

**An investigation into the production of  
phosphoric iron in Eastern England.**

**Neil Stewart Hall, BSc., MSc.**

**Thesis submitted to the University of  
Nottingham  
for the degree of Doctor of Philosophy**

## **Abstract**

Looking at iron slags from Eastern England, this thesis was designed to assess the possibility of inferring the ore type in use by the chemical composition of the slag. A number of case studies are examined. The first is a group of material from the Foulness Valley, East Yorkshire, which is known to be produced from high phosphorus bog ore. This allows direct comparison between this and other assemblages, based on phosphorus content, to infer if bog or bedded ore was in use. Assemblages from Iron Age East Yorkshire, Roman Caistor St Edmund and the Saxon sites of Quarrington and Flixborough were examined to infer on ore exploitation and possible metal production.

The background examination provides a definition of phosphoric iron based upon its material properties and the parameters which govern the creation of the alloy. Further discussion of ore exploitation and the reasoning behind why smelting sites are more difficult to locate are covered, while the current direction of research is examined. The body of experimental work is discussed with notable case studies drawn upon to demonstrate where the literature concentrates its focus. This allows for the suggestion of future possibilities based upon the impacts of these works.

An experimental smelt was carried out in order to inform on the processes and record observations which helped to dictate the choices made on raw material selection. The experimental material was analysed alongside archaeological slags produced from the same ore, and treated in the same way as the material used in the archaeological case studies.

The selection criteria applied to the archaeological assemblages, based on morphology and perceived mass are outlined. A description of the preparation methods for sample examination follows. The physics of electron microscopy are then discussed covering the various effects which govern the generation of the characteristic x-rays which are responsible for the chemical composition data.

Each of the case study assemblages are dealt with individually presenting photographs of the pieces before sampling and backscattered electron images of the material. As this is the first scientific analysis conducted upon the Saxon assemblages from Quarrington and Flixborough, the data generated provides critical, new insight into Early Medieval iron production.

The data using phase composition and phosphorus content are presented on a site by site basis before being assembled into an overall synthesis which further clarifies the inferences of different ore exploitation. Further comparisons of phosphorus and sulphur content are used to demonstrate the use of the bog ore and Frodingham Ironstone available at Flixborough.

The interpretation of the data is then drawn upon for final conclusions and inferences of ore exploitation and the identification of ironstone use at Flixborough which further supports the archaeological and historical evidence for this practice from the 7<sup>th</sup> century A.D.

## **Acknowledgements**

I would like to express my thanks to Dr Lloyd Weeks of the University of Nottingham for his encouragement to start this project and first year supervision during which time the format of this work was decided.

To Prof. Mark Pearce of the University of Nottingham for generously agreeing to assume the role of my lead supervisor following the departure of Dr Weeks.

To Prof. Julian Henderson of the University of Nottingham for his role as second supervisor, and his involvement in suggesting how to present the data.

To Dr Edward Faber for his support during microprobe analysis, and his understanding when stress took hold due to the equipment being unoperational for up to six months at a time.

To Dr Christopher Loveluck of the University of Nottingham, for his enthusiastic support and encouragement when dealing with historical documents and the significance of the data generated from the Saxon material.

To Dr William Bowden of the University of Nottingham for access to the slags from Caistor, and the opportunity to engage with the community archaeologists responsible for the site during a slag training session.

To Mr Antony Lee of the Lincolnshire Archives for access to the iron slags from Quarrington. To Dr Rose Nicholson of the North Lincolnshire Museum for access to the iron slags from Flixborough. To Dr Peter Halkon for access to iron slags and bog ores from the Foulness Valley.

To Mr Jake Keen for the invaluable experience of conducting an iron smelt, including the joys of being badly sunburnt and stained red and black by the end of it.

I would also like to thank the Arts and Humanities Research Council for providing the funding for this project, without which it would not have happened.

Finally, thanks to all my friends and family who have provided both distraction and outlets for the multitude emotions and stress over the past four years, without whom I would not be sane.

# Table of Contents

|   | Page number |
|---|-------------|
| List of Figures   | vi          |
| List of Tables  | xv          |
| List of Abbreviations   | xix         |
| <b>Chapter 1 Introduction</b>   |             |
| 1.1 Aims  | 1           |
| 1.2 Objectives  | 2           |
| 1.3 Site selection  | 2           |
| 1.4 Initial sample strategy   | 14          |
| 1.5 Analytical process  | 15          |
| <b>Chapter 2 Phosphoric Iron in the literature</b>                              |             |
| 2.1 Ferrous materials   | 18          |
| 2.2 Phosphoric iron as a material   | 20          |
| 2.3 Provenance studies  | 38          |
| 2.4 Artefact studies  | 41          |
| 2.5 Iron smelting   | 46          |
| 2.6 Towards a Chaîne Opératoire   | 48          |
| 2.7 Iconographic and Archaeological Representation of<br>specialist ironworkers | 60          |
| 2.8 The occurrence of ironworking and the<br>Utmark/Inmark                      | 68          |
| <b>Chapter 3 Experimental archaeology critique</b>                              |             |
| 3.1 Experimental archaeology: An overview                                       | 74          |
| 3.2 Experimental iron smelting  | 75          |
| 3.3 British iron smelting examples  | 80          |
| 3.4 Bloom smithing: A case study for data collection                            | 87          |
| 3.5 Modern experimental smelts  | 90          |
| 3.6 The Lejre Project   | 94          |
| 3.7 Calculating optimum smelting yields   | 97          |



|   |     |
|---|-----|
| 3.8 The analysis of archaeological material | 100 |
| 3.9 The reduction of phosphoric ores        | 108 |
| 3.10 Summary                                | 109 |
| <b>Chapter 4 Iron Smelting Experiment</b>   |     |
| 4.1 Experimental Design                     | 110 |
| 4.2 Experiment Smelt                        | 112 |
| 4.3 Ore Processing                          | 113 |
| 4.4 Smelt Process                           | 114 |
| 4.5 Experiences and Observations            | 118 |
| 4.6 Products                                | 123 |
| 4.7 Slag Analysis                           | 129 |
| 4.8 Interpretation                          | 131 |
| 4.9 Conclusions                             | 132 |
| <b>Chapter 5 Applied Methods</b>            |     |
| 5.1 Macro examination                       | 133 |
| 5.2 Metallography                           | 136 |
| 5.3 Electron Microscopy                     | 139 |
| 5.4 Sampling Strategy                       | 145 |
| 5.5 Justification of methods                | 147 |
| <b>Chapter 6 Archaeological Material</b>    |     |
| 6.1 East Yorkshire                          | 150 |
| 6.2 Caistor                                 | 158 |
| 6.3 Quarrington                             | 209 |
| 6.4 Flixborough                             | 218 |
| <b>Chapter 7 Data Interpretation</b>        |     |
| 7.1 Introduction                            | 248 |
| 7.2 East Yorkshire                          | 249 |
| 7.3 Caistor                                 | 262 |
| 7.4 Quarrington                             | 268 |
| 7.5 Flixborough                             | 276 |

|  |                        |
|--|------------------------|
| 7.6 Possibility for different reaction conditions and ore exploitation | 285                    |
| 7.7 Implications of the demonstration of the production of fresh metal | 287                    |
| 7.8 Overall Synthesis  | 289                    |
| <b>Chapter 8 Conclusions</b>   |                        |
| 8.1 Conclusions  | 292                    |
| 8.2 Further research suggestions                                       | 294                    |
| <b>Bibliography</b>  | 295                    |
| <b>Appendix</b>  |                        |
| Raw and manipulated data   | Accompanying data disk |

# List of Figures

| Figure Number | Description  | Page Number |
|---------------|--|-------------|
| 1.3.1         | <i>Map of the selected sites in Eastern England.</i>   | 3           |
| 1.3.2         | <i>Map of East Yorkshire and the location of the Foulness river valley (Halkon 2011: 135).</i>   | 4           |
| 1.3.3         | <i>Hasholme Boat with orange staining resulting from iron present in the soil and ground water (Halkon 2011: 137).</i>   | 6           |
| 1.3.4         | <i>The locations of identified iron smithing and smelting sites in East Yorkshire as well as known bronze working locations (Halkon 2008: figure 7.29).</i>  | 7           |
| 1.3.5         | <i>The location of Venta Icenorum (Bowden 2011: Fig 1).</i>  | 9           |
| 1.3.6         | <i>Locations of Quarrington and Flixborough (circled in green and orange respectively) in Lincolnshire (after Ulmschneider 2000: Fig 2).</i>   | 12          |
| 2.2.1         | <i>Hardness (Hv) against phosphorus content (wt%) for pure Fe-P alloys and ternary Fe-P-C and Fe-P-As alloys (Theil and Hošek 2015: Figure 5)</i>  | 22          |
| 2.2.2         | <i>Ghosting in phosphoric iron etched with nital (Theil and Hošek 2015: figure 2)</i>  | 25          |
| 2.2.3         | <i>Ellingham diagram showing metal oxide behaviours</i>  | 27          |
| 2.2.4         | <i>The range of archaeological slag composition (Iron slags dark grey, copper slags mid-grey) in the ternary system FeO-Al<sub>2</sub>O<sub>3</sub>-SiO<sub>2</sub> around the eutectic of Fayalite (Fa) region (Hauptmann 2014: 101).</i>               | 30          |
| 2.2.5         | <i>The binary FeO-Fe<sub>2</sub>O<sub>3</sub>-SiO<sub>2</sub> diagram with a significant increase in melting temperature if either an increased quantity of SiO<sub>2</sub> or iron oxide is present (Hauptmann 2014: 101).</i>                          | 31          |
| 2.2.6         | <i>the morphological differences between bog iron ore (Raseneisenstein) (left) and Orstein (right), most notably the differences in silica grain size (top images) and grain bridging (second top images) (after Kaczorek et al. 2004: 87).</i>          | 36          |
| 2.4.1         | <i>Existing knife typologies demonstrating similarities and differences between classification methods based on blade form the final column is the classification used in Blakelock and McDonnell (2007) (source: Blakelock and McDonnell 2007: 41).</i> | 43          |
| 2.4.2         | <i>Knife blade construction typology (Blakelock and McDonnell 2007: 42).</i>   | 44          |
| 2.6.1         | <i>The chaîne opératoire overview of metallurgical activities with respect to metallic product discussed by Hauptmann (2014: figure 1).</i>  | 49          |

|       |  |     |
|-------|--|-----|
| 2.6.2 | <i>Ore extraction and washing Agricola [1556] (Hoover and Hoover: 291).</i>  | 55  |
| 2.7.1 | <i>Showing a metalworker forging on a horned iron anvil (Stuttgart Psalter: 121r).</i>   | 62  |
| 2.7.2 | <i>The front panel of the Franks Casket with the representation of Weyland (far left).</i>   | 63  |
| 2.7.3 | <i>The smithing scene on Sigurd's portal from the Hylestad stave church, Norway. (<a href="http://www.pitt.edu/~dash/door3932.jpg">http://www.pitt.edu/~dash/door3932.jpg</a>)</i>         | 64  |
| 2.7.4 | <i>Hammer heads in profile from the Tattershall Smith burial (Hinton 2000: Fig. 12).</i>   | 66  |
| 2.8.1 | <i>The model of Utmark and Innmark for iron working according to Birch (after Birch 2011: 9).</i>  | 70  |
| 3.2.1 | <i>The locations of sites KM2 and KM3 (Schmidt and Avery 1983: 423).</i>   | 76  |
| 3.2.2 | <i>The difference between the attempted copy (left) and the original induced draught-furnace constructed in 1910 (van der Merwe and Avery 1987: 152).</i>                                  | 80  |
| 3.4.1 | <i>Major element content (wt%) for ore, smelting slags and smithing slags (solid symbols) and for anvil slags and hammer scale (open symbols) (after Serneels and Crew 1997: figure 1.</i> | 89  |
| 3.5.1 | <i>The effects of higher blast rate upon slag and bloom formation. Lower blast rate (left) and higher blast rate with resultant liquid slag bath (right)(Saunders and Williams 2002).</i>  | 92  |
| 3.6.1 | <i>The experimental pit furnace constructed as part of the Lejre project (Boonstra et al. 1997: 6).</i>  | 95  |
| 4.5.1 | <i>Staining of skin following ore preparation</i>  | 118 |
| 4.5.2 | <i>Ore processing set up.</i>  | 119 |
| 4.5.3 | <i>Large piece of ore (left).</i>  | 120 |
| 4.5.4 | <i>Furnace in use, red 1 indicating location of sealed tapping arch</i>  | 121 |
| 4.5.5 | <i>Opened tapping arch</i>   | 122 |
| 4.6.1 | <i>Composite image showing metallographic sample 1 in the etched condition scale bar 1mm.</i>  | 123 |
| 4.6.2 | <i>Composite image showing metallographic sample 2 in the etched condition scale bar 1mm.</i>  | 124 |
| 4.6.3 | <i>Compositional image with slag inclusion within bloom sample 1 top right and linear porosity visible top right indicative of phosphorus presence.</i>                                    | 125 |
| 4.6.4 | <i>Compositional image of bloom sample 2 showing large pores and linear porosity visible bottom left indicative of phosphorus presence.</i>  | 126 |

|        |  |     |
|--------|--|-----|
| 4.6.5  | <i>Compositional image of feathered fayalite within the first flow slag produced during the experiment.</i>  | 126 |
| 4.6.6  | <i>Compositional image with no free wüstite in pale coloured smelting slag.</i>  | 127 |
| 4.6.7  | <i>Compositional image of slag from the previous smelt conducted in the same furnace with the same ore. Iron rich skin visible top right.</i>  | 127 |
| 4.6.8  | <i>Compositional image of slag from the previous smelt exhibiting severe micro-porosity.</i>   | 128 |
| 4.6.9  | <i>Compositional image of archaeological slag from Tisbury showing well developed fayalite laths and small quantities of wüstite visible centre.</i>   | 128 |
| 4.6.10 | <i>Compositional image of archaeological slag from Tisbury showing close up of fine wüstite dendrites.</i>   | 129 |
| 4.7.1  | <i>Raw fayalite data for experimental assemblage and comparison samples</i>  | 129 |
| 4.7.2  | <i>Raw matrix data for experimental assemblage and comparison samples</i>  | 130 |
| 5.1.1  | <i>A decision tree for desktop iron slag evaluation.</i>   | 135 |
| 5.3.1  | <i>The interaction of a primary electron beam with an analytical sample (grey) producing secondary electrons (S), backscattered electrons (B), X-rays and visible light (after Goodhew et al. 2001: 34).</i> | 143 |
| 5.3.2  | <i>The shape of the area of a specimen which will experience excitement, highlighting the depth of interaction compared to beam to surface contact (Goodhew et al. 2001: 126).</i>                           | 144 |
| 6.1.1  | <i>Thearne smelting slag drips</i>   | 151 |
| 6.1.2  | <i>Hasholme Hall smithing hearth bottom profile</i>  | 152 |
| 6.1.3  | <i>Hasholme Hall smelting slag with fuel inclusion marks – dark central region and surviving fuel inclusions, black charcoal in circular pore below large fuel inclusion impression.</i>                     | 153 |
| 6.1.4  | <i>Hasholme Hall smelting slag showing heterogeneous appearance.</i>   | 154 |
| 6.1.5  | <i>Burse House smithing hearth bottom profile.</i>   | 155 |
| 6.1.6  | <i>Burse House smelting slag.</i>  | 156 |
| 6.1.7  | <i>Burse House green smelting slag.</i>  | 157 |
| 6.2.1  | <i>Trench locations (white squares with numbers) in relation to identified archaeological features at the site of Venta Icenorum.</i>  | 159 |
| 6.2.2  | <i>The distribution of slag by trench and phase within the forum</i>   | 160 |
| 6.2.3  | <i>Quantity of ferrous metallurgical debris per phase.</i>   | 161 |
| 6.2.4  | <i>Sample CRT09/2024 prior to sampling.</i>  | 162 |

|        |  |     |
|--------|--|-----|
| 6.2.5  | <i>Ceramic body of CRT09/2024 with approximately rectangular flint inclusion and silica grains.</i>  | 163 |
| 6.2.6  | <i>Dark field image of red colouration in glassy slag of CRT09/2004.</i>   | 165 |
| 6.2.7  | <i>Bright field image of red colouration in glassy slag of CRT09/2004.</i>   | 166 |
| 6.2.8  | <i>Metallic area in olive green slag in CRT09/2004.</i>  | 167 |
| 6.2.9  | <i>Oxidised metallic area in CRT09/2004.</i>   | 168 |
| 6.2.10 | <i>Yellow colouration in a region of blue/black and olive green glassy slag in CRT09/2004.</i>   | 169 |
| 6.2.11 | <i>Lower and upper surfaces (left and right respectively) of CRT09/2008 prior to sampling.</i>   | 170 |
| 6.2.12 | <i>CRT09/2008 fayalite laths (light grey) with iron prills (white) under optical microscope.</i>   | 171 |
| 6.2.13 | <i>Showing CRT09/2008 large fayalite grains (light grey) in matrix with metallic iron prills (white).</i>  | 172 |
| 6.2.14 | <i>CRT09/2008 large fayalite grains (light grey) in matrix.</i>  | 173 |
| 6.2.15 | <i>The four pieces of slag comprising CRT09/1017</i>   | 175 |
| 6.2.16 | <i>Glassy region with blue colouring with feathered fayalite (white) and silica grains.</i>  | 176 |
| 6.2.17 | <i>A region of glassy slag (grey centre) with feathered fayalite laths (top).</i>  | 176 |
| 6.2.18 | <i>Striking blue colouration in glassy slag of CRT09/1017</i>  | 177 |
| 6.2.19 | <i>Significant fayalite growth, glassy slag and unreacted silica.</i>  | 178 |
| 6.2.20 | <i>Glassy slag surrounding oxidised iron prills</i>  | 179 |
| 6.2.21 | <i>Large iron prill surrounded by glassy slag and silica grains.</i>   | 179 |
| 6.2.22 | <i>Major phases present in CRT09/1137/q6. Large fayalite grains with wüstite and matrix (left) and well developed wüstite dendrites, large fayalite grains and matrix (right).</i> | 180 |
| 6.2.23 | <i>Ultra-fine wüstite dendrites (light grey) within glassy matrix (dark grey) between fayalite grains (mid- grey) in CRT09/1137/q6.</i>  | 181 |
| 6.2.24 | <i>Sample CRTR09/1137/q13 prior to sampling.</i>   | 183 |
| 6.2.25 | <i>Bright field image of silica grains and iron rich matrix of CRT09/1137/q13.</i>   | 184 |
| 6.2.26 | <i>Sample CRT09/1187 prior to sampling.</i>  | 185 |
| 6.2.27 | <i>Dark field image of silica grains in iron rich matrix of CRT09/1187.</i>  | 186 |
| 6.2.28 | <i>Bright field image of silica grains in iron rich matrix of CRT09/1187.</i>  | 187 |

|        |   |     |
|--------|---|-----|
| 6.2.29 | <i>Sample CRT09/1198 prior to sampling.</i>   | 188 |
| 6.2.30 | <i>Singular metal rich inclusion within CRT09/1198.</i>   | 189 |
| 6.2.31 | <i>CRT09/01 unstratified prior to sampling.</i>   | 190 |
| 6.2.32 | <i>Bright field image of slag in close proximity to iron prill (bottom) with limitation of large wüstite development (top right) in sample CRT09/01 unstratified.</i>         | 191 |
| 6.2.33 | <i>CRT09/01 unstratified sample with clear separation of the well-developed wüstite-rich slag (top) from the wüstite-poor slag surrounding the metal prill (bottom left).</i> | 192 |
| 6.2.34 | <i>Bright field image of oxidised iron flake (bright white) in sample CRT9/06.</i>  | 193 |
| 6.2.35 | <i>Fine wüstite dendrite growth surrounded by glassy slag in sample CRT09/06.</i>   | 194 |
| 6.2.36 | <i>CRT09/09a ultra-fine wüstite dendrites and slight coring of wüstite skeletal structures.</i>   | 195 |
| 6.2.37 | <i>CRT09/09a wüstite rich slag (left), probably fuel ash slag inclusion (centre) and fayalite rich slag with well-developed fayalite (right).</i>                             | 196 |
| 6.2.38 | <i>Highly porous, low density nature, vitrified structures (top right) and fine higher density crystals in the optically white region (top left) of CRT09/09b.</i>            | 197 |
| 6.2.39 | <i>CRT09/09b angular crystals in low density matrix with micro-wüstite in the optically white region.</i>   | 197 |
| 6.2.40 | <i>Bright inclusion of weathered cassiterite within fuel ash slag CRT09/09b.</i>  | 198 |
| 6.2.41 | <i>Sample CRT09/200 post-cleaning.</i>  | 199 |
| 6.2.42 | <i>Sample CRT10/2077 post-cleaning.</i>   | 200 |
| 6.2.43 | <i>Sample CRT10/3034 post-cleaning.</i>   | 201 |
| 6.2.44 | <i>Sample CRT10/4006 post-cleaning.</i>   | 202 |
| 6.2.45 | <i>Sample CRT10/4018 post-cleaning.</i>   | 203 |
| 6.2.46 | <i>Sample CRT10/4029 post-cleaning</i>  | 204 |
| 6.2.47 | <i>Sample CRT10/4047 post-cleaning.</i>   | 205 |
| 6.2.48 | <i>Sample CRT11/6605 post-cleaning.</i>   | 206 |
| 6.3.1  | <i>Ejection of slag from a fold weld (after Dungworth and Wilkes 2009)</i>  | 211 |
| 6.3.2  | <i>Profile of slag exhibiting plano-convex form.</i>  | 213 |
| 6.3.3  | <i>Smelting slag from context QCH93 024</i>   | 215 |

|        |   |     |
|--------|---|-----|
| 6.3.4  | <i>Unstratified smelting slag QCH93 +</i>   | 215 |
| 6.3.5  | <i>Backscatter electron image of QCH93+ sample with well developed globular wüstite dendrites, fayalite grains and low density matrix, and significant pores.</i>                                   | 216 |
| 6.3.6  | <i>Unstratified smelting slag drip QCH93 +R.</i>  | 217 |
| 6.3.7  | <i>Backscatter electron image of QCH93 +R sample with well-developed wüstite dendrites, fayalite laths and low density matrix, characteristic of the smelting slags recovered from the site.</i>    | 217 |
| 6.4.1  | <i>Large tapped slag from context FLX89 51.</i>   | 220 |
| 6.4.2  | <i>Backscatter electron image of slag sample from context FLX89 51, with fine wüstite dendrites, fayalite laths, glassy matrix and metallic iron (bright white).</i>                                | 221 |
| 6.4.3  | <i>Smelting slag gromp from context FLX89 51.</i>   | 222 |
| 6.4.4  | <i>Backscatter electron image of slag sample from context FLX89 51, with globular wüstite dendrites, extensive fayalite grains, limited glassy matrix, and notable porosity.</i>                    | 222 |
| 6.4.5  | <i>Flowed smelting slag from context FLX89 2176 (a and b, left and right respectively).</i>   | 223 |
| 6.4.6  | <i>Backscatter electron image of slag sample FLX89 2176a, with fine wüstite dendrites, fayalite laths, glassy matrix, and porosity.</i>   | 224 |
| 6.4.7  | <i>Backscatter electron image of slag sample from context FLX89 2176b, with fine wüstite dendrites and occasional globular wüstite, well developed fayalite laths, glassy matrix, and porosity.</i> | 225 |
| 6.4.8  | <i>Flowed smelting slag from context FLX89 1427.</i>  | 226 |
| 6.4.9  | <i>Backscatter electron image of slag sample from context FLX89 1427, with fine wüstite dendrites and occasional globular wüstite, well developed fayalite laths, glassy matrix, and porosity.</i>  | 226 |
| 6.4.10 | <i>Roasted ore sample from context FLX89 17513.</i>   | 227 |
| 6.4.11 | <i>Smelting slag from context FLX89 2823.</i>   | 228 |
| 6.4.12 | <i>Smelting slag gromp from context FLX89 1995.</i>   | 228 |
| 6.4.13 | <i>Backscatter electron image of slag sample from context FLX89 1995, with no visible wüstite, feathered fayalite laths, glassy matrix, and porosity.</i>   | 229 |
| 6.4.14 | <i>Large smelting slag piece from context FLX89 10393 10449.</i>  | 230 |
| 6.4.15 | <i>Backscatter electron image of slag sample from context FLX89 10393 10449, with well-developed wüstite dendrites, fayalite laths, glassy matrix, and pores.</i>                                   | 231 |



|        |  |     |
|--------|--|-----|
| 6.4.16 | <i>Large smelting slag with flowed surface FLX89 2024.</i>   | 232 |
| 6.4.17 | <i>Backscatter electron image of slag sample from context FLX89 2024, with well-developed wüstite dendrites and occasional globular wüstite, extensive fayalite grains, limited glassy matrix, and significant pores.</i>                          | 233 |
| 6.4.18 | <i>Sample of material from FLX89 800 with slag encasing iron- rich stone.</i>  | 234 |
| 6.4.19 | <i>Smelting slag ribbon from context FLX89 3256 5286.</i>  | 234 |
| 6.4.20 | <i>Backscatter electron image of slag sample from context FLX89 3256 5286, with well-developed wüstite dendrites and occasional globular wüstite, extensive fayalite grains, and glassy matrix.</i>  | 235 |
| 6.4.21 | <i>Smelting slag from context FLX89 674</i>  | 236 |
| 6.4.22 | <i>Smelting slag from context FLX89 10394 10546</i>  | 236 |
| 6.4.23 | <i>Tap slags from context FLX89 3107 – analysed samples tap slag number 2, tap slag number 4 and tap number slag 5 indicated by red numbers. The pieces are arranged to show archaeological and fresh breaks to allow for clearer association.</i> | 237 |
| 6.4.24 | <i>Backscatter electron image of slag sample tap slag number 2 from context FLX89 3107, with wüstite dendrites, extensive fayalite grains, glassy matrix, and occasional metallic iron (bright white).</i>   | 238 |
| 6.4.25 | <i>Backscatter electron image of slag sample tap slag number 4 from context FLX89 3107, with fine wüstite dendrites, fayalite laths and glassy matrix</i>  | 239 |
| 6.4.26 | <i>Backscatter electron image of slag sample tap slag number 5 from context FLX89 3107, with fine wüstite dendrites, fayalite laths, glassy matrix porosity and magnetite skin (far left).</i>   | 240 |
| 6.4.27 | <i>Smelting/furnace slag piece from context FLX89 3107.</i>  | 241 |
| 6.4.28 | <i>Backscatter electron image of furnace slag sample from context FLX89 3107, with fine wüstite dendrites (top right) and globular wüstite (centre), fayalite grains, glassy matrix, and significant porosity.</i>                                 | 242 |
| 6.4.29 | <i>Largest furnace slag piece from context FLX89 3107.</i>   | 243 |
| 6.4.30 | <i>Backscatter electron image of large furnace slag sample from context FLX89 3107, with fine wüstite dendrites, fine fayalite laths, glassy matrix.</i>   | 244 |
| 6.4.31 | <i>Small ore piece from context FLX89 503 14333.</i>   | 245 |
| 6.4.32 | <i>Backscatter electron image of ore sample from context FLX89 503 14333.</i>  | 245 |
| 6.4.33 | <i>Microstructure of ore sample recovered from context FLX89 800, multiple FeS inclusions (bright white) visible within ore body.</i>  | 246 |
| 7.2.1  | <i>Complete phase average compositions for East Yorkshire assemblage.</i>  | 250 |

|        |   |     |
|--------|---|-----|
| 7.2.2  | <i>Complete phase average compositions for East Yorkshire assemblage by site.</i>   | 250 |
| 7.2.3  | <i>Matrix and Fayalite phase average compositions by site with ores for comparison.</i>   | 251 |
| 7.2.4  | <i>Fayalite (red circle) and matrix phase average compositions for all East Yorkshire slag samples.</i>   | 251 |
| 7.2.5  | <i>Wüstite phase average composition per site.</i>  | 252 |
| 7.2.6  | <i>Fayalite phase average composition per site with higher and lower phosphorus groupings circled in blue and red respectively.</i>                       | 253 |
| 7.2.7  | <i>Matrix phase average composition per site.</i>   | 254 |
| 7.2.8  | <i>Complete phase composition analyses for East Yorkshire assemblage.</i>   | 256 |
| 7.2.9  | <i>Complete phase composition analyses for East Yorkshire assemblage by phase.</i>  | 256 |
| 7.2.10 | <i>Complete phase composition analyses of fayalite and matrix phase of East Yorkshire assemblage.</i>   | 257 |
| 7.2.11 | <i>Complete phase composition analyses of fayalite (circled in blue) and matrix phase of East Yorkshire Assemblage after removal of extreme outliers.</i> | 258 |
| 7.2.12 | <i>Complete fayalite phase analyses of East Yorkshire assemblage.</i>   | 259 |
| 7.2.13 | <i>Complete fayalite phase analyses of East Yorkshire assemblage after removal of the green smelting slag.</i>  | 260 |
| 7.2.14 | <i>Complete matrix data with outlier fayalite rich analyses beyond FeO:SiO<sub>2</sub> value of 2 shown by the black line.</i>                            | 261 |
| 7.2.15 | <i>P<sub>2</sub>O<sub>5</sub> against CaO in matrix of analysed East Yorkshire slags</i>  | 261 |
| 7.3.1  | <i>Complete phase average data for the Caistor assemblage.</i>  | 262 |
| 7.3.2  | <i>Complete fayalite, circled in blue, and matrix, circled in red, phase average compositions for Caistor assemblage.</i>                                 | 263 |
| 7.3.3  | <i>Fayalite phase average for Caistor assemblage.</i>   | 263 |
| 7.3.4  | <i>Matrix phase average for Caistor assemblage.</i>   | 264 |
| 7.3.5  | <i>Complete phase composition analyses of fayalite phase Caistor assemblage.</i>  | 266 |
| 7.3.6  | <i>Complete phase composition analyses of matrix phase Caistor assemblage</i>   | 267 |
| 7.3.7  | <i>P<sub>2</sub>O<sub>5</sub> against CaO in matrix of analysed Caistor slags.</i>  | 267 |
| 7.4.1  | <i>Complete phase average compositions for Quarrington assemblage.</i>  | 268 |

|       |  |     |
|-------|--|-----|
| 7.4.2 | <i>Complete fayalite (circled in red) and matrix phase average compositions for Quarrington assemblage.</i>  | 269 |
| 7.4.3 | <i>Wüstite phase average compositions for the Quarrington assemblage.</i>  | 272 |
| 7.4.4 | <i>Complete fayalite (red circle) and matrix phase average compositions for the Quarrington assemblage by sample type.</i>   | 273 |
| 7.4.5 | <i>Complete fayalite data for the analysed Quarrington assemblage.</i>   | 273 |
| 7.4.6 | <i>Complete matrix data for the analysed Quarrington assemblage, showing the fayalite composition limit (black vertical line) at an FeO:SiO<sub>2</sub> value of 2.</i>  | 274 |
| 7.4.7 | <i>P<sub>2</sub>O<sub>5</sub> against CaO in matrix of analysed Quarrington slags.</i>   | 745 |
| 7.5.1 | <i>Phase average for 8<sup>th</sup>-century and 10<sup>th</sup>-century fayalite, circled in red, and matrix to the left of that group.</i>  | 276 |
| 7.5.2 | <i>Fayalite plots with the exclusion of two major outliers from the 8<sup>th</sup>-century, highlighting the major grouping of points from Phases 4 and 6 at FeO:SiO<sub>2</sub> values of 2 and showing clear outliers in the phase 4 data.</i> | 281 |
| 7.5.3 | <i>Matrix phase analyses including mixed signal outliers.</i>  | 282 |
| 7.5.4 | <i>Matrix phase analyses excluding mixed signal outliers with FeO:SiO<sub>2</sub> &gt; 2.</i>  | 282 |
| 7.5.5 | <i>P<sub>2</sub>O<sub>5</sub> against CaO in matrix of analysed Flixborough phase 4 (8<sup>th</sup>-century) slags.</i>  | 283 |
| 7.5.6 | <i>P<sub>2</sub>O<sub>5</sub> against CaO in matrix of analysed Flixborough phase 6 (10<sup>th</sup> century) slags.</i>   | 284 |
| 7.5.7 | <i>P<sub>2</sub>O<sub>5</sub> against CaO in matrix of all analysed Flixborough slags by site phase.</i>   | 285 |
| 7.6.1 | <i>P<sub>2</sub>O<sub>5</sub> against SO<sub>3</sub> scatter plot for Flixborough data</i>   | 286 |
| 7.8.1 | <i>Combined phase average plot for all assemblages, the points circled in black represent the reliable fayalite analyses of the complete assemblage.</i>   | 289 |

# List of Tables

| Table Number | Description   | Page Number |
|--------------|---|-------------|
| 1.3.1        | <i>Quantity of ironworking debris found at Venta Icenorum</i>   | 10          |
| 1.3.2        | <i>Quantity of ironworking evidence recovered from Quarrington (Taylor et al. 2003: 257)</i>  | 11          |
| 1.3.3        | <i>Total combined masses of ironworking debris recovered from Quarrington</i>   | 11          |
| 1.3.4        | <i>Quantity of ironworking debris found at Flixborough.</i>   | 13-14       |
| 1.3.5        | <i>Summary total quantity data of Flixborough assemblage</i>  | 14          |
| 2.2.1        | <i>Weight percent Phosphorus content and associated Vickers hardness (Hv) (Theil and Hošek 2015: Table 2)</i>   | 21          |
| 2.2.2        | <i>Average compositions of major iron ore deposits in Britain, compiled from Zitzmann 1977. * Maximum P content reported by Hallimond (1925).</i>   | 34          |
| 3.8.1        | <i>Analytical data of iron ore samples recovered from Shooters Hill (Dungworth and Mephram 2012:4) and comparative average data from three samples of sideritic ironstone from Braklesham Beds (after Potter 1977).</i> | 107         |
| 4.2.1        | <i>Recorded parameters of the smelt.</i>  | 113         |
| 4.4.1        | <i>The progression of the experimental smelt including duration between charge additions per kg.</i>  | 116         |
| 6.2.1        | <i>Major elements present in the main features of CRT09/2024.</i>   | 163         |
| 6.2.2        | <i>Minor elements present in the main features of CRT09/2024</i>  | 164         |
| 6.2.3        | <i>Major elements and copper content of red coloured area in CRT09/2004.</i>  | 166         |
| 6.2.4        | <i>Minor elements present in red coloured area of CRT09/2004.</i>   | 166         |
| 6.2.5        | <i>Analysis of oxidised metallic region in CRT09/2004.</i>  | 168         |
| 6.2.6        | <i>Major elements detected in yellow coloured area of CRT09/2004, including a notable Barium content.</i>   | 169         |
| 6.2.7        | <i>Minor elements detected in yellow coloured area of CRT09/2004.</i>   | 169         |
| 6.2.8        | <i>Major elements present in observable phases of CRT09/2008.</i>   | 172         |
| 6.2.9        | <i>Minor elements present in observable phases of CRT09/2008.</i>   | 174         |
| 6.2.10       | <i>Elements present in large metallic prills in CRT09/2008</i>  | 174         |
| 6.2.11       | <i>Major elements and appreciable phosphorus content of blue coloured slag in CRT09/1017.</i>   | 177         |

|        |   |     |
|--------|---|-----|
| 6.2.12 | <i>Minor elements present in blue coloured slag in CRT09/1017</i>                                     | 178 |
| 6.2.13 | <i>Major elements detected in iron prill.</i>   | 180 |
| 6.2.14 | <i>Minor elements detected in iron prill.</i>   | 180 |
| 6.2.15 | <i>Major elements present in glassy matrix of CRT09/06.</i>   | 182 |
| 6.2.16 | <i>Minor elements present in glassy matrix of CRT09/06.</i>   | 182 |
| 6.2.17 | <i>Major elements present in the main slag body of CRT09/06.</i>                                      | 182 |
| 6.2.18 | <i>Minor elements present in the main slag body of CRT09/06.</i>                                      | 182 |
| 6.2.19 | <i>Composition of silaceous body of CRT09/1198.</i>   | 189 |
| 6.2.20 | <i>Detected elements in Iron prill of CRT09/01 unstratified.</i>                                      | 191 |
| 6.2.21 | <i>Major elements detected (%) in oxidised iron flake in CRT09/06.</i>                                | 193 |
| 6.2.22 | <i>Major elements detected (%) in the slag body of CRT09/06</i>                                       | 194 |
| 6.2.23 | <i>Minor elements detected (%) in the slag body of CRT09/06</i>                                       | 194 |
| 6.2.24 | <i>Major elements detected (%) in cored structures in figure 6.2.36</i>                               | 195 |
| 6.2.25 | <i>Major elements present in observed crystals in white region of CRT09/09b</i>                       | 198 |
| 6.2.26 | <i>Major elements detected in weathered cassiterite inclusion</i>                                     | 198 |
| 6.3.1  | <i>Revised list of Quarrington smelting slag.</i>   | 214 |
| 6.3.2  | <i>Major elements detected in the main mineral phases of slag QCH93+</i>                              | 216 |
| 6.3.3  | <i>Major elements detected in the main mineral phases of slag QCH93+R</i>                             | 218 |
| 6.4.1  | <i>Major elements detected in the main mineral phases of large tap slag from context FLX89 51.</i>    | 221 |
| 6.4.2  | <i>Major elements detected in the main mineral phases of the smelting group from context FLX89 51</i> | 223 |
| 6.4.3  | <i>Major elements detected in the main mineral phases of the smelting slag FLX89 2176a</i>            | 224 |
| 6.4.4  | <i>Major elements detected in the main mineral phases of the smelting slag FLX89 2176b</i>            | 225 |
| 6.4.5  | <i>Major elements detected in the main mineral phases of the smelting slag FLX89 1427</i>             | 227 |
| 6.4.6  | <i>Major elements detected in the main mineral phases of the smelting slag FLX89 1995</i>             | 229 |
| 6.4.7  | <i>Major elements detected in the main mineral phases of the smelting slag FLX89 10393 10449</i>      | 231 |

|        |  |     |
|--------|--|-----|
| 6.4.8  | <i>Major elements detected in the main mineral phases of the smelting slag FLX89 2024.</i>   | 233 |
| 6.4.9  | <i>Major elements detected in the main mineral phases of the smelting slag FLX89 3256 5286</i>   | 235 |
| 6.4.10 | <i>Major elements detected in the main mineral phases of tap slag 2 from context FLX89 3107.</i>   | 238 |
| 6.4.11 | <i>Major elements detected in the main mineral phases of tap slag 4 from context FLX89 3107.</i>   | 239 |
| 6.4.12 | <i>Major elements detected in the main mineral phases of tap slag 5 from context FLX89 3107.</i>   | 240 |
| 6.4.13 | <i>Major elements detected in the main mineral phases of the medium furnace slag from context FLX89 3107.</i>  | 242 |
| 6.4.14 | <i>Major elements detected in the main mineral phases of the large furnace slag from context FLX89 3107.</i>   | 244 |
| 6.4.15 | <i>Showing major elements detected within the sample of ore FLX89 503 14333.</i>   | 246 |
| 6.4.16 | <i>Main elements detected in the average density ore body of sample recovered from context FLX89 800.</i>  | 246 |
| 6.4.17 | <i>Main elements detected in FeS inclusions found in the ore sample recovered from context FLX89 800.</i>  | 246 |
| 7.2.1  | <i>Phase mean compositions, mean phosphorus content, associated standard deviations, and coefficients of variation for the Foulness Valley fayalite data.</i>                | 253 |
| 7.2.2  | <i>Phase mean compositions, mean phosphorus content, associated standard deviations, and coefficients of variation for the Foulness Valley matrix data.</i>                  | 255 |
| 7.3.1  | <i>Phase mean compositions, mean phosphorus content, associated standard deviations, and coefficients of variation for the Caistor fayalite data.</i>                        | 264 |
| 7.3.2  | <i>Phase mean compositions, mean phosphorus content, associated standard deviations, and coefficients of variation for the Caistor matrix data.</i>                          | 265 |
| 7.4.1  | <i>Phase mean compositions, mean phosphorus content, associated standard deviations, and coefficients of variation for the Quarrington fayalite data.</i>                    | 270 |
| 7.4.2  | <i>Phase mean compositions, mean phosphorus content, associated standard deviations, and coefficients of variation for the Quarrington matrix data.</i>                      | 271 |
| 7.5.1  | <i>Phase mean compositions, mean phosphorus content, associated standard deviations, and coefficients of variation for 8<sup>th</sup>-century Flixborough fayalite data.</i> | 277 |

|       |   |     |
|-------|---|-----|
| 7.5.2 | <i>Phase mean compositions, mean phosphorus content, associated standard deviations, and coefficients of variation for 10<sup>th</sup>-century Flixborough fayalite data.</i> | 278 |
| 7.5.3 | <i>Phase mean compositions, mean phosphorus content, associated standard deviations, and coefficients of variation for 8<sup>th</sup>-century Flixborough matrix data.</i>    | 279 |
| 7.5.4 | <i>Phase mean compositions, mean phosphorus content, associated standard deviations, and coefficients of variation for 10<sup>th</sup> century Flixborough matrix data.</i>   | 280 |

# List of Abbreviations

| Abbreviation       | Full Term                    |
|--------------------|------------------------------|
| SEM                | Scanning electron microscopy |
| EMPA               | Electron Mico-probe analysis |
| XRF                | X-ray fluorescence           |
| XRD                | X-ray diffraction            |
| VHL                | Vitrified hearth lining      |
| SHB                | Smithing hearth bottom       |
| FB                 | Furnace bottom               |
| NDS                | Non-diagnostic slag          |
| $\bar{x}$          | Mean average                 |
| $\sigma$           | Standard deviation           |
| $\sigma / \bar{x}$ | Coefficient of variation     |



# Chapter 1

## Introduction

|            |                                |           |
|------------|--------------------------------|-----------|
| <i>1.1</i> | <i>Aims</i>                    | <i>1</i>  |
| <i>1.2</i> | <i>Objectives</i>              | <i>2</i>  |
| <i>1.3</i> | <i>Site Selection</i>          | <i>2</i>  |
| <i>1.4</i> | <i>Initial sample strategy</i> | <i>14</i> |
| <i>1.5</i> | <i>Analytical process</i>      | <i>15</i> |

### 1.1 Aims

This thesis is designed to investigate the production of phosphoric iron by bloomery smelting. Based upon current theoretical understanding of the direct reduction process, the impact of technology upon bloom and slag chemical composition will be studied by the examination of material from several sites which demonstrate changes in smelting technology over time.

This is important because it would further inform upon the production of phosphoric iron for use in high status objects such as pattern welded blades and high quality craft knives. The aspect of technology, which has yet to be fully understood, may play a role in controlling phosphorus content which may be reflected in the slag produced at sites where high phosphorus ore was available. Currently it is presumed that high phosphorus bog ore will produce phosphoric iron regardless of the technology used. This thesis will attempt to contribute to clarifying this standing assumption.

While the main research into ferrous metallurgy has moved to focus on provenance, this aspect of production has not been fully addressed in an archaeologically valid setting. Previous research has been conducted using a modern laboratory set up with carefully controlled reaction conditions (Godfrey 2007). This was not truly reflective of past smelting practices and thus, while informative, did not replicate the process it attempted to simulate.

For this reason my study will focus on archaeological samples with some experimental pieces for comparison in order to identify the impact of technology and the use of ores to produce phosphorus rich iron.

## **1.2 Objectives**

In order to examine the change of technology sites, dating from the Late Iron Age through to the 4<sup>th</sup>-11<sup>th</sup> centuries A.D. will be selected from predominantly a single region of England. This will allow for a comparison of the archaeological material due to similar geological conditions and relatively continuous chronology across the region of study.

The chemical composition of slag from the selected sites will be determined by electron microprobe analysis (EMPA) which will analyse the different phases present for major, minor, and trace elements. The location of the analyses will be targeted by prior optical microscopy, allowing for the preliminary identification of the major phases present in the slags.

The generated data will then be plotted into XY scatter graphs to determine if there is a general trend between sites which have access, or have evidence of the use of, high-phosphorus bog ores. This may be particularly enlightening for sites which have evidence for the use of both bog and bedded ore deposits, as the difference in phosphorus content may indicate which ore was used or if both were exploited.

## **1.3 Site selection**

For this study, sites from the region of Eastern England were selected.

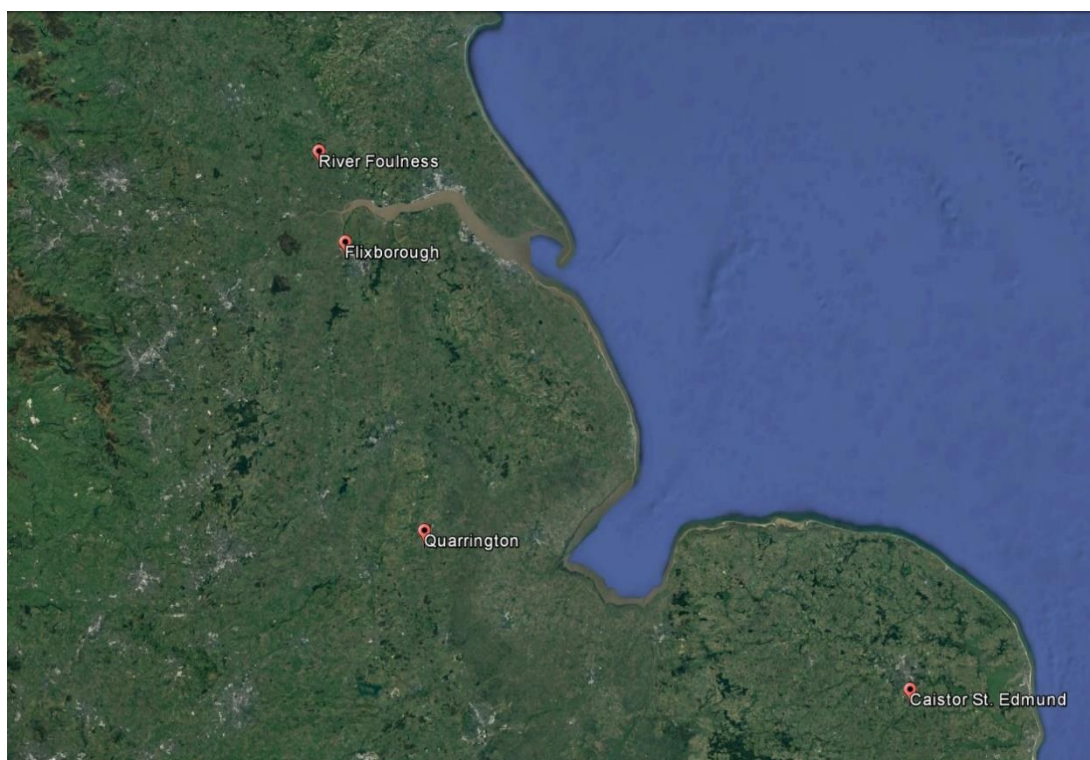


*Figure 1.3.1 Map of the selected sites in Eastern England.*

The earliest sites are drawn from the Foulness Valley, East Yorkshire, where bog iron ore and distinctive smelting technology were in use during the Iron Age. Extensive iron smelting was occurring in the area, as evidenced by the large slag heaps at Moor's Farm and Welham Bridge (Clogg 1999). This site provides a useful reference as the slag was without question produced using high phosphorus bog ore and a non-Roman smelting technique.

The Roman portion of material is taken from the site of Venta Icenorum at Caistor St. Edmund, Norfolk. The metallurgical evidence at this site dates mostly from the late 3<sup>rd</sup>- early 5<sup>th</sup> centuries A.D., with the majority of the pieces found representing iron smithing. There are a small number of pieces which are diagnostic of smelting, which suggest that primary iron production was occurring near the site, although the location of the furnaces lies beyond the area of excavation.

The site representing the next major phase in the history of the region is Quarrington, near Sleaford, Lincolnshire. This site dates from the sixth to seventh centuries, representing the Early-Mid Saxon periods. As with Venta Icenorum (Caistor), the site has evidence of both iron smelting and smithing. Although the morphology of the pieces does not appear to correspond with the usual morphologies associated with these processes. Plates of slag and many flowed slag droplets with no flat surfaces may be indicative of bloom consolidation, which would be anticipated to occur at smelting sites. This

site demonstrates the use of different ore, most likely bog ore, to produce iron when compared to Caistor where the ore type is uncertain.

The last, and possibly most significant, site to be examined is that of Flixborough which dates from the Mid-Late Saxon periods with some iron smelting evidence dating from the eighth century and a far greater quantity dating from the tenth century. This site also has both bog and bedded ore deposits available for exploitation, which may prove to be discernible by electron microprobe analysis. If this proves to be the case then it will further strengthen the argument that bedded iron ore, in this case Frodingham Ironstone, was being used to produce iron significantly before the advent of later blast furnace technology. It may also reveal that smelters at the site were capable of producing both phosphoric and ferritic iron which could then be used independently for specific purposes.

### **Site details and assemblages**

#### **Foulness Valley**

The Foulness Valley is an area of East Yorkshire which is rich in archaeology with large numbers of sites dating to the Bronze and Iron ages as well as the Roman and Romano-British periods.

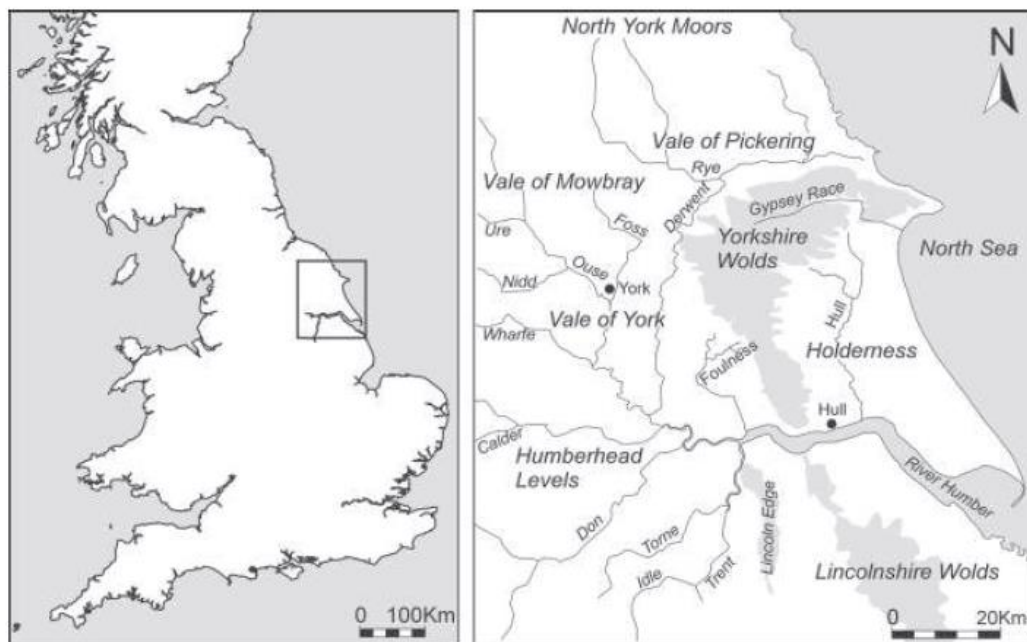


*Figure 1.3.2 Showing map of East Yorkshire and the location of the Foulness river valley (Halkon 2011: 135).*

The Foulness valley was a partially tidal inlet during the Iron Age, as attested by coring studies which have located estuarine clay ranging from the present north bank of the Humber River up to Welham Bridge. The name originates from the colour of the water which was coloured an orange-brown because of the ferruginous ground water draining through the iron rich sands of the holmes (areas of raised drier “islands” amongst the low lying boggy land). The watercourses of the Foulness valley played a significant role in both the settlement of the landscape and the economy at the time. Within the valley there are multiple rivers and springs which, given the low lying nature of the land, would have resulted in portions of the landscape being heavily alluviated. The presence of such a damp, near wetland environment in which there are clear interfaces between clay and ferruginous sand would give rise to the presence of large quantities of bog iron ore which would be highly suitable for smelting.

Iron production in the area appears to have been highly concentrated at Welham Bridge, where the estuarine clays end. This is highly significant as is a distinct absence of other sites outside the Lower Foulness valley concerned with iron production. Because of the apparent concentration of iron smelting in this area, it has been interpreted as an “industrial zone” (Halkon 2008: 170). Many of the identified smelting sites occur in close proximity to either water courses with alluvial flood deposits or peat bogs, further strengthening the case for the exploitation of bog ore (Halkon 2008: 172).

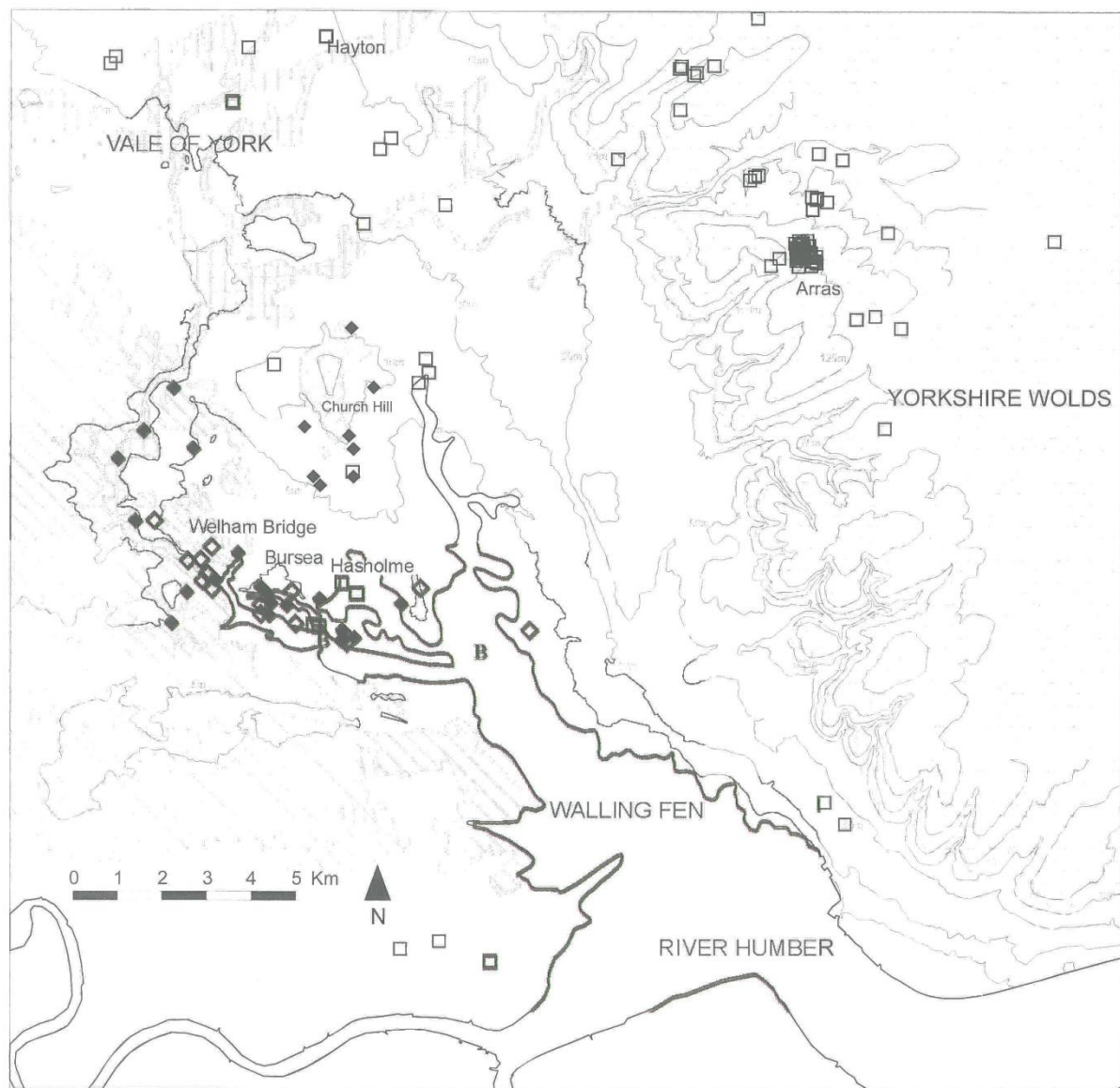
The concentration of iron within the sands of the Foulness Valley is significantly high. Upon excavation the Hasholme Boat exhibited orange staining resulting from the deposition of iron minerals leached from the sands by ground water, as shown below. This is also the case for many large pieces of slag found at the sites of interest which also have iron oxide stained surfaces.



*Figure 1.3.3 Showing the Hasholme Boat with orange staining resulting from iron present in the soil and ground water (Halkon 2011: 137).*

This trend of iron smelting sites being found at locations where the ferruginous sands and estuarine clays meet appears to be a predictive model for the identification of possible smelting locations on both sides of the Humber. The application of this hypothesis is intended to be investigated in future research.





| soils:  |                               | finds:  |                     |
|---|-------------------------------|---|---------------------|
|  | loess                         |  | peat                |
|  | Mercia mudstone               |  | estuarine clay      |
|  | alluvium                      |  | clay                |
|  | peat, alluvium & sand patches |  | sands               |
|   |                               |  | log boats           |
|   |                               |  | square barrows      |
|   |                               |  | iron smelting sites |
|   |                               |  | iron-working sites  |

*Figure 1.3.4 Showing the locations of identified iron smithing and smelting sites in East Yorkshire as well as known bronze working locations (Halkon 2008: figure 7.29).*

Figure 1.3.3 above demonstrates the distribution of iron-working sites, both smelting and smithing, in the region. Each of the sites both the Foulness Valley and nearby Hull Valley are all situated on land where the ferruginous sands and estuarine clays interface. There is a clear concentration of activity

within the Foulness Valley, although other sites may yet remain unidentified in the Hull Valley. The reason for the smelting sites being located at areas where there is an interface between the ferruginous sand and estuarine clay is that bog ore forms at these horizons. The iron in the ground water does not penetrate far into the clay and forms a layer at the interface which builds up into a recognisable iron pan layer. This can either be contiguous as an archetypal “pan” or the ore can form in large nodular blocks.

The actual sites of smelting activity are located some distance from the main areas settlement. It is also apparent that iron production and secondary iron working were carried out in different locations (Halkon 2008: 171). As of 2008, no furnaces had been excavated in the area. However, there is a close resemblance in form between then types 3 and 4 slag blocks identified by Clogg (1999) at Moore’s Farm and blocks produced by slag-pit furnaces dating to the final Hallstatt and early La Tène periods which were excavated in the Paris basin (Cabboi and Dunikowski 2004). Halkon uses the similarities in slag morphology and burial practices between the Foulness valley and the Paris basin to propose a possible cultural link between the regions (Halkon 2008: 171-172) . This may be plausible as the technology in use at Moore’s Farm would appear to be significantly different to that in use elsewhere in England at this time.

Moore’s Farm contained a total of 5,338kg of slag (Halkon 2008: 169), making it one of the largest archaeological slag heaps in the country. Today, almost 30 years after the excavation in 1985, slag is still being found at the site, with multiple slag blocks and pieces of slag being recovered by field walks of which I myself have been involved. This site forms the prehistoric portion of the study, as it is a site that most certainly exploited high phosphorus bog ores to produce iron using a technology that was very different to the later Roman methods.

The rich abundance of archaeology in East Yorkshire suggests that this region has far more to offer researchers, not only in archaeometallurgy but also in many other diverse fields of study. It typically challenges the overwhelmingly South East centric view of British archaeology and technological introduction and cultural adoption. With such a large, prominent waterway it is likely that East Yorkshire experienced a greater flow of human traffic and cultural interaction than is generally assumed as it is not in close proximity to continental Europe as the South East is. The greatly different smelting technology and differing burial practices such as chariot burials may suggest that there was contact between peoples in East Yorkshire and Continental Europe. This appears to receive less attention due to geographical location and hence relatively less intense study in comparison to the South East which becomes significantly more important in later periods following the foundation and establishment of Londinium during the Roman period.

]



## Venta Icenorum

The Roman site of Venta Icenorum at Caistor St Edmund, Norfolk has recently been under excavation. Iron working slags representing both smithing and smelting were recovered and are undergoing analysis as part of this project. The site is located close to the River Tas (Figure 1.3.4), Which due to the low altitude and high water table would suggest a relatively wet local environment with an appreciable chlorine content. As such, little metallic ferrous material is expected to have survived. The majority of the slags date to the late third – early fifth centuries A.D. Two pieces of iron rich material were recovered from the site and may indicate that bog ore was available in the area for smelting. The quantity of smelting evidence is limited with a small quantity of tap slag and wüstite rich slag providing definitive proof of iron production, although possible smelting sites have been identified by magnetometer survey beyond the area of excavation. The smelting technology in use at this site differs greatly from that in the Foulness Valley and later Saxon sites which are considered.

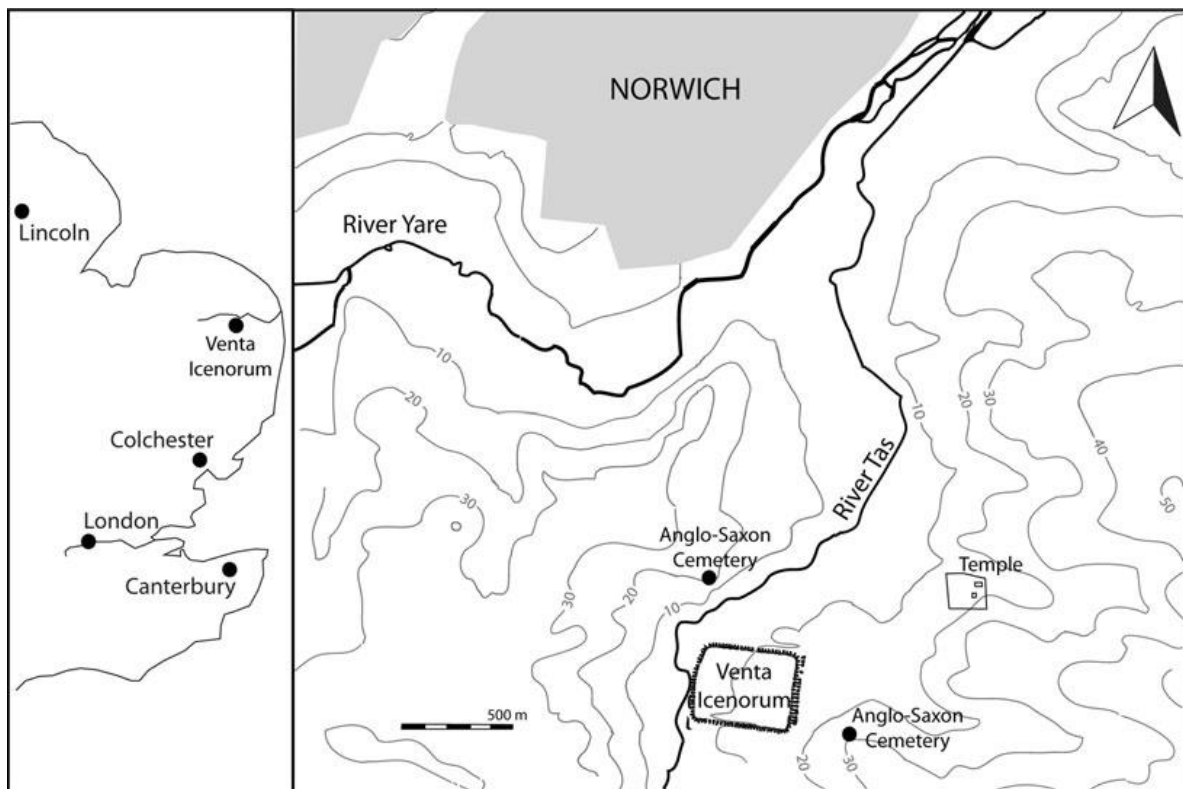


Figure 1.3.5 Showing the location of Venta Icenorum (Bowden 2011: Fig 1).

Preliminary analyses have demonstrated that the possible ores are rich enough in iron to be viable for smelting, although due to the change in hydrology in the area proximal to the site the quantity of ore in the area is likely to be greatly reduced. The table below shows the quantity of material recovered from the site at present.

|                               |  | <b>Vitrified<br/>hearth<br/>lining</b> | <b>Smithing<br/>hearth<br/>bottoms</b> | <b>Smithing<br/>slags</b> | <b>Smelting<br/>slags</b> | <b>Cinder</b> | <b>Non-<br/>diagnostic</b> | <b>Iron<br/>objects</b> |
|-------------------------------|--|--|--|---------------------------|---------------------------|---------------|----------------------------|-------------------------|
| <b>Total<br/>mass<br/>(g)</b> |  | 5593.7                                 | 4785.2                                 | 264.5                     | 443.8                     | 20            | 2382.4                     | 212.3                   |

*Table 1.3.1 showing quantity of ironworking debris found at Venta Icenorum.*

## **Quarrington**

The settlement at Quarrington is an Early to Mid-Saxon site with the majority of the iron slag dating to the 6<sup>th</sup> century A.D. The assemblage is relatively small, detailed below, and does not appear to fit into the standard morphologies associated with either iron smithing or smelting. From the original report (Taylor *et al.* 2003), some of the assemblage namely the small plates of slag and smooth droplets may indicate the process of bloom smithing.

| <b>Context no.</b>             | <b>Description</b>   |
|--------------------------------|--|
| 024, fill of post-hole 023     | 13 tap slag, 158g  |
| 036, fill of gully 038         | 1 hearth bottom, 21g   |
| 267, fill of ditch 257         | 1 smithing slag, 6g  |
| 273, fill of ditch 237         | 1 fuel ash slag, 4g<br>1 ?tap slag, hearth lining on base, 25g<br>1 slag, 2g |
| 291, fill of ditch 257         | 1 hearth bottom, 238g<br>1 smithing slag, 6g                                 |
| 300, fill of ditch 327         | 7 smithing slag, 33g   |
| 333, fill of pit 334           | 1 smithing slag, 10g   |
| 335, fill of pit 336           | 1 vitrified clay, 2g<br>2 tap slag, 52g<br>3 smithing slag, 22g              |
| 339, fill of pit 340           | 1 vitrified hearth lining, ?tuyere, 63g                                      |
| 411, fill of ditch 237         | 1 tap slag, 4g<br>1 hearth bottom, 184g<br>1 smithing slag, 7g               |
| 423, fill of ditch 424         | 1 smithing slag, 41g   |
| 500, fill of ditch 483         | 1 hearth bottom, 41g   |
| 571, fill of ditch 572         | 1 tap slag, 54g  |
| 577, fill of plough groove 578 | 1 tap slag, 37g  |
| 713, soil mound                | 7 tap slag, 433g   |
| 834, fill of ditch 835         | 1 hearth bottom, 84g   |
| 904, fill of ditch 884         | 1 smithing slag, 4g  |
| 1021, fill of 1022             | 1 smithing slag, 2g  |
| 1050, fill of ditch 1051       | 1 smithing slag, 8g  |
| 1120, gully                    | 1 hearth bottom, 26g   |
| 1164, fill of pit 1149         | 1 tap slag, 103g   |
| 1165, fill of 1166             | 1 ?tap slag, 9g  |
| 1168, fill of pit 1247         | 1 ?hearth bottom, 107g   |
| 1169, fill of pit 1170         | 1 vitrified hearth lining, ?tuyere, 107g                                     |
| 1228, fill of gully 1216       | 1 tap slag, 60g  |
| 1272, fill of gully 1216       | 1 smithing slag, 7g  |
| 1389, fill of post-hole 1388   | 15 slag, 36g   |
| 1393, fill of post-hole 1392   | 2 smithing slag, 20g   |
| 1400, subsoil                  | 2 smithing slag, 9g<br>1 vitrified hearth lining, 5g                         |

*Table 1.3.2 showing the quantity of ironworking evidence recovered from Quarrington (Taylor et al. 2003: 257).*

| <b>Material</b>      | <b>VHL</b> | <b>Smithing<br/>hearth<br/>bottoms</b> | <b>Smithing<br/>slags</b> | <b>Tap<br/>slag</b> | <b>Fuel<br/>Ash<br/>slag</b> | <b>Non-<br/>diagnostic</b> |      |
|----------------------|------------|--|---------------------------|---------------------|------------------------------|----------------------------|------|
| Total<br>mass<br>(g) | 177        | 701                                    | 169                       | 935                 | 4                            | 66                         | 2052 |

*Table 1.3.3 Showing total combined masses of ironworking debris recovered from Quarrington.*

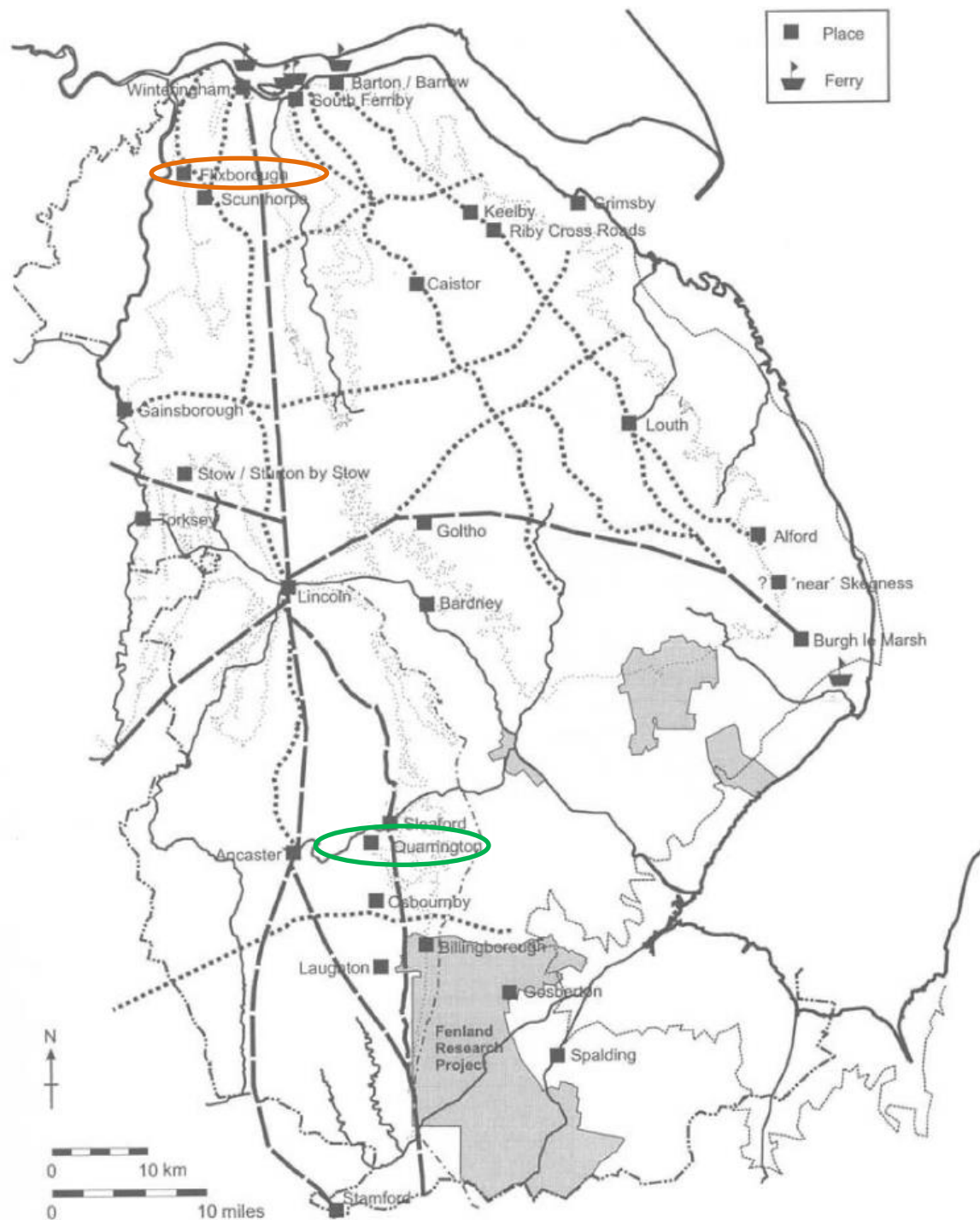


Figure 1.3.6 Showing the locations of Quarrington and Flixborough (circled in green and orange respectively) in Lincolnshire (after Ulmschneider 2000: Fig 2).

### Flixborough

This site, ranging from Early-Late Saxon in date, represents several different phases of activity, with different levels of ironworking intensity. Little evidence of smelting is found in the earlier phases of occupation, with iron smelting becoming more apparent in the record in the ninth century along with high status craft activities represented by window glass and large quantities refuse associated with the

working of copper alloys. In the 10<sup>th</sup> century, much of this high status craft appears to cease, with a marked increase in the production of iron. This is reflected by the large quantities of slag that are dated to this time, including slag blocks, furnace bottoms and tap/flow slag. The site also has access to both bedded and bog iron ores which were both found in during excavation in states suitable for smelting.

This remains contentious within the academic community as it is rare for sites to yield evidence for the exploitation of both major ore types, let alone the use of both for the production of metal.

|                                     | Mass by phase (g) |    |     |      |      |      |     |      |          |       |         |       |
|-------------------------------------|-------------------|----|-----|------|------|------|-----|------|----------|-------|---------|-------|
| Debris Type                         | 1                 | 2  | 2/3 | 3    | 3/4  | 4    | 4/5 | 5    | 5/6      | 6     | unknown | total |
| SMITHING                            |                   |    |     |      |      |      |     |      |          |       |         |       |
| smithing<br>hearth<br>bottoms       |                   |    |     | 1500 | 1310 |      |     | 1300 | 280      | 4250  | 15723   | 24363 |
| Flake<br>hammerscale                |                   |    |     |      |      |      |     |      |          |       | nq      | nq    |
|                                     |                   |    |     |      |      |      |     |      |          |       |         |       |
| SMELTING                            |                   |    |     |      |      |      |     |      |          |       |         |       |
| Tap slag                            |                   |    |     |      |      |      |     |      |          | 1390  | 6015    | 7405  |
| Furnace<br>bottoms                  |                   |    |     |      |      |      |     |      |          | 2220  | 17630   | 19850 |
| Furnace slag                        |                   |    |     |      |      |      |     |      |          | 100   | 7190    | 7290  |
| Slag blocks                         |                   |    |     |      |      |      |     |      |          | 7000  | 4670    | 11670 |
| Possible ore                        |                   |    |     | 662  | 50   |      |     |      | 15       | 400   | 2404    | 3531  |
|                                     |                   |    |     |      |      |      |     |      |          |       |         |       |
| NON-<br>DIAGNOSTI<br>C              |                   |    |     |      |      |      |     |      |          |       |         |       |
| Dense slag                          |                   |    |     | 300  | 440  |      |     |      | 220      | 2101  | 7165    | 10226 |
| Fayalitic runs                      |                   |    |     | 80   |      |      |     |      |          | 175   | 1485    | 1740  |
| Undiagnostic<br>ironworking<br>slag |                   | 60 | 270 | 40   | 1765 | 1775 |     |      | 473<br>0 | 14748 | 38937   | 62325 |
| cinder                              |                   |    |     |      | 226  |      |     |      | 696      | 1235  | 3380    | 5537  |
| Iron-rich<br>cinder                 |                   |    |     |      | 360  |      |     |      | 25       | 165   | 1976    | 2526  |
| Glassy slag                         |                   |    |     |      |      |      |     |      |          | 70    | 650     | 720   |

| Debris Type                         | Mass by phase (g) |            |           |             |             |   |           |             |     |              |               |               |
|-------------------------------------|-------------------|------------|-----------|-------------|-------------|---|-----------|-------------|-----|--------------|---------------|---------------|
|                                     | 1                 | 2          | 2/3       | 3           | 3/4         | 4 | 4/5       | 5           | 5/6 | 6            | unknown       | total         |
| Vitrified hearth/<br>furnace lining | 110               |            |           | 115         | 100         |   | 20        | 245         |     | 1658         | 4146          | 6386          |
| Unexamined<br>topsoil/<br>unstrat   |                   |            |           |             |             |   |           |             |     |              | 8200          | 8200          |
| Misc.                               |                   |            |           |             |             |   |           |             |     |              |               |               |
| clinker                             |                   |            |           |             |             |   |           |             |     | 5            | 5             | 10            |
| Coal                                |                   |            |           |             |             |   |           |             |     | 10           |               | 10            |
| Ferruginous<br>concretion           |                   |            |           |             |             |   |           |             |     | 440          | 975           | 1415          |
| Fired<br>clay/daub                  |                   |            |           | 55          | 25          |   | 15        | 215         |     | 228          | 854           | 1392          |
| Fuel ash slag/<br>cake              |                   |            |           | 44          | 215         |   |           | 65          |     | 108          | 627           | 1059          |
| Iron objects                        |                   |            |           | 135         | 150         |   |           | 185         |     | 515          | 2227          | 3212          |
| Copper alloy,<br>mould,<br>crucible |                   |            |           |             | nq          |   |           | nq          |     |              | 63            | 63            |
| Bone, stone,<br>quern,<br>charcoal  |                   |            |           | 48          | 80          |   |           | 65          |     | 193          | 872           | 1258          |
| <b>Total</b>                        | <b>170</b>        | <b>270</b> | <b>40</b> | <b>5290</b> | <b>4145</b> |   | <b>35</b> | <b>7761</b> |     | <b>37003</b> | <b>125194</b> | <b>180188</b> |
| nq= not<br>quantified               |                   |            |           |             |             |   |           |             |     |              |               |               |

Table 1.3.4 showing quantity of ironworking debris found at Flixborough.

| Material          | VHL  | Smithing<br>hearth<br>bottoms | Tap<br>slag | Furnace<br>bottoms | Furnace<br>slags | Slag<br>blocks | Possible<br>ore | Non-<br>diagnostic |
|-------------------|------|-------------------------------|-------------|--------------------|------------------|----------------|-----------------|--------------------|
| Total<br>mass (g) | 6386 | 24363                         | 7405        | 19850              | 7290             | 11670          | 3531            | 83074              |

Table 1.3.5 showing summary total quantity data of Flixborough assemblage.

## 1.4 Initial sample strategy

In order to record and obtain the maximum quantity of data from the material a suite of slags from each site will be selected. These will include diagnostic smelting evidence, such as tap/flow slags, furnace slags, high density slag, and furnace bottoms if present.

The selection of slags will be based upon morphology, density and colour. These will allow for a sample of likely smelting slags to be identified as the colour of the slag will generally be darker if it has originated from smelting due to greater iron content. A total of 30 to 40 samples per site where possible will be required in order to form a meaningful data set.

Each sample needs to be thick enough to allow for grinding and polishing so that it is suitable for metallographic and electron microscopy. For this reason, the samples must be at least 0.5cm thick,

although thicker samples (approximately 1cm) will allow future researchers to study the material at later dates without needing to re-sample the original material.

The cutting of samples can be taken either by the use of hammer and chisel, or, if the piece of slag is very small or thick to begin with, a diamond cutting wheel. This will ensure that the majority of the original pieces are preserved. Cutting on a diamond wheel will also produce a much flatter surface, reducing the time required for the grinding stage of sample preparation.

The samples will then be mounted in standard 2.5cm diameter blocks, using epo-thin resin mixed to a ratio of ten parts resin to four parts hardener. Each sample will be mounted individually, as the typical size of slag samples is too large to allow for multiple samples per block. The resin takes approximately eight hours to cure.

The cured resin blocks will then undergo grinding and polishing prior to analysis. This will be carried out on a Buehler rotary grinding and polishing machine in steps of 600, 1200 and 2500p grinding paper. The polishing phase will use 6µm, 1µm and final polishing.

### **1.5 Analytical process**

The samples will then be observed and recorded on an Olympus BX-51 metallographic microscope so that areas of interest can be identified and targeted for electron microprobe analysis (EMPA). Once this is done, the blocks will be coated in carbon and analysed by EMPA with an accelerating voltage of 25keV and a spot size of 1µm. Five analyses will be carried out per major phase present, to generate a mean average composition, ensuring the maximum quantity and quality of data possible.

The average compositional data will then be used to plot XY scatter graphs of FeO:SiO<sub>2</sub> against P<sub>2</sub>O<sub>5</sub>, so that the different mineral phases can be plotted per site and a reflection of the phosphorus content can be taken into account. This will not only allow for the probable ore type to be identified by phosphorus content, but also further clarify the behaviour of phosphorus as it appears to exhibit both lithophilic and siderophilic behaviour. If ores from the sites are also available, the compositional data from these will be plotted on the same graphs to aid determining the effect the smelting operation had on the phosphorus content by comparing the ore to products.

This may be particularly enlightening in the case of Flixborough which is known to have both high phosphorus bog ore and roasted Frodingham ironstone on site. As the phosphorus content of these two materials is significantly different, it would be expected that slags produced from these ores would contain drastically different quantities of phosphorus. If the Flixborough data plots into two definable

groups, then it may provide further evidence for the exploitation of both ore sources by smelters in the 10<sup>th</sup> century at the site.

The plots from the other sites will strengthen the argument based upon their appearance, as the technology in use at many of them appears to have undergone relatively little change over the period from the seventh to tenth centuries, with the exception of the production of large slag blocks. These are a result of the method of slag removal, which was either tapped from the furnace into an adjacent pit or collected in a pit at the base of the shaft. In cases where there are no slag blocks, it can be assumed with relative safety that the slag was tapped conventionally in a manner similar to preceding Roman methods.



# Chapter 2

## Phosphoric Iron in the literature

|            |   |           |
|------------|---|-----------|
| <b>2.1</b> | <b>Ferrous materials</b>  | <b>18</b> |
| <b>2.2</b> | <b>Phosphoric iron as a material</b>  | <b>20</b> |
| <b>2.3</b> | <b>Provenance studies</b>   | <b>38</b> |
| <b>2.4</b> | <b>Artefact studies</b>   | <b>41</b> |
| <b>2.5</b> | <b>Iron Smelting</b>  | <b>46</b> |
| <b>2.6</b> | <b>Towards a Chaîne Opératoire</b>  | <b>48</b> |
| <b>2.7</b> | <b>Iconographic and<br/>Archaeological representation<br/>of specialist ironworkers</b> | <b>60</b> |
| <b>2.8</b> | <b>The occurrence of ironworking<br/>and the Utmark/Innmark</b>                         | <b>68</b> |

This chapter outlines the previous work carried out upon phosphoric iron. The initial section (2.1) discusses the various metallic materials which fall into the domain of ferrous metallurgy and defines what is meant by phosphoric iron. Section 2.2 covers phosphoric iron in detail, describing the defining features and the parameters which govern the creation of the alloy. This includes examining the redox conditions required for the successful production of iron, illustrated with an Ellingham diagram. Other engineering parameters, including the chemistry of slag and the presence of phosphorus in the ore are covered along with the extent to which they can be controlled. The chapter then moves on to examine the major field of research in ferrous metallurgy, that of provenance (section 2.3), with the aim of demonstrating that the study of iron alloy production has been less favoured than the pioneering investigation of provenance in recent years. Following from the discussion of the various methods of identifying the provenance of archaeological iron, the use of phosphoric iron is examined through artefact studies (section 2.4). The topic of iron smelting and the remains generated by the activity are described (section 2.5). Particular aspects, such as the difference between Roman and non-Roman technology are discussed, as these may have an impact upon the products produced, as well as the difference in culture which is reflected in the technological choice of furnace design. The stages of smelting are discussed in the next section (2.6), covering the decisions made at each stage. Section 2.7 examines the representation of ironworkers and identifies the lack of smelting representation. Section 2.8 attempts to explain why this might be the case.

## 2.1 Ferrous materials

The identification of metallic materials within the archaeological record is one which has generated a large body of research since the beginning of metallurgical investigation within the discipline of archaeology. Certainly the characterisation of different metals and alloys in terms of their properties has yielded much insight into the metal economies which existed within past societies. Many examples of focused study can be found within the examination of copper alloys, such as the origin of tin for tin-bronze production in the Near and Middle East where it is rare (Weeks 1999), or the identification of possible ancient copper trade routes (Weeks *et al.* 2009)

While the majority of site reports use the term iron objects to describe unidentified artefacts produced from iron and its alloys, there is a body of evidence which not only suggests, but demonstrates, that a more correct term would be ferrous objects (Scott 1991; McDonell 1989; Ottaway 1987; Ottaway 1992). It is well attested that ferrous metallurgy encompasses the examination of several different materials, which can exhibit multiple phases, each of which is distinct (Scott 1991; McDonell 1989; Ottaway 1987; Ottaway 1992). There are three main types of ferrous material which are present within the archaeological record prior to the adoption of blast furnace technology: these are ferritic iron, carbon steels and phosphoric iron. Of these only ferritic iron can be called “iron” as it contains no detectable alloying elements. Carbon steels regularly contain between 0.1-0.8% C, which may comprise of multiple phases of  $\alpha$  ferrite, pearlite and cementite which may exist as a result of varying carbon content. Multiple different features may be present if the artefact underwent heat treatment or cold working during manufacture or repair; ranging from different Fe-C phases such as Martensite to Lower Bainite resulting from heat treatment (Scott 1991), and elongated grains and Neuman bands with respect to cold working, along with the phases previously described as present within carbon steels (Keipura and Sanders 1985; Scott 1991).

Phosphoric iron is an alloy of iron and phosphorus which is distinct from the other ferrous materials of ferritic (clean) iron and carbon steel. There are several material properties that the presence of phosphorus bestows upon iron which make it distinct in behaviour and appearance. Phosphoric iron has mostly been defined iron with a minimum phosphorus content of 0.1% (Vega *et al.* 2003; Godfrey 2007). There is also another state in which iron may exist when produced by bloomery smelting; that of heterogeneous iron. This material contains a natural mixture of ferritic, phosphoric and carburised iron.

This brief description demonstrates that the use of “iron object” is not only insufficient, but most likely also completely inaccurate when describing a ferrous artefact. Just as with copper alloys, each of the ferrous materials must be the result of a specific chaîne opératoire for its successful creation.

Steels may be produced by the secondary addition of carbon to ferritic iron by carburisation. This

process involves the packing of a ferritic iron bar in a sealed container with charcoal, where it is held at an elevated temperature for several hours to allow carbon to diffuse into the metal in the solid state. This results in a carbon gradient with the greatest carbon content being towards the exterior surface of the bar, which gives this process the name of case hardening. The surface of the bar was known to blister due to partial oxidation, resulting in the product also being named blister steel. In some cases carburisation is undertaken in crucibles, producing the aptly named product - crucible steel (Craddock 1998; David and Le Bl  is 1988; Srinivasan and Ranganathan 2004: 37) . The surface of crucible steels are recorded as having a crystalline appearance, particularly when etched (Srinivasan and Ranganathan 2004: 45, 82). In a manner similar to the presumed assessment of copper alloys by colour, the crystalline surface appearance of crucible steel was observed to estimate the carbon content of the alloy (Srinivasan and Ranganathan 2004: 84). Variations in the quality of high carbon steel may be attributed to small quantities of impurities within the iron, such as phosphorus, preventing the absorption of carbon.

As both ferritic iron and carbon steel can be produced unintentionally, deliberately but in an uncontrolled process, or in a deliberate and controlled manner, it stands to reason that the same may be true of phosphoric iron. The nature of the Fe-P alloy, which can be difficult to distinguish from large grained ferrite, has led to a debate as to whether phosphoric iron is a genuine material. Researchers such as McDonnell (1989), Blakelock and McDonnell (2007; 2011) and Robinson (2010) have argued that the material is a separate entity, distinct from the others, due to the very different material properties it possesses. Previously it was not thought of as a distinct substance, but rather as an impure form of ferrite, which exists due to poor control of the smelting conditions on the part of the iron smelter. This view appears to have fallen out of favour with the majority of researchers as phosphoric iron has become more regularly identified and recognised within the archaeological record, as indicated by its inclusion within national ferrous metallurgy guidelines (Paynter 2011).

The existence of phosphorus-bearing iron is not in question. Examples have been recovered from multiple sites across the globe for example in Britain (Ottaway 1992), South Africa (Miller and Van Der Merwe 1994) and India (Balasubramaniam and Kumar 2003). Each location has provided evidence for the use of these materials in specific manners. The South African examples were the only surviving ferrous artefacts from KwaGandaganda to yield any material suitable for metallographic analysis (Miller and Whitelaw 1994: 81-82). This survival in the archaeological record relates to the unique material properties of phosphoric iron, which will now be discussed in order to demonstrate how it differs from the other known ferrous materials which were available to bloomery smelting cultures.

## **2.2 Phosphoric Iron as a material**

As previously stated, phosphoric iron is defined by several characteristic features which set it apart from ferritic iron and carbon steel. The presence of phosphorus results in the multiple differences listed below which are distinct from the effects of the presence of carbon.

The distinct properties and features of phosphoric iron are:

Brighter colour

Large grain size

Increased hardness

Corrosion resistance

Resistance to carburisation

Ghosting

### **Colour**

Firstly the colour of the material is noticeable brighter than both ferritic iron and carbon steel (Thompson 2004). This is a feature which is seen most strikingly in pattern welding. Colour is an aspect of material science which is generally ignored within ferrous metallurgy. This may be due to the inability to observe such a difference in the majority of artefacts after conservation. The artefacts exhibit a rust coloured exterior due to oxidation and hydration experienced during burial within its archaeological context.

The difference in colour is most noticeable in the etch condition during metallographic analysis. In this case the phosphoric material appears significantly brighter than the other ferrous materials due to the lack of carbon content and corrosion resistance.

### **Large grain size**

Phosphoric iron typically exhibits a larger grain size, usually in the order of sizes 3-1 or larger when viewed through an ASTM iron grain size reticule, as compared to ferritic iron (Scott 1991). When a Fe-P alloy is raised to a temperature of 911°C the ferrite transforms into austenite (Kubaschewski 1982), in which both phosphorus and carbon have greater solubility.

### Brittleness, hardness and ductility

Mechanically, phosphorus causes intergranular brittleness, or cold shortness, when in the presence of carbon. This is why Stead refers to the element as ‘treacherous’ to the production of good quality metal (Stead 1918: 309). Phosphorus does however, increase the ductility of iron when minimal carbon is present, allowing phosphoric iron to be drawn into very thin wires which were used for harpsichord strings in the 17<sup>th</sup> century (Goodway 1987).

Phosphorus is also responsible for an increase in hardness, when compared to that of ferritic iron (Stewart *et al.* 2000a: 281). Micro-hardness testing has become part of the standard procedure for metallographic interpretation, regarding ferrous artefacts. This is due to the etch resistance exhibited by phosphoric iron (McDonnell 1992) and the possibility of misinterpretation when compared optically with large grained ferrite. Hardness values between 100-200Hv are regularly recorded for phosphoric iron; this compares to the lower values of 80-100Hv for ferritic iron (Stewart *et al.* 2000a: 278; Hall 2012). The elevated hardness of phosphoric iron, in combination with the other distinguishing features of etch resistance, large grain size and possible ghosting, ensure that the material is correctly identified.

| HV  | P (wt%) | HV  | P (wt%) | HV  | P (wt%) | HV  | P (wt%) |
|-----|---------|-----|---------|-----|---------|-----|---------|
| 140 | 0.25    | 185 | 0.63    | 230 | 1.00    | 275 | 1.38    |
| 145 | 0.29    | 190 | 0.67    | 235 | 1.04    | 280 | 1.42    |
| 150 | 0.33    | 195 | 0.71    | 240 | 1.08    | 285 | 1.46    |
| 155 | 0.37    | 200 | 0.75    | 245 | 1.13    | 290 | 1.50    |
| 160 | 0.42    | 205 | 0.79    | 250 | 1.17    | 295 | 1.54    |
| 165 | 0.46    | 210 | 0.83    | 255 | 1.21    | 300 | 1.59    |
| 170 | 0.50    | 215 | 0.88    | 260 | 1.25    | 305 | 1.63    |
| 175 | 0.54    | 220 | 0.92    | 265 | 1.29    | 310 | 1.67    |
| 180 | 0.58    | 225 | 0.96    | 270 | 1.33    | 315 | 1.71    |

Table 2.2.1 showing weight percent Phosphorus content and associated Vickers hardness (Hv) (Theil and Hošek 2015: Table 2).

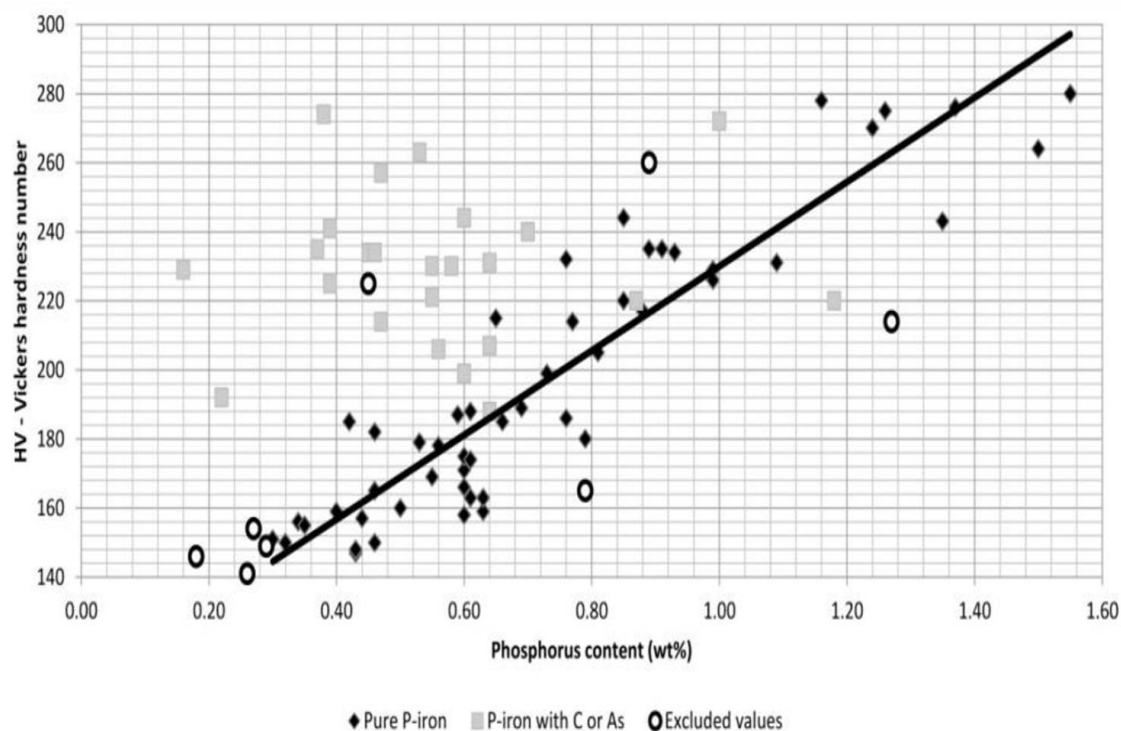


Figure 2.2.1 Showing hardness (Hv) against phosphorus content (wt%) for pure Fe-P alloys and ternary Fe-P-C and Fe-P-As alloys (Theil and Hošek 2015: Figure 5)

The presence of phosphorus is responsible for an increase in hardness when compared to ferritic iron. However, the phosphorus content is not homogeneous across the entirety of a given sample. The uniformity of phosphorus distribution was examined by Piccardo *et al.* (2004) using tint etching with Klemm's reagent. This study demonstrated that phosphorus content can be highly variable within a single material sample (Piccardo *et al.* 2004), which agrees with the variability in hardness test data obtained during experimental investigation of archaeological material (Hall 2012). Without the use of phosphorus detection methods during metallographic analysis, these large, pale grains may be interpreted as large grained ferrite. While the use of tint etching by Piccardo *et al.* (2004) demonstrates the heterogeneous distribution of phosphorus within artefacts, this method should not be utilised as a standalone assessment method of phosphorus content. The interpretation of the colour tint is subjective and can lead to different interpretations based upon the skill of the analyst.

Phosphorus can be segregated at prior austenite grain boundaries as part of an intermetallic ( $\text{Fe}_3\text{P}$ ) which is responsible for the majority of the observed brittleness of phosphoric iron. This segregation is also stimulated by the presence of carbon (Militzer and Weiting 1989: 2592), which contributes to the effects previously observed by Stead (Stead 1918).

A metallographic sample examined by Tylecote from West Runton, Norfolk demonstrated the presence of phosphorus with elevated hardness, between 210-223 HV, very large grains and weak

grain boundaries (Tylecote 1968: 83). Chemical analysis revealed that the phosphorus content of the iron was 1.34%. This is at the upper limit of phosphorus content for most archaeological iron (McDonnell 1989).

Nodular iron ores and iron pan were also found at the site, although the quantity of each is not specified (Tylecote 1968: 83). When analysed they contained 1.32% and 2.79%  $P_2O_5$  respectively (Tylecote 1968:83). Tylecote uses this to question the phosphorus content observed in the metal. Where he states an assumed average phosphorus content in the charge to be about 2% producing a phosphoric iron of approximately 0.5% P (Tylecote 1968: 83). Given the hardness of the artefacts the expected P content would be around 1%, resulting from the ore containing 4%  $P_2O_5$  (Tylecote 1968: 83).

### **Corrosion resistance**

Another property that the presence of phosphorus bestowed on iron is that of corrosion resistance (McDonnell 1992) . Studies carried out upon Indian phosphoric iron, most notably the Delhi and Dhar iron pillars, have demonstrated that Fe-P alloys are more resistant than other ferrous materials to atmospheric corrosion (Balasubramaniam and Kumar 2003: 2463-2464) . Studies on the corrosion products found that weathered Fe-P alloys produce a hydrated iron phosphate which prevents further corrosion of the iron within the artefact. Similar effects were observed when samples of ferritic iron, carbon steel and phosphoric iron were left to corrode in a context of known conditions (Fell 2005: 4) . This suggests that Fe-P alloys are more resistant to corrosion within the context, but, as the study was conducted over a period of 18 months, the time span does not accurately represent archaeological time. Thus any conclusions of the stability of phosphoric iron over extended periods of burial must be carefully drawn. It may be possible that the alloy is more resistant to corrosion over extended durations, which may partially explain why many artefacts found in regions where iron preservation is poor have been found to be made of phosphoric material.

While Fell (2005) and Balasubramaniam and Kumar (2003) identified that phosphoric iron has the potential for better survival over archaeological time than other ferrous materials, the susceptibility of common archaeological Fe-C alloys to further corrosion after excavation has only been examined lately. Recently further study of archaeological iron corrosion products has been undertaken using energy backscatter detection (EBSD) in conjunction with SEM analysis (Azoulay *et al.* 2013). The material studied comprised of 2 archaeological nails, one dating to the Gallo-Roman period, excavated at Angoulins, Charente-Maritime, France, and one dating to the 16th century, excavated near Glinet, Seine-Maritime, France (Azoulay *et al.* 2013: 380). Both of these artefacts were predominantly comprised of hypo-eutectoid steels (0.1-0.7%C) (Azoulay *et al.* 2013: 3798). The samples were polished to a 0.25 $\mu$ m finish, using hexane rather than water, before a final polish of

colloidal silica solution (Azoulay *et al.* 2013: 380). The use of hexane rather than water was a decision based upon the susceptibility of some of the known and possibly present corrosion products to further oxidation by contact with water. The authors hoped to prevent any further corrosion or alteration of the materials present by excluding available oxygen at all stages. Between major corrosion layers, a small quantity of magnetite was observed in both artefacts. This combined with the extensive corrosion of the central material in artefact AN0702 (Azoulay *et al.* 2013: 385), dating to the Gallo-Roman period, demonstrates that artefacts recovered from sites where the soil water content is relatively high will experience significant corrosion and loss of metallic material, while maintaining magnetic properties. The interpretation of heavily corroded ferrous knives by Hall (2012), regarding the possible corrosion products and hence the difficulty of obtaining artefacts suitable for metallographic analysis based upon magnetism, provides further evidence that ferrous artefacts should be analysed as close to the time of excavation and be exposed to as little water as possible to increase the likelihood of the remaining metallic material surviving.

The application of EDS mapping convincingly demonstrated that the identification of different phases was reliable, although the successful characterisation of Chukanovite proved problematic (Azoulay *et al.* 2013: 387). The authors tested regions of this material with multiple acceleration voltages and attempted to use Raman spectroscopy with a range of attenuations from 90-0% (Azoulay *et al.* 2013: 387). Based upon these successive examination conditions, the authors concluded that Chukanovite is highly susceptible to alterations based upon electron beam interaction and thermal degradation (Azoulay *et al.* 2013: 387). This successful study proves that corrosion products can be discriminated, although the full mechanics and understanding of the long term behaviour of ferrous artefacts has yet to be fully understood as other materials, such as phosphoric iron, were not examined as part of the study.

### **Resistance to carburisation**

One of the most significant properties that phosphoric iron possesses is its inhibitive behaviour towards carbon diffusion. It has been observed experimentally that Fe-P alloys can be carburised with limited success (Hall 2008). The cause of the limited carburisation was postulated to be a result of a reduction of the available interstitial space into which carbon atoms could diffuse due to the substitution that phosphorus and iron undergo during alloying (Hall 2008). Within the archaeological record, phosphoric iron contains very little carbon unlike modern ferrous alloys. It would appear that the ability, and possibly knowledge, to manufacture this alloy was lost once blast furnace technology was adopted as the primary means of iron smelting. As phosphoric iron is resistant to carburisation, the alloy was extensively used within pattern welding alongside carbon steels; ensuring that the produced pattern was not lost during subsequent forging of the artefact by secondary carburisation from the charcoal fuel.



The presence of phosphorus also prevents the absorption of carbon (Hall 2008), which is responsible for the formation of pearlite upon cooling below 727°C in the Fe-C system (Samuels 1980). As carbon is not readily absorbed due to the phosphorus content, the austenite grains can convert directly to a Fe-P solid solution with a possibly non-uniform phosphorus content.

## Ghosting

Ghosting is an effect which, while associated with the presence of phosphorus, may not be present in all cases. It is believed by Godfrey (2007) and Rubinson (2010) that the characteristic “watery” features which appear within grains of phosphoric iron result from the non-uniform phosphorus distribution within the specific grains. Evidence of an increase of phosphorus content where ghosting is present has been obtained instrumentally and metallographically (Rubinson 2010; Hall 2012). Hot working is believed to be the cause of ghosting (Rubinson 2010), as it has not been observed within artefacts exhibiting elongated grains associated with cold working: although the mechanics of ghosting formation are yet to be fully understood. Ghosting is revealed in the etched condition with nital, which is most commonly used to examine for carbon content and artefact manufacture methods (Stewart *et al.* 2000c: 291, 292, 299-301) .

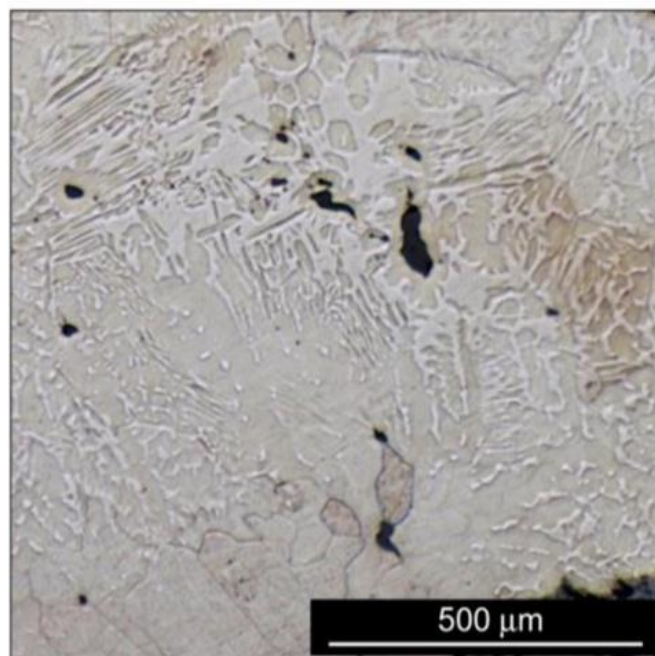


*Figure 2.2.2 showing ghosting in phosphoric iron etched with nital (Theil and Hošek 2015: figure 2).*

Tylecote made a brief note of phosphorus content in the iron found at West Runton in Norfolk (Tylecote 1968: 83). The site was excavated in 1964 and produced no unworked iron. Metallographic

examination of a flattened piece revealed a coarse ferritic structure with evidence of phosphorus coring on half of the artefact and grain boundary carbide in the other half. Well-developed nitride needles were also observed in the artefact within the phosphoric regions, which shows that the metal cooled slowly through a range of 400-200°C. Tylecote also reported that despite this clear evidence of elevated temperature, the artefact displayed no other obvious features related to working (Tylecote 1968: 83). Presumably this relates to elongated grains, rather than strain lines, due to hot worked iron self-annealing.

Tylecote interpreted the metallic finds as pieces struck from blooms and thus representative of the metal being produced at the site. He also suggested that this hard, but brittle metal, would be excellent for nails.

#### Outline of the bloomery process

The bloomery smelting process is the means of producing metallic iron by the direct reduction of iron oxides in the solid state. Within the system roasted iron ore is placed into the furnace operating at approximately 1200°C with an equal or greater quantity of charcoal, and an air blast applied from bellows to provide oxygen, to produce a bloom of solid metallic iron, slag, and waste gases. This is discussed in greater detail in section 2.6.

#### **Engineering parameters**

Lyngstrøm convincingly links high phosphorus ore to phosphoric iron in the case of a single artefact (Lyngstrøm 2011). However, because of the partitioning of phosphorus between metal and slag during smelting (Balasubramaniam and Gouthama 2003: 484; Buchwald 2005: 177), it is difficult to predict the phosphorus contents of smelting products based upon the raw materials used in the smelt (Buchwald 2005: 164). It is also noted that phosphorus content is not solely determined by redox conditions, but also greatly influenced by temperature and slag acidity (Buchwald 2005: 177). Slags with a silica content in excess of 50% rarely host phosphorus at concentrations above 0.2 wt% (Buchwald 2005: 177). This may indicate that phosphoric iron was produced from ores which contained a large proportion of silica rich gangue material, or that silica was intentionally added to the charge in order to produce a more phosphorus rich product. As fayalite, the main iron silicate present in iron slags, has a very limited ability to host phosphorus, an increase in silica in the smelt will result in a slag which has a reduced capacity for phosphorus. This may cause more phosphorus to remain within the metallic product rather than a larger portion partitioning into the slag.

The following Ellingham diagram shown below illustrates the redox conditions required to oxidise and reduce many of the common metal and non-metal elements.



$\text{Fe}_2\text{O}_3$  can be read from the Ellingham diagram as approximately 3/1 and  $1/10^4$  respectively. This demonstrates that a greater proportion of  $\text{CO}/\text{CO}_2$  is required to reduce  $\text{FeO}$  to  $\text{Fe}$  than  $\text{Fe}_2\text{O}_3$  to  $\text{FeO}$ . The ease of reduction is also reflected in the position of the oxidation line on the graph. The higher the line, the more unstable the oxide and the more easily reduced it is. The unusual behaviour of  $\text{CO}$ , in that the line is downward sloping, demonstrates that  $\text{CO}$  is a good reducing agent. Once the  $\text{CO}$  line crosses below that of the oxide of interest then reduction is possible.

Phosphorus is also shown on the graph, with a  $\text{CO}/\text{CO}_2$  value of approximately 1/1 at the average assumed operating temperature of iron smelting of  $1200^\circ\text{C}$ . The oxidation line of  $\text{P}_2\text{O}_5$  is shown above that of  $\text{FeO}$  which indicates that it is more easily reduced. Which, when combined with the high stability of calcium oxide, the lowest line plotted shown in figure 2.2.3, explains why phosphorus and calcium preferentially form calcium phosphate when possible due to substitution of oxygen with available phosphate. This is significant because the formation and preservation of calcium phosphate within the slag can influence the detected phosphorus content. The relationship between the presence of calcium and phosphate is shown during the data discussion in chapter 7.

There is one other aspect of iron slags which is explained within the diagram, the abundance of  $\text{FeO}$  found within bloomery iron slags. This a result not only of the high iron content of the ores being used, but also the partial pressure of  $\text{CO}$  required to successfully fully reduce  $\text{Fe}_2\text{O}_3$  to metallic iron. The significant increase in partial pressure required to fully reduce  $\text{FeO}$  to metallic iron limits the successful reduction of this second stage process when  $\text{Fe}_2\text{O}_3$  is present, which will be reduced first as demonstrated by the position of the line in the Ellingham diagram (Ellingham 1944: 127). There is also the effect of unreacted free oxygen consuming  $\text{CO}$  forming  $\text{CO}_2$ , resulting in a less reducing atmosphere, which further decreases the quantity of reducing agent available. These factors result in a large proportion of the available iron being preserved as  $\text{FeO}$  within the slag, rather than being fully reduced to the desirable metallic state.

### The chemistry of slag

The other major parameter which influences the behaviour of phosphorus is the overall chemistry of the slag in the furnace. Slag is the primary by-product of smelting, which surrounds and is incorporated into the metallic bloom. Current understanding of the formation process indicates that it is formed by the reaction of the iron poor portion of the ore bearing host rock, referred to as gangue, alkali elements within the charcoal and alumina from the furnace walls at high temperature.

As this mixture suggests, iron slags, both smelting and smithing, commonly comprise mostly of iron silicates. In a similar manner to metallic alloys, the materials present within a slag are derived from the overall composition and the rate of cooling it experiences from the temperature of formation.

The study of archaeological iron slags has identified several phases, some of which are characteristic of the reaction conditions. Most commonly, fayalite ( $\text{Fe}_2\text{SiO}_4$ ) is present in smelting slags (Hauptmann 2014: 95). This is the primary iron-silicate which typically forms in distinctive laths, which appear approximately rectangular when observed through a metallographic microscope, the size of which is dependent on cooling rate.

Wüstite, primarily precipitated as dendritic FeO or secondly intergrown with the main fayalite component (Hauptmann 2014: 98), is rarely seen in iron smithing slags. The generation of wüstite requires a fuel to ore ratio on 2:1 or less during the reaction (Tylecote *et al.* 1971). This is very rare during smithing, where the quantity of iron is far outweighed by a large excess of charcoal. The use of sand as a flux during smithing also shifts the quantity of available reactants towards the production of fayalite. The size of wüstite dendrites present in a sample of smelting slag is dependent upon the rate of cooling, the longer the duration of cooling the larger the dendrites become. For this reason, furnace slag which cools within the furnace has larger dendrites of wüstite than slag which has cooled outside the furnace.

The matrix which forms from the material that remains after the formation of fayalite and wüstite, is usually described as glassy. Unlike synthetic glass produced by the reaction of silica with either plant ashes or natron in an oxidising environment, this material is not a true glass. It has a far lower density than the other materials in iron slags, giving it dark appearance during electron microscopy. Compositionally, the matrix contains significantly more silica and alkali than the other phases, with a much smaller quantity of iron which is mostly present in fayalite and wüstite.

Tapped slag is significantly different from furnace slags. It cools far more rapidly having been removed from the furnace, which prevents the development of wüstite dendrites. The low viscosity of the slag results in a flowed, ropey upper surface which can have a maroon through to black colour. The colouration is a result of the surface oxidation, producing  $\text{Fe}_2\text{O}_3$  giving the redder tones, or magnetite ( $\text{Fe}_3\text{O}_4$ ) which is responsible for a black skin on the grey fayalite-rich body.

Other mineral phases, such as Kirschsteinite ( $\text{CaFeSiO}_4$ ) and Anorthite ( $\text{CaAl}_2\text{Si}_2\text{O}_8$ ) may be present depending on the calcium content of the ore in the charge. Anorthite is the most similar material towards which the glassy matrix of bloomery smelting slags will trend.

The rapid cooling experienced by the majority of slags results in the overall composition being highly heterogeneous, with multiple fine grained phases of the above minerals resulting in a complex composition depending upon the bulk chemistry (Hauptmann 2014: 95). For this reason, it may be difficult to acquire a representative bulk chemical analysis and it may be preferable to analyse each phase and other inclusions, such as silica grains and unreacted ore, independently by means of EMPA (Hauptmann: 2014: 97) .

As both smithing and smelting slags share a common mineralogical composition, being dominated by fayalite, the use of chemical and compositional analyses alone is not comprehensive enough to ascertain which process the slag originated from (Hauptmann 2014: 95). This is why a class of non-diagnostic slag, identified as dense ironworking slag, is typically incorporated into site evaluation reports. This allows for the identification of slag which may originate from either process, based upon macroscopic appearance, but may indicate smelting due to density (Starley 1999: 7).

Hauptmann also argues that the concentration of slag compositions does not reflect the skill of smelters, but rather that it is restricted by the operating temperature and the technology available (Hauptmann 2014: 99-100).

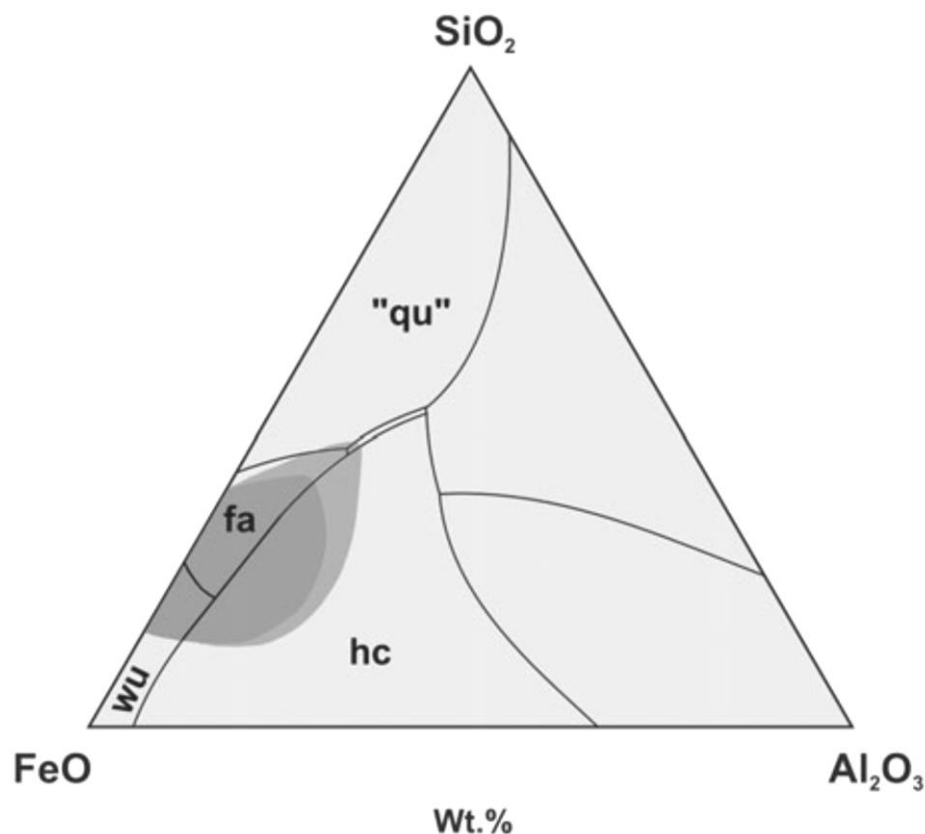


*Figure 2.2.4 Showing the range of archaeological slag composition (Iron slags dark grey, copper slags mid-grey) in the ternary system  $\text{FeO-Al}_2\text{O}_3\text{-SiO}_2$  around the eutectic of Fayalite (Fa) region (Hauptmann 2014: 101).*

The narrow composition range is limited by the temperature at which iron-rich silicate will melt. This has been one of the major defining conditions upon which many iron smelting experiments have been based. A simplified  $\text{FeO}\cdot\text{Fe}_2\text{O}_3\text{-SiO}_2$  binary diagram clearly illustrates that a narrow compositional range, approximating to the composition of fayalite (Figure 2.2.5), will melt at a temperature of  $1200^\circ\text{C}$ .

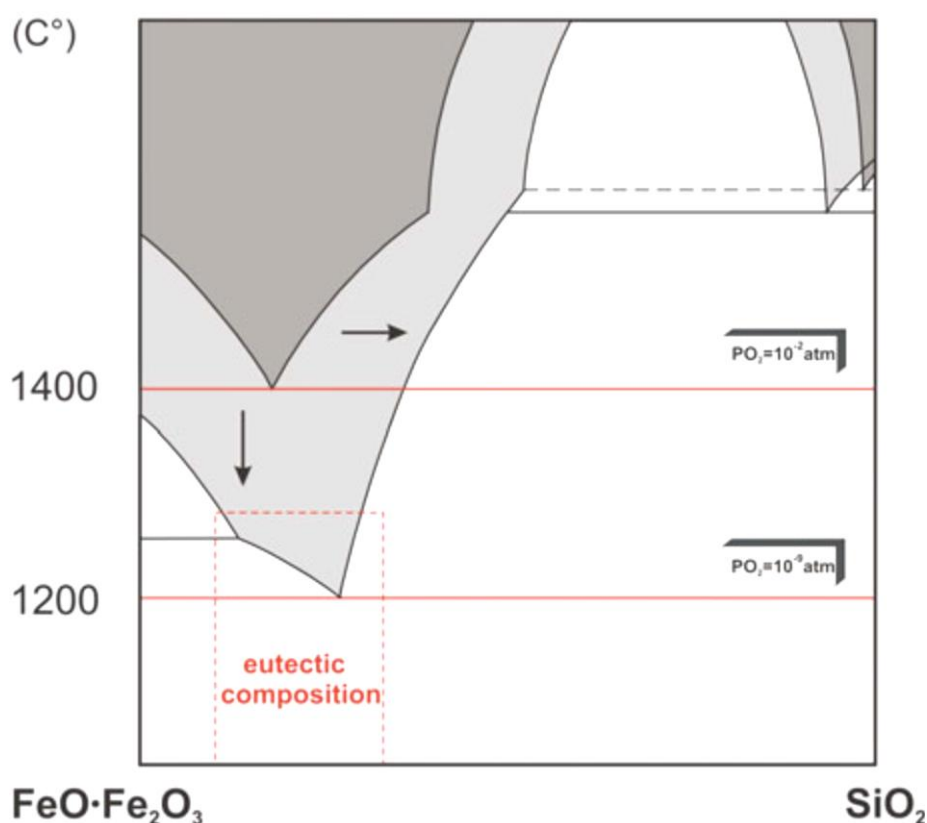


Figure 2.2.5 Showing the binary  $\text{FeO}\cdot\text{Fe}_2\text{O}_3$ – $\text{SiO}_2$  diagram with a significant increase in melting temperature if either an increased quantity of  $\text{SiO}_2$  or iron oxide is present (Hauptmann 2014: 101).

Hauptmann (2007, 2014: 100) goes further to suggest that the presumed limited control of the reaction conditions exercisable by ancient smelters would prevent, or at the very least limit, the production of a regular, standardised product. This view would support the interpretation that the production of different ferrous materials is governed entirely by the raw materials that were used in the charge (Hauptmann 2014: 100), with technology and skill having little to no impact.

However, if this is the case then it would further suggest that skilled smiths were not only capable of a highly sophisticated level of craftsmanship, but also possessed the ability to deliberately select materials from different sources to satisfy their requirements. If smelters could not produce a regular product, this scenario would result in highly fluctuating trade as their product would be extremely variable. This would mean that different blooms could possess very different properties even if they were made from the same raw materials.

To this end it is more likely that, while archaeological slags are concentrated within a specific range of composition, the blooms produced were probably heterogeneous in composition as Hauptmann suggests. This is supported by the multiple experimental smelts conducted by Crew (1991, 2013) and

others (Salter and Crew 1997) who have produced metallic products with multiple phases and variable phosphorus content.

### **To what extent can these parameters be controlled?**

The manufacture of pure iron is one which, certainly within early iron smelting, was dependent upon a relatively clean ore from which to smelt the metal. This can be attested by the production of clean, malleable iron by Catalanian smelters, who were known to use a high purity haematite (Estanislau 1999). By exploiting an ore with a greater phosphorus content, most commonly bog ores, this incorporates a greater proportion of phosphorus in the smelting charge.

The phosphorus found within smelted iron is understood to have originated from the ore that was used. High phosphorus ores originating from lake or bog deposits are most commonly cited as the likely material for Fe-P alloy production (Piaskowski 1989; Vallbona 1997; Godfrey 2007). Several studies have examined iron smelting conditions with the view of identifying the most favourable conditions for the production of clean iron (Cleere 1971; Friede *et al.* 1984; Le Coze 2000; Saunder and Williams 2002). Unfortunately the production of Fe-P alloys has not received the same attention, with the few experimental studies being undertaken predominantly in laboratory conditions. Kumar and Balasubramaniam (2002) attempted to explain the origin of the phosphorus found in ancient Indian phosphoric iron which exhibits a notably high phosphorus content. The researchers examined multiple thermodynamic models for the partition of phosphorus between the metallic and slag portions of a smelt and argued that all of the different conditions studied would produce a similar alloy (Kumar and Balasubramaniam 2002: 10-11). They proposed the reason for the similarity of phosphorus content was due to a lack of lime in the charge. While this may explain the phosphorus content, lime being a common additive in modern smelting to remove phosphorus, it does not identify the origin of the phosphorus. Thus this study has failed to answer the question suggested within the title of the paper – ‘On the origin of high phosphorus content in ancient Indian iron’. It does not identify if a particular ore was deliberately exploited in order to generate a high phosphorus Fe-P material, or if the charge was enriched with a phosphorus bearing agent which may have supplemented the phosphorus provided by a lower phosphorus ore.

The control of redox conditions is determined partially by the quantity of charcoal in the charge, and also by the blast rate which provides the available oxygen. A greater blast will provide a greater proportion of oxygen, which will result in a less reducing atmosphere if the proportion of charcoal is not maintained during the smelt. The increase in temperature as a result of a greater supply of oxygen results in a faster rate of reaction, this causes the charcoal in the charge to burn down faster and the ore to react more readily. Modern experiments using mechanical bellows tend to have a greater O<sub>2</sub> supply (Crew 2013), which results in a greater quantity of CO being produced with a faster rate of



reaction, which will cause a greater recovery of iron to be achieved so less FeO will be present in the slag. Manual bellows do not provide a constant blast, and so give rise to variable and inevitably less reducing conditions, which would explain why archaeological slags contain a far greater quantity of FeO due to incomplete reduction of  $\text{Fe}_2\text{O}_3$ .

The only method available to past bloomery smelters for controlling redox conditions was to observe the colour of the flame at the top of the furnace and, based upon their experience, add charcoal or moderate the blast accordingly. Without the modern understanding of reducing conditions afforded by the above Ellingham diagram, and the use of modern equipment to record the temperature and atmospheric conditions, all of the judgement would be based upon experience and repetition of the standard methods employed by a smelting community when working with their locally available material.

In rare cases it has been observed that very high phosphorus and carbon contents can result in a liquid Fe-P-C alloy being produced which initially has the appearance of cast iron due to the dendritic structure created upon cooling (Navasaitis and Selskiene 2007). The exact mechanics of how this material was produced in the bloomery process is currently unknown as it is such a rarity and may be worthy of further investigation in the future as a way of determining some of the upper limits of reaction conditions within which the process must function.

The unexpected production of a material, such as the Fe-P-C alloy above, is repeated in multiple smelting experiments with blooms being more steel or iron dominated. Very few appear to have been undertaken with the aim of producing a specific metallic end product.

The presence of phosphorus in the charge does not solely determine the production of phosphoric iron, although it is the governing factor which ensures the possibility.

### Phosphoric ores in Britain

Many of the main geological deposits of iron ore in Britain contain an appreciable quantity of phosphorus as the table below demonstrates.

| <b>Ore Deposit</b>         | <b>%Fe</b> | <b>%FeO</b> | <b>%P</b> | <b>%P<sub>2</sub>O<sub>5</sub></b> |
|----------------------------|------------|-------------|-----------|------------------------------------|
| North Devon                | 29.5       | 37.9        | 0         | 0                                  |
| North Pennines             | 14.3       | 18.37       | 0         | 0                                  |
| South Wales                | 29         | 37.26       | 0         | 0                                  |
| Clothister, Shetland       | 63.08      | 81.04       | 0.01      | 0.02                               |
| Skye                       | 37.17      | 47.75       | 0.01      | 0.02                               |
| Skye                       | 41.34      | 53.11       | 0.01      | 0.02                               |
| Furness, Cumberland        | 46         | 59.1        | 0.015     | 0.034                              |
| Llanharry                  | 49         | 62.95       | 0.015     | 0.034                              |
| Llanharry                  | 51         | 65.52       | 0.015     | 0.034                              |
| N. Pennines                | 37.7       | 48.43       | 0.017     | 0.04                               |
| Whitehaven, Cumberland     | 45         | 57.81       | 0.02      | 0.05                               |
| Whitehaven, Cumberland     | 55         | 70.66       | 0.02      | 0.05                               |
| South Staffordshire        | 24.9       | 32          | 0.03      | 0.07                               |
| Yorkshire, Derby, Notts.   | 20         | 25.69       | 0.05      | 0.11                               |
| Bristol and Mendips        | 26         | 33.4        | 0.07      | 0.16                               |
| Bristol and Mendips        | 29.8       | 38.29       | 0.07      | 0.16                               |
| Forest of Dean             | 36.35      | 46.7        | 0.07      | 0.16                               |
| Perran Lode, Cornwall      | 28.8       | 37          | 0.09      | 0.21                               |
| Coalbrookdale, Shrops.     | 35         | 45          | 0.1       | 0.23                               |
| North Staffordshire        | 25         | 32.12       | 0.17      | 0.4                                |
| Banbury Oxon               | 20         | 25.69       | 0.2       | 0.46                               |
| Claxby, Lincs. Wolds       | 20         | 25.69       | 0.2       | 0.46                               |
| Frodingham                 | 21         | 27          | 0.2       | 0.46                               |
| Wealden                    | 30.7       | 39.44       | 0.21      | 0.48                               |
| Tiree                      | 29.8       | 38.3        | 0.27      | 0.62                               |
| Wealden                    | 37.5       | 48.18       | 0.28      | 0.64                               |
| Claxby, Lincs. Wolds       | 30         | 38.54       | 0.3       | 0.69                               |
| Coalbrookdale, Shrops      | 40         | 51.4        | 0.3       | 0.69                               |
| Grantham                   | 25         | 32.12       | 0.3       | 0.69                               |
| North Wales                | 35         | 45          | 0.35      | 0.8                                |
| South Staffordshire        | 42.3       | 54.34       | 0.36      | 0.82                               |
| Banbury Oxon               | 28         | 35.97       | 0.4       | 0.92                               |
| South Wales                | 29         | 37.26       | 0.4       | 0.92                               |
| Cleveland Ironstone        | 28         | 35.97       | 0.45      | 1.03                               |
| Flintshire                 | 36.31      | 46.65       | 0.48      | 1.1                                |
| Westbury, Wiltshire        | 29.7       | 38.16       | 0.475     | 1.1                                |
| Westbury, Wiltshire        | 35.8       | 46          | 0.475     | 1.1                                |
| Frodingham                 | 21         | 27          | 0.5       | 1.15                               |
| Grantham                   | 36.2       | 46.51       | 0.5       | 1.15                               |
| North Devon                | 70.4       | 90.45       | 0.54      | 1.24                               |
| Yorkshire, Derbys, Notts   | 35         | 45          | 0.6       | 1.37                               |
| Northampton                | 30         | 38.54       | 0.7       | 1.6                                |
| Ayrshire, Fife, Midlothian | 40         | 51.39       | 0.75      | 1.72                               |
| Raasay                     | 25.2       | 32.4        | 0.8       | 1.83                               |
| Ayrshire, Fife, Midlothian | 44         | 56.53       | 1         | 2.29                               |
| Northampton                | 30         | 38.54       | 1         | 2.29                               |
| North Staffordshire        | 46         | 59.1        | 1.2       | 2.75                               |
| Cleveland Ironstone *      | 30.2       | 38.8        | 1.44      | 3.3                                |
| Perran Lode, Cornwall      | 56.5       | 72.6        | 2.8       | 6.41                               |
| North Wales                | 35         | 45          | 5         | 11.45                              |

*Table 2.2.2 Showing the average compositions of major iron ore deposits in Britain, compiled from Zitzmann 1977. \* Maximum P content reported by Hallimond (1925).*

Many of these deposits were not available to pre-industrial iron smelters due to the depth at which they occur. The quality of the material is also significantly lower, in terms of iron content, than that of bog iron ores which appear to be the preferred ore type used in bloomery smelting. This preference was suggested in 1920 by MacGregor *et al.* who wrote that “Bog ores are of interest chiefly for their use in the numerous bloomeries of early times” (MacGregor *et al.* 1920: 1). The prevalence of phosphorus proved to be a significant problem for industrial smelters who strove to create phosphorus-free carbon steels and wrought iron. In response to this, haematite had to be imported into Britain from Spain and Sweden to satisfy the demand for non-phosphoric raw materials (MacGregor *et al.* 1920: 10).

### Bog ore formation

The reason that bog ores contain significantly more iron and phosphorus than the bedded ore deposits is because of the processes which result in the ore forming. Bog ore is not a direct product of the standard sulphidic ore degradation process which generates the enriched carbonate and oxide ore deposits typically associated with early metal production (Radivojević 2013). Instead it is formed by weathering of a geological source, or parent ore, and subsequent re-deposition in an aqueous environment (Kaczorek *et al.* 2004).

This process of leaching and deposition results in the ore containing several morphological features which are unique to this species of ore (Kaczorek *et al.* 2004). The composition is enriched in iron, phosphorus and other trace elements as they are removed from the siliceous ore and transported in solution more readily than the silica. As a result of this, bog ores typically contain a smaller proportion of silica than other iron ore types (Kaczorek *et al.* 2004). The silica grains that are included tend to be less angular as they have undergone some weathering due to water action prior to deposition. They then form part of the sediment which precipitates where there is a change in conditions, commonly at the water-table, and where the precipitating context encounters a dense barrier such as a clay rich layer (Kaczorek *et al.* 2004). The rounding of the silica grains by water action results in a characteristic feature of bog ores where there is little bridging, or angular contact, between the silica components. This assists in distinguishing bog ores from similar deposits such as the “Orstein” deposits examined by Kaczorek *et al.* (2004).

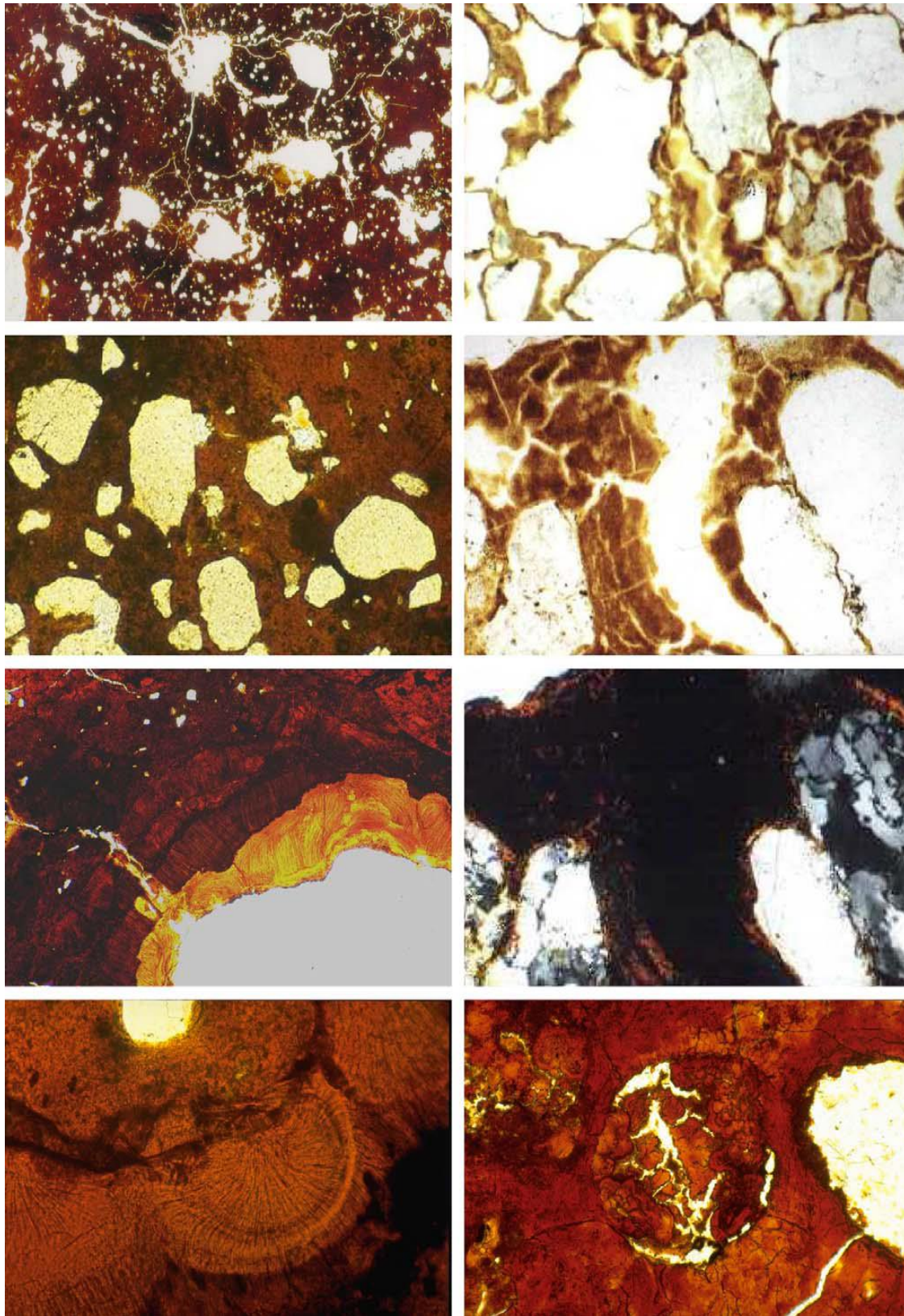


*Figure 2.2.6 Showing the morphological differences between bog iron ore (Raseneisenstein) (left) and Orstein (right), most notably the differences in silica grain size (top images) and grain bridging (second top images) (after Kaczorek et al. 2004: 87).*

The study of Kaczorek *et al.* (2004) examined Orstein deposits found in the Black Forest and compared them with deposits of “Raseneisenstein” (bog iron ores) from the lowlands of Central Poland (Kaczorek *et al.* 2004: 84). All of the bog ore samples were recovered from Holocene deposits in alluvial plains. The ore deposits were identified as being clearly restricted by the hydrological situation of the zone of deposition (Kaczorek *et al.* 2004: 86). The formation environment was found to require a minimum ground water level of 70cm below the surface at the driest part of the year with a mean level of 20cm below the surface during the wettest (Kaczorek *et al.* 2004: 86). This demonstrates that the formation of bog ores is dependent upon a wet environment to allow the precipitation of the iron-bearing minerals and a drier time which then allows the precipitate to stabilise.

One of the other findings of Kaczorek *et al.* was that the bog ores are typically far richer in phosphorus (greater than 0.1%) than the Orstein deposits (<0.1%) (Kaczorek *et al.* 2004: 93). While this may be partly due to the parent material from which the deposits were formed, it also compares well to the known generalisation that bog iron ores are phosphorus rich. The varying level of hydration results in the ores predominantly containing oxidised iron minerals, but also some hydrated species. The presence of a larger quantity of water due to the greater level of hydration explains why some researchers have observed bog ores cracking in an explosive manner during roasting (Boonstra *et al.* 2011).

Bog ores appear to have a significantly higher phosphorus content than the parent bedded ores. The increase in phosphorus content may be a result of the environment in which the bog ores form. If there is a large quantity of vegetation which is decomposing and enriching the surrounding water with phosphorus it is likely that this would result in the production of phosphoric acid which in turn would react with aqueous iron, possibly forming iron phosphates such as vivianite. Many other phosphorus bearing minerals may also be present depending on parent and surrounding geology, such as hydroxyapatite, which can be reduced in the smelting process. It is common for bog ore to contain pieces of vegetative matter which have become incorporated into the bog or mass (Lyngstrøm 2011: 142), which further supports this reasoning for the increased phosphorus content.

There is a marked increase in the occurrence of phosphoric iron in Britain following the arrival of Germanic and Scandinavian settlers. The existing literature (Ottaway 1992, Lyngstrøm 2011) would suggest that the increased production of phosphoric iron for specific uses has some relation to these cultural groups and the technologies they had at their disposal which, certainly in the case of furnaces, differed from the preceding Romano-British and prehistoric technology.

This apparent increase in the production of phosphoric iron may have been a result of two factors: either a preference for the exploitation of bog iron ores, which are more common in the coastal regions associated with the Germanic and Scandinavian settlers, or the technological difference in smelting has a direct effect upon the chemical composition of the product. The first of these, the specific use of bog ores, would cause a greater quantity of phosphorus to be present during a smelt. As a direct result of this, phosphoric iron would be produced in a much larger quantity than ferritic iron. The difference in furnaces, perhaps indicated by the differences in slag composition and a smaller abundance of tap slag, may suggest that the slag produced was of a higher viscosity. This would reduce the quantity of free flowing slag, which can pool at the bottom of the furnace, acting as a heat bath for the developing bloom prior to tapping (Saunders and Williams 2002: 6). If this is the case, then the bloom will be immersed in liquid slag for a shorter period, which may have the effect of reducing the time available for phosphorus to diffuse out of the hot metal. A combination of both factors, the use of bog ore and the possibly higher viscosity of the produced slag, may be responsible for the production of phosphoric iron. This would indicate that technology and raw materials have an impact upon the metallic product composition, although the use of high phosphorus bog ore most likely has the greatest influence.

### **2.3 Provenance studies**

The quest to establish provenance for iron-based artefacts has also been the subject of significant research. Unlike provenancing copper which can be achieved by the study of lead isotope ratios (Weeks 1999; Weeks *et al.* 2009; Pryce *et al.* 2011a), ferrous provenance is a more complex issue. Lead isotope analysis has been applied in a few, limited cases to iron assemblages (Schwab *et al.* 2006). The study conducted by Schwab *et al.* found that iron interferes with the detection of lead isotopes and the samples had to undergo multiple stages of dissolution in acid and ion exchange (Schwab *et al.* 2006: 437). While this made the analytical method a lengthy process, it ensured that meaningful data was generated. The authors proposed that the local bog ores were most likely the source used to produce the iron at Manching, however they acknowledged that the understanding of trace element behaviour within the bloomery process is not sufficient to categorically prove an ore-metal relationship (Schwab *et al.* 2006: 448). One of the major drawbacks of ICP-MS techniques is the fully destructive nature of the analysis. It may also prove difficult to isolate samples of primary slag inclusions for analysis, which may result in isotope ratios becoming skewed by the inclusion of surrounding material. The authors recognised the need for electron microprobe (EPMA) analysis, as this allows for targeted spot analyses of the desired material, while minimising the possibility of surrounding phases or substances altering the data (Schwab *et al.* 2006: 450).

Neutron activation analysis (NAA) had been the most popular method for analysing trace elements for provenance studies due to the ability to simultaneously determine the concentration of multiple elements (Desautly *et al.* 2008). Due to the time consuming and expensive nature of this technique, combined with the requirement of a suitable reactor, this method has been replaced. Tylecote advocated the use of electron microprobe analysis of primary slag inclusions (Tylecote 1970). This has subsequently become one of the major analytical techniques for ferrous artefact provenance studies as it allows the study of slag inclusions to be carried out alongside other evaluations, such as metallographic analysis.

Other techniques, such as the combined study of lead and strontium isotopes by thermal ionisation mass spectrometry (TIMS), have proven to be successful when the likely source of ore is limited and the smelting products are recovered from well-defined contexts. Lead isotopes do not undergo fractionation between metal and slag, unlike many of the other minor and trace elements present within the ore. This results in the concentration of lead being the same in both raw materials and products (Degryse *et al.* 2007: 76). The then novel application of strontium isotope study to iron smelting materials by Degryse *et al.* also relied upon the non-fractionation of the isotopes as a means of providing supporting data which would help to compensate for the broad data ranges generated by lead analysis alone (Degryse *et al.* 2007: 76).

Degryse *et al.* (2007) investigated Roman and Byzantine iron artefacts and ores from Sagalassos in the Taurus Mountains, 120km north of Antalya, south-western Turkey.

The sampled material included iron ore and placer sands from both smelting locations identified in the study as well as iron slags. The raw material used at Sagalassos is distinct from that used at another smelting site at Dereköy, where both ore and associated smelting products were found (Degryse *et al.* 2007: 78), which further aided the researchers in their analyses to distinguish the individual materials (Degryse *et al.* 2007: 77). The slag from Sagalassos was dominated by FeO and SiO<sub>2</sub>, containing high levels of wüstite and fayalite, which is common for Roman slags. This composition is drastically different to the other smelting sites within the nearby Bay Dağları massif which were dominated by magnetite and exhibit exceptionally high TiO<sub>2</sub>, V<sub>2</sub>O<sub>5</sub>, CaO, MgO, Sr, Zr, U, Th and rare earth elements. This was attributed to the locally available magnetite-titanite placer sands (Degryse *et al.* 2007: 77). This demonstrates that even within the territory of a single urban centre, in this case Sagalassos, iron production will exploit the locally available ore sources, rather than import ore from other areas. The researchers advocated the further application of Sr isotope analysis to iron smelting assemblages as the Sr ratios allow for successful differentiation between overlapping lead isotope populations (Degryse *et al.* 2007: 84). Although it appears to require further study to demonstrate successful application of the technique to poorly contextualised material.



The Degryse *et al.* (2007) study was supported by a follow up study published in 2009. In this paper the focus was placed upon identifying the possible ore sources (Degryse *et al.* 2009). Within the paper the Pb and Sr isotopic data are presented, while convincingly demonstrating that the method is successful (Degryse *et al.* 2009: 158). The shortcomings of this particular study are that much of the presented data and therefore the conclusions are a reiteration of their previous research (Degryse *et al.* 2009: fig. 2, Degryse *et al.* 2007: fig. 2). Thus the research may prove to be meaningful and effective, but the lack of further application to other sites limits the successful advocacy of this paper for the use of this technique.

Recently provenance studies have become more reliant upon the study of non-reduced compounds such as  $\text{TiO}_2$  and  $\text{V}_2\text{O}_5$ . This is due to the increasing popularity of targeted analytical methods offered by SEM and EMPA equipment and also the behaviour of major elements during smelting, which typically bear no significance in relating ore to metal (Schwab *et al.* 2006: 442). A preliminary study carried out by Paynter (2006) successfully demonstrated that different known sources of iron ore could be differentiated. Based upon the quantity of the different non-reduced compounds (NRCs) detected by SEM-EDX analysis and comparison with data obtained from raw ores of known provenance from deposits exploited within the operational lifespan of the smelting locations, the possible geological origin for the slag bearing material was identified. It was recognised that the methods used produced an identification of the geological deposit, which can cover a very large area, rather than being able to narrow down the ore source to a specific extraction location (Paynter 2006: 289). To further narrow down the possible geographic point of origin for the ore, the author suggested that models of human effort against reward should be applied, most likely identifying the closest or most easily accessible part of an ore bed as the extraction location. This is most likely to be the case however, if a superior ore was discovered at a further distance it may be possible that the ore would be transported over a distance greater than the optimum distance proposed by effort/reward models. A similar study looking at the major elemental compositions of slag inclusions demonstrated that multiple primary slag inclusions are required for a successful and meaningful analysis, due to the incorporation of secondary elemental signatures during forging (Dillman and L'Heritier 2007).

Blakelock *et al.* (2009) applied further statistical analysis to the NRC concentrations within primary slag inclusions, to further identify smelting site segregation possibilities. This required a far greater mathematical framework than the previous study by Paynter (2006) and a detailed explanation of the statistical processes and their significance (Blakelock *et al.* 2009: 1747-1753). While the process yielded very convincing results and successfully identified different smelting sites and possible sources within the examined assemblage, the explanation of the statistical processes dominated the paper.



Current research has also targeted Os for isotopic analysis in an attempt to find a simpler isotopic method for establishing geological origin for archaeological iron (Brauns *et al.* 2013).

The Brauns *et al.* (2013) study successfully demonstrated that the radiogenic Os isotopes can be used to identify different iron ore sources. It was found that each deposit does not contain a single level of isotope concentration, but that there is a range of Os content with which each source may be identified. This occurs because of the radiogenic nature of Os. The parent element ( $^{187}\text{Re}$ ) which can be present in significant quantities undergoes a beta decay, generating  $^{187}\text{Os}$ . This results in highly variable quantities of  $^{187}\text{Os}$  which causes wide ranges in the  $^{187}\text{Os}:^{188}\text{Os}$  ratio (Brauns *et al.* 2013: 843). The study involved the experimental smelting of ores recovered from two archaeological sites and then comparing the Os data generated from the experimental material with archaeological data from slag found *in situ* on the sites (Brauns *et al.* 2013: 842). This allowed a direct comparison between archaeological smelting slag and slag produced from what was assumed to be the same raw material. This assumption may be problematic, as the ore found on site may have been rejected during the ore selection process as unsuitable for smelting.

Recognising that this method does not produce a single value with which to categorise and segregate ores based on geological origin, the researchers proposed that other ongoing studies being carried out at the time of publication would further strengthen the case for the application of the technique. (Brauns *et al.* 2013: 841) This development may prove to be useful in the future once a larger body of reference data is available as this technique only requires analysis of a single element and the corresponding isotopes, rather than the isotopes of multiple elements. The data will still require some level of knowledge to interpret as the geological deposits will contain a range of values; such subjective interpretation is commonplace in ferrous analysis techniques, most notably within metallographic analysis, which will be discussed later.

The major obstacle to the determination of provenance is the number of methods which have proven to be partially successful. All of the studies have, to some extent, demonstrated that it is possible to discriminate between different smelting sites based upon the raw materials which were exploited. One of the greatest failings of these studies is that not one of them has stated what material surrounded the primary slag inclusions which were analysed. This flaw within the provenance studies limits the understanding of the use of raw materials in the intentional production of different ferrous materials.

## **2.4 Artefact studies**

The work of Sim (1998) is a rare example of a study examining the entire process of artefact manufacture, examining the stages of smelting, consolidation and forging to produce several replica Roman artefacts. This is a practical investigation building upon the work of McDonnell (1988), who examined the life cycle of the metal from raw material to deposition and subsequent corrosion (McDonnell 1988). Due to the size of the blooms produced, a metallographic analysis of the

consolidated billets produced was not feasible. This is a common problem with many iron smelting projects, where the product is too large to analyse in its entirety. In order to conduct metallographic analysis, samples must be removed from the object. The problem that occurs here is that the samples may not be representative of the entire artefact. As previously described, blooms are commonly heterogeneous in composition, which may make small sample analyses obsolete. To produce more reliable metallographic interpretations, the bloom should be sectioned, to better understand the process of consolidation (Sim 1998: 42-52) and small samples from the various different regions removed for analysis. Unfortunately, the removal of samples from central regions is not always possible due to the damage this will cause to the artefact if it is archaeological. In the case of experimental material, the damage caused is less important when compared to the data produced.

Knife typology has undergone multiple studies which have generated several different classification systems. Blakelock and McDonnell (2007) undertook a study of Early Medieval knives from multiple Anglo-Saxon sites, both urban and rural, in order to identify the major manufacturing methods used to produce knives and to generate a simplified typology which would be more applicable than the several preceding frameworks.

Previously knife typology was based on the shape of blade as well as the construction method. This lead to multiple typologies which differentiated knife types based upon blade shape, rather than construction. The problem of categorising archaeological knives by blade shape is that many artefacts will have undergone extensive corrosion which makes identifying the original blade form problematic. The typologies of Evison (Evison 1987) and Ottaway (Ottaway 1987) in particular segregate knife groups in a seemingly arbitrary manner based on the shape of the blades, without accounting for construction, this explains why the attribution of blades in the different typologies does not appear to be related.

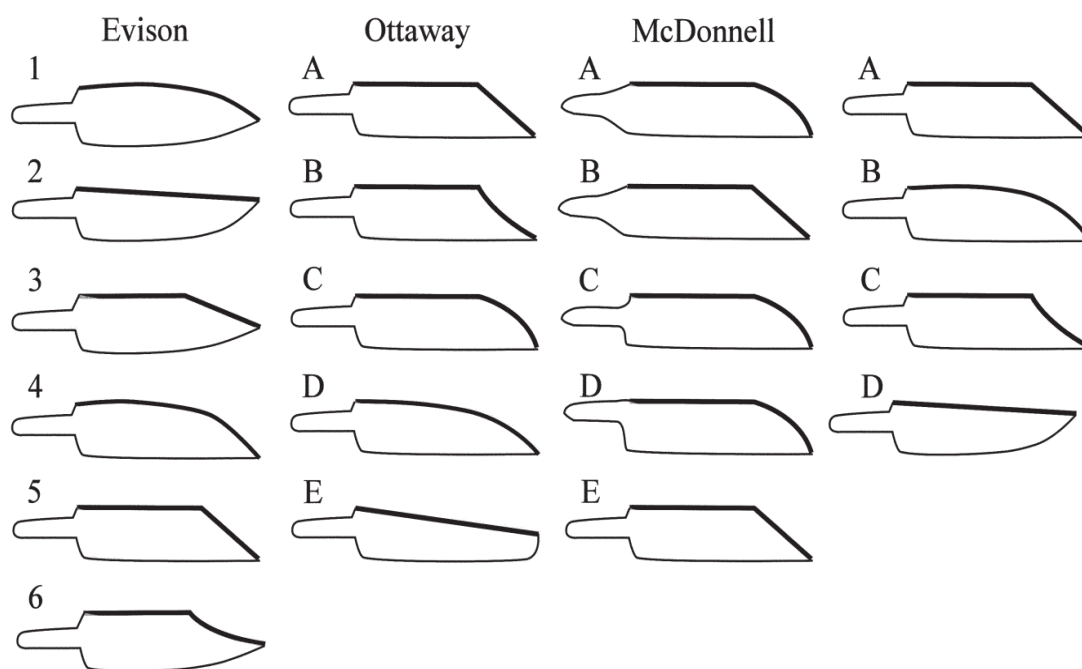


*Figure 2.4.1. Existing knife typologies demonstrating similarities and differences between classification methods based on blade form the final column is the classification used in Blakelock and McDonnell (2007) (source: Blakelock and McDonnell 2007: 41).*

The methods employed by Evison (1987) used classification by the shapes of both the knife back and cutting edge (Evison 1987: 133-137). The major disadvantage of using the cutting edge as a diagnostic tool is that it may have undergone extensive alteration during the lifespan of the blade. This can be the result of several factors including extensive use, improper sharpening and preferential corrosion in the burial environment. Due to the possibility of cutting edge alteration Ottaway developed a typology reliant upon the knife back, which is less likely to be significantly altered by use (Ottaway 1992). McDonnell further developed this by including the interface between blade and tang as part of the criteria based upon Ottaway's earlier work (Ottaway 1987: 86). This required the identification of the tang to blade interface, identifying distinct interfaces on both sides of the blade, a single side or blades with no clear interface present. The shortcoming of this method was that it relied upon the assumption that a smith would routinely forge knives in the same manner, preferentially forging the knife on a particular side. This method has only been applied to knives from Hamwic as it is almost impossible to classify artefacts without the presence of these interfaces.

As a result of the multiple typologies available Blakelock and McDonnell created a simplified typological series which incorporated several of the preceding types into groups. Basing these upon knife back form, angle backed blades were grouped together as Form A, rounded backed types as Form B, knives exhibiting incurving towards the tip as Form C and lastly, straight backed knives as Form D (Blakelock and McDonnell 2007: 41-42).

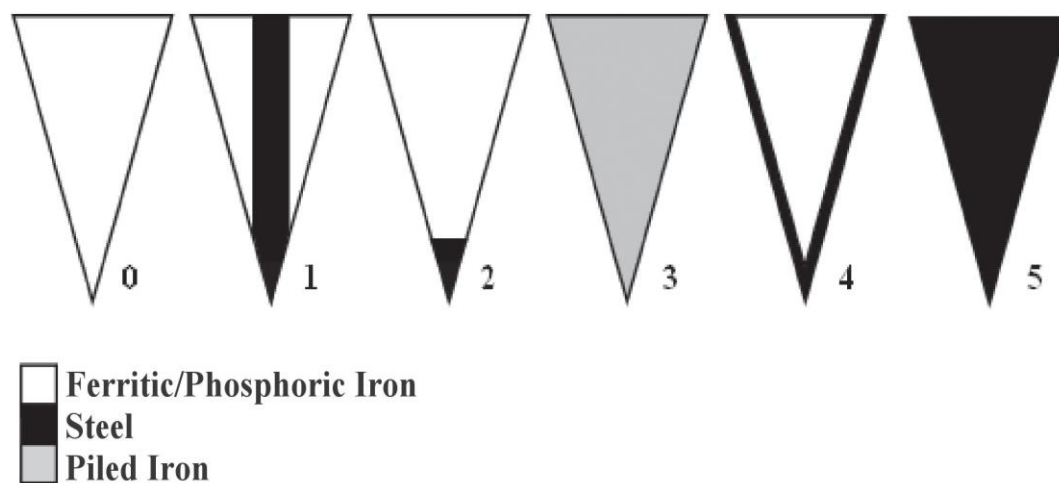


*Figure 2.4.2 Showing knife blade construction typology (Blakelock and McDonnell 2007: 42).*

This particular study identified that the major types of knives present were of either type 1 or types 2a or 2b. Types 2a and 2b are sub groups based upon the angle of the weld between the steel edge and the knife back. Type 2a is represented above in figure 2.4.2, type 2b has an oblique weld. It was found that phosphoric iron was used extensively within knife backs where high carbon steel was incorporated as a cutting edge. This study generated a useful typology which incorporates the major blade types which are encountered within the archaeological record between the 8<sup>th</sup> and 11<sup>th</sup> centuries A.D. (Blakelock and McDonnell 2007). A second study was undertaken to examine the differences between urban and rural settlements to identify if the quality of knives varied (Blakelock and McDonnell 2011). However, it did not account for the differences between the sites, such as Hamwic, which was a major urban centre, and Thetford which was more rural, or the chronological difference which may account for trends within blade manufacturing techniques (Dungworth 2012). It was found that more type 2 knives were present in urban settlements, which may reflect either a demand for a better quality knife from the urban populace, a greater proportion of specialist craft blades or a reflection of greater smithing skill being possessed by urban smiths. It may also be possible that type 2 knives, which contained a smaller quantity of carbon steel, may have been produced in greater quantity in urban settlements due to the greater economic spending of the inhabitants. Type 2 knives could be repaired, providing smiths with further income as knives could be renewed with fresh cutting edges. In rural settlements where the majority of the population could not afford as many high quality items, type 1 knives predominated, due to their longer useful lifespan. This property resulted from the steel core of the type 1 knife which provided a constant and more durable edge as the blade was used.

Type 2 knives are described as being of greater quality than type 1 because of the higher quality materials regularly observed in their construction. Type 2 knives may be misinterpreted as Type 0 knives, which are manufactured from a single material, either ferritic or phosphoric iron, and possess no carbon steel cutting edge, if the blade is severely corroded and no evidence of welding can be observed.

While phosphoric iron blades are not as common as composite ones, a sword produced entirely of phosphoric iron was found at Coppergate, York (Ottaway 1992: 716-718). This interpretation is recognised to have the same problem as identifying a type 2 knife, where the steel cutting edge may have been lost due to corrosion (Ottaway 1992: 718). Certainly, if the blade had been manufactured solely from phosphoric iron, it would have had limited practical application – being more brittle and softer than a steel edged sword, it would not have survived prolonged use without significant damage. The brighter colour of phosphoric iron may further support the possibility that this object was more decorative than functional.

Pattern welding is most commonly seen as a signifier of status, where it is found in objects which either have a strong element of public display within their characteristics (Gilmour 2007), or in artefacts for which there is no functional reason for pattern welding being used in their construction. A good example of functionally needless pattern welding are the arrow heads from Arminna West Cemetery B, such small objects gain no major mechanical benefits from being produced by pattern welding (Abdu and Gordon 2004: 983, 993). The likelihood of these objects being lost, or significantly damaged, through use is also relatively high, so they are interpreted as being for a decorative purpose to display the status of the owner.

The method of material selection for pattern welding is not addressed within any of the papers which examine such artefacts. This is most likely because it was based on specialised knowledge of the materials, such as different colour, which is no longer observable, and the sound the material produces when struck. These selection criteria cannot be used with archaeological artefacts, and are generally presumed to have been applied by smiths in the past. Other criteria such as hot working properties are mostly neglected as very few smiths now work with phosphoric iron in the production of pattern welding, relying predominantly upon wrought iron and carbon steel. There is a case for deliberate selection not taking place in all cases, with phosphoric and ferritic iron being used for the same purpose within the same artefact type, as observed in knives from York (McDonnell 1992) and Hamwic (McDonnell 1987b). As with many decisions made within knife manufacture, the choice of material with which to produce the artefact may have been driven by economic factors such as material availability, rather than technological properties; this may explain the apparently interchangeable use of phosphoric and ferritic materials.

Phosphoric iron was also utilised in the manufacture of other ferrous edged tools which required a harder cutting edge, such as knives, augers and chisels. The incorporation of phosphoric material into the tool or knife back ensured that the carbon present in the high carbon steel used for the cutting edge did not diffuse causing a loss of carbon and a reduction in hardness. In some cases phosphoric iron was used solely in the production of knives; such blades are assumed to be of lower quality as they lack a complex production method and would not have maintained a cutting edge for as long as a knife which contained a steel component.

## **2.5 Iron smelting**

Furnaces of Roman origin are generally tapping furnaces. In order to remove the slag from the furnace, a hole was opened in the tapping arch of the furnace wall so that liquid slag could flow out before the removal of the developed bloom. This process produces a characteristic slag with a ropey upper surface, caused by the solidifying liquid slag flows (Fulford *et al.* 1992: Plate XI; Bayley *et al.* 2001). There is a lack of surviving superstructures within the archaeological record. As a result, model of furnace appearance remains fairly consistent based upon past interpretations of furnace construction (Tylecote 1990; Mihok 2006; Pryce *et al.* 2011b). It is likely that some earlier furnaces also exhibited some form of decoration as it seems unlikely that the process of turning ore into workable metal would be completely unassociated with ritual practices. Decorated furnaces are well attested within the anthropological record in Africa, although the decorations themselves are culturally specific (Childs 1991).

Roman tapping technology appears to have been abandoned in Northern Europe at approximately 200 A.D. during the Late Roman Iron Age, in favour of a slag pit furnace (Carlie 2012: 58). The geographic origin of the technology is unclear, but it appears most prevalently within Denmark, Germany and the Netherlands. This technology differs from the previous furnace type by constructing the furnace body over a pit into which the liquid slag drains. This may allow for more efficient bloomery production as the furnace is less likely to become choked with slag and the bloom can grow constantly providing the slag remains in a liquid state. There are possible disadvantages to smelting in this manner as the constant removal of slag can result in a bloom which is poorly consolidated. This results in a bloom which is more difficult to forge and will typically fragment due to a greater quantity of incorporated slag (Saunders and Williams 2002). There are sites where upwards of 1000 of these furnaces have been found, such as Heeten in the Netherlands, used for approximately 25 years (Godfrey and van Nie 2004: 1118), and Snorup, Denmark, with in excess of 4000 furnaces, occupied for 240 years (Carlie 2012: 58). These high concentrations of furnaces may be used to argue for specialised, intensive production, where local materials were exploited to produce specific materials over a substantial period of time, as is similarly seen in the Foulness Valley, East Yorkshire (Halkon

2008, 2011). It is also recorded that bog iron ore is extensively available in Jutland, blanketing most of the country at a depth of 30-60cm (Lyngstrøm 2011: 139). Unlike other mineral forms of iron ore, bog ore will regenerate if the peat bogs or areas of deposition are left undisturbed for extended periods of time (Kazorek and Sommer 2003: 394, 395 ). Over-exploitation results in the depletion of the resource to the point where it is exhausted and cannot recover, as is the case with many renewable resources. This occurred in Lithuania during the Medieval period, where the bogs were dredged to the point of complete exhaustion, potentially producing 250-330 thousand tonnes of iron, and have still not recovered (Navasaitis *et al.* 2010: 114) .

Concentrated iron production in regions where the quality of raw materials is recognised as being superior to others for the production of specific products is also known in Britain. The iron producing areas of the Weald are well documented as being important both during the Roman period and the 16<sup>th</sup>-17<sup>th</sup> centuries. The level of activity was so great that a dedicated research group has been cataloguing and evaluating the iron production and working sites and methods in the Weald since 1969. Another region which exhibits concentrated iron production and working is that of Northamptonshire, where iron ore deposits, most commonly limonite, are accessible at depths of up to 3m below the surface (Condron 1997). This depth is recognised as being a limiting factor in pre-industrial ore exploitation due to the difficulty of extracting the material, the quantity of ore available and the value of the material (Craddock and Gale 1988). Where deeper mines exist, it is interpreted as being a result of great economic demand or value of either the ore, which may have been used as pigment, or smelting products.

Such concentrations of iron smelting in areas of easily accessible, good quality material commonly leads to the suggestion of specialised production. In some cases this could suggest the manufacture of a specific product, such as clean ferritic iron (Estanislau 1999), or possibly the controlled, intentional production of an iron alloy, whether it is a carbon steel or phosphoric iron (Godfrey and van Nie 2004).

Examples of specific materials being produced in relation to the quality of raw materials are recorded throughout history. One of the most notable is the production by Catalan forges of clean “malleable” iron which was exported to Coastal Italy, France and Valencia (Estanislau 1999: 226).

Within Britain, the nature of high phosphorus secondary ores, like bog ore, has made the use of phosphorus as a provenance aid more difficult, while the bedded ores which contain either none or high levels of phosphorous may be reflected more accurately within locally produced material which was not subsequently exported (Rubinson 2010). This is because of the changes made to the hydrology of the landscape since the main periods of bog ore exploitation in Britain. Since many of the bog ore deposits that were used no longer exist, it is difficult to obtain material from the probable locations for use in trace element comparisons. As bedded ores are not dependent upon hydrology for

their formation, any outcrops or accessible beds which occur in close proximity to smelting sites may have been exploited in the past. This would mean that the iron produced from these ores would be more easily recognised as related to the ore deposits by minor and trace element analyses.

## 2.6 Towards a Chaîne Opératoire

While the majority of the literature deals with the specifics of iron ores, smelting methods, and the metallographic identification of Fe-P alloys, there is a distinct lack of consideration for the *chaîne opératoire* for ferrous materials. This section will attempt to address this by demonstrating that not only is a *chaîne opératoire* required but also that the concept may not be applied correctly in many studies.

When examining the production of a material and its subsequent uses the concept of a *chaîne opératoire* becomes central to the conceptualisation of stages and processes enacted to bring about the desired outcome. The primary model of a *chaîne opératoire* developed by Leroi-Gourhan was not adopted widely within archaeology before the translation of his major work “Le Geste et la parole” into English. While this work is solely focussed on the lithic periods of prehistory, it does inform on the development of a *chaîne opératoire* as both a progression of actions as well as a psychological chain of thoughts and interactions. Looking at the development of lithic tools, Leroi-Gourhan coined several stages of “industry” which were denoted with increasing complexity and an increase of the quantity of working required to produce the finished product (Leroi-Gourhan 1993: 92, 93, 96, 101). The linear progression of stages and complexity of form illustrated in the diagrams showing the manufacture of tools from one stage to the next, has become a central tool for the conceptualisation of the multiple stages of activity presented in other artefact production. This has resulted in many of models being predominantly linear in progression from a given start point to a distinct end point without considering agencies outside of the examined activity.

In the case of metallurgical studies the primary *chaîne opératoire* models are concerned with the transformation of metallic ores into artefacts. So much so that there are papers and projects entirely devoted to the study of a single manufacturing process or highlighting the proposed steps of the *chaîne opératoire* for a given material or as a general overview of a collective discipline.



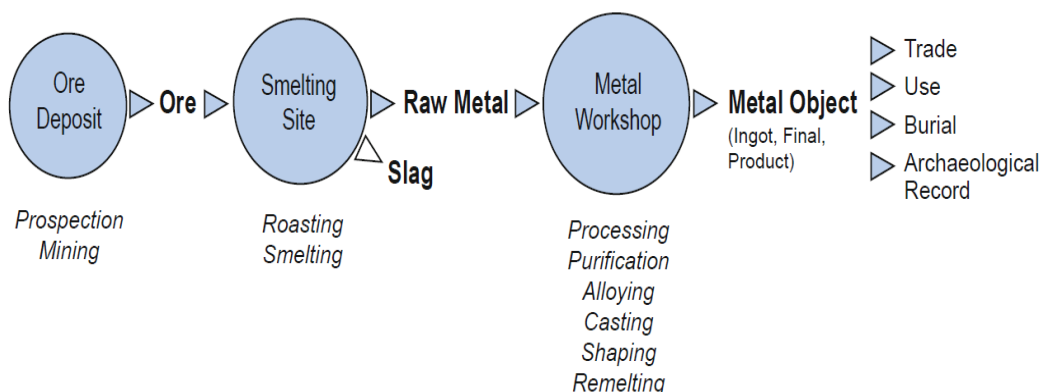


Figure 2.6.1 showing the *chaîne opératoire* overview of metallurgical activities with respect to metallic product discussed by Hauptmann (2014: figure 1).

Typically these models which highlight the progressive stages of working and actions taken to reach the desired end product do not elaborate upon the decisions taken during the stages in order to achieve the preferred results. In the case of the Hauptmann example in Figure 2.6.1 the inclusion of ore prospecting and mining is important, although it does not illustrate all of the actions undertaken to change an ore deposit into an ore suitable for smelting. Many ores have to undergo some beneficiation prior to smelting due to the quantity of gangue present. This activity is missing from the above diagram and has a fundamental impact upon the success of any smelt. Some ores, such as bog ore may require less beneficiation than bedded ores due to the precipitation formation processes which generate them in the wet environment. During roasting bog ore will likely suffer from self-fracture due to trapped water expanding as steam. This will not only reduce the pieces of ore to more suitable sizes for further preparation but also help to remove incorporated stones and grit, improving quantity of metal-rich material with minimal effort.

The inclusion of the archaeological record at the end of the diagram is also important, however it should be correctly placed after the other stages of trade, use and burial as these actions occur prior to the artefact in question becoming incorporated in the archaeological record. The complexities involved in smelting and the secondary processes of purification, alloying and artefact manufacture are not discussed in detail within this diagram as they can be multiple-stage processes which contain cyclical stages of repeat actions before reaching the desired result. Hauptmann does discuss that slags are also formed as part of the secondary processes of processing, purification and casting and alloying within the caption of the diagram (Hauptman 2014:92). This could have been incorporated onto the original diagram to further illustrate the existence of primary and secondary slags which form the majority of metallurgical assemblages.

Further to this, the cyclical section involving the transformation of metal ingots by workshops is hidden by the term “use” at the end of the diagram. Certainly by later periods the use of purified metal ingots to produce alloys of controlled, known composition is a major activity in its own right as discussed by both Biringuccio [1540] (Smith and Gnudi 1990) and Agricola [1556] (Hoover and Hoover 1950). These two historical sources are important because they are the first major works to be concerned with metallurgical activity which were written following first hand observation. The earlier work of Theophilus clearly relies upon second or third party information; as reflected in the section discussing “Spanish gold” (Hawthorn and Smith 1979: 119-120), where the practices described are impossibly fantastical and in no way accurate.

The other fault with this form of model is that it represents the activity almost as a standalone entity. This diagram does not illustrate any interaction with other areas of human activity outside of the trade, use and burial of the metallic artefacts produced. By identifying secondary stages such as purifying, casting, re-melting and alloying, the stages of metallurgical activity must surely include the procurement of materials and vessels with which to undertake these processes. Many purification and alloying applications require a reaction vessel for the process to occur within due to the need to exclude high levels of oxygen. The production of these vessels and other materials associated with workshop activities would add further branches of contributing activity to the primary chain illustrated by Hauptmann.

While the Hauptmann paper is mainly concerned with the study of archaeological slags, it is important to emphasise that a *chaîne opératoire* for a metallurgical process is not as simple as the linear progression that was put forward. For this reason, the simple step by step operation of a *chaîne opératoire* needs to be altered to include other, external factors which directly impact upon or permit the processes to happen. These may include the manufacture or trade of crucibles, the production of bone ash and cupels, the sourcing of the materials to build a furnace and the maintenance and provision of fuel for the pyrotechnological activity. While this inclusion may divert away from the primary chain of actions undertaken to produce a metallic product from raw materials, the additional interactions are no less important as they demonstrate how the metallurgical activity and practitioners fit within the greater community of which they are a part. These additional inclusions would lead away from a linear *chaîne opératoire* and towards an integrated operations web that demonstrates community interactions as well as the technological choices made by a group concerned with a specific activity.

This increased social understanding is an aspect which recently has become a more integral part of archaeological thought (Birch 2011), taking study away from the sole focus of process and production and incorporating it within a greater framework of materiality and social connections.

## Ore procurement

The first stage of a successful metal production process is the identification and extraction of suitable ore for smelting. Many experimental studies begin with sourced ore which is ready for processing (Girbal 2013: 83). In these cases the chaîne opératoire begins with either ore roasting or crushing, which avoids the preliminary stages of suitable ore selection and washing ahead of the roasting and crushing stages. The identification of suitable ore is rarely covered in the literature, however it appears to be governed by the colour of the ore which is dependent upon the iron content (Kaczorek and Sommer 2003: 60, Keen pers. comm. 2015). The method of ore extraction is different depending if the ore is a bedded variety or a bog ore. Bedded ores typically require a level of mining either of an exposed outcrop or by digging down into an ore vein. In these cases different techniques may be applied if the extraction takes place on the surface or below ground.

Near surface mining of an outcrop may involve the process of fire setting (Hoover and Hoover 1950: 120). Here a fire is built against or in close proximity to the ore and host rock to cause fracturing due to the differing coefficients of expansion of the rock and ore. This also has the benefit of partially roasting the material prior to extraction which allows the ore to be more readily identified from the host rock. Stone and bone tools were typically used in prehistory for the extraction of bedded ores (Lewis 1994: 33-34), presumably due to the higher value of metal. Later historical accounts illustrate the use of iron or steel tools as the cost of the metal and alloys had reduced due to increased quantities being produced more effectively. Certainly by the Roman period, iron tools were much in evidence elsewhere and would also be present during ore extraction, although few artefacts have been identified it would be improbable that stone masons would have access to metal tools while other rock breaking activities did not. The fired face of the outcrop would then be struck to break off further pieces of weakened rock and ore (Hoover and Hoover 1950: 121), typically resulting in the low overhangs observed in several ancient mining sites.

Deep mining may develop from a surface mining operation when the high quality ore continues deeper in the ground. In these cases the requirement for light and limited oxygen may result in several different approaches to extracting the best quality material. Certainly in cases such as the Great Orme (Lewis 1994: 36), some of the mined tunnels are too small for adults which would suggest that children were employed to exploit some of the narrower veins. By today's standards the use of child labour seems abhorrent to Western thinking, however it may have been a necessity in the past when a community's main source of income was the metal produced from the ore.

Bog ores may exist either as a horizon layer or as nodules overlaid by peat and loose, near waterlogged soil. In these cases, different methods of prospection and extraction are required compared to those employed as discussed for the acquisition of secondary ores such as haematite. Firstly the ore has to be located which can be done by observation of the water in the surrounding area which will typically be enriched in iron and have a characteristic orange tint. If the ore is found to be in nodular formations it can be identified by probing the ground to find the hard pieces. These can then be dug out for use. If the ore exists as a horizon, as is the case in Denmark (Lyngstrøm 2011), it is more practical to strip back the peat or overlying soil and remove the ore by breaking the pan into manageable pieces. In both of these cases the overlying material should be returned so that the ore has a chance to regenerate as it is a near renewable resource compared to bedded ores which has a finite accessible quantity.

The possibility of ore regeneration may lead to some interesting inferences concerning the thoughts and world view of those involved in ore exploitation. While the reconstruction and understanding of mining technology and techniques has been more prominently addressed within the literature, the reasoning behind the activities involved and surrounding the removal of ore from a deposit remains an area of debate. Pearce highlights the backfilling of mines as an activity which previously was considered as a utilitarian means of spoil disposal, to have a more significant purpose regarding the operation of ancient mines (Pearce 2014). Ancient historical sources, describe the formation of metallic ores, including iron varieties, as paralleling foetal development. Pliny the Elder when writing about Spanish lead mines states that -

*“Mirum in his solis metallis, quod derelicti fertilius reviviscunt”* (“It is a remarkable fact in the case of these mines only that when they have been abandoned they replenish themselves and become more productive”).

The explanation he provides for this apparent renewal and increased ore yield is highly obstetric: *“Hoc videtur facere laxatis spiramentis ad satietatem infusus aër, aequè ut feminae quasdam fecundiores facere abortus”* (“This seems due to the air infusing itself to saturation through the open orifices, just as a miscarriage seems to make some women more prolific”. (*Natural Historiae*, 34, 49, 164-165).

Early first century A.D. sources also describe similar backfilling and apparent mineral regeneration. The Greek geographer Strabo writing about the iron mines on Elba states that “there is also the fact that the diggings which have been mined are in time filled up again”. This he also claims to be the case for mines in Rhodes, Paros and India (*Geography*: 2, 5, 6). Virgil (*Aeneid*: 10, 174), writing at around the same time describes Elba as *“insula, inexhaustis Chalybum generosa metallis”* (“an island rich in the Chalubes’ inexhaustible mines”). Taken together these comments highlight a belief that the

practices of backfilling old excavations and leaving them for a time allows the excavation to recover, much as leaving fields fallow to restore fertility, but also to allow the remaining ore as rarely veins were completely removed to regrow.

The much later Renaissance author Girolamo Cardano (*De subtilitate*, Book 6) writes of a belief that metals and minerals were living entities birthed inside mountains providing an analogy with plants which grow underground.

This evidently long held belief lasting for over a recorded millennium that ores grow within the earth may be connected to even earlier beliefs about the nurturing nature of accessible areas below ground. There are cases of ritual activities being centred on caves which exhibit iron ochre staining similar to blood (Gutiérrez-Zugasti and Cuenca-Solana 2015). It may have been believed that such entrances either represented or actually were entrances into mother earth from which humans were born. In such cases it is highly credible that other substances such as ores, once discovered, would also be believed to be alive, although slower growing, than people.

Bog ores, which are found on land which is waterlogged but not stagnant, may also have had a relationship with other ritual understandings of the environment. Bogs have been recognised as the sites of deposition for many types of artefacts and human remains in situations which have been described as ritual. The potential for the bog to be seen as where the land and waterscapes meet may be tempting to be interpreted as a place where different worlds interact and the barrier is thinner. Thus extracting ore from a bog may be seen as removing something of value from an “other world”. This concept has parallels within present day cultures where mining transcends the material world into the supernatural (Pearce 2014).

The *Bergbüchlein* published anonymously around 1500 (Ross *et al.* 2015) presents an alchemical theory that different metals are produced as a result of the union between Sulphur and Mercury. The species of metal produced was dependent upon the influence of different astral bodies: the Moon producing Silver, the Sun - Gold, Venus – Copper, Mars – Iron and Saturn – Lead. It may be noteworthy that the red planet Mars is linked to Iron. When related to people, this astrological framework relates to the character people are said to possess, which again connects back to the different characters of metal produced based on which body was of greatest influence.

While the later alchemical and earlier embryonic theories do not parallel, they do offer insight into the connection made between human behaviour and development with that of the surrounding natural world.

Bog ores have a partial seasonality to their formation processes as discussed by Kaczorek *et al.* (2004). This may also suggest that the exploitation of the ore was conducted with a seasonal preference. The extraction of waterlogged material from a boggy environment is a physically hard

activity. The additional weight of water held within many porous bog ores significantly increases the mass of the piece being lifted. For this reason it may have been that bog ores were preferentially exploited during the somewhat drier conditions of summer when the ore and overlying peat is less likely to be heavily waterlogged. This is certainly the case when peat is cut for fuel in the summer in preparation for winter, and in some cases it may have been that both operations were undertaken simultaneously to maximise the economic reward for effort. This seasonality in a landscape which is waterlogged in winter and considerably drier in summer may be influenced not only by the practical consideration of how easily the ore may be extracted but may also be connected to the wider world view of the people in the past. In the Iron Age water played a major part in religious and ritual activity (Pearson 1999: 50). This is typified by the deposition of artefacts in bodies of water. If these depositions are taken as offerings and the boundaries between the known physical world and the spiritual domain can be crossed in such locations as rivers, pools and waterlogged land, then it may be a reasonable supposition that bog land which is cyclically wetter and drier through the year may have some significance. It may be reasonable to suggest that bog ore, which forms in winter when the bog is heavily waterlogged and is accessible during the drier summer, may have been thought of as something valuable that came from this other domain. In which case the belief that the bog was home to this material that would re-grow may have resulted in the practice of rituals similar to those discussed in (Pearce 2014) where offerings were made to deities for protection, in exchange for the ore, and also in some cases in the intention to deceive the deity so that the extraction may go unnoticed.

In later periods this proposal of rituals ahead of ore exploitation may be more difficult to support as little to no comparable evidence has been recorded. It may have been likely that offerings were made at temples or churches ahead of mining activity, although there are no historical accounts that explicitly state this.

In cases where bedded ores may be exposed beneath water, or a plentiful quantity of tertiary ore nodules have formed at depth, the method of dredging may be a more practical solution. Here rakes and nets would be used to drag the desired material from the bed of the body of water.

The assessment of the quality of the obtained ore would be undertaken after the following phase of roasting which provides a clearer indication of the iron content of the ore.

In order to identify the higher quality ore hosting rock from the gangue rich portion of the roasted material the gathered pieces may have had to undergo washing. In historical sources this is shown being done using a series of sluices and shoots in which water flows over the ore and pieces are picked out by hand based on appearance Agricola [1556] (Hoover and Hoover: 291). Simpler washing

operations are also represented which may more closely resemble earlier ore washing processes. The image below illustrates an example of sorting and washing from Agricola.



*Figure 2.6.2 Showing ore extraction and washing Agricola [1556] (Hoover and Hoover: 291).*

This helps in cases where the ore has been removed from clay rich beds, as the additional clay coating the ore may prevent or impede complete reaction as well as contributing more material for slag formation, reducing the yield of metallic iron. Further washing of bog ore would mostly add extra water to the ore, which is not desirable in the furnace. It is unlikely that bog ore would undergo supplementary stages of washing following roasting as the presence of sand within the ore would act as a flux, helping the ore to react and form liquid slag which is required to produce a consolidated bloom.

## Roasting

This is a process which is covered extensively in experimental studies as it is recognised as essential due to its recurring description and emphasis within historical texts Biringuccio [1540] (Smith and Gnudi: 65), Agricola [1556] (Hoover and Hoover: 274, 275). This step is required because not only does it remove impurities such as sulphur, but it also ensures that the metal bearing ore is in a condition that allows for maximum reducibility and thus metal extraction during smelting.

Many ores have a porous structure which accommodates water. This is particularly prevalent in the case of bog ore and is an important factor during roasting. Even after being allowed to air dry ahead of roasting, many ores will still contain an appreciable quantity of water. During roasting this water transforms to steam which results in the ore fracturing into smaller pieces. As the ore is heated in oxidising conditions the vast majority of the iron bearing phases are converted to  $\text{Fe}_2\text{O}_3$ , this results in the ore changing colour from the typical dark orange-brown to a maroon-red (Smith 2013: 100).

The roasting stage would typically be undertaken on an open fire such as those indicated by the long oval pits found at Wakerley (Fell, D. 2007: 25, 28). These features tend to be interpreted by the presence of fire debris such as charcoal and evidence of burning indicated by a red-brown colour (Fell, D. 2007: 25). Roasted ore is relatively rare as it would have been carefully gathered from the hearth following roasting due to the previous effort required to obtain it and then processing for smelting.

## Crushing and selection for smelting

The roasted ore is typically still too large for smelting as many pieces will be in excess of “pea size”. Many experimental smelts have found that the ore has to be relatively very small in order to achieve a good rate of reaction (Crew 2013, Boonstra et al 1997, Cleere 1971, Saunder 2013). In these studies the ore used is typically crushed into pieces approximately  $1\text{cm}^3$ . This ensures a large surface area to volume ratio, which allows the reduction to occur at an appreciable rate so the experiments can be finished within a day, as seen in experimental smelts including my own discussed in chapter 3. It would be a reasonable assumption that past smelting operations were also conducted within a single day and as such the ore preparation would have been to a similar to higher level of control.

The ore was likely crushed using stone hammers and anvils in most cases prior to the advent of significantly increased iron production during Roman and later periods (Craddock and Craddock 1996: 60). The behaviour of the ore during crushing would also provide another indicator of the quality of the material, acting as the final selection criterion ahead of preparing the furnace charge.



Following the roasting the ore is sorted based on the observable colour as well as the density and feel of the material. During my own experimental experience, discussed in chapter 4, I found that the best quality ore was significantly lighter and felt softer than gangue-rich pieces. This coupled with the darker colour and ease with which it broke during crushing provided several clear indicators that these pieces were the most suitable for smelting. For example, a piece that required a relatively large amount of force to break and had a light fracture surface was rejected as it contained too little ore.

The broken material would be carefully sorted to regulate the size of pieces used in the charge. This also has an effect of influencing the size of pieces being introduced into the archaeological record. Many sieves that may have been used in the past to assist the regulation of piece size would have been made from organic materials as wire was very valuable when produced from bloom iron. This may help to explain why few are known archaeologically and it is assumed during modern experiments that sieves are a suitable control method, such as those made of wood depicted in Figure 2.7.2. The same applies to the charcoal used in the charge, which must also be of an approximately regular size to ensure a reasonable reaction rate. By sieving the charcoal any fines, the smallest fraction present usually ranging from less than 0.5cm to dust, are removed which can be used for lining the bottoms of tapping furnaces or in other processes. Fines can collect and effectively choke a furnace by preventing airflow. The pieces of charcoal selected for use are typically at least two to three times the size of the ore (Girbal 2013: 81, Smith 2013: 100, 102). This allows for a large enough surface to volume ratio to produce a reducing atmosphere, while allowing a slow enough consumption rate that charge does not have to be added every few minutes.

The quantities of crushed ore and charcoal used in the charge would then most likely be judged by eye to an approximate volume based upon the experience of the smelting team rather than being measured to a known ratio as with modern experiments before being added to the furnace (Saunders 2013: 70, Girbal 2013: 85, Keen Pers. Comm. 2015). The regularity of the charge ensures that the reaction conditions are controlled and remain at least semi-predictable throughout the duration of the smelt.

### The smelt

As outlined in the section covering experimental smelting, several conscious decisions are made during each individual smelt that are partly repetition of previous successful smelts and partly based upon the individual circumstances of the current event. The need to pre-heat the furnace ahead of the addition of the first charge is widely accepted within the experimental community, as the positive impact of starting close to the desired operating temperature has been demonstrated by Crew (Crew 2013). This allows the charge to be introduced at a near working temperature with the result that the production of metallic products occurs as quickly as possible without the consumption of excessive quantities of fuel and a significant loss of ore through incomplete reaction.

The force of the blast applied is guided by the experience of the head smelter (Edmonds 1990) and this is interpreted by the colour and height of the flames rising from the top of the furnace, as well as the sound produced from within. Optimal conditions appear to be signalled by a lack of smoke rising from the furnace, an indicator that no non-combusted carbon is escaping. Flames that are low in height again demonstrate a lack of combustible waste gases and a not too aggressive blast which does not force oxygen through the furnace too rapidly.

The addition of further charge to the furnace is governed by the available space. This changes from smelt to smelt depending on the rate of reaction achieved. In the experimental smelt conducted as part of this study discussed in a chapter 4, the reaction rate was very rapid, with charge being added every ten minutes or less. In other cases the charge may be added every 15 minutes. The reason for the difference in charge times is not fully understood, however it may be a result of a combination of blast force and the resulting temperature (Crew 2013: 28).

After the last of the charge is added and more space is available in the furnace, several experiments have added extra charcoal to allow the furnace to burn down (Cleere 1971, Boonstra *et al* 1997, Saunder and Williams 2002), allowing extra time for the bloom to consolidate by maintaining a high temperature at which the surrounding slag remains liquid. While this has proven to be successful (Saunder and Williams 2002), the addition of further carbon to the system may result in further carburisation of the bloom, particularly at the surface. This may be observed during sampling of the bloom where the surface is significantly harder than the centre.

Once the burn down has been completed the metallic bloom and slag must be removed. Again the judgement of the lead smelter is paramount in this process as they have a greater knowledge of where the bloom may have formed. If the tapping of slag occurs quickly enough then the slag will still be fluid enough to flow from the furnace as free flowing tap slag (Crew 2013: 38). This is optimal as much of the slag will flow from the furnace and not require removal by force. If on the other hand the furnace has cooled too much, the slag will begin to solidify into a viscous mass which will have to be pried away and separated from the furnace walls and bloom. The bloom itself will remain hotter than the slag and can be seen glowing within the furnace which allows the smelters to remove it, while trying to minimise the damage caused to the furnace. It is common for a bloom to become attached to the furnace wall close to the tuyère where the temperature is greatest.

Once the bloom is removed, the smelting activity is complete and the final stage of primary processing beings.

### Bloom consolidation

The bloom removed from the furnace still contains a significant quantity of slag and requires a phase of smithing before it is in a workable condition for the production of artefacts (Crew 2013). In order to reduce the quantity of brittle, unworkable material the bloom it is forged into a billet. During this primary smithing the slag remaining on the exterior surface is removed and slag contained within may be ejected during compression.

The method of smithing the bloom into a billet differs depending on the individual team undertaking this stage. Some practitioners exercise a far more vigorous consolidation using large metal sledge hammers (Crew 2013: figure 1), while others prefer a more gentle approach with wooden mallets. The first of these methods results in the loss of large pieces of material containing both slag and metal, while producing a well consolidated, if somewhat reduced billet. The second method appears to be more akin to the historical representations of billet production (Crew 2013: figure 18c).

These billets could then be traded or forged into smaller sized bars before being supplied to secondary smiths for artefact manufacture. At this point the primary production of material is at an end, with the finished forgable materials ready for use.

### Predictable production

The stages of production described above highlight the conscious decisions required to successfully produce a viable product from iron ore. The major consideration that is not addressed within individual experiment reports is the predictability of the properties which that product possesses. It is not possible that ancient smelters recognised that phosphorus was responsible for a billet or bar being harder and more resistant to corrosion. Instead it is more reasonable to assume the recognition that a specific type of ore produced metal with a distinct behaviour. This understanding of the material properties of a given iron, such as that produced from a bog ore compared to that made from a haematite, would give rise to distinct and deliberate selection of materials for use.

Studies which have examined the reaction conditions required for the production of phosphoric iron such as the work by Godfrey (2007) are studying the reducing atmosphere in ways that simply were not available in the past. While they have yielded a greater understanding of the means to conserve phosphorus as part of the metallic product they have not addressed the process in the same way that ancient smelters approached their work. The risk of adopting the highly scientific mind-set of modern research as the primary standpoint is that it colours our perception by informing the way in which studies are carried out. The belief that ancient production was carried out with the aim of producing a known material every time is questionable. While it is likely that ancient smelters regarded the quality

of their product as greater or lesser depending on behaviour, such as how malleable it was, the overall highly predictable production of batch based materials such as bloom iron is less likely.

This view relates to the discussion of control and intentionality in relation to ancient alloy production. The level of control involved in the production of phosphoric iron is evidently high with the multiple stages of material selection and preparation prior to smelting, as well as the control of the reaction conditions within the furnace to ensure a successful smelt. The level of intentionality involved when discussing the material as phosphoric is where modern retrospective viewpoints, such as those held by Godfrey differ from the practical and experiential understanding of ancient smelters. Godfrey argues that it could be produced intentionally by carefully controlling the reaction conditions and using a known ore. This is contrary to the practical ability to accurately control the partial pressure of reducing gasses within the internal atmosphere during an authentic smelt. It is more credible to say that the production of an “iron” bloom is controlled and intentional, however to say without doubt that the production of a phosphoric iron bloom is also highly intentional is not possible. This would rely upon the identification of an ore as phosphoric, or phosphorus rich. Without access to the suite of modern knowledge and methods that have resulted in the identification of phosphorus rich ores, ancient smelters would likely produce a batch product that was regular in quantity and approximately regular in material properties, identified as the “iron” produced from the ore available to them.

In conclusion it would appear that by following the current understanding of the chaîne opératoire as outlined here production of phosphoric iron was a controlled and unintentional process. The overall intention was to produce forgable iron from the ore available, where this ore contained significant levels of phosphorus then the product reflected that with possessing a greater phosphoric character. Without the knowledge of the presence and effect of phosphorus the end product will have been entirely governed by the raw materials and reaction conditions.

## **2.7 Iconographic and Archaeological Representation of specialist ironworkers.**

The representation of iron workers during the Early Medieval period in Britain in the archaeological record is something which highlights a disparity in the perceived importance of the different roles. This section addresses the representation of iron smithing and smelting in identified burials as well as iconographic and literary sources. Other comparisons will be drawn upon from continental Europe as well as earlier periods where some interesting emphases may be found.

The two professions considered here occupy different social spheres. Smithing happens within settlements or in close proximity to areas of occupation, such as Roman forts with Vici. Smelting by contrast occurs beyond the boundaries of settlement, away from the majority of the population who would not regularly observe or associate the sounds of the process with the end result.

In Early Saxon England the distinct lack of identified large scale iron smelting locations suggests that iron was either produced from ore sources in areas away from the ore beds exploited during the Roman period, or that some was imported. Smithing evidence is far more common although with the lack of primary production sites it raises questions of not only where the iron came from, but also how the smiths obtained or knew about when and where the iron would be available. This leads to the concept of the itinerant smith, who moved from place to place to work.

Early Saxon laws do attest the presence of travelling groups and travellers. The laws of Hlothhere and Eadric, kings of Kent (Attenborough 1922: 19), state:

*“Gif man cuman feormæþ III niht an his agenum hame, cepeman oþþe oðerne þe sio ofer mearce cuman, 7 hine þonne his mete fede, 7 he þonne ænigum mæn yfel gedo, se man þane oðerne æt rihte gebrenge oþþe riht forewyrce”*

The translation made by Attenborough describes “strangers” which are interpreted as “traders or anyone else who has come over the border” (Attenborough 1922: 20-21).

Within the laws of King Wihtred of Kent there is further evidence for itinerancy (Attenborough 1922: 30-31). Here it states that:

*“Gif feorran cuman man oþþe fræmde buton wege gange, 7 he þonne nawðer ne hryme ne horn ne blawe, for ðeof he bið to profianne: oþþe to sleanne oþþe to alysenne.”*

Which requires people leaving the road to shout, or blow a horn in order to signal their intent. Failure to do so would permit others to consider them as thieves (Attenborough 1922: 30-31).

King Ine also issued a similar law:

*“Gif feorcund, mon oððe fremde dutan wege geond wudu gonge 7 ne hrieme ne horn blawe, for ðeof he bið to profianne, oððe to sleanne oððe to aliesanne.”*

This iteration of the same behaviours of itinerants leaving roads comments specifically of travelling through woods (Attenborough 1922: 42-43). This is a reflection of the differing landscapes ruled by Ine, although the same expectations are held of travellers.

These decrees are an indication of how commonplace itinerancy was at this time, and that laws were required to govern its conduct. The common theme of the laws regarding leaving the roadway is the issuing of a loud noise, which may explain why the Tattershall Smith burial included a large iron bell (Hinton 2000). This may have been used for such signalling as many of the laws would likely have had some level of interpretation associated with their application. There may have been cases where individuals possessed of great talent or unique skills did travel to produce artefacts at the behest of others, as we will discuss later, however it seems unlikely that the majority of smiths did this.

While commonly iron smiths are referred to as blacksmiths, due to the blackening of the iron in the forge, there is a distinct difference in ability between a smith who makes artefacts for day to day use and those who produce bespoke artefacts such as pattern welded swords, sheilds and armour. The level of skill required to produce a balanced sword is far higher than that required to make a usable knife. Thus the classification of all iron smiths as blacksmiths is somewhat misleading. It would be better to refer to the highly skilled craftspeople involved in the production of arms and armour as swordsmiths or armourers to avoid any ambiguity. Just as fine metalsmiths (Swanton 1993: 174), and other crafts (Swanton 1993: 169-175; Attenborough 1922: 75), are differentiated in textual sources by the late 10<sup>th</sup>-century.

Several iconographic representations of smithing exist which typically contain several common features. The most recognisable is the anvil and hammers being used, but there are also other objects being represented



*Figure 2.7.1 showing a metalworker forging on a horned iron anvil (Stuttgart Psalter: 121r).*

The image from the Stuttgart Psalter (Anon. 820-830) illustrates the common toolkit used by iron smiths during the 8<sup>th</sup>-10<sup>th</sup> centuries A.D. A staked anvil held in place on a wooden block, hinged iron tongs, and an iron hammer with a wedge shaped head. While the image itself concerns the biblical forging of bronze, the artefacts are sourced directly from the illustrator's experience of iron working (Anon. 820-830). This is corroborated in other sources, both textual and archaeological, with the same common features appearing in multiple representations and contexts (Swanton 1993: 175, Hinton 2000, Fig. 12).

The Franks Casket, dating to approximately 800 A.D. depicts another smithing scene, here the smith is shown with a hammer, tongs, and two staked anvils imbedded into a wooden block (Figure 2.8.2). This is a representation of Weyland (Hinton 2003) shows the smith with a large beard and clothing comparable to those of the wealthy individuals in the other image on the right half of the front panel. This demonstrates that the master smith was in a position to accrue and display wealth, while the beard may be seen as an outward presentation of age and knowledge (Wood 1990, Webster 1991: 101-103).



*Figure 2.7.2 showing the front panel of the Franks Casket with the representation of Weyland (far left) (British Museum Collection Database, “1867,0120.1, AN98117001” <http://www.britishmuseum.org/collection>, British Museum Accessed 06/06/2016).*

A similar representation of iron smithing can be found in a later 13<sup>th</sup> century carving on Sigurd’s Portal, found in the Hylestad stave church (Lindholm *et al.* 1969).





*Figure 2.7.3 Showing the smithing scene on Sigurd's portal from the Hylestad stave church, Norway. (<http://www.pitt.edu/~dash/door3932.jpg>)*

Another feature of both figure 2.8.1 and figure 2.8.3 is the relationship between the smith and the apparent apprentice. The smith in both cases is shown to be in more affluent attire, with evidence of decoration in both cases. The poorer apprentice is also shown to be dissociated from the actual working of the metal as both are shown to be working the bellows. The attribution of rank within the forge can also be seen in the appearance of the two men. The smith has a full beard while the apprentice is clean shaven. This is a reflection not just of age, but also the accrued experience and knowledge that grants the smith his position. This status division is further emphasised in the second example where the apprentice is clearly shown to be behind the other figures. This reflects the social position of the apprentice within the domain of ironworking, where they would be expected to be at work, learning and providing the less technically demanding labour. The smith, by contrast, is placed in the foreground but more importantly overlapping the surrounding frame of the scene. This may not only be a result of the cultural artistic style, but may also be a reflection of the smith's position in



society. A master smith would not only be the first contact for a client entering the forge, but they would also be in a position to interact outside that domain, unlike the apprentice who would be concerned with activities within the forge.

Notably the shape of the bellows has changed between the two images, while the anvil and hammers remain fairly consistent. This demonstrates that technological advancement as well as conservatism occurred at the same time.

The common association of smiths with this toolkit of anvil, hammer, tongs, punches and snips is attested in the archaeological record. It is also apparent that skilled individuals could attain significant wealth and social status as evidenced by the remains of the Tattershall Smith.

The Tattershall Smith burial is a unique example of a recognised metalworker in the archaeological record. The grave was discovered in 1981 in advance of gravel extraction in the flood plain of the River Bain at Tattershall Thorpe, Lincolnshire. The site consisted of three Roman pits, a medieval ditch and a sub rectangular feature from which the artefact assemblage was recovered (Hinton 2000: 1). Due to the state of preservation, many of the artefacts were removed in blocks to undergo further work and conservation at the Trust for Lincolnshire Archaeology conservation laboratory (Hinton 2000:1).

The feature interpreted as the grave was 1.72m in length by 0.70m wide and reached a depth of 0.40m (Hinton 2000: 4). Some skeletal remains were described in a letter dated 12<sup>th</sup> March 1981 to Mr Glyn Coppack (Inspector of ancient monuments for Lincolnshire) as

“... an inhumation... most of the bones had dissolved owing to the acidity of the soil... some vertebrae and part of the pelvis preserved... I think the head was facing east and feet to the west” (Hinton 2000: 5).

Photographic records of the grave do not provide any conclusive evidence of a body being present. Neither stain nor any of the described bones that were lifted are seen (Hinton 2000: 5). The conservation effort took 18 years (Hinton 2000: 7), and revealed many artefacts both ferrous and copper alloy which provide a detailed insight into Saxon metal working techniques beyond that available through pictorial representation (Hinton 2000: 11).

The artefacts accompanying the body, provide a near complete assemblage of tools, commonly referred to as a smithing toolkit, and scrap interpreted as a smith's working hoard (Hinton 2000:1). In particular, the staked anvil with a flat, square top parallels the artistic representations previously discussed (Hinton 2000: 14). The hammers appear to be very similar to those shown in the Stutgarter Psalter, with a tapered head and quadrilateral cross section (Hinton 2000: 22).

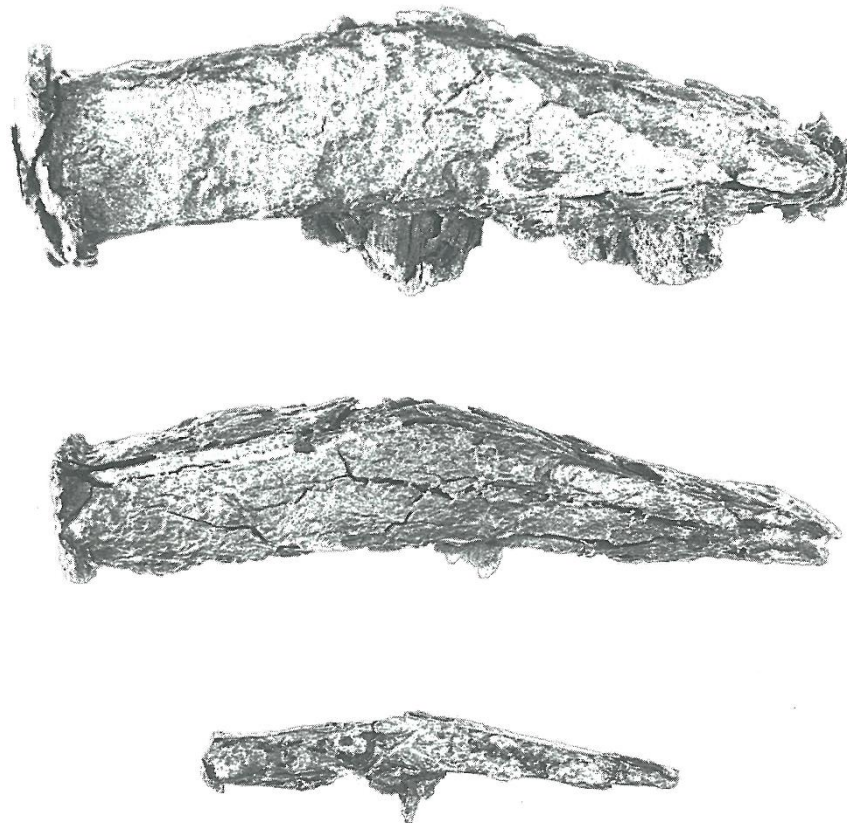


*Figure 2.7.4 showing hammer heads in profile from the Tattershall Smith burial (Hinton 2000: Fig. 12).*

The smallest of these would not have been suitable for ironwork, which suggests that the individual was also employed working copper alloys and potentially precious metals. The iron fragments found that may have been the remains of bars were not in excess of 50mm in length, other pieces may have been tools that can no longer be reconstructed due to corrosion. The entire collection of ferrous scrap was probably not large enough to produce a single sax blade, however the hoarding of the metal was interpreted as a reflection of the inherent value of workable quality iron at that time (Hinton 2000: 105).

The dating of the grave is highly tenuous due to the age of some of the artefacts recovered, in particular the Roman coins ranging in date through 161-380 A.D. (Hinton 2000: 63-65), and the later continental openwork disc attributed to between c. 550-600 A.D. (Hinton 2000: 54). The hazarded date put forward by the researcher was 660-670 A.D. to account for the later objects in the assemblage (Hinton 2000: 100).

The coins which date to preceding centuries and were most likely kept by the smith as tokens. Other artefacts found in the grave indicate that the individual was a privileged, potentially affluent individual. Roman glass fragments, including a cobalt blue bag beaker (Hinton 2000: 17), garnets classified by XRF (Hinton 2000: 18), and silk (Hinton 2000: 94-95) were all identified. These characterise this person as someone who benefitted from connections with high status clients, allowing them to accrue a selection of highly valuable materials rarely seen in the possession of non-elite individuals. Within the standard view of society craftspeople are usually seen as being below the status of those regularly associated with silk. As such, that this individual owned a silk bag is either a measure of the wealth they possessed, or the esteem their skills warranted from wealthy clients. The lack of gold, both in the form of finished objects and raw material may suggest that if the smith did work precious metals they were provided to him by his employers, rather than being part of stock materials possessed by the smith themselves (Hinton 2000: 108).

The location of the grave suggests that the individual was distinctly different from the community they served. The grave being located 7km from the nearest known cemetery at Horncastle to the north and the nearest to the south are on the far side of the River Witham at Ruskington and Sleaford (Hinton 2000: 102). This places the grave firmly within the territory of Lindsey but far away from other recognised burial sites. The body appears to have been buried facing west, rather than east, overlooking the flood plain and boggy ground beyond (Hinton 2000: 101, 102). This would further support the potential interpretation that this individual was an outsider (Hinton 2000: 115), although the apparent isolation of the grave may have been a result of the later quarrying rather than burial placement (Hinton 2000: 101) . What is clear however is that the smith was a skilled metalworker and this is represented in the assortment of artefacts included in the burial.

In comparison to the clear identification of metalworker burials by tool association, little identification of metal producers has been done. The only direct connection between individuals and iron slag, or iron production, in burials that I am aware of is found in Finland, where there appears to be a ritual importance to the placement of iron slags in graves (Shepherd 1997) . This is unrelated to practices in Britain however and there are no known comparable examples. For this reason the identification of metal producers has been neglected as part of archaeological study as it requires human remains that are associated with evidence that links the people with the activity, or extensive isotope examination.

## 2.8 The occurrence of ironworking and the Utmark/Innmark

The two Saxon sites examined in this work, show distinct differences in the nature of their iron production. Quarrington is a site that is in a rural setting within a small settlement (Taylor *et al.* 2003), while Flixborough demonstrates an increasing urbanisation through its occupational phases (Loveluck 2007). The difference in the environment in which the smelting activity occurred may indicate a change in not only the demand for iron but also the social positioning of the iron producing community within the wider Saxon social framework. Birch discusses the social landscape in terms of the Scandinavian Utmark/Innmark model (Birch 2011: 9). Here the physical and conceptual positioning of iron smelting activity is explained as being between the known and unknown as well as being on the periphery of society because of the abstract nature of the unobservable processes occurring.

Within Scandinavian archaeology there has been a focus upon a distinction between the occupational core and the periphery which has been coined the Utmark/Innmark (outfield/infield) opposition (Holm *et al.* 2005). This concept was explored by Birch in his 2011 study looking at early Saxon iron working. This idea is different from the centre-periphery model as discussed by Champion (1989). In the most simple and general of forms, the infield is the area of occupation, while the outfield is what lies beyond the boundaries. The subjective nature of the interpretation of this model has led to significant debate and remains a difficult concept to fully crystallise as a single, agreed concept. In British archaeology this is partly due to the lack of a corresponding terminology for the concept of Utmark (Øye 2005: 9). Diinhoff states that the notion of the Utmark/Outfield should always be understood in relation to the infield of the particular setting involved (Diinhoff 2005: 109). For this reason Birch is careful to explain that the utmark/innmark model is subjective as one person's utmark areas and activities may not be someone else's (Birch 2011: 9).

This level of subjectivity also transcends the physical environment where concepts of the unknown relate to actual practicalities and reach into the seemingly magical occurrences which are imbedded in iron production contributing to the utmark understanding of iron smelting. Many of these abstract factors are known to the group of smelters which isolates them from the majority of the society with which they interact. This is demonstrated within the body of ethnographic literature, as discussed in chapter 3, but also provides an indication of why smelting occurs away from the main concentration of social activity. Iron smithing also possesses some of this specialist and isolating knowledge, but the process of forging an object is a more approachable procedure to the general populace which places smiths in a unique place within the utmark/innmark model. Many smithing sites are associated with settlements where they operate within the boundaries of the occupational zone. While the smiths may be isolated from the consumer populace, their activity is less mysterious as it can be observed and at least simplistically understood by onlookers. In these cases smithing appears to straddle the boundary

between utmark and innmark depending upon the location and perceived interactions with the rest of the community.

By the 10<sup>th</sup>-century, with greater urbanisation and settlement nucleation in the rural world, ironworking appears to have become more integrated within the established social framework. This would explain the occurrence of smelting to supply larger urban centres where demand for iron would be significantly higher. By including both the primary production and secondary working of ferrous materials within the influence sphere of these larger settlements it would ensure that not only was there enough material and objects produced to satisfy demand, but also that it directly enhanced the economic power of the settlement within the surrounding area. This can be related to iron production in Rockingham Forest, close to 10<sup>th</sup>-11<sup>th</sup> century Stamford, Lincolnshire, where it has been argued that smelting occurred close to high status locations which may add further weight to not only the importance of iron in the Mid-Late Saxon period but also that the control of iron production was becoming increasingly important. This would suggest that the production of iron was becoming part of the understanding of a greater proportion of the population, most likely this was in relation to the elite who required knowledge of the production of the materials they consumed and controlled. The shift into urban production may demonstrate that iron production was moving from an Utmark activity to a more liminal one, similar to how smithing appears to have occurred in both zones of familiarity. Similarly with the establishment of urban smithies the otherness of smithing activity would be slightly reduced as the general populace would be exposed to its occurrence and accept the noise and observable processes as part of life, which is also reflected in the Aelfric Colloquy (Swanton 1993) shifting the entire iron working stages, both primary and secondary towards Innmark with time.

The diagram below attempts to illustrate the distinction between utmark and innmark while representing the conceptual placement of ironworking activities within the framework.

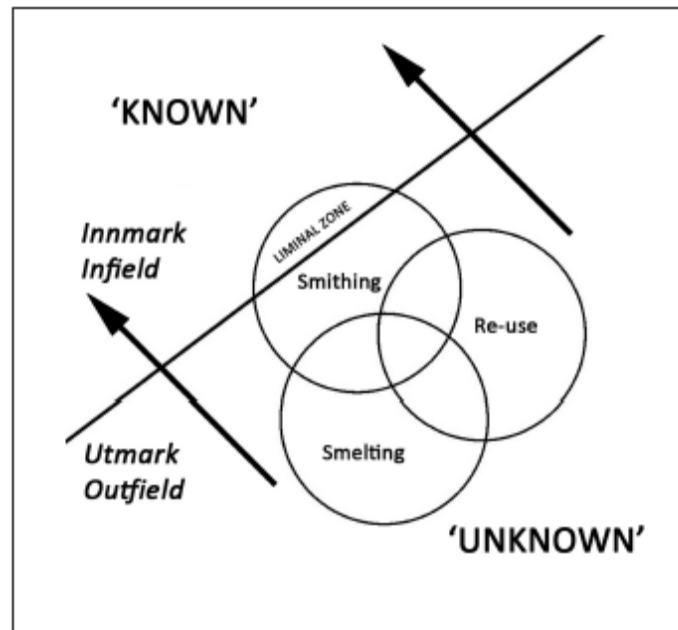


*Figure 2.8.1 Showing the model of Utmark and Innmark for iron working according to Birch (after Birch 2011: 9).*

The sphere of re-use shown within figure 2.8.1 is a more questionable interpretation than the main processes of smelting and smithing. The re-use of an object or product, such as slag, may have been more apparent and understandable than the initial production of metal. This also falls into the discussion of scrap metal and recycling.

Scrap metal exists as three distinct classes of potentially re-usable metal waste. The first is primary scrap, also called in house scrap, which is the material deemed unsuitable following smelting. This class may include products such as hypoeutectic steels or cast iron that may be produced during bloomery smelting. The second class is new scrap which is the collective term for material and flawed artefacts rejected after artefact smithing. The final class of scrap metal is that of old scrap which is what is typically thought of as scrap today. Old scrap consists of used artefacts which have broken or have suffered extensive use wear and cannot be fixed. In some cases the re-use of old scrap and new scrap to produce an entirely different artefact may be more difficult to comprehend as the original and final form taken by the metal may be drastically different. This does not however place this form of re-use significantly further away from the known region of the diagram compared to smithing. The use of a venn diagram to represent the regions of the activities has resulted in this distancing of re-use from the activities in which it may take place. The separate region of re-use may be better related to the re-use of artefacts for different purposes to those they were originally intended for, however this is not discussed by Birch in his paper.

Birch also discusses the major sources of iron ores in Britain, listing the major bedded ore deposits which are known to have been heavily exploited as well as giving reference to bog ore in the highland zones of Wales, Scotland and Ireland (Birch 2011: 6). This neglects the evidence for the potential identification of the bog ore deposits in East Yorkshire recorded in a charter of 959 A.D. (Hart 1975: 119-120) due to the rusty colour of the water within the river Foulness, listed as “*fulanea*” as part of the boundaries of Howden (Hart 1975: 120). Birch highlights the near complete lack of identified smelting sites in regions such as the Weald and the Forest of Dean during the Anglo-Saxon period (Birch 2011: 7). This potentially provides an insight into the possibly different ore procurement strategies of that time as iron production was extensive in both the preceding Roman and subsequent later Medieval periods (McDonnell 1989: 347). If this is the case then it may be likely that Early Anglo-Saxon smelting relied more heavily on bog ore sources than the significantly larger bedded ore deposits. The occurrence of bog ore in areas which are not as suitable for large scale settlement may have influenced the apparently more rural early smelting activity. Alternatively, the later Medieval ore extraction may have removed earlier evidence from many locations where bedded ores were easily accessible.

Birch recognises that the lack of smelting evidence in these important iron producing regions conflicts with the distribution of pattern welded swords which date to the Saxon period (Birch 2011: 11,12). While discussing the potential origins of the blades as well as the iron and steel they are made from, he does not suggest that the iron producing sites beyond the south east may have been reliant upon bog ore rather than bedded deposits (Birch 2011: 12).

There is however historical evidence for the exploitation of bedded ore during the Saxon period. A charter from 689 A.D. states that King Oswaine of Kent granted a sulung of iron-bearing land previously belonging to the vill of Lyminge (Kelly 1995: 33-34). This demonstrates that bedded ores were known and used by Saxon smelters as early as the late 7th century A.D. This appears to be a rare occurrence however, as little is recorded either historically or archaeologically regarding ore use prior to the later Saxon periods where both bog and bedded ores have been found in the roasted condition at Flixborough.

Quarrington is a site which Birch does not list as it was under excavation at the time of publication (Birch 2011: 7). The list of sites dated as early numbers only three which makes Quarrington even more important as it is the only site of the four not in the South-East of England.

## **CONCLUSION**

The body of literature concerning iron smelting has demonstrated that there is a clear link between the raw materials and the metallic products. The main problem that smelters would have encountered in Britain would be the presence of phosphorus in the majority of the ores available. This would have resulted in the production of ferritic iron and steel being significantly more difficult than making phosphoric iron.

This would suggest that there is an aspect of technology also involved in the production of ferrous materials which can offset or mitigate the phosphoric content of the ore used.



# Chapter 3

## Experimental archaeology critique

|      |   |     |
|------|---|-----|
| 3.1  | <i>Experimental archaeology: An overview</i>            | 74  |
| 3.2  | <i>Experimental iron smelting</i>                       | 75  |
| 3.3  | <i>British iron smelting examples</i>                   | 80  |
| 3.4  | <i>Bloom smithing: A case study for data collection</i> | 87  |
| 3.5  | <i>Modern experimental smelts</i>                       | 90  |
| 3.6  | <i>The Lejre Project</i>                                | 94  |
| 3.7  | <i>Calculating optimum smelting yields</i>              | 97  |
| 3.8  | <i>The analysis of archaeological material</i>          | 100 |
| 3.10 | <i>The reduction of phosphoric ores</i>                 | 108 |
| 3.11 | <i>Summary</i>  | 109 |

This chapter provides an overview of experimental archaeology and the application of experimental methods to the investigation of ironworking. Drawing upon case studies, the major characteristics of successful investigations are highlighted. By examining both the practical and theoretical studies of the production of iron in the bloomery process, the difficulties in translating the theoretical into a practical model will be demonstrated. This leads into the discussion of the methods used in the analysis of archaeological metallurgical remains. Here the difficulties of direct dating, the use of morphology and the application of archaeometric methods are examined to demonstrate both the instrumental and subjective nature of the analysis of ironworking slags.

### **3.1 Experimental archaeology: An overview**

Within the multifaceted discipline of archaeology, experimental investigation has become an increasingly popular and successful aspect. While the majority of archaeological study is concerned with the detailed examination of archaeological remains to extract the maximum quantity and quality of data on which to base an informed interpretation, experimental investigations provide a more tactile and experience-based understanding of past processes.

Archaeological experiments can be conducted for several reasons including understanding of site formation processes (Dixon 2004), the use of technologies, and the manufacture of objects (Sim 1998). There is a danger in any experimental study that the experimental techniques may not reflect the archaeological processes they claim to replicate.

Recreating the past in a physical event is dependent upon a suitable level of archaeological validity to be judged as justified. An experiment which, for example, attempts to replicate an artefact but does so using tools which would have been unavailable to the original craft-workers suffers from a lack of archaeological validity. While in many cases researchers begin an investigation with the intent of being as close to 100% archaeologically valid as possible, some factors may result in compromises being made to ensure a successful test of given parameters.

The majority of experimental studies lie within this region of compromise. Very few studies manage to maintain a complete replication of ancient processes. Some compromises may be made due to material availability, where a specific material used in the past may no longer be obtainable by the researcher. Other cases where time constraints may result in a hastening of experimental stages may cause slight, unpredicted changes in the overall outcome.

### 3.2 Experimental iron smelting

One of the most popular areas for experimental investigation is that of metal smelting. Many experiments have been carried out in order to examine the different methods of obtaining a given metal from its ore. In some cases experiments were conducted to evaluate smelting technologies from a cultural perspective, this has particularly been the case in African iron smelting studies (Schmidt and Avery 1983, Chirikure 2006). These investigations have resulted in a more sophisticated view of the traditional indigenous iron smelting practices which precede the introduction of later European smelting technologies.

The examination of iron smelting techniques has relied predominantly upon the reconstruction of furnaces based either upon archaeological or ethnographic evidence. The following sections will look at several cases of experimental iron smelting which drew upon different sources for their respective furnace reconstructions.

As previously mentioned multiple experiments have been conducted relating to African bloomery smelting since the 1970s. Schmidt and Avery (1983) conducted a study based upon ethnographic and technological observation coupled with excavated evidence over a period of 3 years from 1976 to 1979 (Schmidt and Avery 1983: 421). The authors recognise that prior to their investigation the main argument adduced for continuity in smelting technology was analogy (Schmidt and Avery 1983: 422). The underlying problem of the use of analogy within any ethnographic or anthropological work is that an analogy is only applicable if the compared sites, or features, are directly comparable (Binford 1967).

Binford's analogy between ethnographic observation of hide smoking and the pits he interpreted as having the exact same function is a rare case where the modern and the archaeological examples are direct parallels of each other (Binford 1967: 8). This is not the case with the majority of archaeological sites. Direct analogy between ethnographic work and archaeological material can only be proposed in cases where the culture, environment and technologies are approximately the same.

This is problematic in the case of bloomery iron smelting within any region as the technology will exhibit differences based upon multiple factors, including the surrounding environment, the geological setting, the raw materials which are available and, importantly, the culture in which the smelting occurs. For these reasons Schmidt and Avery obtained new excavated evidence with which to support the ethnographic observations and also to remove the need for analogy (Schmidt and Avery 1983: 425). One aspect of the smelting process that was identified both ethnographically and archaeologically was the spiritual dimension of the smelting process for the parties involved. In the cases observed, objects and substances were used in the belief that they would increase the

productivity of the smelt and ensure the smelt was successful and with the aim of imparting desirable properties to the bloom (Schmidt and Avery 1983: 424-425). This is a symbolic and ritualised area within the overall endeavour, which is not as yet attested in any form within the prehistoric European archaeological record.

The excavated furnaces found in 1977 (site KM2) and 1978 (Site KM3) in the Kemondo Bay basin, Lake Victoria, Tanzania were identified as ‘bowl furnaces’ (Schmidt and Avery 1983: 423-424).

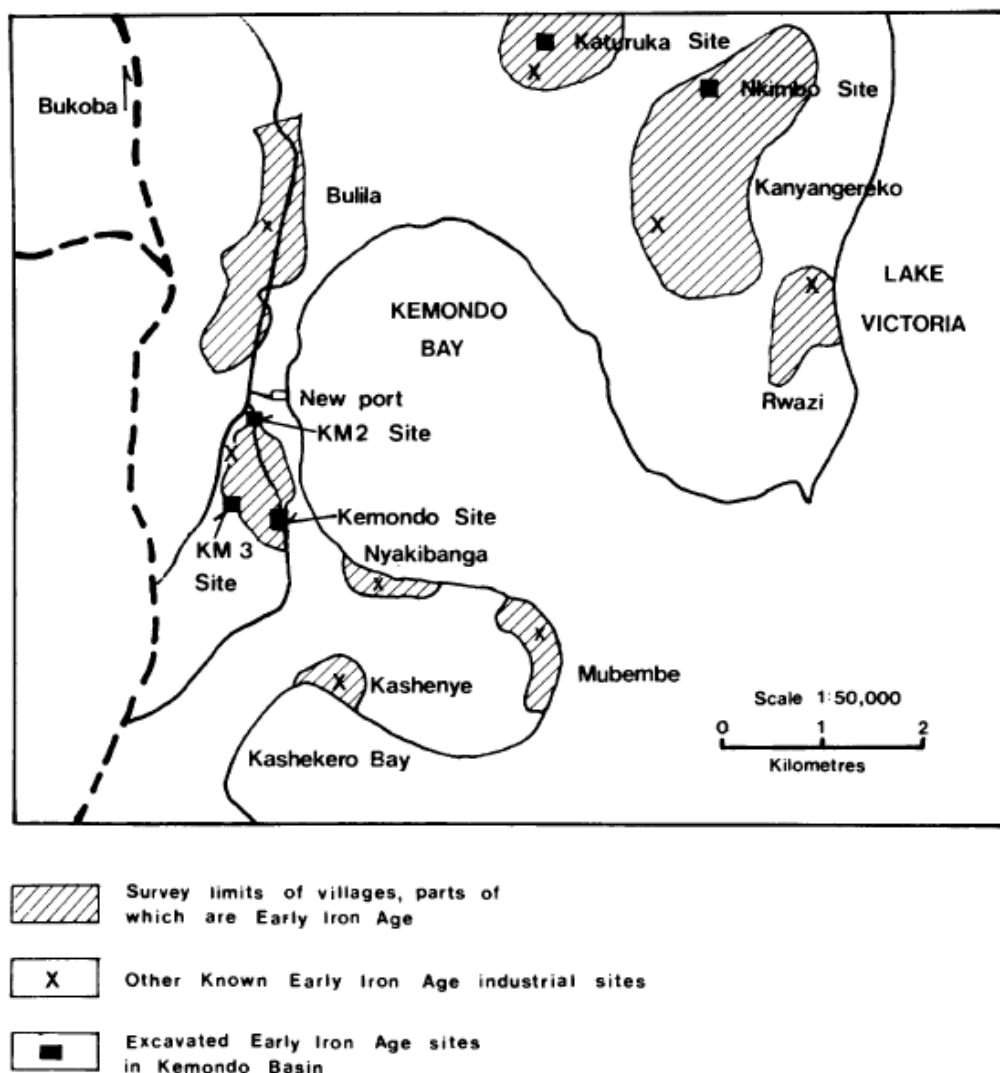


Figure 3.2.1 Showing the locations of sites KM2 and KM3 (Schmidt and Avery 1983: 423).

This term has more recently fallen out of favour within the archaeometallurgical community due to the ambiguity of distinguishing between a bowl furnace and a pit furnace (Starley, Pers. Comm. 2013). In the case of the furnaces studied by Schmidt and Avery the pit features are significantly wide, up to 1.15m in diameter at the original excavated boundaries, and 0.25m deep (Schmidt and

Avery 1983: 424). This would suggest that the furnaces were not only substantial in size but also representative of fully developed pit furnace technology. The two sites also demonstrated differences in the technological choices by the smelters. The furnaces excavated at the KM2 site had earthen liners applied to the pits, which allowed the re-use of the furnace to be recognised more easily. The smelters at the KM3 site did not make use of liners, however the numerous sandstone blocks found in the pits may have acted as refractory buffers instead of applied clay lining (Schmidt 1997: 185). The lack of surviving liners in the KM3 furnace pits was also interpreted as a signature of potential extensive re-use until the liner became severely degraded and was replaced with logs. This interpretation may indicate that the significance of lining of the pits changed from being a true technological choice to a more stylistic, cultural tradition (Schmidt 1997: 188).

Further experimentation was undertaken to investigate the degradation of tuyères under high-temperature reducing conditions (Schmidt 1997: 155). It was observed that different clays were used to make the tuyères used for smelting and smithing (Schmidt 1997: 156). The use of slag particles as temper was recorded in the case of smithing tuyères which was found to have a negative impact upon the stability of the ceramic in a highly reducing atmosphere (Schmidt 1997: 156). Over the course of the smelting experiments conducted between 1976-1984, the majority of tuyère degradation was derived from high FeO content, particularly when slag was used as temper, and back pressure in the furnace stack resulting from the use of damp charcoal (Schmidt 1997: 156-157). Further experimentation was undertaken to resolve the instability of the tuyères and a traditional smelting clay was sourced and grog used as temper. This proved to be far more successful with a total of 17.1% loss over an 8 hour exposure compared to losses between 25-52.8% experienced with the previous clays (Schmidt 1997: 167-158).

While the production of more stable tuyères was successful with the use of clay and temper with low FeO content, the largest blooms were produced by smelts during which the tuyères were replaced due to cracking (Schmidt 1997: 158-159). This factor leads to questioning what is desirable during a smelt and what may be judged as a “success” by researchers, in this case tuyère stability, may not always be what was sought after.

During the 1984 experiments there were several problems that had a direct impact upon the effectiveness of the smelts. The tuyères rested on a flat rim rather than a curved pivot as in previous experiments, resulting in a restriction of the positioning of the draft. This also prevented the tuyères being placed in an “ashy zone” of the furnace, significantly altering the dynamics of the smelt from previous iterations (Schmidt 1997: 159). If the tuyères were not in contact with an ash rich area there would be significantly less vitrification and reaction with fuel ashes. This would result in a greater survival rate of the tuyère body. It was also noted that the bellowing of the smelts was not up to the standard of previous years due to old age and death amongst the original smelters (Schmidt 1997:

159). This would impact upon the strength of the reducing conditions and the overall temperature, which again would reduce the likelihood of tuyère failure. These factors are deemed to be the cause of the tuyères suffering only 9.3% loss in length over the first smelt in 1984 (Schmidt 1997: 159). As previously suggested the reduced rate of failure would indicate less than suitable conditions for iron production in this case.

Combining the fully developed nature of the technology seen at the Kemondo Bay sites with the implied size of the iron blooms produced and the metallographic evidence that these blooms were carburised to steel within a pit beneath the furnace, would further indicate that experienced smelters were more than capable of producing both ferritic iron and carbon steel with a notable degree of intentionality.

The identification of grass impressions on a bloom would indicate that damp grasses, most likely obtained from near to the site (Schmidt and Avery 1983: 425, 431), were used to fill the pit prior to smelting in order to support the growing bloom and allow the slag to drain away. This technology differs from other sites where wood was used instead of grass. This difference most likely arises due to the surrounding environment and the availability of material, but may also reflect a cultural or ritual difference specific to that community, rather than being a direct technological choice as both methods serve the same purpose with approximately the same efficiency.

Tylecote's earlier reconstructions of this type of furnace was based upon Roman tapping furnaces (Schmidt and Avery 1983: 430). This has since proved to be inaccurate, with revised pit furnace models being more closely related to the archaeological evidence (Schmidt and Avery 1983: 431). The dangers of reconstructing a furnace based on archaeological evidence alone is that the superstructure very rarely survives (Fell 2007: 42, 43). This is partly why Tylecote's initial attempt was based upon a furnace type that was more familiar (Schmidt and Avery 1983: 430). Only later, when further excavated evidence and ethnographic observations were applied, did the interpretation become more accurate (Schmidt and Avery 1983: 430-431). This case study demonstrates the nature of scientific investigation where interpretations and conclusions can be drastically altered when new evidence comes to light.

Chirikure (2006) further examined the application of metallurgical study and ethnography. This study examined tap slags and technical ceramics that were found in association with a well-defined smelting site at Gandamasungu, Wedza Mountains, Zimbabwe (Chirikure 2006: 146-148). The slag proved to consist predominantly of fayalite with an interstitial glass matrix. The extremely low wüstite content signifies that the smelting operation was highly efficient as almost all of the available iron was liberated during reduction (Chirikure 2006: 148). The author recognises that distinguishing between tap and flow slag can be difficult, as both can exhibit similar features under reflected light

microscopy, particularly if the flow slag was formed by raking molten slag from the furnace. One distinguishing feature of tap slag is the formation of a magnetite skin on the outside of the material due to the molten slag contacting oxygen from the atmosphere (Chirikure 2006: 147). Not all flow slag, which the author describes as “forming within the furnace, but not joining the furnace bottom”, is exposed to enough available oxygen to result in magnetite formation (Chirikure 2006: 147).

The evidence from Gadanmasungu demonstrates that when smelters had access to high quality ores it was possible for bloomery smelting to extract a high proportion of metal. As this is possible within the specific setting of African iron smelting, it may be possible that ancient European smelters also possessed greater skill than they are regularly attributed by researchers approaching the archaeological context from the modern viewpoint. This is an example of temporal chauvinism – a term coined by Cherry (1990: 201) where the technological capabilities of past peoples are seen in a dismissive way, commonly because of the belief that people in the past were more “primitive” – usually taken to mean less sophisticated, or stupid, than we are today (Michell 1989:45). There are two models which deal with the way past societies are regarded, these are the primitivism, or minimalism, model and the modernist model. From the primitivism perspective people living in the past are perceived as behaving in a different manner to our own due to the society in which they existed being fundamentally different (Horden and Purcell 2000: 146-50). The counter view to this is that of modernist thinking where past people are essentially similar to ourselves, although they have access to a different level of technology in less complex societies.

Reconstructive experiments based upon the ethnographic accounts have a limited validity due to the loss of knowledge that has occurred between the time of the archaeological instance and the modern-day recounting of events. This is particularly noticeable within the van der Merwe and Avery study of 1987. Here a free standing induced draught furnace, originally constructed in 1910, was compared to an attempted copy that was produced in 1982. The drastic difference in shape reflects how the modern Chulu smelters had a different understanding of the construction process than the original master smelter of 1910, as can be seen in figure 2.2.2 below.

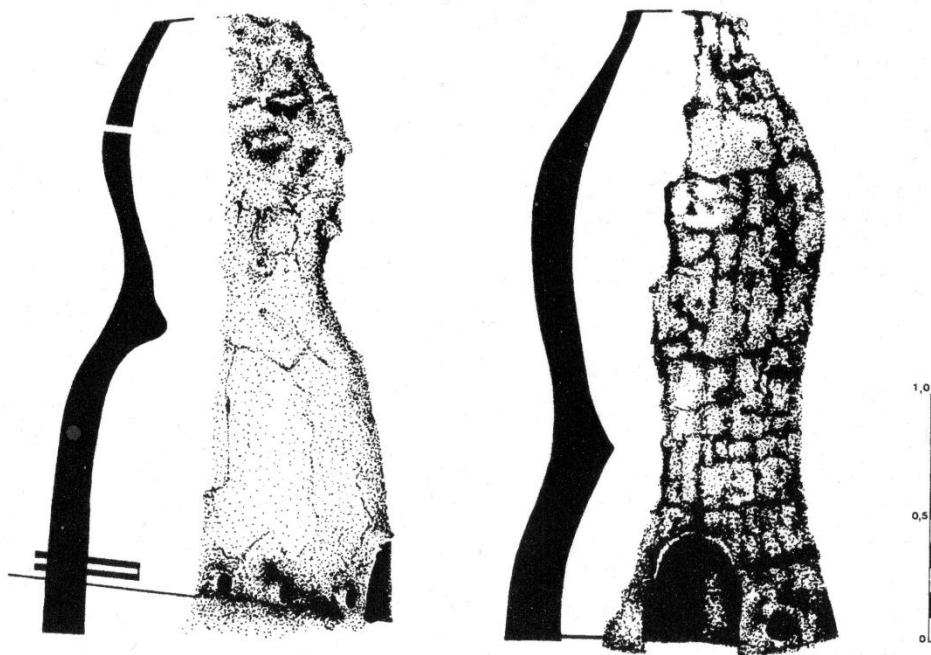


*Figure 3.2.2: Showing the difference between the attempted copy (left) and the original induced draught-furnace constructed in 1910 (van der Merwe and Avery 1987: 152).*

This example clearly illustrates the potential inaccuracy that can occur by basing an experiment upon modern interpretation and recollection. This is an inherent risk when undertaking experimental smelting of prehistoric or early medieval smelting, where the furnace superstructure is generally not recorded in any form. Whether this lack of information is due to the poor survival of records, the level of detail of knowledge transferred verbally, or the potential beginnings of industrial secrecy, the true form of ancient furnace superstructures may never be known. Applied decoration and ritual aspects are typically not represented in modern experiments as the scientific knowledge of physical chemistry of modern metallurgists has superseded the ritual and experience-based understanding of past peoples.

### **3.3 British iron smelting examples**

The early development and establishment of archaeometallurgy as a discipline was largely a result of the work of Tylecote. Much of the early work carried out looked at the examination of metal producing technologies examining both cupric and ferrous fields. During the 1970s the majority of research was driven by the need to understand the production of metal from ores and the identification of smelting sites. This can be seen in the earlier models of bloomery furnace operation where the development of the bloom is represented with reasonable accuracy, but the production of slag differs greatly as discussed below. The experimental work carried out by Tylecote in collaboration with others not only informed us greatly upon the process of bloomery smelting but also instigated a



framework for further, subsequent studies. The investigation published in 1971 demonstrates the level of understanding and detailed recording of method and results which have since become commonplace within experimental studies (Tylecote *et al.* 1971). This study was designed as a systematic investigation into the variables that have a direct affect upon the performance of a smelt with the express aim of deriving an effective routine that would inform the archaeological understanding of bloomery iron smelting (Tylecote *et al.* 1971: 343). The furnace used in the initial stages of the investigation was based upon excavated evidence from Ashwicken in 1957-58. Five shaft furnaces were found with an internal diameter of 30cm and a height of approximately 1.4m. The inner walls of the furnaces were vertical with a slight expansion towards the bottom (Tylecote *et al.* 1971: 342-3). The tapping arch was also identified as the point of bloom removal and draught delivery based upon the size of the opening. The estimated complete height of the furnace was 1.5-2m, which would allow for a good draught through a 60cm deep bed of charge and the ejection of the produced smoke from the pit in which the furnaces were built (Tylecote *et al.* 1971: 343). Furnaces of the same description were also identified at Pickworth, Lincolnshire (Tylecote 1970). This would suggest that Roman tapping furnaces were of similar construction and have similar operating conditions. The ore used in the experiments was Cumbrian hematite, which is known to be an ore with a low phosphorus content, Labrador limonite, West Lothian siderite and Northamptonshire siderite (Tylecote *et al.* 1971: 347). Like many early smelting investigations, the study was mostly concerned with the production of a suitable yield of metal, this was discussed extensively with regards to the effects of fuel to ore ratio in the charge (Tylecote *et al.* 1971: 351-352). The description of the desired bloomery process as having “reduced yields” while having “large iron losses in the slag” is indicative of the metallurgical thought of the time that a more successful iron smelt has a high yield of metallic iron and a low loss of iron within the produced slag (Tylecote *et al.* 1971: 352). The negative description of the desired bloomery conditions indicates that the preference for producing what could be considered as a high quantity of metal resulted in the slower acceptance of the importance of slag production. This is problematic as the concentration on metal extraction resulted in experiments failing to produce slag in quantities which are archaeologically comparable (Cowgill pers. com. 2013). Two iron smelts were undertaken, one in an outdoor environment and one in laboratory conditions (Tylecote *et al.* 1971: 344). This was done to enable temperature readings and gas composition data to be collected in a controlled manner. Upon the examination of the products of the various smelts, it was recorded that wüstite does not appear until the FeO content of the slag exceeds 50%. This results from a fuel to ore ratio of 1:2 or less (Tylecote *et al.* 1971: 359). The experimental identification of this diagnostic feature was a crucial step in the understanding of direct process iron smelting. This observation has resulted in the standardisation of the fuel to ore ratio used in all experimental smelting to date, with the aim of producing metal and slag which is comparable with archaeological material. The results of the bloom analysis demonstrated that the microstructure of raw blooms can be heterogeneous, particularly with respect to carbon content (Tylecote *et al.* 1971:355),

although particular microstructures will be predominant depending upon major and minor element distribution. This is particularly apparent in the case of sulphur which causes a pale-grey globular sulphide phase when present in excess of 0.1% (Tylecote *et al.* 1971: 355). The lack of observable phosphide in any of the analysed samples indicated that the phosphorus content was below the limit of solid solubility. The increased hardness of some of the specimens studied was attributed to the presence of phosphorus, in keeping with the mechanical properties bestowed upon iron by the element (Tylecote *et al.* 1971: 355). The microstructures observed were generally well developed, as evidenced by the coarse pearlite and large grains. The bloom formation process was also partially revealed during macroanalysis. The structure of the blooms, while exhibiting some variation, all tended towards a similar overall trend. As a bloom forms throughout the smelting process once the production of metallic iron has begun, the macrostructure of the piece develops and conforms to a particular form. The bottom of a bloom comprises the first metal to be produced; this results in the bottom being less dense, with large gaps between the separate metallic areas as the metal is formed in the available space between the charcoal below the tuyère. The main body of the bloom is more compact, this results from the agglomeration of iron particles gradually compacting. This also forces slag out of the bloom, producing large areas of solid metal (Tylecote *et al.* 1971: 354,355). Large pores may still exist in the bloom due to the presence of large pieces of charcoal; this may also be demonstrated by an increased quantity of carburisation in proximity to these voids (Tylecote *et al.* 1971: 355).

The interpretation of the macrostructure of the blooms produced in the experiments would suggest that free-flowing slag, the kind associated with Roman tap slag, is highly desirable for the production of well-consolidated, low carbon blooms (Tylecote *et al.* 1971: 362,363). They also found that easily reducible ores with a high water content were the most suitable for smelting (Tylecote *et al.* 1971: 362). These include the siderite and limonite ores which were tested as part of the study and the findings further support the potential exploitation of weathered bedded ores, for example limonite, in locations such as Northamptonshire (Condron 1997).

This study has influenced several experimental investigations, carried out with the aim of producing both metal and slag (Dungworth and Doonan 2013). The successful identification of slag which was comparable with archaeological material, and the conditions which produced the slag, has become a central aspect of the current understanding of the operation of iron smelting furnaces.

The archaeological record of iron production in Britain exhibits apparent different intensities of activity depending upon the time period. This is however most likely due to the varying intensity of investigation that has occurred with respect to the different periods and the survival of identifiable diagnostic features. Roman iron production is somewhat better attested than that of either the preceding Iron Age or the later Early Medieval periods. This may be partly due to a possibly greater

demand for iron from the population and the quantity of research undertaken into the organisation of the Roman territory of Britannia. A good example of the level of identified iron production and working sites would be the study of Leicestershire, Rutland and Northampton region undertaken by Condon (1997). The identification of the intensity of iron production and working in the East Midlands by Condon was acknowledged as being “far from comprehensive” (Condon 1997: 2). This suggests that the major sites identified within the site distribution were the focus of work due to the relative ease with which they could be located. Other sites may have been overlooked due to subsequent plough damage (Condon 1997: 2), or because they were seen as minor sites in comparison. Condon recognised that while there is a group of smelting sites located on a deposit of iron stone, the smelters may have had access to other iron-bearing raw materials. Other sites in the region within the Fenland environments have access to bog ore, this is stated as a presumption by Condon (Condon 1997: 2).

A total of 19 major smelting sites are addressed within Condon’s study. The complete range of sites is listed in a gazetteer at the end of the paper, which categorises the sites based upon operation intensity as measured by quantity of recovered material. In the case of iron working, the classification appears to have been more linguistic than meaningful as both smithing and forging can be interpreted as the same process (Condon 1997: 15-16). The paper further describes the availability of iron ores to smelters based upon the depth at which the deposit occurs. The argument is that Roman smelters would only access materials that were available at depths of up to 3m based upon the quarry pits found in the region (Condon 1997: 2). This may be partly due to the size of the exploitable deposits which cover a relatively large area, and thus would not require extensive excavation to extract efficiently until the depth reached beyond 1m. This may explain why bog ores appear to be sought during the Iron Age rather than bedded ores.

Much of Condon’s study is concerned with the analysis and conveying of the assumed increase in organisation that occurred with the appearance of Roman administration. The recognition of skilled Iron Age iron workers is noteworthy (Condon 1997: 4). Although the reported lack of evidence for specialist production may reflect the level of identification and importance placed upon prehistoric sites, rather than there being a genuine lack of specialism. The sites themselves are split into 3 general categories, based upon size and geographic setting. Beginning with household production the author describes limited, apparently short-term iron working as the least sophisticated, being reliant upon itinerant smiths to repair broken tools and forge replacements. Condon also suggests, most likely erroneously, that the inhabitants of these minor agricultural settlements were capable of operating a successful smelting operation (Condon 1997: 4). Here he suggests that the populace would gather the materials for an iron smelt and conduct the production themselves. Given that agriculture is a very different occupation to iron smelting, there would be a distinct lack of specialist knowledge in this circumstance which would likely prevent the smelting being successful. The ability to carefully

control the reaction conditions is more complex than the firing of pottery, which was a relatively common household practice prior to the Roman conquest.

The next stage in the categorisation is that of specialists supported by villa-complexes. This is a natural progression resulting from a larger sedentary community based around a single administrative hub. Within this context iron production had a reliable demand for both primary and secondary products. These being iron from smelting operations, most likely iron billets produced from consolidated blooms, and worked ferrous object produced by smiths. Condrón finishes the categorisation by considering urban-based workshops and specialised production centres. These most likely reflect an increase in scale and a concentration of Roman manufacturing ability, which are more identifiable in both the archaeological record.

A large body of work has been conducted by Peter Crew examining all stages of ironworking from ore processing to iron bar production. Some of the work was experiential, while other aspects were deliberate experiments to examine the impact and behaviour of specific variables (Crew 2013). Some of this work has been highly influential in shaping out current understanding of the mechanics and underlying chemistry of successful iron production. One such instance was the use of multiple thermocouples in XP41 (experiment 41) to record the temperature gradient within the furnace across the blowing axis (Crew 2013: 34, 35). The temperatures recorded during this experiment showed that the hottest part of the furnace is approximately level with, and slightly above the tuyère opening during pre-heating, while the bloom typically forms just below this as the 1100°C isotherm descends during bloom formation (Crew 2013: figure 12, figure 14). This isothermic region can be deflected by the developing bloom towards the furnace wall (Crew 2013: 34), which explains why in many cases the iron bloom is found to be very close, or adhering to the furnace wall near the tuyère.

Crew has undertaken multiple smelts investigating the use of different ore types, including bog ore, sideritic ironstones and hard rock ores such as haematite (Crew 2013: 37-42). The reaction conditions for each ore type were recorded as being different for optimal metal recovery. The hard rock ores were the most challenging from which to produce a well consolidated bloom when using hand bellows capable of a 1000l/min draught (Crew 2013: 39). When mechanical bellows were used to produce a similar air supply, it was found that the resultant conditions were too reducing, producing slags with low iron content which could not be tapped from the furnace. While the steely bloom was well consolidated there was also a notable quantity of cast iron produced as a block on top of the bloom (Crew 2013: figure 19). This result provides information concerning two distinct aspects of the successful smelting of hard rock ores in Cumbria and the Forest of Dean where haematite ores were exploited by both Roman and Medieval smelters. Firstly, as the ores contain little gangue when compared to sideritic ironstones and bog ore, a significant contribution must be made by the furnace

clay in order to produce appreciable quantities of tapable slag (Crew 2013: 39). Secondly the impact of mechanical bellows upon the smelt, even when set to produce a draft of mathematically the same volume per minute, resulted in a greater reducing atmosphere. This would strongly suggest that hand bellows need to be operated at a faster rate to produce a similar draft. The intermittent draught produced by hand bellows will cause the overall air supply to be less than that of mechanical bellows which run constantly. This constant and consistently greater oxygen supply results in a more reducing atmosphere which causes the greater iron recovery and iron poor slags observed in several experimental smelts (Crew 2013). Crew suggests that the design of the furnace may have been different and that a more efficient air delivery system may be required to smelt these types of ore with greater success (Crew 2013: 39).

Smelting sideritic and bog ores was generally more successful. Crew began smelting bog ores in small bowl furnaces, with a domed top and then a later small chimney. Small spongy blooms were produced although the slag formed was noted as being “quite unlike those from excavations” (Crew 2013: 32). These smelts were based upon work by Wynne and Tylecote (1958), and illustrate the early beginnings of iron smelting experiments which usually met with limited success. In 1987 Crew made an attempt to replicate results obtained by Tylecote *et al.* (1971) in a low shaft furnace. This again met with limited success as the proposed draught of 300l/min was found to be too great for the clay furnace, even with the thin, 150mm thick walls (Crew 2013: 32).

Following the limited success of the third furnace design, Crew increased both the wall thickness and the furnace bed depth to 200mm and 350mm respectively in furnace 4 (Crew 2013: 32). The furnace was built in 1988, and the first smelt conducted in 1991 (XP17) which produced the first reasonable consolidated bloom (Crew 1991). The reasons suggested for the more successful bloom production were the greater heat retention afforded by the increased thickness of the furnace walls, which allows a larger desirable hot zone to occur, and the increased residence time of the ore due to the greater height, which allows for more complete reduction and consolidation of the metal (Crew 2013: 32). These proposals would appear to be fairly reliable, due to the increased success of subsequent smelts (Crew 2013). The slags produced from these early experiments were green and glassy, with low iron content. This was attributed to the high blowing rate causing the reaction atmosphere to be too reducing (Crew 2013: 32). The variability of the ores used in these early experiments was one of the factors identified for the limited successes. Crew’s statement (2013: 32) that some of the ores were of too poor quality, but that this was only known when they were analysed years later, would seem to indicate that there was a lack of direct observation of the ore quality during preparation. As I have experienced in my own experiment discussed in chapter 4, it is noticeable when ore is of poor quality. This is due to increases in both the hardness and perceived mass of the ores observed during processing. By recording these observations, the later use of instrumental analysis would have

confirmed that the ore used by Crew in his early work was of poorer quality, rather than demonstrating it for the first time.

Experiment 56 was the first to produce tap slag (Crew 2013: 39), which would demonstrate the increased familiarity and understanding of the processes involved between the earlier experiments, where even bloom production was unreliable, to the successful production of a consolidated bloom with associated flowing tap slags. Crew attributes the more successful smelting of the sideritic ironstones when compared to the bog ore smelting to increased experience based upon previous attempts (Crew 2013: 39).

In light of the large body of research and the gradual improvements towards replicating ancient iron production, Crew made several suggestions for progressing experimental smelting. He states that ores benefit from hand sorting during crushing to remove the “obviously poor or contaminated material” (Crew 2013: 46), and that washing can also remove or reduce the clayey and sandy fractions which accompany the desired ore (Crew 2013: 46). The impact of this sorting is also noted by the finding of discarded ore during excavation (Crew 2013: 46), although the quality of the pieces found during excavation may not always be representative of what was incorporated into the smelting charge.

The continuing experimental investigation of iron smelting requires the reporting of both success and failure in order to present both positive and negative findings which may inform future work and interpretations (Crew 2013: 47). Crew rightly points out that not all ancient smelts met with success (Crew 2013: 46), which demonstrates how, even with far greater experience, a smelt may not function as anticipated.

To increase the reliability and comparability of experimental results it was proposed that a permanent, universal experimental platform be established at which all raw materials and products could be stored for use and study (Crew 2013: 47). By doing so, it would enable more detailed and more easily repeatable sets of experiments to be conducted investigating specific aspects or mechanics of iron production. This would be far more informative than comparing multiple experiments from different locations with several different variables between them, and allow for longer periods of experimentation approximating more closely to what may have occurred in the past. Lastly a permanent platform would also allow for a closer assessment of bloom refining techniques and production of workable bars as the conditions in which the smithing occurred would have greater similarity, reducing the variables impacting upon the finished product to the bloom and charcoal compositions.

### **3.4 Bloom smithing: A case study for data collection**

Building upon the known distribution and production of Roman ferrous artefacts, as described by studies such as the Condron paper, Sim (1998) undertook an experimental study of secondary iron working.

Initially undertaken as a PhD thesis, and later published as a British Archaeological Report volume, Sim's work is a significant demonstration of a successful experimental investigation into ferrous metallurgy. Sim undertook experimental replication projects examining the processes of bloom consolidation and refining as well as artefact manufacture (Sim 1998). During the processes of forging both the bloom and the refined iron into the various artefacts concerned with his study, Sim collected as much data and material as possible to produce the most complete account of the processes. This included hammerscale distribution and quantity (Sim 1998: 140-145), metallographic examinations of the material at the different stages of working, alterations in mass throughout working and the time taken to complete the operation for each artefact.

Notably the collection of hammerscale data is rarely undertaken during experimental work. This is an important step in understanding the site formation processes of smithy sites, as on the basis of the quantity of hammerscale produced from a single artefact the quantity of material worked at a site during a given period can then be estimated from the material recovered from the floor. Naturally this is based on the assumption that hammerscale was not regularly gathered and removed from the workspace. This assumption may be slightly flawed in that intensive ironworking will produce large quantities of hammerscale which would have to be removed. The processes of folding and welding produce spheroidal slags (Dungworth and Wilkes 2009) which can be dangerous underfoot, and would have to be removed, or at least swept away from the main work area for safety.

Unfortunately the collection of hammerscale from contexts associated with iron smithing hearths during excavation is still relatively rare. This is partly due to the difficulty of identifying hammerscale during excavation, although this can be remedied by applying magnetic detection to a soil sample. The identification of hammerscale during excavation can provide greater evidence for iron smithing as smithing hearth bottoms may not always be present.

The direct comparison between the experimental replica material and the archaeological originals is a crucial part of any experimental work. This allows for the success of the experiment to be assessed based upon microscopic features and analytical data such as hardness values and elemental composition, rather than macroscopic appearance alone.

One aspect of bloom refining which Crew investigated in detail was the production and possible reason for the shape of currency bars. The first aspect of forging the bloom is the consolidation of the metallic portions which comprise the irregular bloom body. Crew discusses the effect of leaving the

bloom in the hearth for too long, where the incorporated slag will fully liquefy and cause the separate iron pieces to become dissociated and lost (Crew 1991). For this reason, it is more likely that the first consolidation occurred immediately after bloom extraction while the slag was still hot, but not fully liquid. Crew described the colour of the bloom as bright red, and the process of hammering to be done very gently (Crew 1991: 163). This is preferable to aggressive, hard hammering as it will prevent the larger, cooling slag inclusions from fracturing and the subsequent loss of metallic portions. Regular heating between every two or three strikes is required to keep the bloom warm, this prevents it shattering during working on the anvil (Crew 1991: 163). This is a lengthy process, with the half bloom used having a mass of 792g taking 12 reheats over five hours (Crew 1991: 163). The final billet had a mass of 642g, while the combined mass of slags produced from the process 385g. The mass of the billet when adjusted to account for the entire bloom represents a yield of approximately 36% from the original ore. The net increase in mass of smithing slag is a result of fuel ash incorporation and interaction with the billet surface during smithing (Crew 1991: 163).

The billet itself was found to be unsuitable for forging due to a great quantity of trapped slag, with a further three hours of vigorous hammering required before it was considered workable (Crew 1991: 163). This would suggest that the bloom did not have a sufficiently high enough internal temperature during the initial consolidation.

The properties of the produced metal have a significant impact on the how it behaves during forging. The three bar productions discussed by Wang and Crew (2013) demonstrate how heterogeneous material can have different working properties depending on carbon and phosphorus content, as well as the presence of slag inclusions, and the possible influence of trace element abundance (Wang and Crew 2013: 399, 400).

Problems of bar and billet fracturing are observed by Wang and Crew (2013) where transverse cracks appeared during cooling, which were thought to be caused by slag inclusions with high melting temperatures (Wang and Crew 2013: 394). As many slag inclusions were reduced and elongated during working, it is difficult to attribute the bar fracturing entirely to the presence of slag inclusions. It is likely that they may facilitate fracture propagation when in greater abundance by providing a point of force concentration for fractures to begin at when in high enough abundance (Wang and Crew 2013: 399). This may provide some insight into why currency bars possess their distinctive shape. In order to produce a long, thin bar, with a forged socket on one end, very little slag must be present. This would suggest that the shape of the bar would be seen as some form of quality assurance, particularly in the case of long distance trade via intermediaries (Crew 1994: 346, 347). While the insights of Crew into the production and technical requirements of currency bars has furthered the understanding of bloom to bar ironworking it highlights the current lack of capability possessed by modern experimenters regarding the working of bloomery iron.



Serneels and Crew (1997) compiled a series of analyses examining the composition of smelting and smithing slags. This study clearly demonstrates the declining Fe and P content of the material from ore to large smithing slags (Serneels and Crew 1997: 80). The hammerscale and anvil slags are significantly richer in iron than any of the large scale slags. This is to be expected as they are formed from the surface of the worked metal interacting with fuel ash, and as such contain less silica than the ore derived smelting slags and bloom refining slags comprised mainly from adhering or trapped smelting slag.

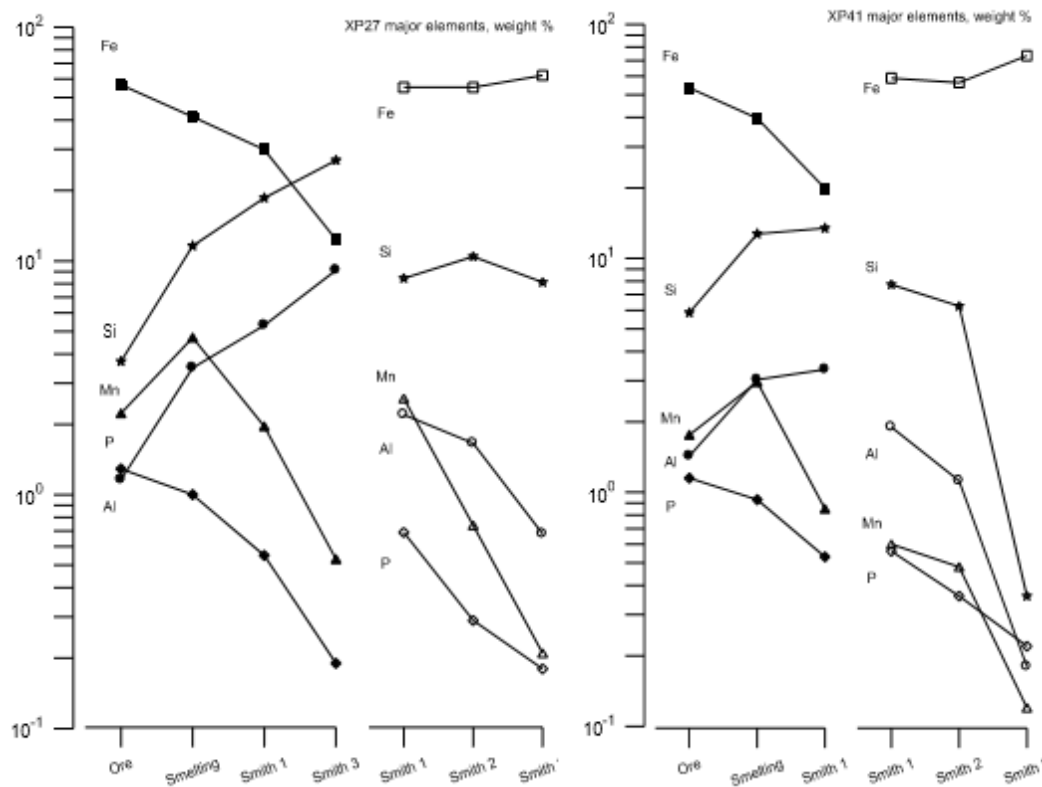


Figure 3.4.1 showing major element content (wt%) for ore, smelting slags and smithing slags (solid symbols) and for anvil slags and hammer scale (open symbols) (after Serneels and Crew 1997: figure 1).

The difference in perceived mass between smelting and smithing slags is due to a decrease in iron content. This difference in perceived mass is one of the major criteria for identification during desktop assessment.

### 3.5 Modern experimental smelts

Experimental smelting has also experienced some systematic investigations. As reflected by Condrón (Condrón 1997: 5), smithing is seen as the more sophisticated process, as the effort and skill required to produce an artefact from a bar is more clearly apparent than the skills required to produce a specific material from ore. The major difference between the two processes is that smelting is a system which is not directly observable, as the metal production occurs within the furnace where only very limited direct observation is possible, giving rise to the presumed simplicity of metal extraction.

Taking the successes of Sim's work into consideration, the experimental portion of this study will also compare the material produced by an experimental smelt series to that of archaeological material produced by a similar process. This can be assessed by both the morphology of the pieces and also the microstructures which are present within the materials.

Cleere undertook a series of experimental smelts based upon Roman tap furnaces excavated at Holbeanwood, Sussex (Cleere 1971: 206). Drawing upon the extensive history of Wealden iron production, the local carbonate ores were used. The analysis of the ore by Cleere showed that the iron content was approximately 50%, with 10% SiO<sub>2</sub>, 3% CaO and a considerable quantity of CO<sub>2</sub> and water. The high carbon dioxide content would be expected as the ore is predominantly a hydrated carbonate mineral. The presence of 10% silica would act as a natural flux and aid slagging. These features combined with the natural lime would have helped to produce a clean ferritic iron, which explains why iron production in the Weald had been so successful and dominant within the literature.

The fuel used by Cleere was a carefully prepared charcoal, in line with excavated evidence. A random sample of the charcoal was assessed for which species of tree were represented. Birch and oak were found to dominate the fuel, which is reflective of the general distribution of trees within the mature Wealden forest (Cleere 1971: 207). The charcoal was initially sieved in order to remove material that was smaller than 2.5cm in size. This was done so that the fuel would more closely resemble fuel samples recovered from archaeological contexts, although the subsequent trials did not sieve the material as approximate only 5% of the fuel proved to be smaller than the desired dimensions (Cleere 1971: 207). Cleere also recognised that by sourcing fuel from a modern supplier other materials were incorporated within the charcoal, such as a piece of plywood, which would not have been available to smelters within the past.

Samples of the original furnace walls were analysed to identify a suitable clay for the experimental furnace construction. No traces of additional filler material were found to be present within the archaeological furnace walls. Ashdown Sand, a sand bearing clay which overlays the ore deposit, was found to correspond with the archaeological material. In order to maintain the maximum level of archaeological validity, and thus comparability between the experimental and archaeological material,

the furnace for the study was also constructed using Ashdown Sand from a nearby smelting site at Horam (Cleere 1971: 209).

The ore preparation undertaken by Cleere followed the archaeologically confirmed process of crushing, roasting and size selection. It was found that crushing the ore into pieces of approximately 7.5cm in size was the most efficient method to produce roasted ore of a size suitable for use with the 2.5cm charcoal (Cleere 1971: 208). The process of roasting was conducted in a roasting pit 2.4m x 0.3m x 0.3m in size. Unlike the archaeological example found at Bardow in 1968, the pit for Cleere's study was not lined with stone, but puddled clay (Cleere 1971: 208). This may have been due to the lack of available stone with which to line the pit, although the success of the roasting operation was not adversely affected. Observation of the ore during roasting proved to be the most effective way of assessing the progress of the reduction. The colour of the ore being a clear and very important indicator of the redox state of the iron, starting at a creamy-pink or light grey due to natural variability in the carbonate ore, to a maroon when reduced to  $\text{Fe}_2\text{O}_3$  and later a blue-black when further reduced to  $\text{Fe}_3\text{O}_4$  (Cleere 1971: 208).

This further state of ore reduction may not be required for a successful smelt as the ore will be further reduced in the furnace. In the case of carbonate ores the roasting process causes further fragmentation by cracking and explosion. Cleere's recorded observations at every stage of the smelting process assist readers to fully understand the thought process of the researcher, particularly with regards to the events of the smelting trials where the cracking and repair of the furnace was well recorded (Cleere 1971: 209-10).

Cleere acknowledges that no examples of bellows used for smelting are known (Cleere 1971: 210). This leaves the means of delivering the draught for the smelt open to interpretation. Whether it was achieved using bag bellows, as most commonly seen in African smelting, and assumed to be utilised in prehistoric Europe, or by the use of more sophisticated board-based varieties is unknown.

By regulating the quantity of the charge placed into the furnace at each charging the quantity and ratio of ore and charcoal was controlled. This allowed the different trials to be compared more effectively as the charge additions were accounted for. In order that the slag could be tapped from the furnace a sandstone block was used to block the tap arch. This proved to be an unsuitable material as the block became fused to a mass of cold slag at the bottom of the furnace. In recognition of this, Cleere adapted the tap arch plug and used turf in place of sandstone. This alteration was far more successful as the organic portion of the turf was burnt away by the high temperatures, in excess of  $1200^\circ\text{C}$ , leaving an aperture through which hot molten slag flowed continuously (Cleere 1971: 212).

The use of organic material as a means of providing a heat source through which liquid slag can drain may also have an impact upon pit furnace technology. Here unseasoned wood or wet straw is placed

in the base of the furnace, mostly in order to support the developing bloom; however as it combusts the heat generated will ensure that the slag around the bloom is kept hot as it drains into the pit.

Research conducted by Saunder and Williams in 2002 suggests that the success of a smelt depends largely upon the blast rate. By experimentation the optimal blast was determined as being between 1.2- 1.5 l/min (Saunder and Williams 2002) . Lower blast rates appear to limit the production of liquid slag, this is accepted as being of critical importance for the successful production of a metallic bloom, as the liquid slag will surround the reduced metal and prevent oxidation (Saunder and Williams III 2002: 6). The figure below illustrates the effect of different blast rates upon bloom development.

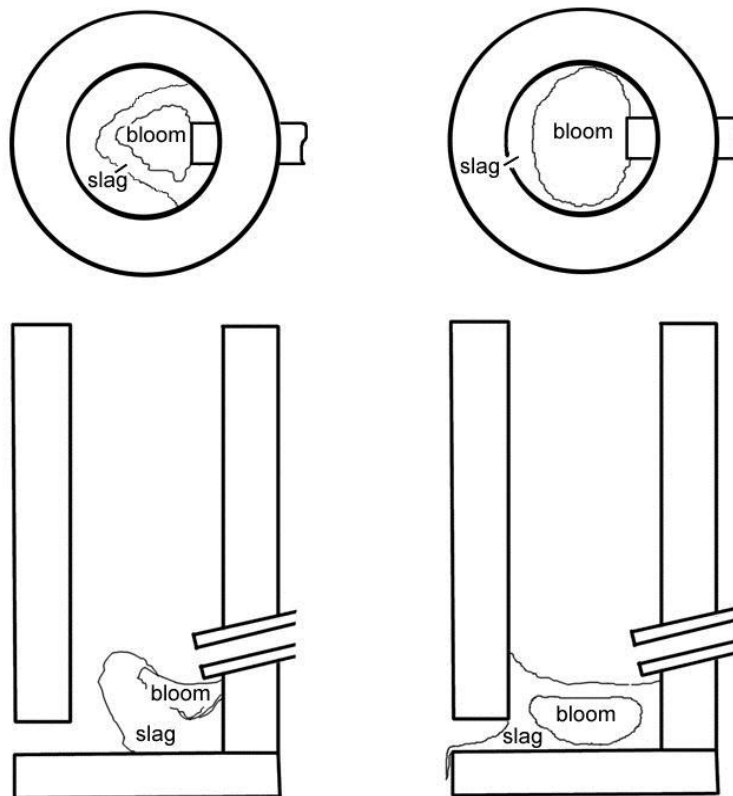


*Figure 3.5.1: Showing the effects of higher blast rate upon slag and bloom formation. Lower blast rate (left) and higher blast rate with resultant liquid slag bath (right) (Saunder and Williams III 2002: figure 3, 4).*

The production of ferritic iron is dependent upon having a significant proportion of available iron within the slag for successful decarburisation of the solid bloom. Saunder and Williams (2002) hypothesized, based upon the work of Espelund (1997), that the reaction between the available FeO in the liquid slag and carbon within the bloom results in a dilution of carbon content and the production of more reducing agent (CO) (Saunder and Williams 2002: 7). Further to this, the lack of “slag bath” reactions is identified as the possible reason that previous researchers experienced difficulty when consolidating blooms. This is because the majority of the metallic iron is produced in stack reduction,

where it exists as isolated, loosely accumulated particles, rather than lower down in the shaft within the slag, forming a denser bloom (Saunders and Williams 2002: 7).

The other method of decarburising blooms during smelting is to introduce slag as part of the smelting charge. It is possible that slags were recycled as a means of maximising the quantity of iron produced when demand was particularly high (Saunders and Williams 2002: 8). This works in a similar manner to the reactions within the liquid slag by producing more metallic iron from the partially-reduced iron oxides. If the slag was formed at the same or lower temperature as the smelt it is introduced to, it will melt and add to the quantity of liquid slag at the furnace base. Saunders and Williams propose that this further enhances the smelt process by increasing the thermal and chemical resources around the developing bloom, enabling it to grow larger and with a greater quantity of malleable iron present (Saunders and Williams 2002: 7-8).

Another aspect of this particular bloomery smelting study that demonstrates the success of the experiment is the comparison of data generated with that of previously undertaken attempts. By doing so the improvements in iron retention, in terms of quantity per hour with regards to the finished bloom, is highly distinct (Saunders and Williams 2002: 8). They suggested that the increase in quantity was derived from the increased production of liquid slag during the smelt.

The shortcomings of this particular study were well examined by the researchers, who acknowledge that “the first goal of any investigator in experimental archaeology should be to match the results of the ancient craftsman” (Saunders and Williams 2002: 9). With this in mind the use of mechanical air blowers for bloomery iron smelting experiments is highlighted as being incompatible with the aims of matching and replicating ancient processes. Based upon the work of Rehder (2000: 77) a blast rate of 3600 l/min could be maintained indefinitely by a single operator. This is based upon the use of large bellows more akin to those represented within the historical texts of Biringuccio [1540] and Agricola [1556], rather than smaller types seen in ethnographic studies. There is a clear discrepancy between the two blast rates of the Saunders and Williams study and that calculated by Rehder. The former suggests a very low blast rate which would seem overly small given the size of most bellows used experimentally, while the latter proposes a blast rate which would seem excessively large for a single operator to maintain without the use of mechanical assistance.

Crew modified a series of bog ore smelts based upon this higher blast rate proposed by Saunders and Williams (2002), and found that it had several negative impacts upon the process and resultant products (Crew *et al.* 2011). In one case, Crew’s experiment 92, a block of cast iron was produced in place of a bloom and low iron slags were formed (Crew *et al.* 2011). These smelts were conducted using a lower grade ore than the smelts of Saunders and Williams, which led Crew

to argue that the use of a higher grade ore, with a lower blowing rate and a reduced charcoal to ore ratio would have yielded a more normal bloom and tap slags (Crew *et al.* 2011).

The experimental examination of pit furnaces appears to have been less intensive. This may in part be due to the prevalence of tapping furnaces within the archaeological record, as pit furnaces appear to have a more restricted geographic distribution. Saunder and Williams (2002: 9) stated that future work would be carried out into the production of iron within pit furnaces, although this has yet to be published.

### **3.6 The Lejre Project**

A major experimental comparative study of pit and tapping furnace smelting was undertaken at Lejre by members of the Prehistoric open-air museum, Eindhoven (Boonstra *et al.* 1997). This study appears to have been designed with the goal of producing an iron bloom in a pit furnace. This represents the typical mentality of experimental iron smelting that producing a bloom is the definition of success, while not considering the production of slag. While accurately recording the smelting process and the materials used, the objective of producing a specific material appears to have been neglected in preference of simply producing a metallic bloom. The researchers did not state within the paper what material they aimed to produce, whether it was ferritic iron, phosphoric iron or a hypo-eutectoid carbon steel.

The two furnaces were constructed to approximately the same dimensions, conical superstructures with internal diameters of 36cm at ground level and 25cm at the top of the cone. The tapping furnace was slightly shorter at 72cm tall, while the pit furnace was 80cm tall (Boonstra *et al.* 1997: 2, 6).

The ore used in both smelts was a local bog ore from Stiphout with a significant P content of 4.46%. The ore itself also contained vivianite (Boonstra *et al.* 1997: 2), a blue coloured hydrated iron phosphate mineral. It is unknown if the presence of this blue mineral would have aided prehistoric smelters in the identification of suitable ores, although it is a possibility. The ore was processed firstly by breaking the bog ore into pieces approximately the size of a fist and then roasted for 4 hours in a charcoal fire (Boonstra *et al.* 1997: 2). The ore had previously been allowed to dry before being processed as freshly extracted bog ores tend to contain a significant level of moisture.

The roasted ore varied in colour from a dull maroon red to a grey-blue similar to that described by Cleere (Cleere 1971: 208). This demonstrates the varying levels of reduction achieved within the heterogeneous environment of the roasting pit.

The experimental procedure for both smelts included a 3 hour preheating with 2 hours using wood and the final hour charcoal and bellows (Boonstra *et al.* 1997: 4, 7). The more recent work of Saunder

and Williams has argued that this stage may not need to be as lengthy (Saunders and Williams 2002: 3), although the use of bellows by Boonstra *et al.* may have reduced the blast rate resulting in the furnace taking longer to reach optimum operating temperature. As such a preheat cycle will aid the smelting process by introducing the initial charge of charcoal at an elevated temperature, although the temperature achieved by the preheating will be dependent upon the quantity of fuel consumed.

The pit furnace constructed by Boonstra *et al.* had an unusual floor, constructed as a temporary platform supported by piles, rather than the more common interpretation of wood or straw packing.

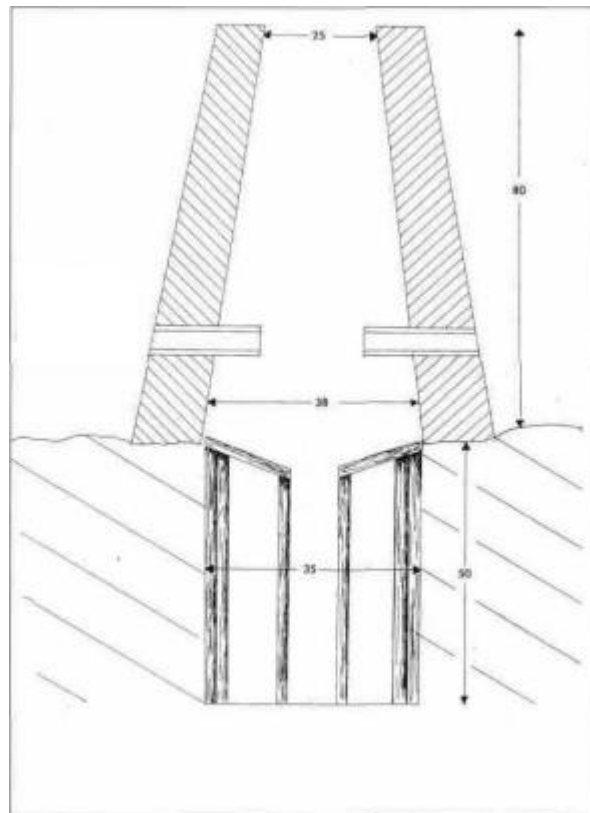


*Figure 3.6.1: Showing the experimental pit furnace constructed as part of the Lejre project (Boonstra et al. 1997: 6).*

The pit itself was dug to 50cm deep, which would suggest that it was intended for the production of large blooms. The researchers admit that the furnace is not based upon any specific excavation (Boonstra *et al.* 1997: 1) which may place an element of doubt over the validity of the final construction.

The smelt used 45kg of ore in a fuel:ore ratio of 1:1 over a duration of 5.5 hours. This was half the quantity of material used in the first smelt in the tapping furnace. The duration was drastically reduced from the 14 hours operating time of the previous experiment; the authors cite the reduction in operating time was due to adverse weather conditions (Boonstra *et al.* 1997: 7). A pair of bellows,

one positioned on either side of the furnace, was used to supply the blast for the smelt, each delivering a volume of approximately 40l. A small recharging of 1.5kg of both ore and charcoal was undertaken every 10-15 minutes as space at the top of the cone became available.

Even with this significantly shorter smelting time, a comparably substantial raw bloom of 18.7kg was produced in comparison to the tapping furnace raw bloom had a mass of 27kg (Boonstra *et al.* 1997: 4, 7).

The iron produced by the tapping furnace, which was carefully monitored so that slag was constantly removed during operation, was found to contain 0.7% P (Boonstra *et al.* 1997: 5). This provides very strong evidence for the production of phosphoric iron based upon the use of bog ore and slag-bloom contact time being kept to a minimum. Taking the findings of these experiments into account, the experimental element of my study will also attempt to reduce the time that slag remains in contact with the bloom, while ensuring that the slag produced is not in the solid state.

The main fault of this study was the temporary floor used in the pit furnace. This required a relatively significant level of engineering to function, with the angling of the temporary surface, lining with clay and covering with wet boards during the firing of the furnace itself prior to use (Boonstra *et al.* 1997: 6). A pit filling of combustible material, which appears to be more regularly encountered within the archaeological record, would have been simpler to use. In the case of the conical furnace design it would be more likely that straw would have been used as it would be easier to load into the pit through the narrower opening, rather than larger pieces of wood. The straw could be placed after firing the superstructure, which may account for the lower surface of some furnace bottoms encountered at locations in East Yorkshire being irregular and containing some larger fuel impressions.

The excavation of the pit furnace after smelting allowed for the maximum recovery of produced material, and also for the observation of the furnace bottom formation process. This also revealed why slag had escaped through one of the tuyères (Boonstra *et al.* 1997: 7). As the slag could not drain through the fired ceramic that formed on the temporary furnace floor, it had to drain through the central hole. Once this became clogged, slag accumulated on the furnace floor and formed a seal over it so that no slag could drain but through the central aperture when it was re-opened. As this proved difficult due to bloom formation, the slag continued to pool in the bottom of the furnace, until it surrounded the tuyères, when the only available avenue of escape for the liquid slag was via the tuyères. This proves that the furnace floor, being lined with the same clay that the shaft was built from, did not allow the slag to fully drain into the pit, suggesting that this method was not likely to have been employed in the past.



### 3.7 Calculating optimum smelting yields

Senn *et al.* (2010) undertook a series of five smelts in order to assess the overall success of experimental smelting in comparison to archaeological examples from sites near the Gonzen Mountains, Switzerland. The experiments were undertaken using a hematite ore with a mean Fe content of 54% and 0.06% P (Senn *et al.* 2010: 137). This demonstrates the difference between a hematite-based iron source and a bog ore which contains significantly more phosphorus.

This study, unlike those previously discussed, illustrates how both the optimum and actual yield of iron is calculated. Within the experiments the quantity of iron produced varied from 1.5kg to 4.4kg. The experimental yields were calculated by dividing the quantity of produced iron by the amount of iron present in 30kg of roasted ore, which constituted the total charge of ore for each smelt. As a result of the varying mass of iron produced by the smelts, the yield ranged from 9-26% (Senn *et al.* 2010: 136). The optimum yield for the experiments was calculated by:

$$\frac{[(\text{Quantity of iron in 30kg ore} - \text{amount of iron bound in slag}) / \text{Quantity of iron in 30kg ore}] \times 100}{\text{Quantity of iron in 30kg ore}} = \text{yield \%}.$$

This is based upon the assumption that slags produced from smelting ores of low calcium content can be described as a mixture of fayalite ( $\text{Fe}_2\text{SiO}_4$ ), hercynite ( $\text{FeAl}_2\text{O}_4$ ) and a glassy matrix (Senn *et al.* 2010: 136).

Taking the calculated average values for the materials used in the study, the 16.8kg of iron present in the roasted ore is divided between 5.7kg being retained in the slag and 11.1kg being reduced to metallic iron. This represents an optimum yield of 66% for the direct process using the given materials. The problem with this optimum calculation is that it does not take into account the existence of wüstite ( $\text{FeO}$ ), which can also crystallize in bloomery slag. The researchers recognise that it is not possible to estimate the quantity of iron that will be partially reduced to wüstite, rather than fully reduced to metallic iron, thus the effective yield of all of the experimental smelts were expected to be below the optimum 66% (Senn *et al.* 2010: 136).

These calculations alone are not enough to provide a sufficiently accurate mass balance and yield. For this chemical compositions of ore, slag, ash and furnace lining are required and they allow for better comparison between optimum and practical yields. The calculations will not alter the mass balances of the experiments, but they will take into account the different types of slag (tap and furnace slags) formed. This will also allow for an interpretation of the effects of the different types of slag in the smelting process.

All elements, with the exception of trace elements, are expressed as oxides in accordance with geochemical examinations. The generated data are then normalised to 100% and the major contributors, ferric oxide, silica and alumina, are recalculated as elements for subsequent calculations (Senn *et al.* 2010: 138). The researchers based the mean values for unroasted ore upon nine analyses on single rock fragments which exhibited a maximum of morphological variations, in an attempt to account for the heterogeneity within the raw material. For the roasted ore, three analyses were made upon each of several similar fragments as the processing of the roasted ore limited the variation across the material (Senn *et al.* 2010: 138).

The composition of the ore, as detected by instrumental analysis, was found to be dominated by ferric oxide, with minor components of silica, calcium oxide and manganese oxide. It was poor in alumina compared to other Swiss ores and had a relatively high abundant trace of barium (Senn *et al.* 2010: 138).

Within the smelt, ferric oxide, part of the  $P_2O_5$  present and the siderophile trace elements Ni, Co, Cu and As are reduced, while the other components of the ore contribute towards slag formation. Sulphur is lost to the atmosphere during reduction and was not found in either the metallic bloom or the associated slags.

The slags were found to contain a more consistent Al/Si ratio than that which occurs within the ores. As the Al level is elevated in comparison to the ore, its source was interpreted to be the furnace lining.

The fuel ash contribution was based upon a sample of modern charcoal ash produced in other experiments conducted by Serneels (2002). Providing that the species and relative proportion of trees represented within the charcoal are the same as that which occurred within the charcoal used in the Senn *et al.* study, the use of different charcoal ash for analytical purposes does not invalidate the conclusions.

In comparison with Early Medieval Swiss archaeological material (Eschenlohr and Serneels 1991, Serneels 1993, Serneels and Beck 1998, Beck and Senn 2000, Eschenlohr 2001), it was found that the experimental furnace slags contained a greater proportion of iron. This was interpreted as arising from poor reduction of ore during the experiments (Senn *et al.* 2010: 142). Such a different outcome most likely reflects the difference in skill between the early medieval smelters and those undertaking the modern experimental reconstruction attempts. Many of the trace element concentrations varied between the archaeological and experimental material, this is due to the different ores used in the smelts.

Following the comparison between the archaeological and experimental slags, which, in this case, exhibit a relatively close degree of similarity, the optimal operating temperature of the furnace was identified as being between 1100 - 1200°C (Senn *et al.* 2010: 144). This temperature range is

commonly identified within the literature and appears to have been the standard operating temperature for direct process smelting. A blast of 370 l/min and 620 l/min was delivered by bellows in the first and second experiments respectively (Senn *et al.* 2010: 133). Both experiments produced metallic iron and slag; however the second experiment proved to be more successful due to the higher blast rate and resultant higher temperature achieved (Senn *et al.* 2010). The researchers did not record the temperatures achieved at various parts of the furnace during smelting (Senn *et al.* 2010). This is one of the major shortcomings of this experimental series, as it prevents a full understanding of the smelting conditions.

Karbowniczek (2006) examined the theoretical basis of iron smelting from a scientific perspective. His study evaluates the conditions at which direct reduction occurs at a temperature of 1200°C. Beginning with the most common form of iron oxide ( $\text{Fe}_2\text{O}_3$ ), he details the full reduction process for temperatures above and below 572°C. The reason for this being that below this temperature metallic iron can be produced directly from  $\text{Fe}_2\text{O}_3$  without experiencing partial reduction to FeO (Karbowniczek 2006: 150), unlike what occurs within iron smelting furnaces operating at the previously identified optimum temperature of 1200°C.

The mass balance equations for the theoretical model are clearly stated based upon the use of 1kg of ore and the production of a 1kg slag block for calculation simplicity (Kerbowniczek 2006: 151-153). This is on a very small scale for a real iron smelt, although the quantities of ore and fuel can be increased to compensate for the increase in scale.

The findings of the theoretical framework show that 1kg  $\text{Fe}_2\text{O}_3$ , containing approximately 50-60% Fe, requires 0.954kg CO to be fully reduced, yielding 0.700kg Fe and 1.493Kg  $\text{CO}_2$  (Karbowniczek 2006: 152).

Similarly 1.500kg of ore containing 60% Fe would be required for a 1kg slag block, assuming that the slag contained 60% FeO. The results of the calculations are presented in a short table which do not truly represent or clarify the different starting parameters of varying iron content. Thus the conditions are present as a range, rather than fixed values (Kerbowniczek 2006: 154). In reality this does not mean that the maximum starting iron content will result in the stated maximum quantity of metallic iron being produced.

The major shortcoming of this study is the lack of practical testing, which the researcher acknowledges towards the end of the paper (Kerbowniczek 2006: 154). Overall Kerbowniczek's (2006) examination gives a brief overview of the process which this study aims to undertake. It does not provide any actual material or results on which to base firm conclusions. Theoretical models can explain what occurs within a process which is not directly observable, like smelting; however they illustrate an idealised case where the process operates in the ideal manner with no heterogeneity within the reaction conditions. This lack of real experimental data makes my study less useful than

those which have undertaken physical experimentation which have generated real data with which to derive meaningful understanding.

### **3.8 The analysis of archaeological material**

*In situ* bloom and slag material are rarely recovered archaeologically from the same site. A notable exception is that of Heeten in the Netherlands (Godfrey 2007). Here a metallic bloom, slag and ferrous objects were recovered and, following subsequent metallographic and instrumental analysis of the artefacts and bloom, were found to be of phosphoric iron (Godfrey 2007: 186, Godfrey and van Nie 2004: 1119).

The slag block from Heeten examined by Godfrey underwent both microscopy and x-ray diffraction (XRD) in order to identify the various mineral phases that were present. Godfrey states that the mineralogical makeup of the slag indicates that the smelting conditions were relatively oxidising and that a large proportion of phosphorus was portioned into the slag. This is represented by the quantity of iron phosphate and newly formed calcium phosphate, which is not found in the original ore (Godfrey 2007: 182, 183). The quantity of calcium phosphate in the slag in comparison to the quantity of phosphorus in both slag and bloom material, indicate that a calcium phosphate material was not used as the source of phosphorus. As this material is stable in the slag, it is not possible for it have been responsible for the phosphorus content detected in the metallic bloom. This further supports findings that calcium phosphate cannot be used as a free phosphorus source for enrichment processes (Hall 2012).

The smelting site at Snorup, Jutland, was investigated preliminarily using magnetic susceptibility prospection. This identified a significant number (approximately 4000) of furnaces and possible furnaces within a relatively small area (Smekalova *et al.* 1993). Given favourable conditions, where slag pits were not covered with alluvial deposits of soil or sand, Smekalova *et al.* (1993: 101) state that it was possible to discern individual pits within clusters, their respective dimensions and approximate mass of slag responsible for the magnetic anomaly. The successful prospection of the site led to the identification of several large slag blocks and metal-bearing smelting products.

The material exhibits less regular phosphoric characteristics than the artefacts from Heeten (Godfrey 2007). Here it is observed that the objects contain greater proportions of arsenic, which has a similar effect upon iron as phosphorus, both in terms of colour and hardness. This is most commonly seen at weld joins where arsenic is segregated into a “white weld line”. Much like phosphorus, the arsenic content is dependent upon the ore used in the smelt. Both elements behave in a similar manner regarding the atomic lattice of iron, with regions of higher arsenic content typically containing less phosphorus. The slag blocks from the site are far larger than those of Heeten, in some cases as large

as 200kg (Voss 1996, Høst-Madsen and Buchwald 1999). The size of these slag blocks is a clear indication of the scale of production, and the furnaces in which they were generated. Jöns (1999) indicated that the phosphorus-rich bog ore available at the site had evidently been used, which is to be expected due to the distribution of bog ores across Denmark (Lyngstrøm 2011). Ganzelewski undertook metallurgical analysis of the ore and metallic products, describing the ferrous materials as ferritic iron with only a small quantity of phosphorus present (Ganzelewski 1997). The compositional range of phosphorus in this context is generally below 1%, so it is unclear what Ganzelewski classifies as a small quantity. To account for the difference in phosphorus content the researcher hypothesises that iron containing several percent phosphorus could have been produced, although the greater proportion had been lost by partitioning into the slag.

The studies of the archaeological material from Heeten and Snorup have demonstrated that the application of the correct instrumental techniques, in combination with microscopic observation, can yield a significant quantity of meaningful data upon which to base interpretations of the represented processes. It is worth noting that the description of elemental composition needs to be more accurate than that given by Ganzelewski (1997) to be truly meaningful. By presenting the data generated by this examination of phosphoric iron production in a numerical manner, this ambiguity will be mitigated.

Analysing both slags and metallic products will also help to illustrate the partitioning effect between metal and slag. This may also help to support or disprove the hypothesis of Ganzelewski (1997) concerning the possibility of producing phosphoric iron with an exceptionally high phosphorus content, which then undergoes a de-phosphorisation due to partitioning. The local de-phosphorisation effect on iron in the presence of slag inclusions with high basicity is recorded by Vega *et al.* (2003), which may result in the presence of high Ca/P inclusions within the slag (Wang and Crew 2013: 399).

Mineral identification by XRD analysis (Henderson 2000: 10-11), as demonstrated by Godfrey (2007), can yield further data with which to support the interpretations made during examination under the metallurgical microscope. The difficulty with this method is that the samples used for XRD may, or may not be, fully representative of the original material. This may particularly be the case if the slag produced during an experimental smelt is formed in heterogeneous conditions. To reduce the likelihood of misrepresentative data, multiple samples from several locations within the produced slag block and adhering slags should be taken. This would ensure a fuller picture in terms of the mineral phases formed within each distinct slag type, being more representative of the varying conditions within the furnace column.

The examination of iron smelting slags from the Holme region of East Yorkshire, particularly in proximity to Hasholme, was undertaken using both physical and chemical analytical methods (Clogg 1999: 82). The physical examination of a representative sample of the 5338kg of iron slags from

Welham Bridge identified 4 distinct morphological types; plano-convex furnace bottoms, elongated convex furnace bottoms, dense hemispherical chunks and large elliptical vesicular masses (Clogg 1999: 83). It was noted by Clogg that much of the material appeared complete, exhibiting well defined outer curved surfaces shaped by the associated furnace structures with which the slag was in contact (Clogg 1999: 83).

Of the 37 samples included within Clogg's representative corpus, 20 pieces were considered to be of the typical plano-convex form. The mean dimensions of these pieces were a radius of 180mm, a depth of 170mm and a mass of 12.7kg. These plano-convex furnace bottoms indicated that the furnaces in which they were formed had internal diameters between 300-400mm. The other characteristic features exhibited by these furnace bottoms were that the upper surface displayed a flowed texture and the curved base was comprised of small globules or dribbles of slag that were welded into the main mass. Little charcoal was evident upon the external surfaces, which is to be expected as it would be consumed by combustion as the furnace bottom forms (Clogg 1999: 83).

The group of elongated convex hearth bottoms was represented by 4 examples, with mean dimensions of 525mm in length, 373mm in breadth and 245mm in depth and an mean mass of 26.6kg (Clogg 1999: 83-84). In comparison with the typical plano-convex furnace hearth bottoms, these larger examples have a much more irregular upper surface with evidence of large charcoal inclusions and 2 well defined hollows in one example (Clogg 1999: 84). The presentation of the measurements of each piece clarified the distinction between the different classes, this allows the reader to quickly compare the groups and assess the differences in form, without having to rely on lengthy descriptions of each piece (Clogg 1999: 85).

The third group, comprised of 4 examples, exhibited a very regular shape, with a smooth, flat upper surface and a deep bowl. While the report describes these as large hemispherical pieces (Clogg 1999: 84), this description would appear to match that of a plano-convex hearth bottom (Bayley *et al.* 2001). Again the mean values of the radii, depth and mass are given as 255mm, 386mm and 45.75kg respectively (Clogg 1999: 84).

The final distinct class of slag forms from Welham Bridge included the largest pieces. These tended to exhibit compacted, clearly defined curved edges, suggesting that they were formed within a vertical containing structure. The overall form of the pieces was generally an irregular elliptical shape, with a mean radius of 327mm, mean depth of 354mm and a mean mass of 59.7kg. Large, clearly visible charcoal inclusions were present within the 7 examples that represented this group, some of this material was subsequently extracted for use in radiocarbon dating (Clogg 1999: 84).

The methods of dating slag assemblages rely predominantly upon associated finds to date the context in which the slags were found, such as ceramics, as well as slag morphology and charcoal inclusions for radiocarbon dating (Clogg 1999, Pine 2003: 57). A rough means of establishing chronological

period is by assessing the morphology of the iron slag. Iron Age slag for example is typically coarse, exhibiting larger charcoal inclusions in comparison to slags of later periods, whereas Roman slags tend to be far finer than those of the preceding Iron Age (Bayley *et al.* 2001). The size and form also inform regarding the technology that was employed in the smelting, which can also provide a loose chronological date which may be used as a preliminary measure when assessing a site (Bayley *et al.* 2001).

Internal examination of a selection of the representative sample revealed that group 1 (plano-convex furnace bottoms) exhibited increasing vesicularity away from the upper surface, with the slag forming a fairly solid mass, concentrating towards the upper corners. The charcoal inclusions were concentrated towards the extreme edges and the material displayed no form of zoning or layer separation within the examined cross sections (Clogg 1999: 84).

The group two material was far less dense, with large quantities of charcoal concentrated towards upper central regions with many pieces being up to 20mm in length. The slag within the elongated furnace bottoms was thinly distributed throughout the blocks, but did not show any apparent layering or concentration of solid slag material (Clogg 1999: 84-85).

The microstructural analysis of these slags showed the predominant components were wüstite, fayalite and a glassy non-crystalline phase. This is in line with the findings of other slag analyses, demonstrating that these three substances form the majority of all direct process iron smelting slags. Electron microprobe analysis (EMPA) was also undertaken on mounted samples after optical analyses to strengthen the identification of the phases present. Here the optical identification of fayalite was confirmed by iron: silicon ratios between 2.1:1 to 2.3:1.

The quantity of wüstite present had a very large variation across the analysed samples ranging from almost none to 55%. The size and shape of the basically dendritic wüstite was affected by the varied cooling regimes within different areas of the slag. Fine, well developed dendrites were present within the heterogeneous vesicular regions, whereas within the homogenous masses very little wüstite was evident (Clogg 1999: 85).

The identified glass phase was recorded in concentrations between 4-27%, being more prevalent within samples taken from larger homogenous regions. This directly reflects the temperature and slower cooling rates experienced in these homogenous slaggy areas. Very fine inclusions of high titanium content were observed within the glassy phase which consisted of approximately equal proportions of FeO and SiO<sub>2</sub>. Aluminium was present between levels of 12-18%, while there were also consistently high concentrations of calcium, potassium and phosphorus oxides (Clogg 1999: 87-88).

Following the work of Morton and Wingrove (1969), a ternary diagram of iron oxide, silica and anorthite ( $\text{Al}_2\text{CaSiO}_8$ ) was created based upon the bulk chemical composition of the representative material. Following this, the diagram demonstrated a working furnace temperature of approximately  $1150^\circ\text{C}$  in all cases (Clogg 1999: 89). This could indicate a significant level of control over the operating parameters within the furnaces or possibly indicate the consistent use of the same raw materials.

The shape and dimensions of the slag may imply an aspect of technology that was employed in their creation. Plano-convex material is well attested throughout early iron production, forming at the base of furnaces with the bloom resting on top and therefore taking on some of the features of the internal furnace structure. The evidence from Welham Bridge does not allow for a direct argument for the employment of a bowl or shaft furnace (Clogg 1999: 89). The slag pieces are generally smaller than those reported in McDonnell's 1988 report of the excavated ironworking slags found at North Cave, East Yorkshire. However, comparable elongated hearth bottoms were recovered from North Cave, which may suggest that a similar technology was in use at both sites, although the blocks from Welham Bridge are far larger. The depression in the upper surface of the slag blocks was used to argue for a double tuyère within the furnace structure (Clogg 1999: 90), although this may have more likely arisen from the metallic bloom resting upon the block of slag towards the end of the smelt. This would indicate that the smelting technology was of the pit furnace variety, rather than the tapping furnace system. Magnetic susceptibility testing would be able to resolve this outstanding issue regarding technological identification, following the work of Smekalova *et al.* 1993.

Recently in 2013, two furnace bottoms which approximately match the description of the group two samples in Clogg's (1999) study were found during a field walk, in which I participated as part of the HMS spring workshop (22-24 March 2013). This involved field visits to Holme-on-Spalding Moor, Hasholme Hall and Moores Farm, as well as a small piece of slag which is examined later in this thesis.

Clogg (1999: 90-91) further discusses the raw materials used in the Foulness Valley. Ore recovered from the same region as the recently found furnace bottoms proved to be of low quality, in terms of iron content, but this may not be representative of the iron ores used during the operational lifetime of the industry. It may be possible that the richest bog ores were exploited to the point of depletion and thus are no longer available. Other iron ore sources, such as the Frodingham ironstone beds on the south side of the Humber, have been discounted due to the difficulty of successfully smelting these ores and also the proximity of more easily accessible material (Clogg 1999: 91).

There is also another aspect to bog ores which makes their use in modern reconstruction experiments problematic. Bog ores form in a similar way to iron pan, typically where the iron is precipitated at a horizon where clay encounters the iron carrying water. Naturally this depends upon the hydrology and



geology of the location in question. If the hydrology has undergone significant change, such as by the implementation of modern field drains, the water content of the iron deposition horizon will be reduced, which prevents the formation of bog ore or iron pan. Areas where iron working has occurred in the past have, in some cases, experienced significant draining due to modern farming practices. This partially explains why some iron smelting sites occur in regions where there are no apparent iron ore sources available.

Another aspect of ore identification which may be problematic is the associating of ore fragments found at smelting sites to the material that was used during smelting. The site of Wakerley, Northamptonshire was excavated in 2005 and several iron smelting furnaces and associated features were discovered (Fell 2007). These features included three distinct oval pits which displayed a very clear red/brown colour indicative of burning. This combined with charcoal recovered from one of these features lead to their interpretation as ore roasting pits or channel hearths dating to the Saxon period (Fell 2007: 9, 22, 25).

Iron ore was found associated with the earlier Roman iron production on site. This is where the interpretation of surviving ore fragments becomes contentious. The report interprets the material as possible waste from the Roman iron smelting (Fell 2007: 92). By describing the remaining ore and charcoal as possible waste, this would suggest that the surviving ore was not deemed desirable by the smelters. If this is the case, then the material that was found on site is not representative of the ore that was placed within the furnace. This would bring into question the interpretation of ore samples found during excavation and any experiments based upon the use of material which closely matches the recovered pieces, which are likely to contain elevated levels of gangue materials in comparison to the ore that was actually smelted.

Combining this with the inherent problems encountered with bog ores as previously described, it may be more suitable to substitute a more reliable mineral ore for experimental smelting replications, as this material will not have undergone significant alteration in chemical composition, unlike the bog ores which are accessible today. This is a good example of the compromise that many experimental studies have to accept in order to have a degree of success.

The recording of the mass of iron working slags is a common practice within archaeological reports (Pine 2003; Hall 2009). This is due to the typically large quantities of indistinct pieces which are recovered. This is particularly apparent in the report of Pine (2003) regarding the late Iron Age/Roman settlement and iron production site at the Whitehall Brick and Tile Works, Arborfield Garrison, Berkshire. Here 9.842kg of furnace bottoms was examined, in comparison to the 20.360kg of slag attributed to smelting origin (Pine 2003: 57). The study of Hall (2009) had predominantly non-diagnostic slag pieces, but which were identified as smithing slag due to the lighter colour and relatively low density of the material (Hall 2009: 166). Many reports examine a representative

sample as this reduces the quantity of material which has to be analysed.

This method of recording the mass of slag produced will also be applied to this study. It may also help to generate a clearer understanding of the conditions within the furnace as the slag morphology is highly dependent upon the fluidity resulting from temperature and silica content.

A recent study by Dungworth and Mephram (2012) of prehistoric iron smelting slag from Shooters Hill, London demonstrates the current standard of investigation undertaken upon this material. During limited excavation in 2007, a ditch containing ceramics identified as probably dating to the Early Iron Age (8<sup>th</sup>-century B.C.) also yielded an assemblage of approximately 63kg of slag and related material (Dungworth and Mephram 2012: 1, 2). This material proved to contain slag, furnace lining and possibly ore which would further help to characterise the overall production process (Dungworth and Mephram 2012: 2, 3).

The ore samples were shown to contain higher proportions of iron and phosphorus, while containing significantly less silica than the nearest geological iron ore outcrop of the Bracklesham Group.

|        | Na <sub>2</sub> O | MgO  | Al <sub>2</sub> O <sub>3</sub> | SiO <sub>2</sub> | P <sub>2</sub> O <sub>5</sub> | SO <sub>3</sub> | K <sub>2</sub> O | CaO  | TiO <sub>2</sub> | MnO  | FeO  |
|--------|-------------------|------|--------------------------------|------------------|-------------------------------|-----------------|------------------|------|------------------|------|------|
| 19a    | 0.1               | <0.1 | <0.1                           | 2.4              | 0.2                           | <0.2            | <0.1             | <0.1 | <0.1             | <0.1 | 96.8 |
| 21     | 0.1               | <0.1 | 0.6                            | 8.0              | 0.6                           | <0.2            | <0.1             | 0.1  | <0.1             | <0.1 | 90.4 |
| 22     | <0.1              | 0.4  | 2.6                            | 3.1              | 0.9                           | <0.2            | <0.1             | 0.6  | <0.1             | <0.1 | 92.3 |
| 23a    | <0.1              | <0.1 | 0.3                            | 3.2              | 0.5                           | <0.2            | <0.1             | 0.1  | <0.1             | <0.1 | 95.6 |
| Potter | 0.05              | 0.5  | 3.7                            | 18.7             | 0.1                           | 0.5             | 1.0              | 0.9  | <0.1             | nr   | 74.0 |

*Table 3.8.1: Showing analytical data of iron ore samples recovered from Shooters Hill (Dungworth and Mephram 2012:4) and comparative average data from three samples of sideritic ironstone from the Bracklesham Group (after Potter 1977: 238).*

The marked increase in iron and phosphorus content is most likely a result of weathering of the source deposit (Bracklesham Group ore). The ore samples also exhibited vughy microstructure which was infilled with radially distributed iron oxide needles (Dungworth and Mephram 2012:4). This is consistent with geologically recent iron-rich formations which form at the top of the water table, in particular bog iron ores (Kaczorek *et al.* 2004; Landuydt 1990; Stoops 1983; Young 1993).

Following the analysis of the assemblage, the data are presented in several XY scatter graphs plotting iron and silicon oxides, titanium and aluminium oxides and calcium and phosphorus oxides respectively (Dungworth and Mephram 2012: figure 5-7). These highlight the association and grouping of the different materials within the assemblage, with clear separation of ore, slag and furnace lining. The grouping of the slag indicates that all of the analysed samples were produced from similar raw materials by the same process.

By plotting similar graphs of the material examined as part of this study, the different sites should be identifiable and it is hoped that the slag from the sites will also exhibit different phosphorus content, reflecting the slightly different raw material, but also the production processes involved.

### 3.9 The reduction of phosphoric ores

In order for phosphoric iron ore to be successfully reduced to produce a metallic bloom during smelting, the inevitable mixture of iron oxides and phosphates present must undergo interaction with both the reducing atmosphere of CO and the slag. Schürmann (1958) postulated a theoretical framework for the effect of CO volume at 900°C upon the reduction of a wüstite-iron phosphate mixture, fayalite-silica-iron phosphate mixture and pure iron phosphate. This investigation was based entirely upon thermodynamic calculations and graphical extrapolation.

This temperature has since been regarded as to being too low for efficient bloomery smelting as temperatures closer to 1200°C are viewed as being more efficient operating temperature in terms of both metal recovery and overall smelt duration. The theoretical temperature of Schürmann has also been disregarded as practical due to the experimental work of Godfrey who investigated this framework in a controlled atmosphere furnace. Under the conditions given by Schürmann and between temperatures of 800-1100°C, no metallic bloom will be produced, but instead a mixture of wüstite-rich silica and magnetite will result (Godfrey 2007: 78, 79).

Schürmann predicted that the wüstite-iron phosphate mixture would produce metallic iron with a phosphorus content of 0.07% at 900°C in an atmosphere of 69 vol% CO. The reaction involving fayalite and silica would produce metallic iron of 0.9% P in an atmosphere of 86 vol% CO (Schürmann 1958). This consideration is more relevant and significantly more valid archaeologically, as pure iron phosphate does not exist as an ore material and silica will always be present, producing fayalite as the reaction proceeds.

Schürmann suggests that a carbon free product could be produced at either 69 vol% CO or 86 vol% CO ratios, but at the greater CO concentration of 89.4 vol% 0.02% would be present in a 1.8% P iron (Schürmann 1958). This phosphorus content of 1.8% is contended by Schürmann to be the saturation composition, whereby no carbon can be absorbed into the ferrite. This figure is significantly lower than other identifications, contemporary with the work of Schürmann, of the phosphorus saturation limit as being in excess of 2.5% (Hansen 1958, Raghaven 1988).

Further to this, Schürmann continues by suggesting that, under suitable environmental conditions, either phosphorus-rich low-carbon ferrite (phosphoric iron), or high-carbon low-phosphorus austenite could be produced. The problem with this theory is that the overall environment within a bloomery smelt is highly heterogeneous. Interaction between carbon, reducing ore and fully reduced metal will have an impact, and most likely due to the available quantity of carbon, dominate the behaviour of the present phosphorus.

The major flaw with all of these predictions is that the stated temperature of 900°C is significantly lower than those identified more recently as being best suited to the production of iron at an appreciable rate (Tylecote *et al.* 1971).

The recording of the atmospheric conditions, while being very scientific, does not reflect archaeological practice. Inevitably the reaction conditions would have been monitored and controlled by means other than observation of numerical data. Such methods include the observation of flame colour, which is derived from the escape gas composition and can give an experienced smelter a relatively reliable indication of the atmospheric conditions of the reaction.

### **3.10 Summary**

In summary, ironworking has been examined from multiple standpoints. Primary production experiments have proven to be useful but still do not match the archaeological process. Instead researchers are reliant upon the use of analytical data and mass balance equations to compensate for the overall lack of experiential knowledge that past smelters had. The recent developments in provenance study are proving to be more useful for including the trade of iron with the other notable commodities of the examined period.

It is also notable that a large body of experimental work has been conducted, to which the smelt undertaken as part of this study does not contribute any new information. It will however, expand upon my own understanding and greatly inform on the interpretation of archaeological assemblages based upon the experience gained.

# Chapter 4

## Iron Smelting Experiment

|            |  |                   |
|------------|--|-------------------|
| <b>4.1</b> | <b><i>Experimental Design</i></b>          | <b><i>110</i></b> |
| <b>4.2</b> | <b><i>Experimental Smelt</i></b>           | <b><i>112</i></b> |
| <b>4.3</b> | <b><i>Ore Processing</i></b>               | <b><i>113</i></b> |
| <b>4.4</b> | <b><i>Smelt Process</i></b>                | <b><i>114</i></b> |
| <b>4.5</b> | <b><i>Experiences and Observations</i></b> | <b><i>118</i></b> |
| <b>4.6</b> | <b><i>Products</i></b>                     | <b><i>123</i></b> |
| <b>4.7</b> | <b><i>Slag Analysis</i></b>                | <b><i>129</i></b> |
| <b>4.8</b> | <b><i>Interpretation</i></b>               | <b><i>131</i></b> |
| <b>4.9</b> | <b><i>Conclusions</i></b>                  | <b><i>132</i></b> |

### 4.1 Experimental design

This section outlines the design of the experiment carried out as part of the investigation into iron smelting. The design of an experiment is important as it allows the work to be modified and improved depending upon the observations made during and the results recorded at the end of the experimental run.

For this thesis, the primary aim of the experiment was to demonstrate and experience the number of variables that have an impact upon the bloomery smelting of iron. This served to further expand upon my knowledge of the production of iron and the numerous challenges that directly influence the successful production of a bloom. Many studies, discussed in chapter two, worked to produce a bloom and demonstrate how the modern understanding of a successful smelt is the production of a large bloom from a given quantity of ore, usually with a yield of 40-60% metallic iron (Senn *et al.* 2010) As I have argued, this concept of success based upon percent yield is a modern conception. Smelters in the past possessed no way of knowing the percentage of iron present in a given ore sample and thus judged success by different standards.

Thus my experiment was conducted under the direction of experienced smelter Jake Keen, with the aim of completing a smelt and assessing the end products, rather than producing an assumed quantity of iron at the end. The objectives of the exercise were defined in order to maximise my understanding of the practical aspects of a smelt and the knowledge gained by personally observing and doing the

activities, as much of the experiential knowledge is not discussed in historical or modern experimental accounts.

### Experimental aims and objectives

#### Aims:

- I) To successfully undertake the major stages of a smelt from ore preparation to bloom extraction.
- II) Assess the products of the smelt and compare with archaeological material.

#### Objectives:

- I) Personally undertake as many stages of the process as possible, gaining insight into the experiential understanding of the materials for example the differentiation between “good” and “bad” ore.
- II) To record the multiple stages of the experiment in terms of personal experience to gain a more human understanding to supplement the empirical scientific description of the processes.
- III) Apply metallographic and electron microscopic techniques to allow for comparison between the experimental and known archaeological materials.

In order to produce a bloom of iron from the iron ore identified as suitable for the investigation of the production of phosphoric iron and the potential technological impact upon phosphorus content, experimental smelting was a necessary process.

## 4.2 Experimental Smelt

This section documents an experimental smelt undertaken as part of this thesis for purposes of experiential learning and generating analytical samples. The processes and experiences of processing ore, loading charge into a working furnace, tapping slag and bloom removal are described below. Following this outlining of how the experiment progressed, the products of the smelt are described and illustrated along with analytical data and interpretation of results. The smelt was conducted using ore gathered from the iron smelting site at Tisbury which was in operation at the same time as the construction of Salisbury Cathedral.

### Smelting location and conditions

The smelting took place on 14 June 2014 at Down Farm, Dorset. The weather had been dry for several days prior to the smelt and the ambient temperature on the day was approximately 27°C. This meant that the charcoal had no opportunity to absorb water from the atmosphere, making it optimal for use as damp charcoal has a negative impact upon smelt performance. The hot ambient temperature also had a direct effect upon those working around the furnace, with a greater risk of dehydration and fatigue.

The furnace, which has been used multiple times over the past 5 years, underwent a slight change with the addition of a new top to the cone. This was taken from a previous furnace and provided a narrower, tall top to the cone which allowed for easier loading of charge with less risk of scorching. It is of little concern that the top of the furnace was not part of the original, as the reaction zone was far below the join between furnace components. Little to no reduction occurs within the top zone of the furnace as the escape gases are cooler than the main operating temperature (Crew 2013: 34, 35, figure 12).



Recorded below in table 4.2.1 is a summary of the experimental parameters.

|   |  |
|---|--|
| Furnace dimensions                            | Height x Diameter<br>1.8 x 60cm (approx.)  |
| Materials used in furnace construction        | Locally available white and yellow clay  |
| Charcoal wood species                         | Sweet chestnut   |
| Charge ratio                                  | 1kg ore : 1kg charcoal (approximately every 10 minutes)  |
| Furnace ventilation                           | Electric vacuum cleaner  |
| Quantity of material that entered the furnace | 14kg charcoal preheat, 14kg charcoal during the smelt. 28kg total<br>11kg ore during the smelt |
| Quantity of material removed from the furnace | Bloom – 2kg<br>Slag – Total unrecorded due to partial recovery                                 |

*Table 4.2.1 Showing the recorded parameters of the smelt.*

### 4.3 Ore processing

The ore was sourced from Tisbury, which was a Medieval iron smelting site in use when Salisbury Cathedral was under construction. The ore was broken into pieces approximately the size of a fist and the most gangue-rich portion removed prior to roasting. The material was roasted with wood for fuel for 2 hours in a perforated drum to prevent exploding ore fragments from causing injury. After roasting the ore was allowed to cool to allow for maximum fragmentation ahead of sorting and crushing.

The ore crushing was undertaken using modern metal hammers weighing approximately 1kg and both metal and stone anvils. During the crushing process ore was selected for use in the smelt based upon colour and texture. Ore that was deemed “good” was typically a deep red/maroon or purple hue in colour and much softer than the rest of the material (Cleere 1971:208, Smith 2013: 100). Gangue rich material was again rejected and placed to one side away from the desired ore. This material was easily distinguished by how hard it was in comparison to the good ore and by the far paler colour exhibited by the fresh fractured surfaces.

The ore was crushed to pea sized pieces which were sieved through a 1cm<sup>2</sup> riddle. This ensured that any larger pieces would be identified and re-processed to the correct size. Pieces which got stuck in the riddle (those of approximately 1cm maximum thickness) were removed and added to the charge. Jake observed that the overall quality of the ore used in this smelt was somewhat lower than had been

used previously in similar experiments he had carried out. The reduction in ore quality was judged by the increasing hardness of the ore that was being crushed, which is a consequence of a greater gangue content. This resulted in a total ore charge of 12kg being prepared for use, with a significant amount being lost to unsuitable silica rich waste.

From the experience of preparing the ore, it became clear that the selection of suitable material is a highly subjective process. The good ore was identifiable not only by colour and texture after breaking, but also felt significantly softer and slightly lighter in the hand. In many cases, gentle tapping with the hammer was all that was required to break the ore into small enough pieces for use. This contrasted greatly with the poorest grade material which would not fracture without the application of significant force. This was surprising as it is not discussed in great detail in many publications (Crew 2013, Cleere 1971, Girbal 2013, Smith 2013) and further demonstrates the benefit of undertaking practical investigations as part of academic research. This also highlights a significant difference between iron and copper smelting. In many cases the malachite used to produce copper is not roasted to allow for the beneficial thermal decomposition of the carbonate ore during smelting. This results in the crushing being more laborious in terms of applied effort in comparison to the crushing of roasted iron ores.

As with many experimental attempts at undertaking past processes, the level of experience possessed by the investigators is significantly less than that of the original practitioners. This resulted in the processing of the ore taking longer than expected, as the recognition of better quality material initially required more care and attention.

A large quantity of dust was produced during the crushing stage. This resulted in my clothing and arms becoming coated in red dust due to sweat. This demonstrates that the process of ore preparation was and is not a clean one. This dust coating would also make the smelters very distinct in the community during times of smelting activity, which might further suggest why they occupy places of separation within ethnographically observed modern societies (Childs 1991, David and Bléis 1988).

#### **4.4 Smelt process**

The furnace was pre-heated for 2 hours ahead of the addition of the first charge. The charge was made of 2kg of prepared ore poured on top of 2kg of charcoal. The charcoal was weighed and sieved to remove fines before being incorporated as the fines would choke the furnace and prevent successful smelting by falling through the charge and collecting towards the active zone. The prepared charge was fed into the top of the furnace using a hand-held metal hopper. This allowed for a controlled delivery of charge, so that it did not risk choking the furnace by adding too much too quickly, or taking too long to add the measure of charge.

During loading the flames emerging from the top of the furnace lapped around the end of the hopper. If the loading of charge was too slow, then the flames were drawn up the outside of hopper towards my hands by the smaller particles of charcoal which inevitably survived the sieving. This provided further incentive to load the charge faster so that my hands did not get burnt.

Occasionally a large piece of charcoal would become lodged in the neck of the furnace. This was remedied by using a metal rod to break the piece and cause it to fall into the furnace body. It was observed that this caused a slight delay in charge delivery because of a charge being suspended in the neck. This was a problem which was partially a result of not being able to observe the entirety of the smelt within the furnace. As it was unknown that charcoal had become lodged until it became apparent by the suspension of charge at the top of the furnace.

The charging of the furnace occurred as shown in the table below, the original facsimile of which is presented in the appendices.

| Time  | Charcoal (kg) | Ore (kg) | Charge time (mins) |
|-------|---------------|----------|--------------------|
| 8:30  |               |          |                    |
| 9:00  | 1             |          |                    |
| 9:07  | 1             |          |                    |
| 9:25  | 1             |          |                    |
| 9:35  | 1             |          |                    |
| 9:45  | 1             |          |                    |
| 9:58  | 1             |          |                    |
| 10:11 | 1             |          |                    |
| 10:21 | 1             |          |                    |
| 10:30 |               |          |                    |
| 10:35 | 1             |          |                    |
| 10:43 | 1             |          |                    |
| 10:50 | 1             |          |                    |
| 10:54 | 1             |          |                    |
| 10:56 | 1             |          |                    |
| 11:02 | 1             |          |                    |
| 11:10 | 1             | 0.5      |                    |
| 11:19 | 1             | 0.5      | 9                  |
| 11:26 | 1             | 0.75     | -                  |
| 11:30 | 1             | 0.25     | 11                 |
| 11:34 | 1             | 0.75     | -                  |
| 11:41 | 1             | 0.25     | 11                 |
| 11:46 | 1             | 1        | 5                  |
| 11:54 | 1             | 1        | 8                  |
| 12:02 | 1             | 1        | 8                  |
| 12:10 | 1             | 1        | 8                  |
| 12:18 | 1             | 1        | 8                  |
| 12:29 | 1             | 1        | 11                 |
| 12:41 | 1             | 1        | 11                 |
| 12:50 | 1             | 1        | 9                  |

*Table 4.4.1 showing the progression of the experimental smelt including duration between charge additions per kg.*

After the last addition of charge, the furnace was allowed to burn down for thirty minutes. This was done to allow the slag to collect prior to tapping. Unfortunately, when the furnace was tapped it was found that the slag had started to solidify in the base of the furnace. This resulted in less tap slag being produced than was hoped for. A large quantity of slag was found to be “stickier” than was expected. The reason for this was unclear as the conventional tap slag flowed very freely. It only became apparent the following week, when the furnace was undergoing repair in preparation for another smelt, that the furnace had been built upon a thermalite block which, over the past 5 years had gradually become exposed and reacted with the slag during the smelt discussed here.

The bloom itself had adhered to the furnace wall on the left side of the tapping arch. This was expected as blooms from smelts conducted the previous week had also coalesced in that region. Initially the bloom was difficult to identify as a large proportion of the slag had remained in the furnace. This was pried free with a long iron bar and a hammer before being levered away from the walls and removed before air cooling. This process of cooling was selected as it would allow the longest time for phases within the slag to develop and finalise form, rather than submerging the pieces in water which would have resulted in the phases being finer and potentially harder to identify during optical microscopy.

The slag itself had a mid-grey surface for the most part; however some regions had a cream yellow colour. This was unexpected and had previously not been observed when smelting the Tisbury ore. Initially it was thought that this colour difference may have originated from the use of a different, yellow clay to patch the interior of the furnace prior to smelting. However it became apparent that the interaction between the slag and the thermalite block was most likely responsible for the distinct colour due to a change in slag composition when the furnace was under repair.

Upon examination after sampling all of the slag from the smelt possessed this yellow colour regardless of the colour of the surface. It was found that there were no observable wüstite dendrites in any of the slag under optical microscopy, as discussed in section 4.6. This highlights that the characteristic, dark grey colour of archaeological smelting slags is a direct result of the presence of high quantities of wüstite. The observed yellow colour is not unknown archaeologically, as samples from Caistor St. Edmund, discussed in chapter 6, have demonstrated.

It may also be noteworthy that the modern experimental slags produced both in this smelt and in those conducted previously by Jake Keen, have been significantly more brittle than archaeological pieces. This may indicate that iron slags undergo some alteration in character when buried over archaeological time which, as of yet, has not been fully studied or considered.

Upon removal, the bloom was somewhat smaller than expected when compared to previous smelts using the same ore. This was adjudged to be a result of both the quantity and quality of the ore used. Initially the smelt was deemed a failure because of the quantity of metal, however upon debate the conclusion was that the smelt had not failed as metal had been successfully produced from the lower grade material available.

#### **4.5 Experiences and observations**

From a personal aspect I learned much from undertaking the experiment, having previously only smelted copper and produced copper alloys on a small scale in laboratory conditions. The most notable experience was being able to differentiate between good and bad ore by touch. The other experience of ore processing with the quantity of dust produced during crushing. Even after processing only the 11kg used in this smelt much of my exposed skin was stained as can be seen below.



*Figure 4.5.1 Showing staining of skin following ore preparation.*





*Figure 4.5.2 Showing ore processing set up.*

The ore sorting was done during crushing, working right to left selecting ore pieces from the roasted pile, crushing on the anvil and then sweeping it to the left. Rejected pieces were thrown away to the top right of the image above, creating a small scatter of material while the majority was processed, sieved into the bucket and the separated larger fraction re-processed. This generated a large quantity of dust which can be seen covering the anvil, and surrounding surfaces.



*Figure 4.5.3 Showing large piece of ore (left).*

The figure above (figure 4.5.3) illustrates the nature of the roasted ore. This larger piece shows the heterogeneous nature of the ore and host rock, and the significant fracturing that occurs with roasting. The best ore was found to be the bright rusty-red coloured portions with the darker surface, seen on the top left of the piece, while the other iron bearing regions were not as suitable due to an increased proportion of host rock.





*Figure 4.5.4 Showing furnace in use, red 1 indicating location of sealed tapping arch.*

The furnace was powered by a two directional vacuum cleaner. This greatly reduced the physical effort required to provide a draught to the smelt while also ensuring that the supply of oxygen was consistent. Previous bellows-powered experiments conducted at Rievaulx Abbey have demonstrated that fluctuating draughts from bellows operated by different individuals result in less reliable reaction conditions which alter the rate of iron reduction (McDonnell pers. comm. 2014).

The tapping arch was sealed with a removable block and covered by a mixture of charcoal and sand. This allowed for faster opening of the furnace and subsequent slag and bloom extraction.



*Figure 4.5.5 Showing opened tapping arch.*

Upon opening the furnace there was no initial slag flow. The slag was contained within the furnace behind the quantity of charcoal visible in the above image. The first flow of slag fell between the two blocks and was significantly paler in colour than the slag from previous smelts. The rest of the slag remained within the furnace and had to be pried out along with the bloom, as discussed in section 5.4. The bloom itself had adhered to the left of the furnace close to the tuyere. The blooms from previous smelts in this furnace were also found in similar positions, although the bloom from this event had caused more damage to the interior wall than had occurred in previous smelts. Due to time constraints the bloom was placed in water to cool before sampling.



#### 4.6 Products

Two samples of the bloom were cut using an angle grinder and then subjected to metallographic and electron microprobe analyses to determine the predominant compositions present. The following composite images (figures 4.6.1 and 4.6.2) show the metallographic samples in the etched condition following etching with nital.

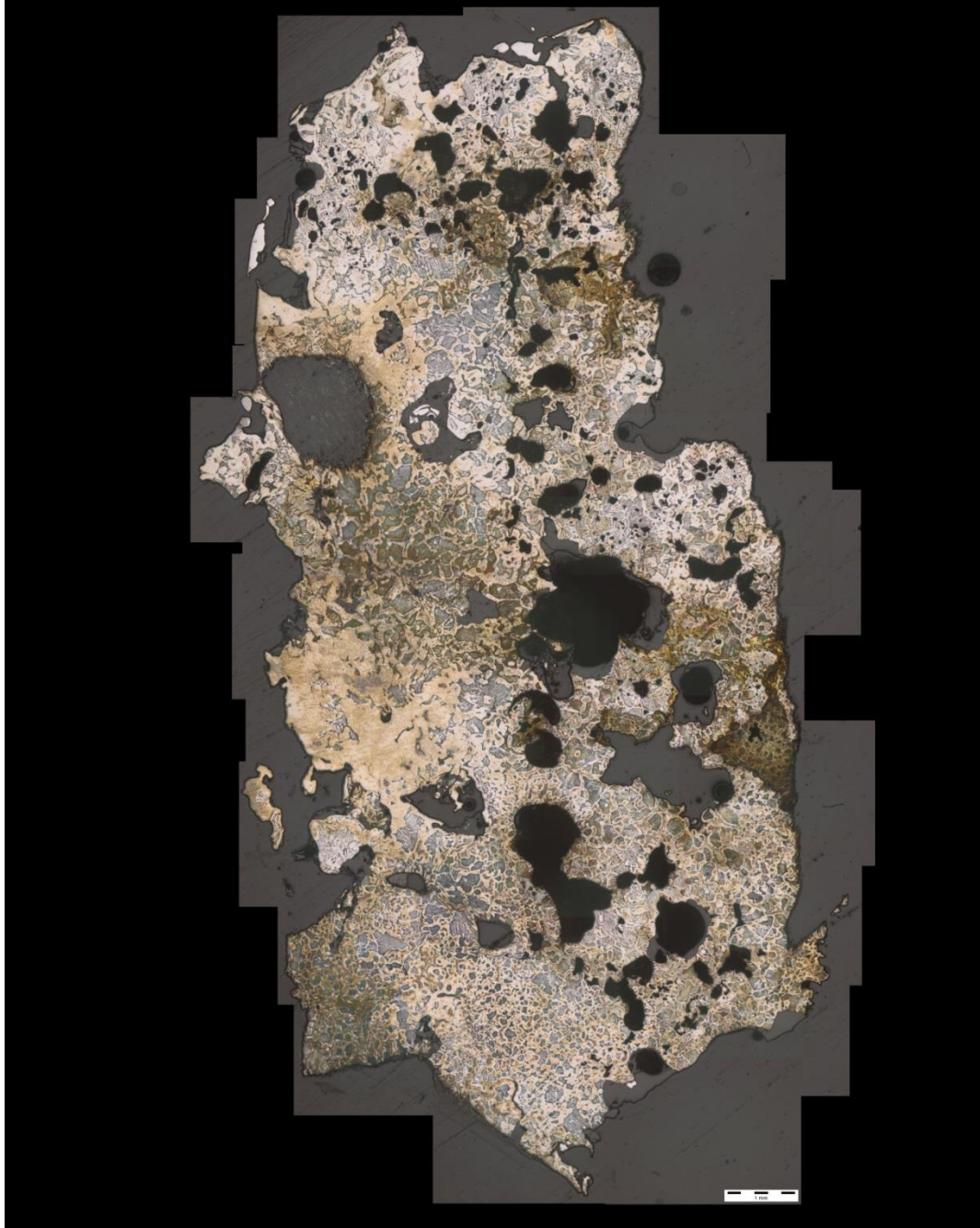


*Figure 4.6.1 Composite image showing metallographic sample 1 in the etched condition scale bar 1mm.*

As can be seen in figure 4.6.1 above, there are regions of limited carburisation and regions exhibiting no carburisation with a pale colour. This is diagnostic of the presence of phosphorus as has been observed by Hall (2008, 2012). The limited carburisation close to the surface of the bloom, from which both of these samples were taken, demonstrates the impact upon carbon diffusion that the presence of phosphorus has. The pores which are visible, as irregular black spaces, in both samples also posed a problem with etchant and alcohol retention, which is responsible for some of the dark yellow colouration in close proximity to these hollow spaces.

Hardness testing was also conducted upon the sample shown in figure 4.6.2 to provide supplementary data to further clarify the interpretation of the optical analysis. While the dark colouration of the carburised regions is diagnostic of carbon steel and the pale colour, and extremely large grains are indicative of phosphoric iron. The subsequent hardness testing of these different regions helps to confirm the initial interpretation as well as providing recognisable locations for EMPA study from which to gather chemical composition data for definitive proof.



*Figure 4.6.2 Composite image showing metallographic sample 2 in the etched condition scale bar 1mm.*

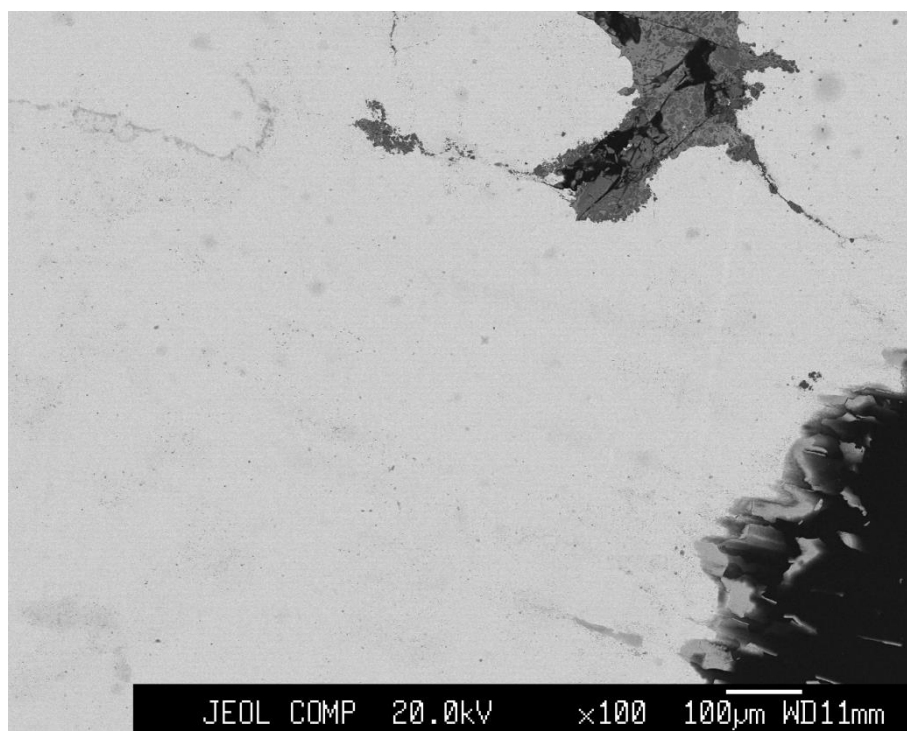


*Figure 4.6.3 showing compositional image with slag inclusion within bloom sample 1 top right and linear porosity visible top right indicative of phosphorus presence.*

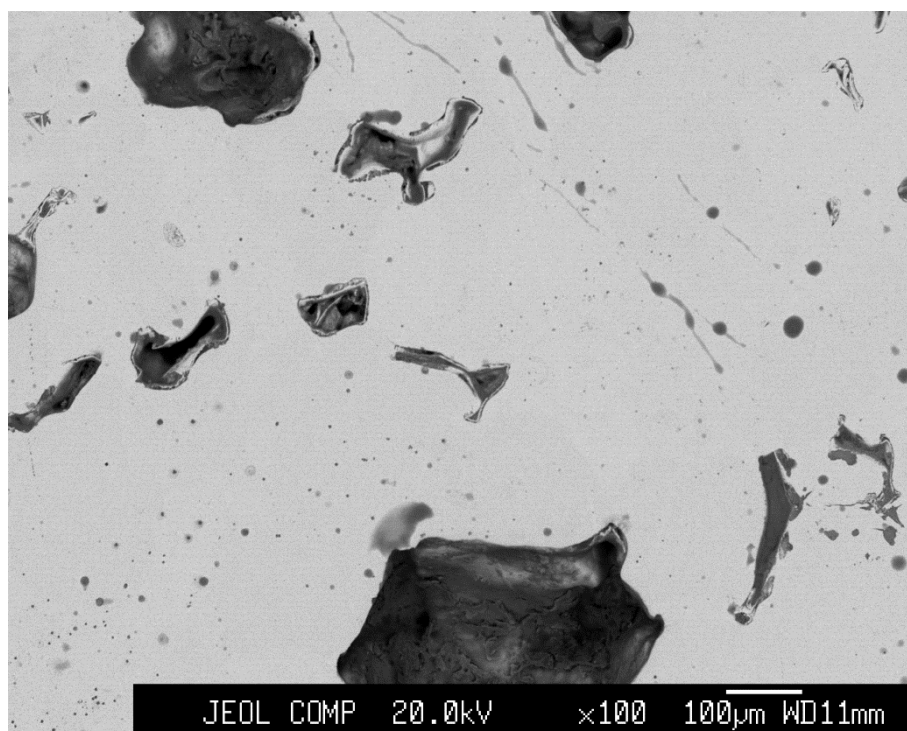


*Figure 4.6.4 showing compositional image of bloom sample 2 showing large pores and linear porosity visible bottom left indicative of phosphorus presence.*

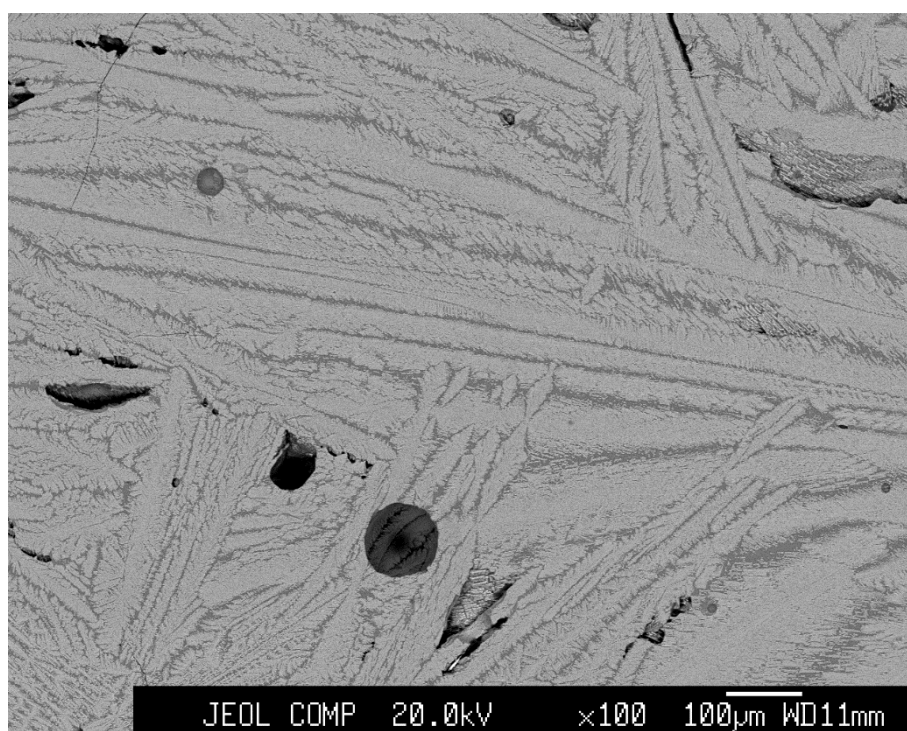


*Figure 4.6.5 showing compositional image of feathered fayalite within the first flow slag produced during the experiment.*

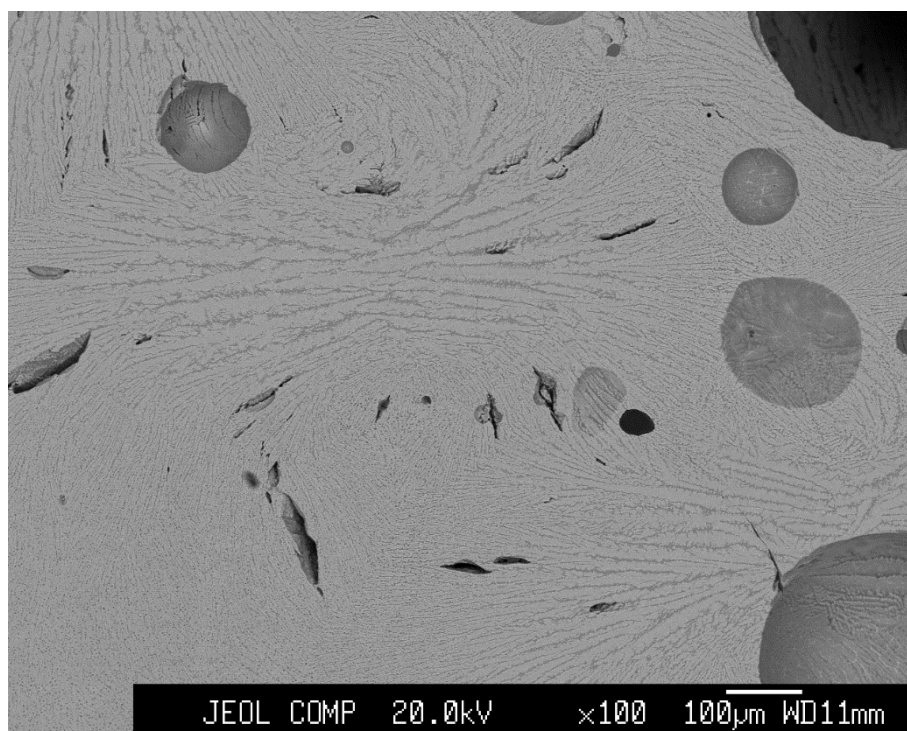


*Figure 4.6.6 showing compositional image with no free wüstite in pale coloured smelting slag.*

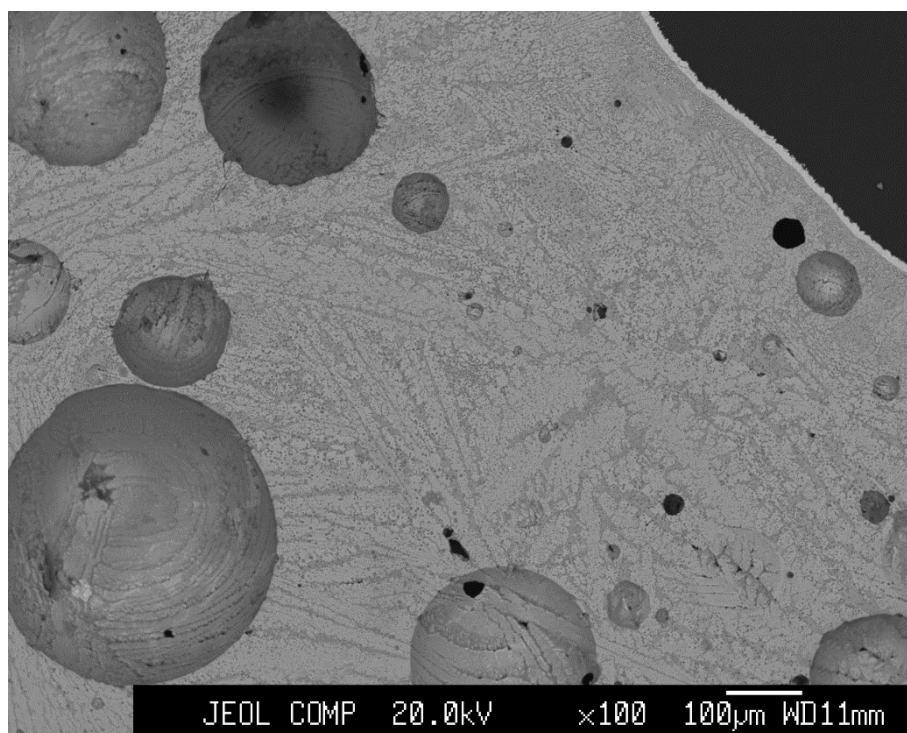


*Figure 4.6.7 showing compositional image of slag from the previous smelt conducted in the same furnace with the same ore. Iron rich skin visible top right.*



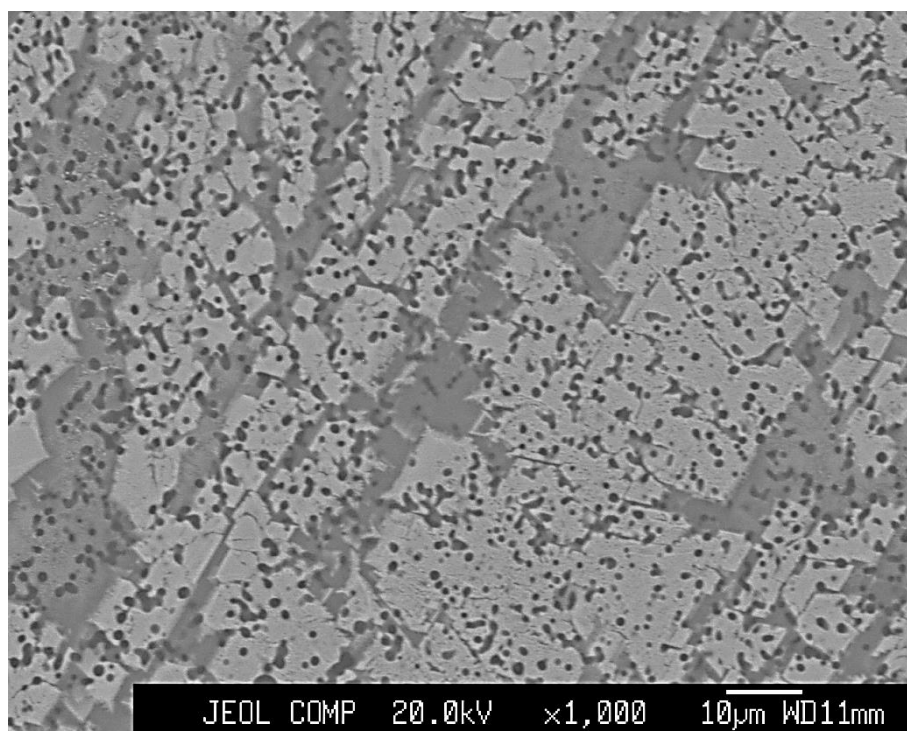


*Figure 4.6.8 compositional image of slag from the previous smelt exhibiting severe micro-porosity.*

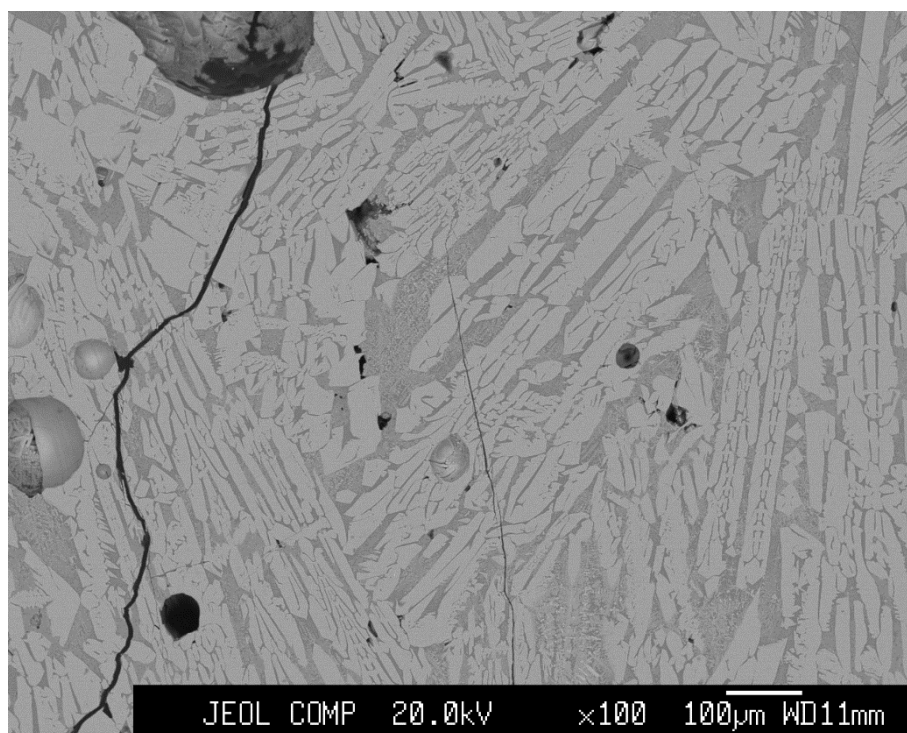


*Figure 4.6.9 compositional image of archaeological slag from Tisbury showing well developed fayalite laths and small quantities of wüstite visible centre.*



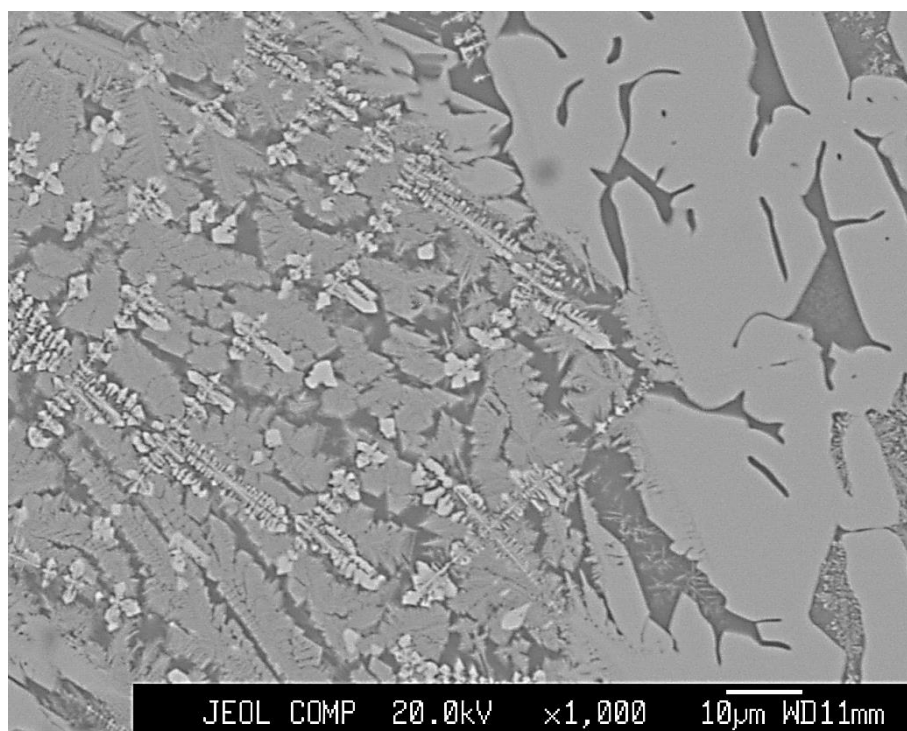


Figure 4.6.10 compositional image of archaeological slag from Tisbury showing close up of fine wüstite dendrites.

#### 4.7 Slag Analysis

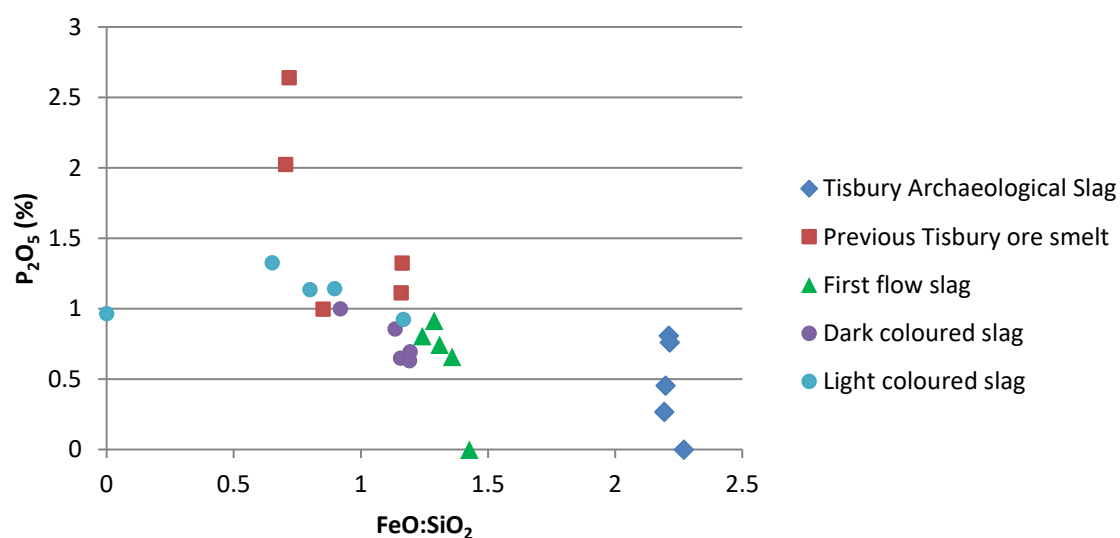


Figure 4.7.1 showing raw fayalite data for experimental assemblage and comparison samples

The experimental fayalite composition shows a skew towards the left, this is due to mixed signal responses caused by analysing a portion of the matrix phase along with the intended fayalite. The slag cooled very quickly resulting in very fine fayalite and narrow bands of matrix, making reliable point

analyses difficult. The archaeological material appears to have cooled more slowly, due to the greater thickness of the tap slag plates produced, providing better sampling locations for the fayalite phase data with resultant values in excess of 2, much closer to the  $\text{FeO}:\text{SiO}_2$  value of the mineral.

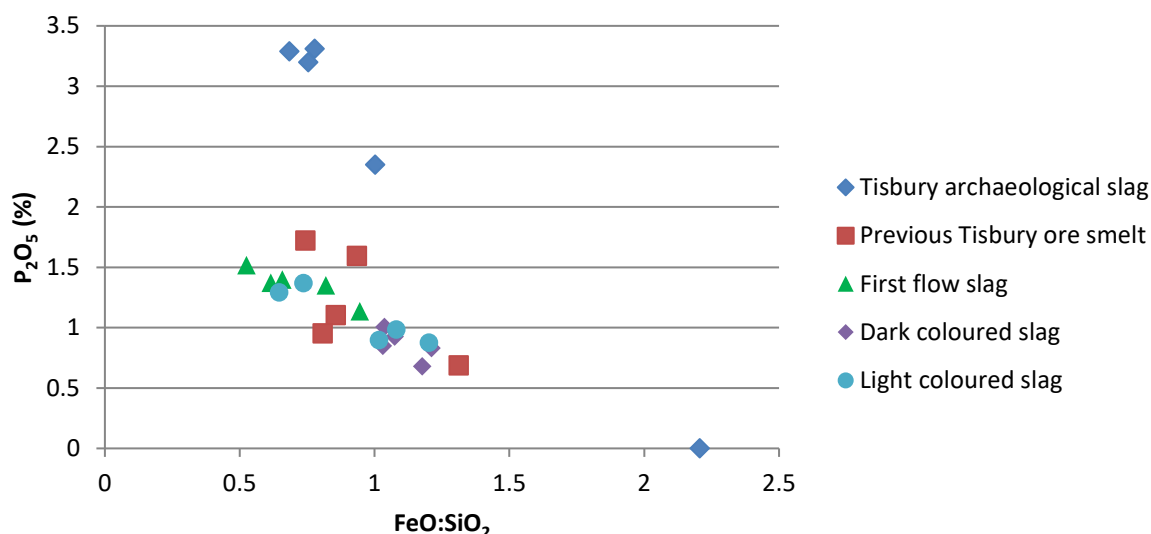


Figure 4.7.2 showing raw matrix data for experimental assemblage and comparison samples

The graph showing the matrix analyses (figure 4.7.2 above) shows that the experimental slags have  $\text{FeO}:\text{SiO}_2$  ratio range between 0.52 and 1.3. The archaeological material also has a similar ratio, between 0.6 and 1.0, although the outlier, is a result of analysing mostly fayalite, hence a ratio exceeding a value of 2. The archaeological matrix analyses, excluding the outlier, show there is a significantly higher proportion of  $\text{P}_2\text{O}_5$ . This can be explained due to the higher  $\text{CaO}$  content found in the archaeological material which would suggest that the ore included in the archaeological charge contained more calcium than that used in either of the modern experiments.

As the ore originated for a marine deposit, as evidenced by the presence of shell within the host rock, the higher calcium content may be a result of different processing decisions, with more of the shell being included amongst the selected charge material.

The difference in colour between the dark and light coloured slags can be attributed to the  $\text{FeO}$  content. It is noticeable in both data plots that the dark coloured slag plotted with a higher ratio, all around a value of 1 than the lighter slags which have several points with values of less than 1. This supports the interpretation that the inclusion of the furnace material that broke and became included in the smelt during the experiment was the cause of the lighter colour due to the addition of an increased quantity of silicates.

## 4.8 Interpretation

The hardness testing of the etched samples proved that the bloom had undergone significant hardening. This is a result of it being placed in water to cool down fast enough for sampling due to time constraints. Both samples show regions with distinctly restricted carburisation, which is due to the presence of phosphorus in the surrounding metal grains. I have seen similar restricted carburisation in other experiments investigating the effect of phosphorus on the production of steel (Hall 2008). The large number of pores present in both samples are a result of the bloom formation processes where individual flakes of reduced metallic iron coalesce to form the spongy mass of the bloom. As these samples were taken from close to the surface the pores have not been closed due to the smaller quantity of metal applying pressure and thus not compacting those regions of the sample as greatly as would be found closer to the core. These pores also caused some of the staining seen on the samples as it was very difficult to remove all of the etchant and water from the deepest pores.

The lack of ghosting seen in the phosphoric regions is due to the bloom being in the original unworked state. This is commonly seen in finished artefacts such as knives and currency bars which have undergone significant hot working, and it is likely that if the bloom was to be forged the distinctive watery appearance of ghosting would appear across the phosphoric regions along with the reduction in grain size which results from the compression of the material.

The highly heterogeneous nature of the bloom samples, even this close to the surface where the material is exposed to a greater quantity of carbon and thus more susceptible to carburisation, demonstrates that the production of a homogenous bloom is extremely difficult if not impossible when using a phosphorus-containing ore.

## 4.9 Conclusion

Based on the experience gained from undertaking a smelt, and the analytical study of the materials produced, it is possible to make some broad statements which have guided the interpretation of the archaeological material considered in the following sections.

Firstly, the processing of the ore used is guided largely by colour, texture and the experience of the smelting team. The regulation of piece size and ore content can be maintained by the use of sieves and gauging the appearance of the pieces.

Secondly, the quantity of slag produced during modern smelts is significantly less than that found in archaeological examples. This is most likely a result of a difference in scale between the more likely smaller modern experiments when compared to archaeological smelting. The result of which would be that a larger quantity of ore and gangue would be present in archaeological smelts, which should result in a greater quantity of both metal and slag being produced.

A second potential cause of the discrepancy in slag production may be the inclusion of a greater quantity of poorer ore in archaeological smelts. This would help to account for the lack of large quantities of discarded material seen at identified smelting sites, and further demonstrate that archaeological smelts occurred on a greater scale than modern experimental replication studies.

Thirdly, the pale interior colour of the smelting slag produced appears to have resulted from the slump and subsequent inclusion of part of the furnace wall into the smelt. This would explain why some archaeological slag is found to have a pale interior in the same way. The distinct lack of free wüstite in this slag demonstrates that the reaction conditions were too reducing, as a result of using mechanical bellows. The additional contribution from the slumped furnace ceramic to the overall process may also have reacted with some of the wüstite producing a greater quantity of fayalite and matrix, making the slag appear pale in colour.

Lastly, the analytical data demonstrates that the products of a given smelt are directly influenced by the raw materials used. It has been shown, based upon our current experience using authentic methods, that it is not possible to carefully manipulate the reaction atmosphere in such a way as to remove or preserve phosphorus.

# Chapter 5

## Applied Methods

|            |  |                   |
|------------|--|-------------------|
| <b>5.1</b> | <b><i>Macro examination</i></b>        | <b><i>133</i></b> |
| <b>5.2</b> | <b><i>Metallography</i></b>            | <b><i>136</i></b> |
| <b>5.3</b> | <b><i>Electron Microscopy</i></b>      | <b><i>139</i></b> |
| <b>5.4</b> | <b><i>Sampling Strategy</i></b>        | <b><i>145</i></b> |
| <b>5.5</b> | <b><i>Justification of methods</i></b> | <b><i>147</i></b> |

This section is intended to explain how the investigative techniques applied to the material studied in this work function. Each method will be addressed individually in order to demonstrate the thought process and staged progression of investigation that is central to the study of metallurgical evidence. This begins with a macro desktop examination of the pieces in question, with basic classification and identification of materials suitable for further study, followed by sampling, preparation metallographic analysis and finally electron microscopy.

### 5.1 Macro examination

Prior to any invasive and destructive investigation an assemblage of metallurgical materials must be observed, recorded and classified. This first, preliminary stage of study is crucial to the successful application of any further methods and techniques to the assemblage. Before any meaningful classification can be placed upon the assemblage, the material must first be clean of adhering soil where possible. Cleaning the samples in water with a toothbrush ensures that the minimum damage is caused to the sometimes fragile materials, ceramic material exhibiting exposure to oxidising firing conditions are typically amongst the most fragile metallurgical remains along with corroded ferrous pieces. During the cleaning process, some pieces may prove to be too fragile to be cleaned and may be separated due to their highly friable nature. Other samples, such as the slags that make up the majority of primary metallurgical evidence are far more robust and can be cleaned with ease. If charcoal is present as inclusions within the slag then care must be taken to not remove this significantly softer material by excessively vigorous brushing.

All of these observations and decisions are based upon the experience of the investigator. In many cases observing the material when damp immediately post cleaning can provide a greater level of clarity than when the samples have dried. The remaining water can help to reduce the effect of adhering dust and soil that forms a thin layer over the surface upon drying. It is impossible to remove all of the accompanying soil from samples, particularly those of a porous nature, however if the majority is removed then a better interpretation may be reached.

During cleaning other characteristics may be taken into account, such as the density of the piece in hand. This judgement of density is subjective, but in combination with colour and morphology allows the investigator to preliminarily classify the material ahead of a second confirmation. Pieces with distinct morphologies such as smithing hearth bottoms and tap slags are the easiest pieces to classify and can generally be done on first sight. The more complex identification of the dense seemingly non-diagnostic pieces may require the application of further methods.

Prior to any destructive sampling for use in microscopic analytical methods, the pieces must be recorded in their original, complete state. Photographing the pieces ensures that there is a visual record that, unlike archaeological illustration, does not have a subjective aspect regarding the surface and texture represented in the image. It is also a far faster means of recording singular and groups of pieces which may then proceed to destructive sampling.

The following flow diagram provides an overview of the decision making process when conducting a desktop evaluation of iron slags.

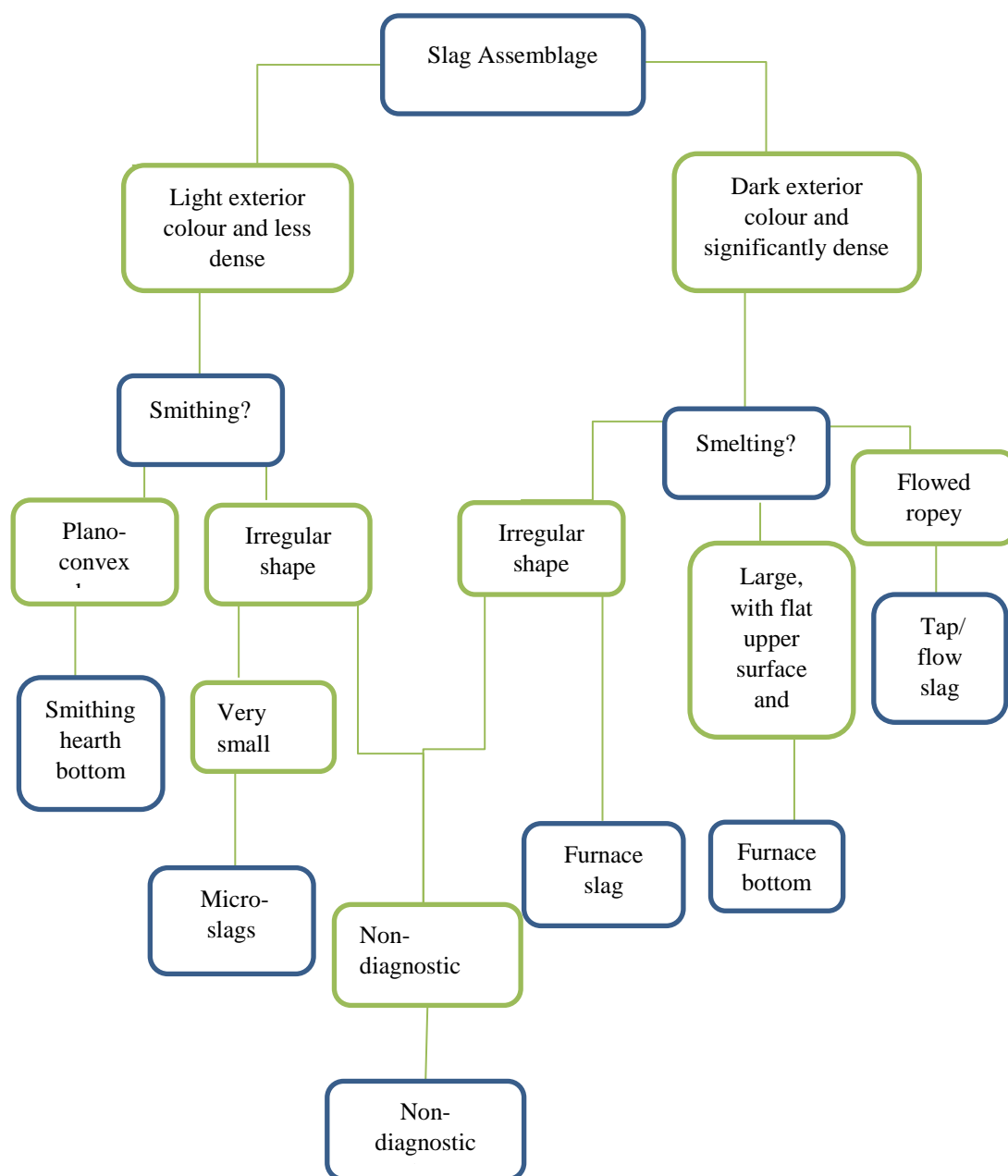


Figure 5.1.1 Showing a decision tree for desktop iron slag evaluation.

## 5.2 Metallography

The successful application of metallographic analysis is entirely dependent upon the level of skill possessed by the investigator. Unlike other methods where the data produced is entirely quantitative in the form of numeric data, such as that produced by isotopic analysis using mass spectrometry, the data produced by metallographic study is qualitative and requires a degree of interpretation and supplementation with additional quantitative data to ensure a sound conclusion is reached.

Metallography is one of the most established means of examining metal artefacts and associated metallurgical slags. The process of preparing a sample involves mounting the piece in resin and then grinding and polishing the sample to a less than 1  $\mu\text{m}$  finish before observation under a metallographic microscope. While machines exist that can prepare samples, it is best that an investigator is capable of sample preparation themselves. This ensures that the individual understands the process and possesses the skills required, rather than simply letting a machine do the work and not comprehending why a sample may prove problematic.

In my own experience of preparing samples, it can be quite easy to accidentally grind a sample at an extreme angle which can result in a significant loss of material. This occurs when the sample is not held correctly, or pressure is applied to the block unevenly when in contact with the grinding paper. While this is not an analysis ruining error for metallography, if the sample proves to be worthy of further examination, then the existence of a significant slope may make electron microscopic study extremely difficult or impossible. For this reason it is best if the ground surface of the sample block is as close to horizontal as possible.

When grinding a sample it is important to ensure that the grit from the previous stage does not transfer to the following, finer stage. This transfer of coarser grit will cause larger scratches to the sample surface than expected and at a different angle to the previous stage. This can make taking images difficult as scratches may not appear significant until the sample is etched to reveal the metallographic features which inform of the processes the artefact has experienced.

At the end of each stage of grinding and polishing the sample is cleaned and observed under the microscope when necessary to assess how well the sample is prepared. For the coarser grits it is possible to judge by eye if the scratches are all in the same direction while during polishing the use of the microscope ensures a greater quality of finish.

Once polished a metallic sample may require etching to reveal the internal structure and features that inform the assessor of the fabrication and formation processes that the piece has experienced, depending on if the piece was taken from an artefact or a slag. The etchant applied to the surface depends upon what the sample is made from and questions the investigator is asking of the sample.



Nital is an etchant commonly used on ferrous objects to reveal the presence of grain boundaries, carbon, arsenical (white) weld lines and phosphorus ghosting. Comparatively, alcoholic ferric chloride is commonly used on copper based artefacts to reveal internal features.

The recognition of the metallographic features is dependent upon the quality of finish achieved on the sample surface and the length of exposure the sample has to the etchant. The now seminal work by Scott (1991) provides a clear identification of the features generated by each of the major stages of metalworking. The origins of each of which are also carefully explained as to avoid confusion between different features of seemingly similar appearance, most notably the difference between strain lines and mechanical twinning (Scott 1991: 79, 142, 144).

The majority of the metallographic features described by Scott are generally not present in directly reduced iron and certainly not found in slags. However, some of the features such as phosphorus ghosting may be found in metallic inclusions within slag bodies. Scott does not discuss ghosting in his work, which highlights the focus of metallurgical study on the Fe-C system.

When etched with nital the metallic sample or metallic region within the sample will colour depending upon carbon content. Phosphoric regions will be paler in appearance due to greater etch resistance in comparison to ferritic iron. Regions of perlite, the lamellar phase of ferritic iron and cementite, etch dark while cementite ( $\text{Fe}_3\text{C}$ ) as an individual phase etches bright white. This allows for an easy interpretation of a sample based on carbon content and thus construction.

The identification of ghosting during metallography requires that the sample is etched with nital in order to reveal the grain boundaries and the ghosting effect. This distinct feature as revealed by nital etching appears as a watery looking feature which can be within phosphorus containing grains which are typically larger than non-phosphorus bearing regions, but may also occur across several grains. Ghosting is mostly observable when the surface of the sample is out of focus, this makes obtaining a clear image of the feature problematic. The ghosting effect is diagnostic of phosphorus presence in that it only appears in regions which definitely contain phosphorus following hot working. The difficulty of using phosphorus ghosting as a means of material categorisation arises when the other features of phosphorus presence are observable without ghosting. This occurs when a region has exceptionally large grains with little to no carbon content and no apparent ghosting. In this case the use of nital alone may not be enough to confirm the nature of the material.

To further strengthen interpretations of such qualitative, non-diagnostic data further etchants that are sensitive to phosphorus such as Oberhoffer's or Stead's reagent may be applied. Both of these reagents deposit copper onto the surface of the sample while leaving phosphoric areas with little colouration. Combining images taken in the etched condition with nital and images when etched with one of these phosphorus sensitive reagents it is possible to clarify the classification of the material. Further quantitative data from hardness testing may also be used to provide further evidence to support the interpretation of the optical metallographic results as each material has a fixed, known hardness range. Commonly ferritic iron has a hardness no greater than 90Hv while phosphoric iron by comparison is between 100-120Hv.

The metallographic microscope upon which this analysis is undertaken is an optical reflection microscope. The light from the light source passes through condensing lenses before passing through the objective lenses and being directed onto the polished surface of the sample where it is reflected towards the objective lenses. These focus the light and magnify the image depending on which lens is in use. This initial magnification is dependent upon the focal length of the objective lens, with a shorter focal length resulting in a greater magnification. The reflected light beams then pass through the eyepiece lens which further magnifies the image by another six to 10 times depending upon the lens in use.

The microscope has two main illumination modes. Bright field illumination produces images with a bright flat surface and dark non-flat features such as pores and edges. Dark field illumination by contrast produces images with bright non-flat features on a dark surface. Typically dark field imaging can be used to successfully assess the quality of finish achieved on a sample as it highlights the edges of remaining scratches.

Once the optical recording of a sample is complete it may then progress onto electron microscopy for chemical analysis to obtain the required quantitative data to confirm or inform the standing qualitative interpretation.

### 5.3 Electron Microscopy

The development and application of electron microscopic analytical techniques to material science has yielded significant advances in the study of archaeological materials. Before the use of scanning electron microscopes and electron microprobes, the majority of analyses were conducted using destructive wet chemistry. Such methods are not suitable for archaeological samples which, by their very nature, are highly fragile and of extremely limited quantity.

The process of obtaining a sample for use in an electron microscope is destructive to the original artefact, but once the sample is prepared analysis can be conducted with minimal damage. This allows analytical samples to be preserved and studied again at a later date if so desired. The retention of prepared material is of great benefit to researchers as it reduces the damage caused by multiple sampling to an assemblage of material. In other words, a sample that has been prepared and stored correctly can be made available for future research, increasing the speed of subsequent repeat analyses and project completion.

While the use of optical microscopy allows the identification of metallographic features in artefacts they cannot be used to produce accurate quantitative data concerning chemical composition. The wavelength of visible light also limits the size of features that can be observed as the smallest detectable features are approximately 150nm when using green light which is detectable by the human eye (Goodhew *et al.* 2001: 12). With this limit upon resolution it is not always possible to observe the features of interest in a sample. Electron microscopy methods have a far higher resolution, in theory up to 0.02nm (Goodhew *et al.* 2001: 19). This is however, significantly smaller than an individual atom, which proves that this is an idealised case. However, it does indicate that features far smaller than those observable using visible light may be recorded and analysed if required.

The wavelength of the electron is dependent upon the potential difference it is accelerated through prior to interaction with the sample. The accelerating voltages which are the most useful for electron microscopy are in excess of  $2 \times 10^4 \text{V}$  which has an impact upon the calculation of the resulting wavelength.

The overall formula is presented as:

$$\lambda^2 = h^2 / (2eVm_e + e^2V^2/c^2)$$

Where h is the Planck constant, eV is the energy given to the electron,  $m_e$  is the mass of the electron and c is the speed of light. This can be simplified by substituting the values for h, e,  $m_e$  and c to

$$\lambda = [1.5 / (V + 10^{-6}V^2)]^{1/2} \text{ nm}$$

The above equation is used because of the relativistic effects that act upon the electrons at the velocity they are accelerated to. This results in the wavelength correction reaching 25% at one million volts (Goodhew *et al.* 2001: 23).

Electron microprobe analysis provides a greater level of precision over other, electron excitation techniques such as XRF. While SEM and EPMA methods are slower, they can determine the elemental composition of a sample to a far greater precision (0.01%) when compared to XRF (0.1%) which is best used for a snapshot view of what elements are present.

The electron microscope functions by generating a beam of high energy electrons from a filament. This is typically part of a thermionic gun which emits electrons by heating to a temperature of approximately 2800 K and being held at a high negative potential with respect to the anode (Goodhew *et al.* 2001: 24). A Wehnelt cap, which is held at a slightly more negative voltage than the filament, is used as a collimator to help control the area of the filament which emits electrons.

The produced beam passes through the Wehnelt cap, which acts as the grid of a triode valve which gives the electron gun the name of a triode gun. The important feature of this kind of gun is that the paths taken by the emitted electrons cross, making the gun the primary lense of the microscope. The brightness of the projected beam is defined as the “measure of how many electrons per second can be directed at a given area of the specimen” (Goodhew *et al.* 2001: 26). The brightness of a beam increases rapidly as the temperature of the filament and the thermionic work function ( $\phi$ ) decreases, thus it is preferable to use a filament with a high melting point and low  $\phi$  value. Tungsten is a common material used in filaments with a high melting point of 2653K and a  $\phi$  of 4.53V (Goodhew *et al.* 2001: 26). The brightness of a tungsten filament is approximately  $10^9 \text{ Am}^{-2}\text{sr}^{-1}$  (Goodhew *et al.* 2001: 26). This value can be increased by a factor of 10 or more if  $\text{LaB}_6$  is used in place of tungsten, which also has a lower  $\phi$  value of 3.0eV. Such filaments are used frequently in analytical and high resolution work due to the desirably higher brightness (Goodhew *et al.* 2001: 26).

In the case of the equipment used for specimen analysis in this study, a tungsten filament was used as

this was adequate for the purposes of slag analysis and the greater brightness level provided by a LaB<sub>6</sub> filament was not required.

The beam of electrons produced by the emitter gun then passes through several electromagnetic lenses and a collimator to produce a highly focused beam. The lenses are designed to exert a force almost parallel to the direction of travel of the moving electrons. This results in the electrons taking a helical path forming a tighter beam similar to the behaviour of light passing through a glass lense (Goodhew *et al.* 2001: 27, 28). This beam can be manipulated by adjusting the focus to make the area of analysis larger or smaller. This is also the case when deflecting the entire beam to scan back and forth across a given area as in a scanning electron microscope (SEM) (Goodhew *et al.* 2001: 29). This produces an image of the sample based on the kind of electrons being detected. Here is where the different machines exhibit their first major application differences. SEMs can examine large areas for bulk samples, this can be highly useful for heterogeneous materials where data for an “average” composition may be desired. Electron microprobes are typically more suitable for examining small features or individual phases, this combined with a greater sensitivity and precision, particularly to the lower mass elements from Na through Ca, make them the ideal choice for examining small samples where trace elements are highly important. In the case of this study, the common practice of bulk analysis has been replaced with the electron microprobe analysis of specific phases within the specimens to provide data to further examine the behaviour of phosphorus in the smelting environment. Bulk analyses mask the location of phosphorus as well as possibly misrepresenting the distribution of less mobile elements of which phosphorus is an example. This further demonstrates that bulk sampling may not always be representative of slag composition as areas of exceptionally high or low minor element concentrations may be included and skew the sample totals due to undetected heterogeneity.

The beam of electrons that interacts with the sample is composed of primary electrons (Goodhew *et al.* 2001: 29). They are called primary electrons because they have not interacted, or been generated from, an analytical sample. The images observed during the operation of an electron microscope are comprised of the same and also different electrons which leave the sample after beam-sample interaction. The beam of high energy electrons produced from the filament of the electron microprobe penetrates the sample to a depth of 5 microns. Here the electrons can undergo one of two processes, they can either experience scattering or can cause excitation. Within these interactions there are two major types, elastic and inelastic scattering which covers the excitation effects (Goodhew *et al.* 2001: 30, 31).

Elastic scattering is the major mechanism by which electrons are deflected from the sample. This means that elastically scattered electrons are the major contributors to diffraction patterns. The angle of diffraction is specific to the scattering element, which is a result of either Rutherford scattering or the

electron exploiting the mean free path which is highly dependent upon the atomic number of the scattering atom (Goodhew *et al.* 2001: 30).

Inelastic scattering is a far more general term which covers the effects experienced by primary electrons which are responsible for a detectable loss of energy. The process of Phonon scattering is responsible for the heating of a solid sample by the electron beam during analysis. Phonon scattering also deflects electrons through a relatively large angle, approximately 10 degrees, which has significant impact upon image contrast (Goodhew *et al.* 2001: 31). Inelastic scattering also covers two major forms of electron excitement, single valence excitation and inner shell excitation.

Single valence excitation is a less likely process which involves the transfer of energy from a high energy electron from the beam to a single valence electron of an atom. With the small energy loss and small scattering angle, this process is not exploited during electron microscopy. Inner shell excitation involves the knocking out of an electron from an inner electron shell and thus requires a far higher energy transfer for example 1100eV to excite a copper L electron (Goodhew *et al.* 2001: 32)

The most important form of interaction is inner shell excitation. This is responsible for the generation of diagnostic X-rays which are required for compositional analysis. The energies required to produce these X-rays are generally high, for this reason a typical voltage of 25KeV is selected to ensure that X-rays will be generated from all of the detectable elements that are present within any given sample. The process of excitation involves the transfer of energy from a high energy electron in the beam to an electron situated in an inner shell of an atom. This gives the atomic electron a greater quantity of energy, making it excited. When this electron returns to its original energy level, during relaxation, the excess energy is emitted as an X-ray of characteristic wavelength which is dependent upon the excited species of atom (Goodhew *et al.* 2001: 32, 35).

In addition to these primary effects there are also two significantly important secondary effects of the interaction of the electron beam with the analytical sample. The first of these are secondary electrons which have relatively low energies and are produced from the surface of the sample. They may originate from electrons in the beam which have little energy remaining or are electrons from the surface of the sample which have had a small quantity of energy transferred to them (Goodhew *et al.* 2001: 34). Secondary electrons are abundant with a yield of 1 per primary electron or higher (Goodhew *et al.* 2001: 34). This lower energy and high abundance means that they are commonly used for imaging rather than compositional interpretation of a sample.

The other major secondary effect is backscattered electrons. Unlike secondary electrons, those that undergo backscattering typically have a much higher proportion of their incident energy remaining (Goodhew *et al.* 2001: 34, 35). In this case the electrons are reflected back directly to the detectors with far less energy transfer occurring as they do not excite inner electrons. The diagram below illustrates the various effects as generated in a sample during analysis.

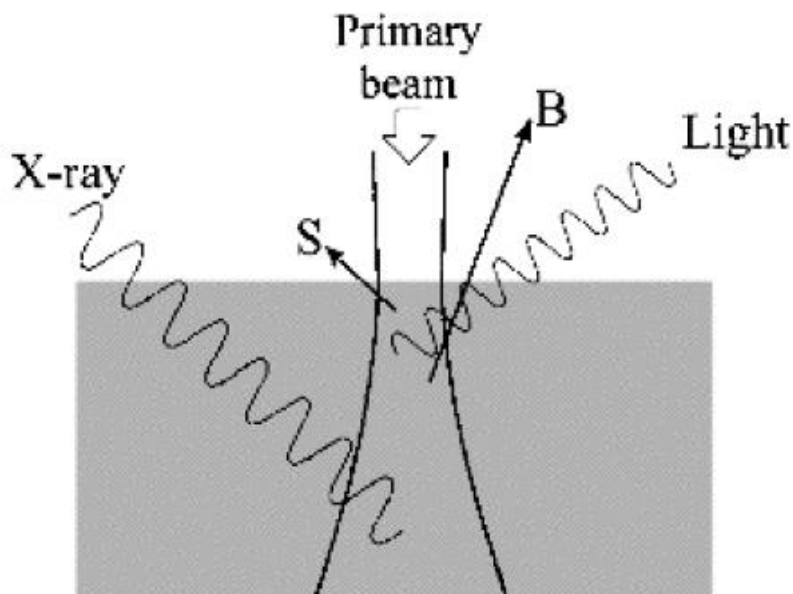


Figure 5.3.1 Showing the interaction of a primary electron beam with an analytical sample (grey) producing secondary electrons (S), backscattered electrons (B), X-rays and visible light (after Goodhew *et al.* 2001: 34).

Backscattered electrons are used for compositional imaging, diffraction and analysis as the angle of backscatter, and quantity of returned electrons is dependent upon the density of the examined material. The use of compositional imaging not only reveals the presence of different materials in a sample, but also allows for interpretation of manufacture or formation techniques. The examination of manufacturing techniques is a particularly important application of backscatter electron microscopy, with insightful studies examining the experimental welding of bronze (Azéma *et al.* 2011) and the identification of how gilt silver thread was produced (Hall 2007).

Other electrons may also be produced with the energy emitted by excited electrons being released as another electron. This effect produces Auger electrons which are best used to examine the surfaces of samples, which is rarely used in archaeological projects

For this study, compositional analysis is the chosen method. This method utilises the characteristic X-rays to identify the elements present. Compositional imaging produces a greyscale image which represents the density of the material in view. The brighter the area, the greater the density of the material present. This increase in brightness is due to the number of X-rays being detected, denser materials contain a greater number of atoms per unit volume which produce more X-rays when compared to lower density substances.

The drawback of all electron microscopy techniques is that the machine operates on the assumption that the material being analysed is homogeneous. This is entirely correct for the majority of single

colour glass samples, which due to their size can be safely assumed to be of a single composition. The other extreme is the material examined in this thesis. Iron slags are some of the most heterogeneous of all archaeological materials. Multiple mineral phases are typically present and due to the depth of analysis, it is highly likely that the bulb of analysis will penetrate more phases than those observable on the polished surface.

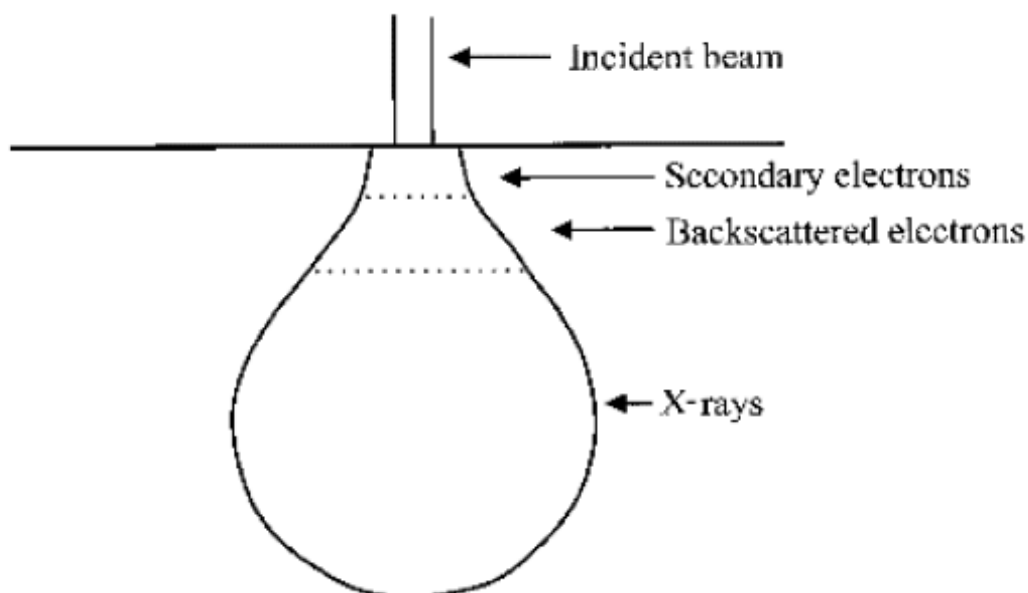


*Figure 5.3.2 showing the shape of the area of a specimen which will experience excitement, highlighting the depth of interaction compared to beam to surface contact (Goodhew et al. 2001: 126).*

In some cases voids and concealed inclusions may lie beneath, this will drastically affect the end total for that analysis spot. Typically analytical data of 70% or greater is acceptable for the analysis of iron slags. This is because of the heterogeneity of the substance, the hydration which occurs over archaeological time producing a non-detectable percentage of the total composition, and in some cases the absorption of X-rays by higher density atoms within the sample.

While SEM bulk sampling may produce an overall idea of the composition, it does not guarantee that the data is representative of the whole piece from which the sample was taken, let alone other regions within the same sample. Electron microscopy has the added benefit of being able to analyse the individual phases of the slag. The accuracy of sampling is central to this study, where the behaviour of phosphorus within slag is under examination. Bulk sampling masks the behaviour of individual elements by producing an overall composition rather than demonstrating which phase they are hosted by. This is particularly important with respect to phosphorus which exhibits both lithophilic and



siderophilic characteristics, meaning that it can, to some degree, be hosted by almost all of the phases present.

In order to achieve the best results possible from the very unpredictable material an accelerating voltage of 50keV was chosen as this would give a high count rate and a spot size of 1µm to ensure that the analyses were conducted as exclusively as possible to a single phase. This was more difficult when analysing the matrix phase in comparison to the other major phases of wüstite and fayalite. The matrix while containing the majority of the alkali and alkali earth elements, forming an approximately glassy phase, also contains many super and ultra-fine particles of wüstite. The presence of this FeO results in the matrix occasionally containing more FeO than would normally be expected. Similarly, fayalite can exhibit a secondary wüstite growth which alters the composition of the phase. This is easily identified in the data as the FeO:SiO<sub>2</sub> ratio is skewed away from the value of 2 associated with fayalite.

#### **5.4 Sampling strategy**

The material from each site was assessed following the guidance provided in Bayley *et al.* (2001) and Paynter (2011). As the slag from all of the sites was in unwashed condition it was cleaned with cold water and toothbrush to remove adhering soil to reveal the full morphology of the pieces for assessment. The masses of the metallurgical material were then recorded to allow an indication of activity level per phase of occupation to be identified. Prior to any sampling the pieces were photographed to record their original state post-excavation. This was done to mitigate any damage caused during sampling, as slag is a heterogeneous material there is no certainty that a piece will survive sampling comparably intact. This way, even if a piece suffered catastrophic fracture due to heterogeneity a record of the original appearance is preserved allowing for a fuller interpretation of the origin and conditions the piece experienced. The pieces selected for sampling were chosen based upon their morphology, colour and density. These characteristics are the most important in terms of preliminary identification of metallurgical material.

The use of perceived mass – how heavy the piece appears in comparison to its size, referred to as density here for simplicity, as a criterion for sample selection is particularly important in the case of this assemblage where a large proportion of the material originated from smithing processes. In the case of iron slags the density is derived from the quantity of high iron content phases present. It is for this reason that smelting slags which contain significantly more wüstite and metallic iron are possessed of higher density. This directly impacts upon the colour of the slag as well, with higher wüstite content resulting in a darker slag.

By cutting on the diamond saw to obtain analytical samples the damage caused to the slag pieces, whether intact or previously broken, was kept to a minimum. The orientation of the cut was selected based upon how stable the piece was held in the grip of the saw to prevent damage to the saw blade during use. Samples of a thickness not in excess of 1cm were taken so that further analyses could be conducted in future without requiring further sampling of the original material.

Pieces that were not cut using the saw were ground using p220 silicon carbide paper prior to mounting. This produced a flatter surface on the sample which reduced the time required for grinding and polishing.

The larger pieces were sampled using a hammer and chisel to break a piece off the main body of the artefact. As some of the larger pieces were too large for the saw this was the only means available, which unfortunately does cause more damage to the piece. These samples were ground on p220 paper to flatten the surface prior to mounting to reduce the amount of preparation required before analysis.

Each site had its own individual considerations when selecting samples, which are detailed below.

### East Yorkshire

All of the material from the sites in the Foulness Valley and Hull Valley is unstratified surface collection finds. The lack of later smelting in the same areas limits the origin of the slag to the Iron Age as a working hypothesis. Representative pieces from each site were selected in order to produce micro-assemblages which could be analysed efficiently.

### Caistor

The Caistor assemblage is dominated by smithing slag with a small quantity of unstratified evidence for smelting. These pieces were preferentially selected first in order to include primary production evidence.

### Quarrington

The material from Quarrington had previously been examined and so the initial report was taken as guidance for this study. Where stratified material was examined first as this was previously reported in Taylor *et al.* (2003). The majority of the slag exhibited a flowed appearance with a dark surface which is diagnostic of tap slag. Other pieces which were possessed of high density were placed to one side for consideration as possible furnace slags.

The unstratified material was examined as this would provide further evidence of activity on the site as no other ironworking evidence had been recovered from the site except that of Early Saxon date. The two largest pieces of unstratified slag were broken on an anvil using hammer and chisel. This was done to reveal their internal structures to further clarify their nature and origin. One was a smithing hearth bottom, with a light grey interior and the other was a far darker grey synonymous with iron smelting. This characteristic colour combined with the high density lead to the interpretation of this piece being either a small furnace bottom or a large piece of furnace slag. The piece removed from the large smelting slag body was then cut on a rotary diamond saw for analysis.

Within the assemblage there were also two pieces of red stained stone. These may have been ore bearing rock, however the quantity of the red probable ore material remaining made it unlikely that a suitable sample could be taken for analysis without causing significant damage to the pieces. Their presence was recorded and then they were discounted from the pool of desirable analytical material.

### Flixborough

The quantity of material taken in preliminary selection was limited by my ability to carry the box on public transport. This restricted the size of pieces and overall mass of material I could select, however it did ensure that many of the pieces were of diagnostic nature, rather than non-diagnostic meaning that they were directly suitable for sampling and analysis.

A second selection of material was conducted in order to ensure that material from both periods of iron production were included. This was done in the hope of identifying any changes in phosphorus content in the material over time, which may be indicative of different ore exploitation strategies between periods.

## **5.5 Justification of methods**

There are two major techniques used in the selection and analysis of samples as part of this work. The first is the method of sample selection based on morphology, colour, and perceived mass. The study of Serneels and Crew (1997) demonstrates that there is a reduction in iron content from ore to large smithing slags as the processes of metal extraction and refining progress. This directly affects the perceived mass of the pieces, as iron is the heaviest element present in an appreciable abundance, a reduction of which causes a reduced perceived mass. The morphology is a result of the process which produced the specimens. The colour of the pieces is influenced by the redox conditions experienced by the slag during formation and cooling. A more oxidising environment will result in the slags displaying a redder colour due to the greater presence of more oxidised iron species such as  $\text{Fe}_2\text{O}_3$ , when compared to  $\text{FeO}$  which is a duller grey/black colour.

The use of morphology is a good starting point when describing and categorising iron slags. The diagram shown in figure 5.1.1 illustrates how many of the slag types can be separated during desktop study, allowing for a broad, but reasonably quick assessment of ironworking activity at a given site. There is the possibility of non-diagnostic slags with no distinct morphology. This could be due to the presence of archaeological breaks, or flowed morphology with a lower perceived mass such as fayalitic runs. These may originate from either smelting or smithing depending on the quantity of fayalite present and the redox conditions the slag experienced. Post-depositional processes can also have an influence on the appearance of iron slags. In the case of the East Yorkshire slags, this includes the deposition of hydrated iron oxides on the surface of the material, which causes some specimens to have an oxidised orange surface. Oxidation may also occur following removal from the furnace or hearth, resulting in partial oxidation of iron-rich areas. For these reason only diagnostic pieces were selected for electron microscopy examination, to ensure that the data was more representative of identifiable processes, removing possible ambiguity from the interpretation of each assemblage.

The electron microscopy technique used here is not the more common bulk analysis method. Bulk sampling has the benefits of being quicker and providing a more general overview of the specimen composition. By mapping an area for x-ray generation and producing the data from a region of mixed phase composition, bulk sampling provides a closer to mean average composition for the specimen. The downfall of this is that it operates on the presumption that the sampled area is representative of the overall mineral distribution within the slag. As phosphorus concentrates predominantly in the glassy matrix, the proportion of matrix present in a given sample will provide an indication of how much phosphorus is present in the overall sample. However, this is an assumption based on the limited observable area of the prepared piece. The appearance and composition of a mounted slag sample may vary dramatically across the observable surface, so to infer that the examined bulk sample areas are representative may not always be reliable.

Examining each phase independently by microprobe allows for spots to be placed on areas of matrix which are distant from each other within the sample. This will highlight the possibility of heterogeneous phosphorus distribution, but has the shortcoming of being influenced by the effect of phosphorus concentration in a smaller quantity of matrix. This concentration can result in seemingly high phosphorus content in the spot, which in reality reflects a lower overall phosphorus content in the entire sample due to the overall volume of phosphorus hosting material. To mitigate this possibility having a significantly detrimental impact on the integrity of the data, multiple points are plotted across the sample in different areas and the results used to calculate a mean average.

As any investigation is limited by the equipment available, the use of microprobe analysis and the averaging of compositions taken across samples is the best compromise for not having access to SEM bulk sampling. By taking multiple points and averaging the phase composition this allows the phosphorus content across the sample to be more accurately represented. Bulk sampling would effectively dilute the phosphorus content on a point by point basis by analysing phases, such as wüstite, which do not host phosphorus, and so make taking a greater number of analyses a necessity to provide similar indications. The other major benefit of employing EMPA is that trace element data can also be gathered from the same plots in the matrix phase. This will supply a new dataset which can be utilised in the future for provenance studies, without the need to re-analyse the samples to obtain a significant quantity of data.

# Chapter 6

## Archaeological Material

|            |                              |                   |
|------------|------------------------------|-------------------|
| <b>6.1</b> | <b><i>East Yorkshire</i></b> | <b><i>150</i></b> |
| <b>6.2</b> | <b><i>Caistor</i></b>        | <b><i>158</i></b> |
| <b>6.3</b> | <b><i>Quarrington</i></b>    | <b><i>209</i></b> |
| <b>6.4</b> | <b><i>Flixborough</i></b>    | <b><i>218</i></b> |

### 6.1 East Yorkshire material

As the material from East Yorkshire was recovered as surface finds from working agricultural fields it is not currently possible to provide specific site data regarding the number of furnaces or exact location of production due to the lack of excavation undertaken at many of the sites. The following section describes the material examined to provide data from slag which is known to be produced from high phosphorus bog ore as a control set. The sites are all low lying no more than 3m above sea level. This results in them being waterlogged during wet winters, as I have experienced during a visit to the sites in 2015. The site at Thearne has an unexcavated furnace with slag in situ, unlike the others (Hasholm Hall and Bursea House farm), which have not provided any other finds except those brought up by ploughing. The seasonal waterlogged and dry nature of the sites, results in regenerating bog ore deposits which form rapidly over the space of a few years into large, thick nodules. These are ideal for smelting due to the inclusion of the sand rich soil acting as a self-contained flux, which helps to explain why iron production was so concentrated in the area during the Iron Age.



*Figure 6.1.1 Thearne smelting slag drips*

The drips shown above in figure 6.1.1 are a representative selection of slag drips from the site at Thearne. They typify the arrested flowed appearance of rapidly cooled slag which appears during smelting. Commonly these drips contain large pores resulting from trapped gas, this combined with the flow direction of the cooling slag is what gives the drips their bulbous features.



*Figure 6.1.2 Hasholme Hall smithing hearth bottom profile*

This piece from Hasholme Hall (Figure 6.1.2) exhibits the classic diagnostic plano-convex profile associated with smithing hearth bottoms. The appearance of these characteristic slags both here and also at Bursea house (see figure 6.1.3 below) demonstrate that the iron production centres were not solely concerned with the manufacture of raw, bloom iron, but were also responsible for the production of at least workable bars for later smithing.





*Figure 6.1.3 Hasholme Hall smelting slag with fuel inclusion marks – dark central region and surviving fuel inclusions, black charcoal in circular pore below large fuel inclusion impression.*

The smelting slag from Halsholme Hall above clearly shows surviving fuel inclusions within pores where larger pieces of charcoal had been and the impressions of large charcoal pieces. Such an appearance is typical of prehistoric iron slag and is used as a diagnostic tool in order to provide a preliminary proxy-date during excavation.



*Figure 6.1.4 Hasholme Hall smelting slag showing heterogeneous appearance.*

This piece of smelting slag illustrates the heterogeneous nature of the material. This piece has three distinct different colours within the main slag body; the dark grey commonly associated with smelting slag (1), a lighter grey potentially a result of weathering as indicated by the patches of orange/brown oxidation (2), and a pale grey-green seen as a band towards the centre (3). There is also a region where the natural bog ore deposition has occurred upon the surface of the material to the left of the image. The inclusion of small pebbles (pale/off-white colour), top left, may have entered the smelt with the ore as they are encased in slag.



*Figure 6.1.5 Bursea House smithing hearth bottom profile.*

The smithing hearth bottom from Bursea House has the diagnostic plano-convex shape and clear fuel inclusion marks. While smithing slag is not diagnostic of the ore used to produce the metal that was worked, due to the addition of oxides from secondary fuel and flux, it can give an indication of the composition of the metal that was forged. In the case of the Bursea House smithing slag it is likely to have been made during smithing of the metal produced there, as such the phosphorus content should be elevated due to forging phosphorus rich metal produced from the bog ores found there.



*Figure 6.1.6 Bursea House smelting slag.*

This piece of smelting slag from Bursea House has a flowed upper surface comprising of several separate slag flows which formed this thick plate of tapped slag.





*Figure 6.1.7 Bursae House green smelting slag.*

This piece has a very different appearance to all of the Iron Age slag previously recovered and examined. The pale green, Munsell soil chart reference 7.5GY 6/1, flowed and unusually un-rusty surface of this piece suggests that it originated from different reaction conditions to those which produced the rest of the slag found at Bursae House. An oolitic piece of slag such as this is commonly associated with blast furnace production as there is such a high fayalite content that it appears green. However it may have been caused by a significant failure within the furnace and the inclusion of a large quantity of furnace fabric, resulting in a portion of slag which has absolutely no free wüstite to produce a dark surface or interior as seen in the fracture surfaces at the top and bottom of the piece.

## **6.2 Roman smelting: Caistor Ironworking debris**

The Roman site of Venta Icenorum at Caistor St. Edmund, Norfolk has been excavated over the past four years and has thus far yielded extensive evidence of metallurgical activity. This section is a report briefly describing the analysis undertaken upon a small selection of pieces as a preliminary investigation with the aim of determining both the kinds of material that will be encountered and the methodology for future examination.

The sample group numbered a total of twelve pieces, many of which were small drips of dark coloured, highly porous slag. One of the pieces was considerably larger and of lighter colour than the rest of the sample, the reasons for which will be discussed later.

Ironworking debris is an umbrella term which encompasses both primary and secondary iron slags. Primary slags are produced during iron smelting and as such are the first slags to be produced from the raw materials. Secondary slags are those produced during subsequent working of iron by smithing. Due to the different process the different slag types of primary and secondary are also referred to as smelting and smithing slags respectively.

## Spatial distribution

The trench locations are presented on figure 6.2.1 below.

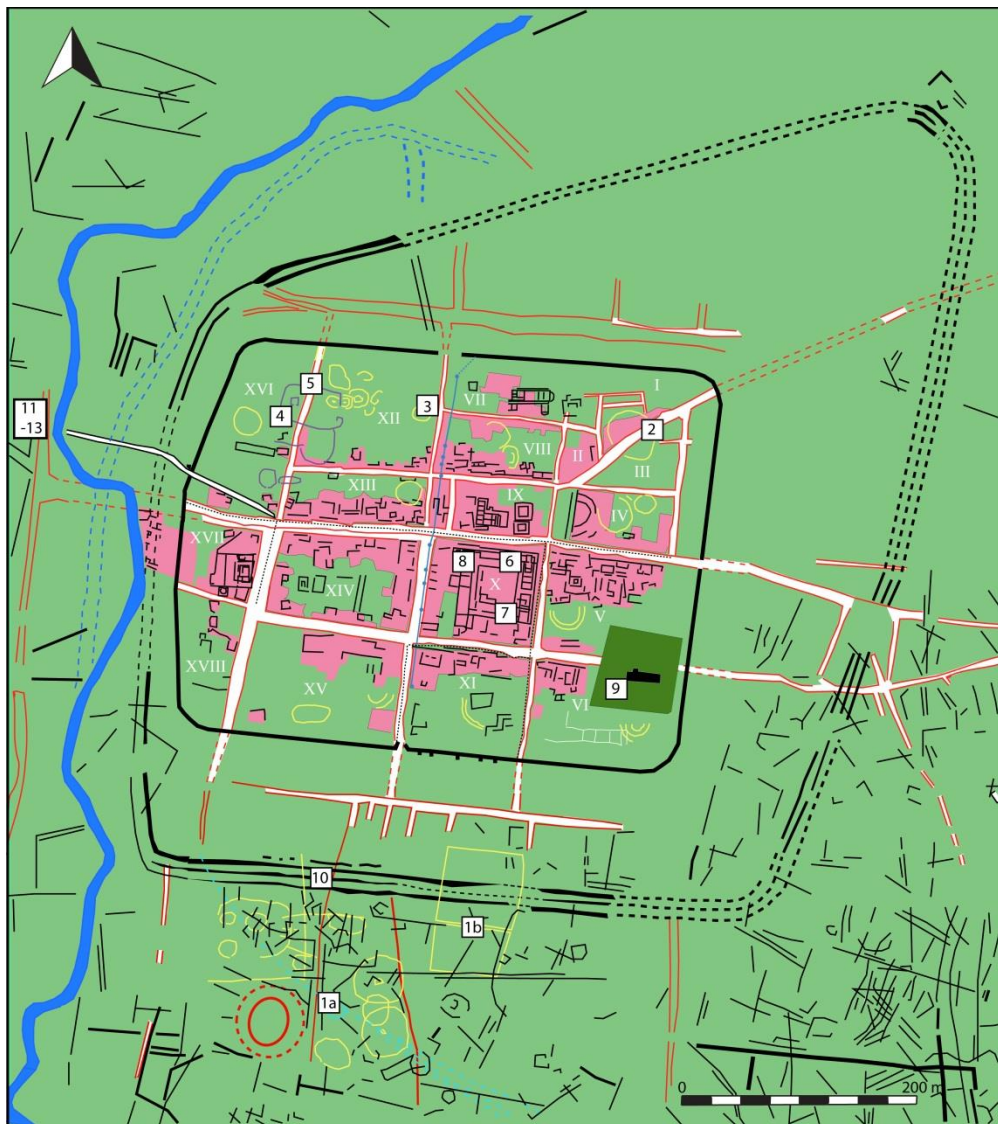


*Figure 6.2.1 showing trench location (white squares with numbers) in relation to identified archaeological features at the site of Venta Icenorum.*

The distribution of slag at the site was found to occur in two major concentrations, the main deposits being within the forum and the smaller concentration being outside the settlement at Trenches 11 and 12. The majority of the material discovered in the forum was found in trench 7 in the South-East corner. Figure 1.2 below shows the distribution of material within trenches 6 and 7 per phase highlighting the peak period of activity and slag deposition.

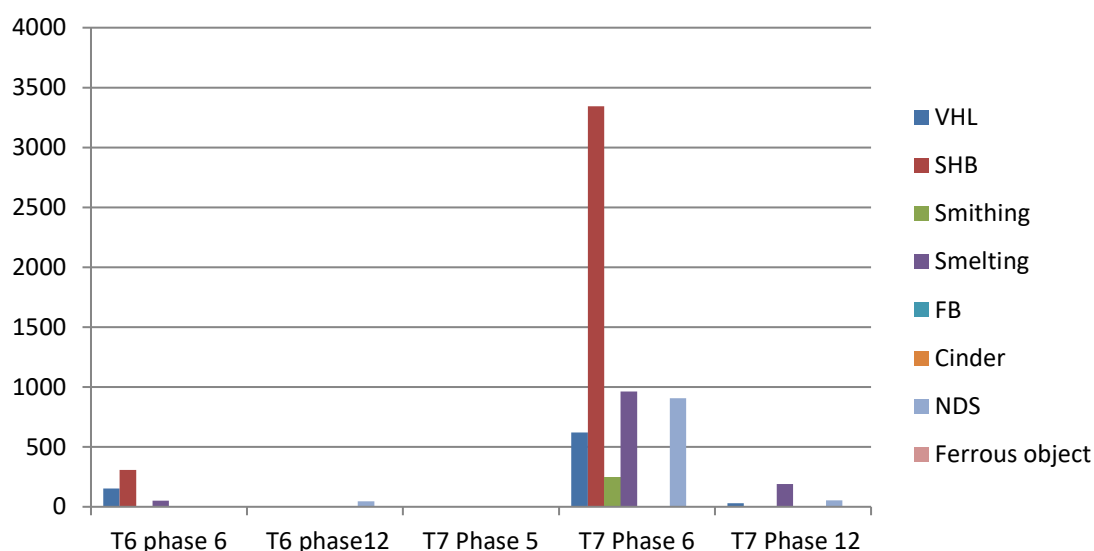


Figure 6.2.2 showing the distribution of slag by trench and phase within the forum.

The deposition of slag in the area within trench 7 may suggest that the South-East corner of the forum was adopted as the location for slag deposition, rather than the location of the actual smithing activity. The distance of approximately 50m between trenches 6 and 7, combined with the appearance of all major slags and small ferrous objects – potentially scrap, may further indicate that the smithing activity occurred in the region of trench 6 with the slag being removed to the other side of the forum in order to keep the smithy tidy and in a working condition. The precise location of the smithy cannot be confirmed as the hammerscale distribution study has not been completed.

The total lack of slag from Trench 8 would suggest that the west side of the forum did not experience metallurgical activity.

The earlier material, being mostly vitrified hearth lining (Figure 12.1), was recovered from Trench 10 which was situated across the main ditch to the south of the fort. The deposition of waste material in fort ditches is common as they form a convenient location for dumping waste. Similar behaviour is seen at Housesteads where metallurgical waste, both ferrous and non-ferrous, was deposited in the ditches surrounding the fort (Dungworth 2001).

The material from Trenches 11 and 12 was found beyond the boundaries of the settlement and may be from contexts dating to the Saxon period, however the lack of morphological differences between it and the other securely date Roman finds may suggest that it is residual Roman material which has been redeposited rather than being definite Saxon evidence.



## Phasing of material

The majority of the material was recovered from phases dated to the late 3<sup>rd</sup> to early 5<sup>th</sup> centuries AD, this is represented by phase 6 in the site phasing scheme. The earliest material dates to the 2<sup>nd</sup> century AD (phase 4) and small quantities date to both the late 2<sup>nd</sup> to late 3<sup>rd</sup> (phase 5) centuries and 5<sup>th</sup> to 6<sup>th</sup> centuries (phase 7). Little morphological difference is observable between the material dating to the Roman and Post-Roman periods, suggesting that changes in smelting technology did not occur immediately after the main Roman period of site occupation. This interpretation of technological continuity is limited by the lack of evidence for smelting recovered from the excavated areas and further excavation of the large anomalies found by magnetometer survey may yield more significant proof of iron production methods at the site.

The remaining material excavated from contexts belonging to phase 12 may belong to phases of several dates. Many of the phase 12 contexts considered here are either trench backfills from previous excavations, spoil heaps or plough soils. Many of the plough soils occur directly above contexts dated to phase 6. This restricts the dating of material recovered from these plough disturbed layers as being no later than the late 3<sup>rd</sup> to early 5<sup>th</sup> centuries.

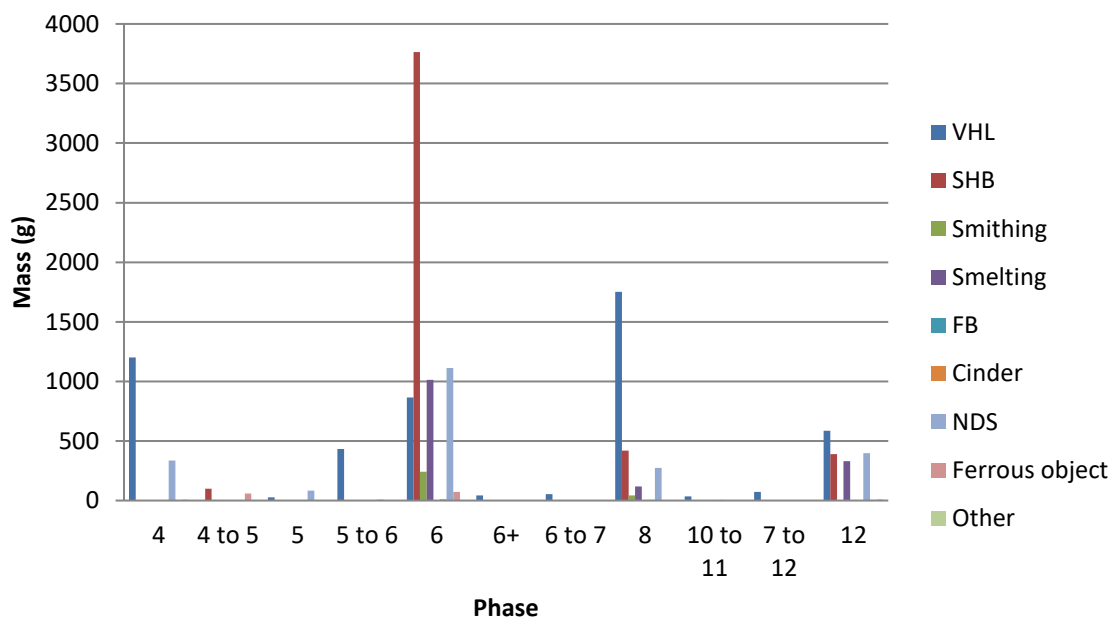


Figure 6.2.3 showing the quantity of ferrous metallurgical debris per phase.

The distinct lack of morphological differences between the phase 6 and phase 8 materials may suggest that the later samples are residual Roman pieces rather than being Early Saxon. However, it may also be possible that if the same ore source was being exploited the resultant slag would be near indistinguishable without a significant change in technology. As there is no evidence of a distinct technological change during the Early Saxon period, it is likely that the majority of slags produced would be physically indistinguishable from earlier Roman examples.

### **Analysed samples**

#### **CRT09/2024**

This sample comprised of a fired clay tempered with flint inclusions. There were some regions of high iron content and some vitrification which can also have a similar appearance to some slag.



*Figure 6.2.4 Showing sample CRT09/2024 prior to sampling.*

While sampling this piece, some of the larger flint inclusions became separated from the ceramic body. The flint appears to have been added in order to increase the refractory properties of the clay as it is not a kaolin clay of high silica content.

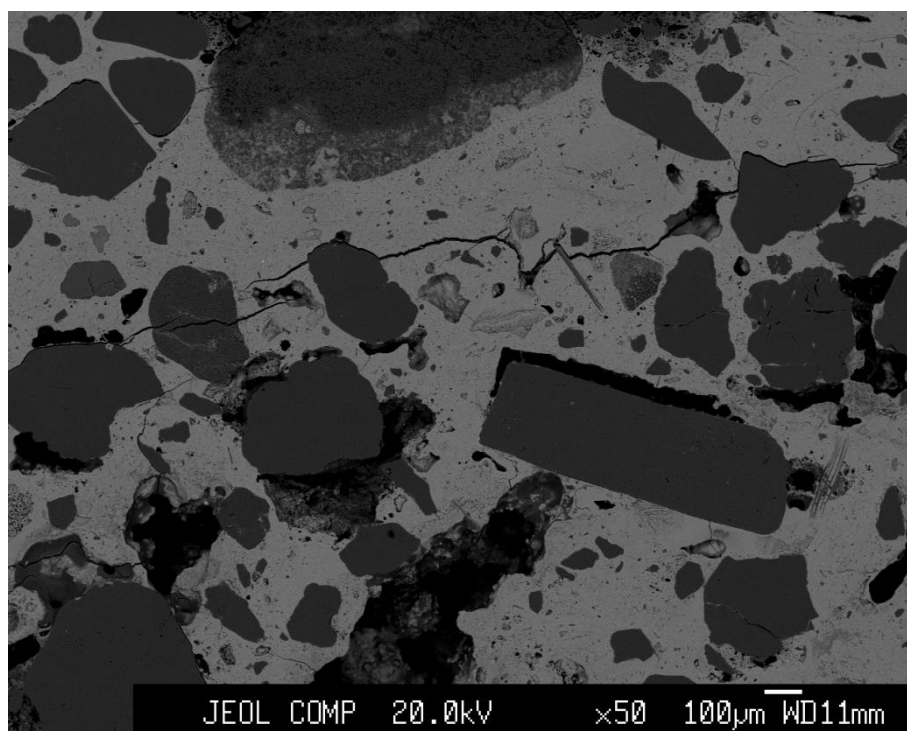


*Figure 6.2.5 Showing ceramic body of CRT09/2024 with approximately rectangular flint inclusion and silica grains.*

The orange colouration of the clay indicates that it was exposed to elevated temperature in an oxidising environment; however it is not possible to attribute this to an iron smelting operation as several other processes, including iron smithing, could produce a similar material. Parts of the ceramic body were notably iron rich, which may also suggest that this material had been exposed to reducing conditions as well as oxidising conditions.

| Element                | FeO   | SiO <sub>2</sub> | P <sub>2</sub> O <sub>5</sub> | Al <sub>2</sub> O <sub>3</sub> | CaO  | MnO  |
|------------------------|-------|------------------|-------------------------------|--------------------------------|------|------|
| Iron rich ceramic body | 70.29 | 2.36             | 1.49                          | 0.86                           | 0.93 | 0.63 |
| Flint inclusion        | 0.27  | 95.16            | 0.02                          | 0.04                           | 0.03 | BDL  |

*Table 6.2.1 Showing major elements present in the main features of CRT09/2024.*

| <b>Element</b>         | <b>MgO</b> | <b>SO<sub>3</sub></b> | <b>K<sub>2</sub>O</b> | <b>CoO</b> | <b>NiO</b> | <b>CuO</b> | <b>ZnO</b> | <b>As<sub>2</sub>O<sub>5</sub></b> |
|------------------------|------------|-----------------------|-----------------------|------------|------------|------------|------------|------------------------------------|
| Iron rich ceramic body | 0.18       | 0.06                  | 0.01                  | 0.12       | 0.03       | 0.13       | 0.27       | 0.05                               |
| Flint inclusion        | BDL        | 0.02                  | 0.02                  | BDL        | 0.004      | 0.09       | 0.02       | BDL                                |

*Table 6.2.2 Showing minor elements present in the main features of CRT09/2024*

#### CRT09/2004

This specimen comprised of slag adhering to ceramic material. The ceramic exhibits extensive vitrification and there are multiple colours present within the glassy slag.

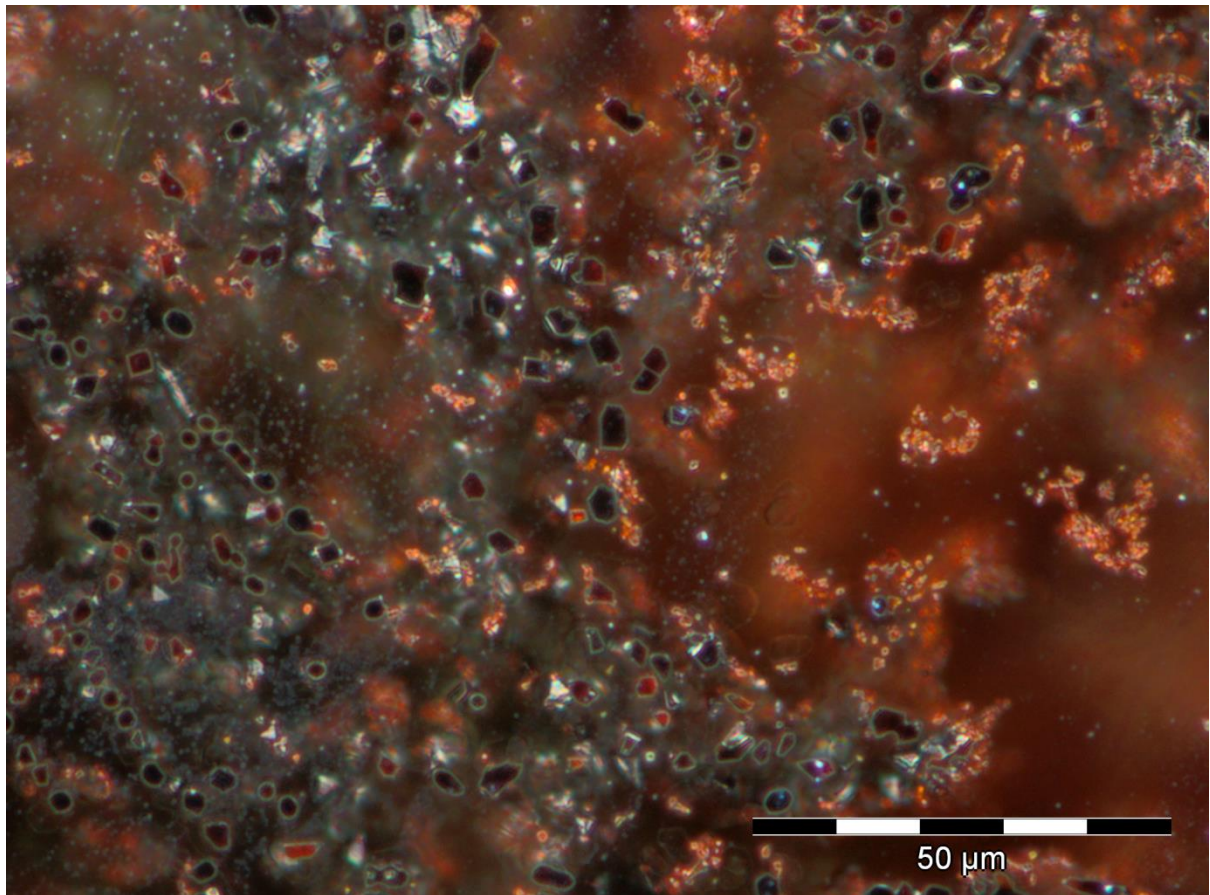


*Figure 6.2.6 Showing dark field image of red colouration in glassy slag of CRT09/2004.*

The red colouration may be due to the presence of a small quantity of reduced copper. Small areas of metallic copper are observable both in dark field (bright orange) and bright field images.

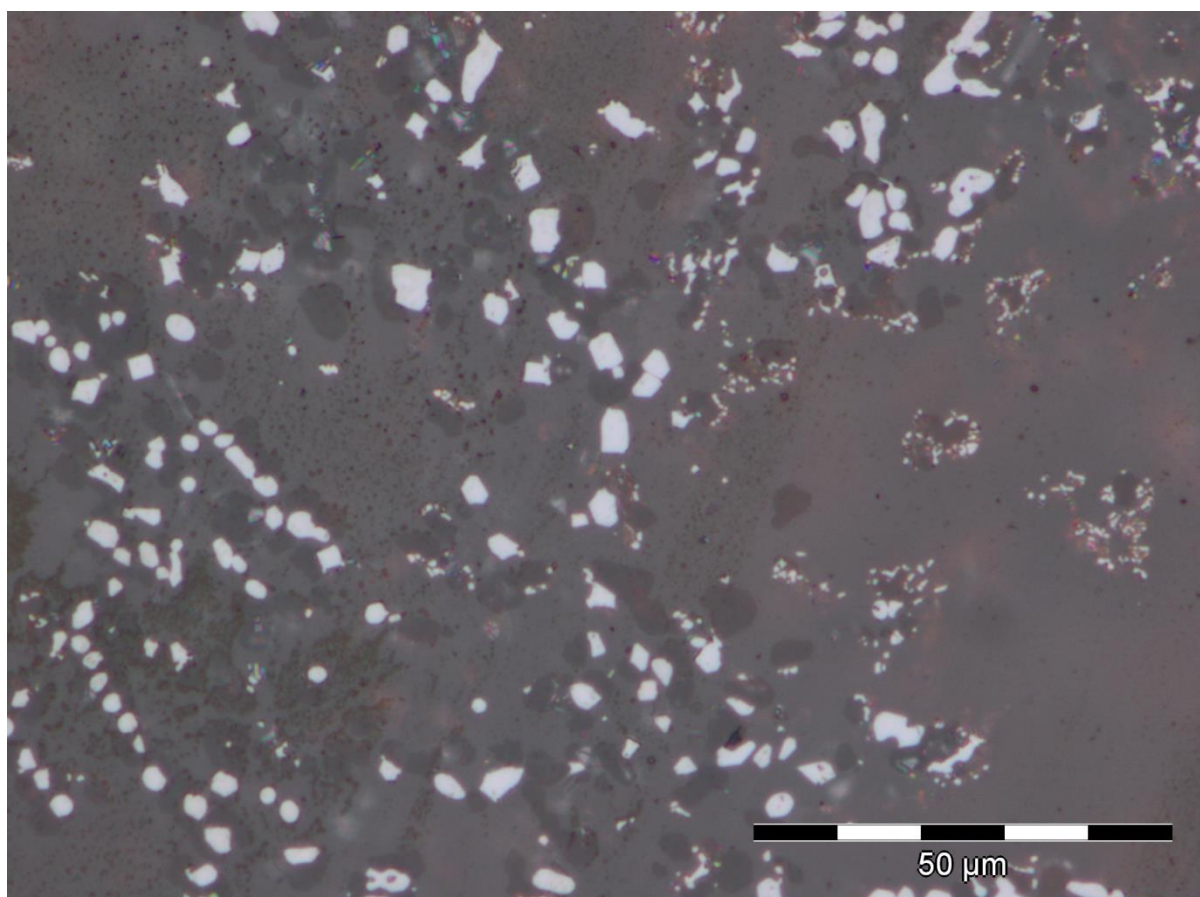


Figure 6.2.7 Showing bright field image of red colouration in glassy slag of CRT09/2004.

Fine wüstite dendrites are also present, which indicate that the sample cooled relatively rapidly, preventing dendrite growth.

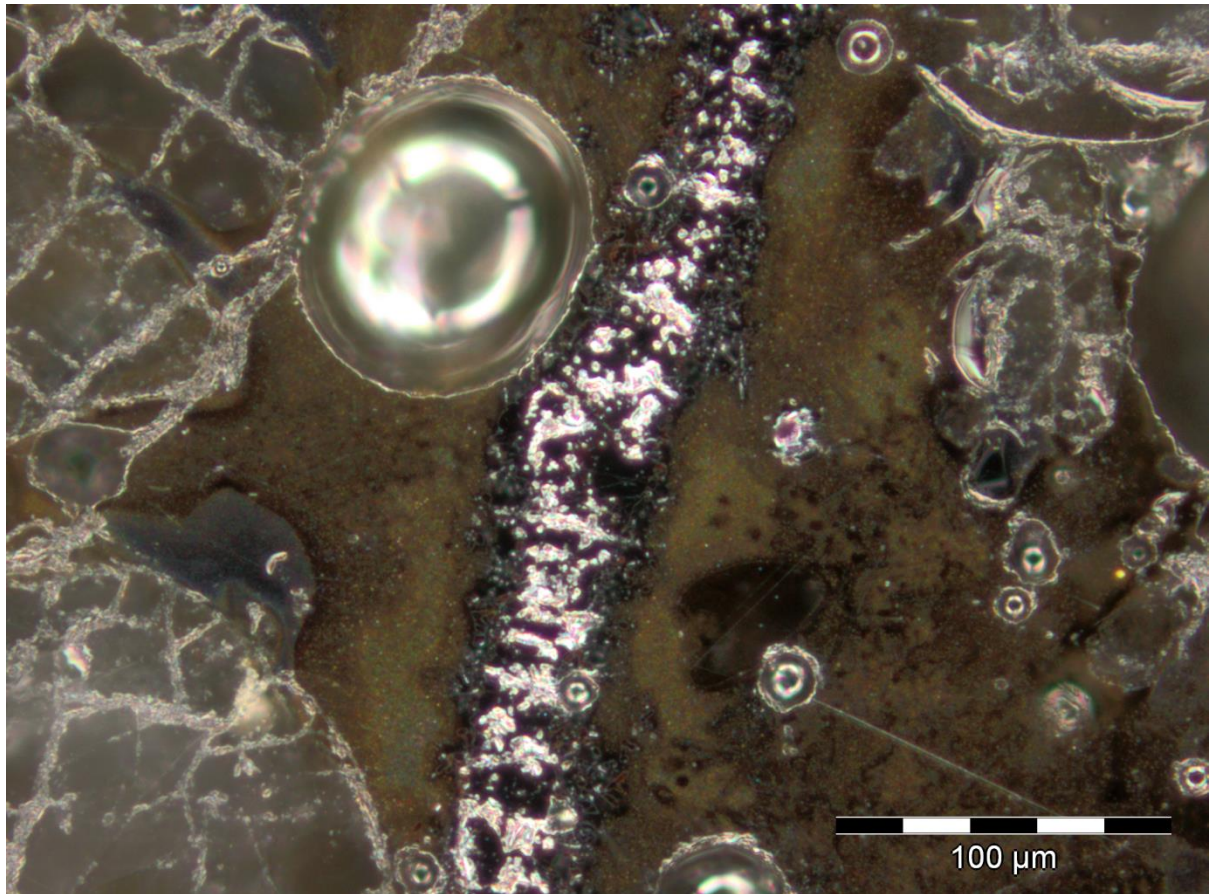
| Element                  | FeO  | SiO <sub>2</sub> | P <sub>2</sub> O <sub>5</sub> | MgO  | Al <sub>2</sub> O <sub>3</sub> | K <sub>2</sub> O | CaO   | CuO  | MnO  |
|--------------------------|------|------------------|-------------------------------|------|--------------------------------|------------------|-------|------|------|
| CRT09-2004<br>red colour | 9.05 | 52.87            | 1.12                          | 2.83 | 8.20                           | 1.37             | 18.67 | 0.04 | 0.64 |

Table 6.2.3 Showing major elements and copper content of red coloured area in CRT09/2004.

| Element                  | Na <sub>2</sub> O | SO <sub>3</sub> | TiO <sub>2</sub> | V <sub>2</sub> O <sub>5</sub> | Cr <sub>2</sub> O <sub>3</sub> | CoO  | NiO  | ZnO  | BaO  |
|--------------------------|-------------------|-----------------|------------------|-------------------------------|--------------------------------|------|------|------|------|
| CRT09-2004 red<br>colour | 0.24              | 0.02            | 0.39             | 0.01                          | 0.002                          | 0.02 | 0.01 | 0.02 | 0.08 |

Table 6.2.4 Showing minor elements present in red coloured area of CRT09/2004.





*Figure 6.2.8 showing metallic area in olive green slag in CRT09/2004.*

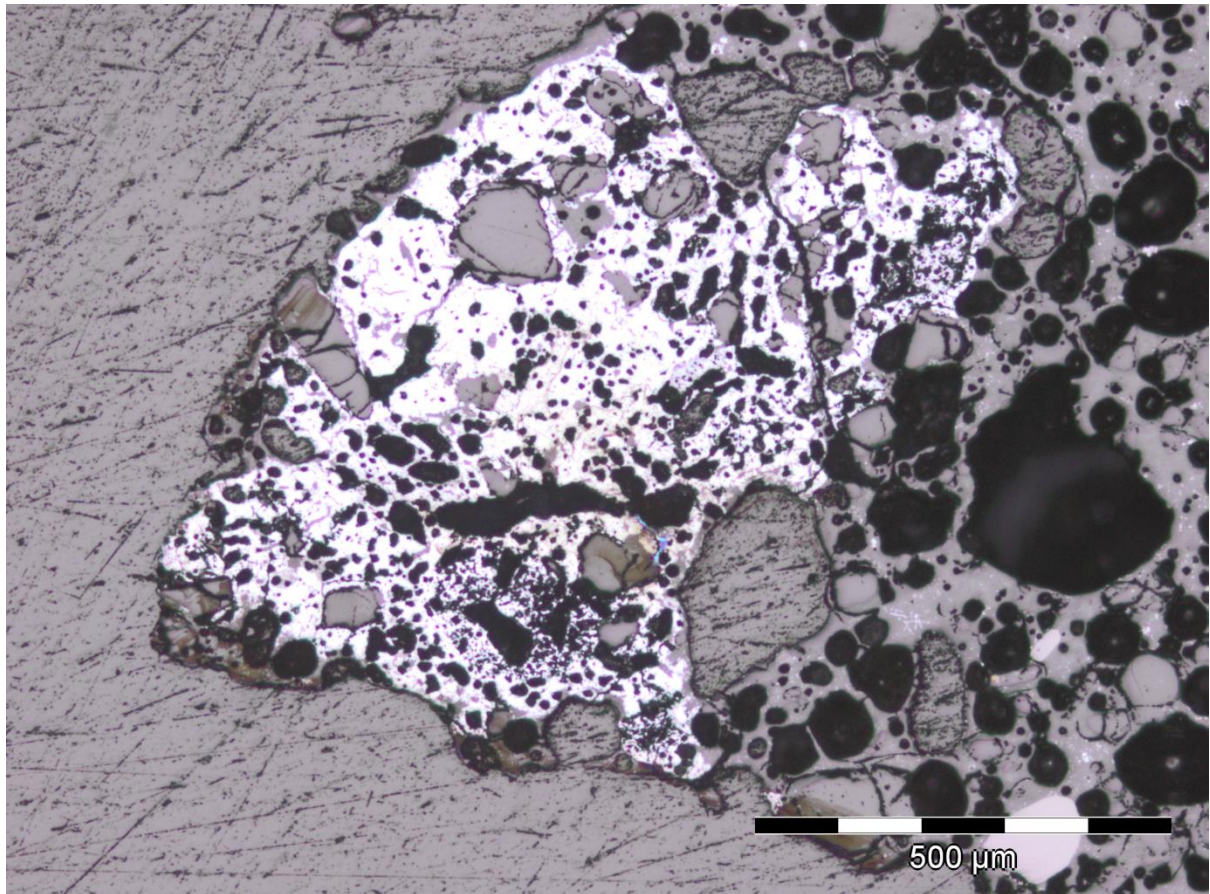


Figure 6.2.9 showing oxidised metallic area in CRT09/2004.

| Element                | Fe | Si   | P    | Al   | O     |
|------------------------|----|------|------|------|-------|
| oxidised metallic area | 54 | 7.14 | 0.25 | 2.54 | 27.99 |

Table 6.2.5 Showing analysis of oxidised metallic region in CRT09/2004.



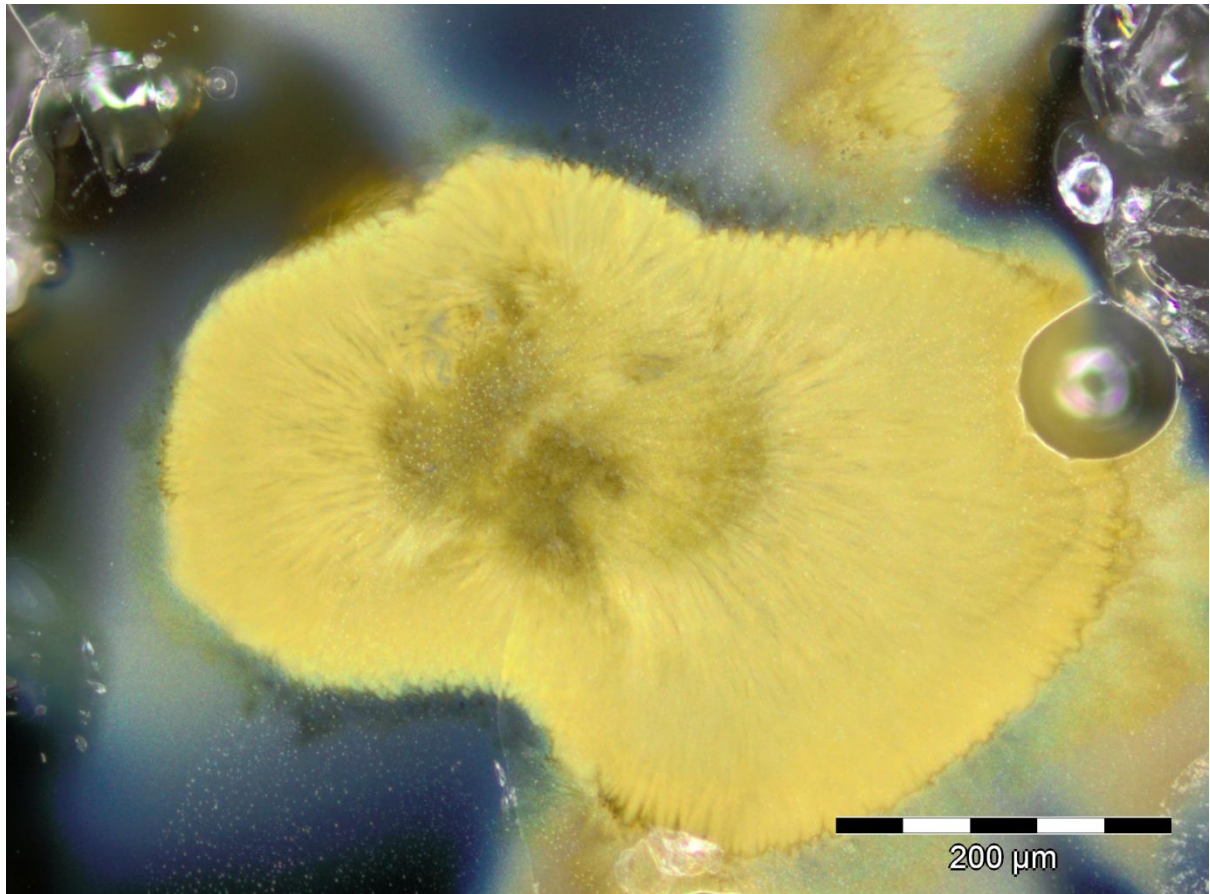


Figure 6.2.10 showing yellow colouration in a region of blue/black and olive green glassy slag in CRT09/2004.

This distinct yellow colouring shown above was not observable as a distinct area in backscatter detection during EMPA. The analysis did return slightly higher values for Barium than many of the other phases present. The higher barium content may have resulted in the lemon yellow colour observed.

| Element       | FeO   | SiO <sub>2</sub> | P <sub>2</sub> O <sub>5</sub> | MgO  | Al <sub>2</sub> O <sub>3</sub> | K <sub>2</sub> O | CaO   | BaO  |
|---------------|-------|------------------|-------------------------------|------|--------------------------------|------------------|-------|------|
| yellow colour | 12.67 | 56.22            | 0.71                          | 1.69 | 6.02                           | 3.16             | 12.95 | 0.05 |

Table 6.2.6 Showing major elements detected in yellow coloured area of CRT09/2004, including a notable Barium content.

| Element       | Na <sub>2</sub> O | SO <sub>3</sub> | TiO <sub>2</sub> | V <sub>2</sub> O <sub>5</sub> | Cr <sub>2</sub> O <sub>3</sub> | MnO  | CoO  | NiO  | CuO  | ZnO  |
|---------------|-------------------|-----------------|------------------|-------------------------------|--------------------------------|------|------|------|------|------|
| yellow colour | 0.41              | 0.02            | 0.46             | 0.004                         | 0.01                           | 0.45 | 0.02 | 0.01 | 0.04 | 0.01 |

Table 6.2.7 Showing minor elements detected in yellow coloured area of CRT09/2004, including a notable Barium content.

**CRT09/2008**



*Figure 6.2.11 Showing the lower and upper surfaces (left and right respectively) of CRT09/2008 prior to sampling.*

Within the initial sample examined here, the largest slag body, sample CRT09/2008 recovered from Church Trench 2, proved to be far richer in fayalite than any other piece. This combined with the approximate plano-convex form would lend itself towards the interpretation of this piece as a smithing hearth bottom.

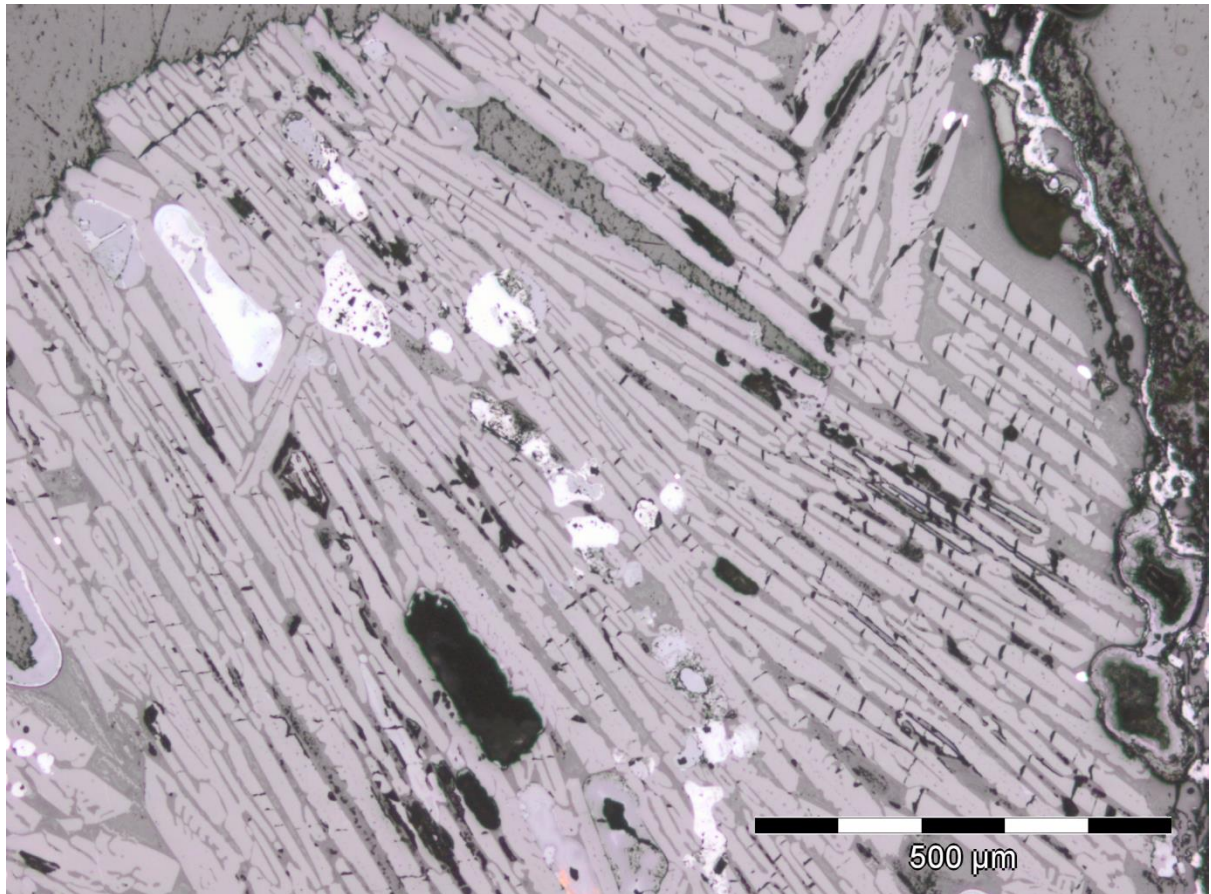


*Figure 6.2.12 Showing CRT09/2008 fayalite laths (light grey) with iron prills (white) under optical microscope.*



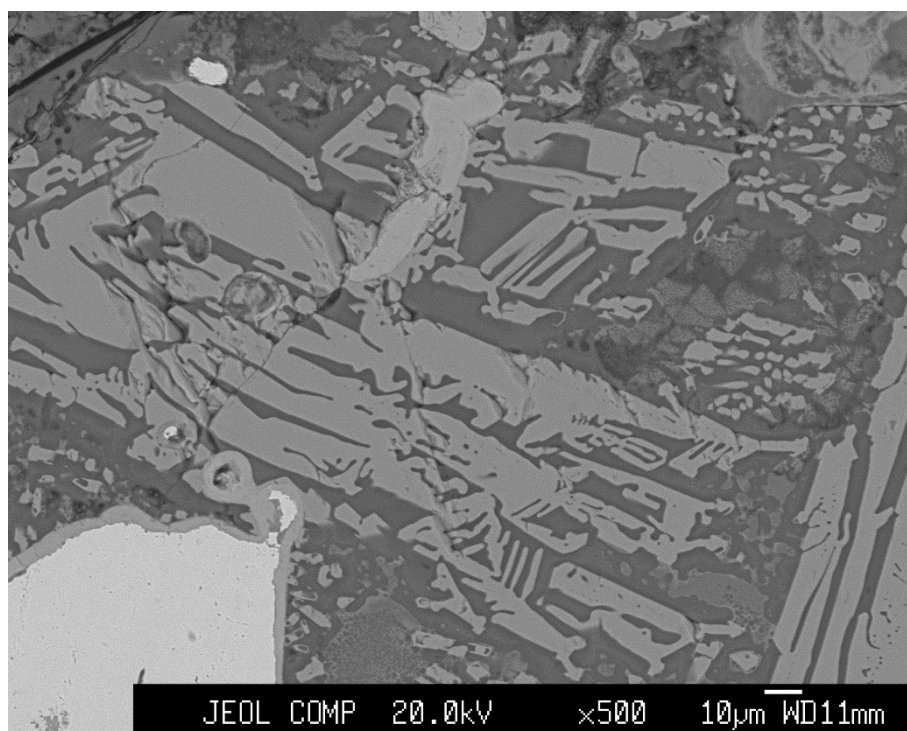


*Figure 6.2.13 Showing CRT09/2008 large fayalite grains (light grey) in matrix with metallic iron prills (white).*

| Element                                       | FeO   | P <sub>2</sub> O <sub>5</sub> | Al <sub>2</sub> O <sub>3</sub> | CaO   |
|---|-------|-------------------------------|--------------------------------|-------|
| CRT09-2008 Lath near large prill              | 64.58 | 0.11                          | 0.03                           | 0.75  |
| CRT09-2008 Inter-lath material nr large prill | 29.27 | 0.20                          | 5.43                           | 3.11  |
| CRT09-2008 Large grain/lath                   | 65.27 | 0.02                          | BDL                            | 0.97  |
| CRT09-2008 Inter grain/lath mid-density       | 23.12 | 0.82                          | 7.29                           | 12.21 |
| CRT09-2008 Matrix1                            | 19.10 | 0.30                          | 10.44                          | 5.66  |
| CRT09-2008 Lath nr second prill               | 63.04 | 0.06                          | 0.38                           | 0.79  |
| CRT09-2008 Matrix nr second prill             | 17.09 | 0.40                          | 7.57                           | 5.11  |

*Table 6.2.8 Showing major elements present in observable phases of CRT09/2008.*

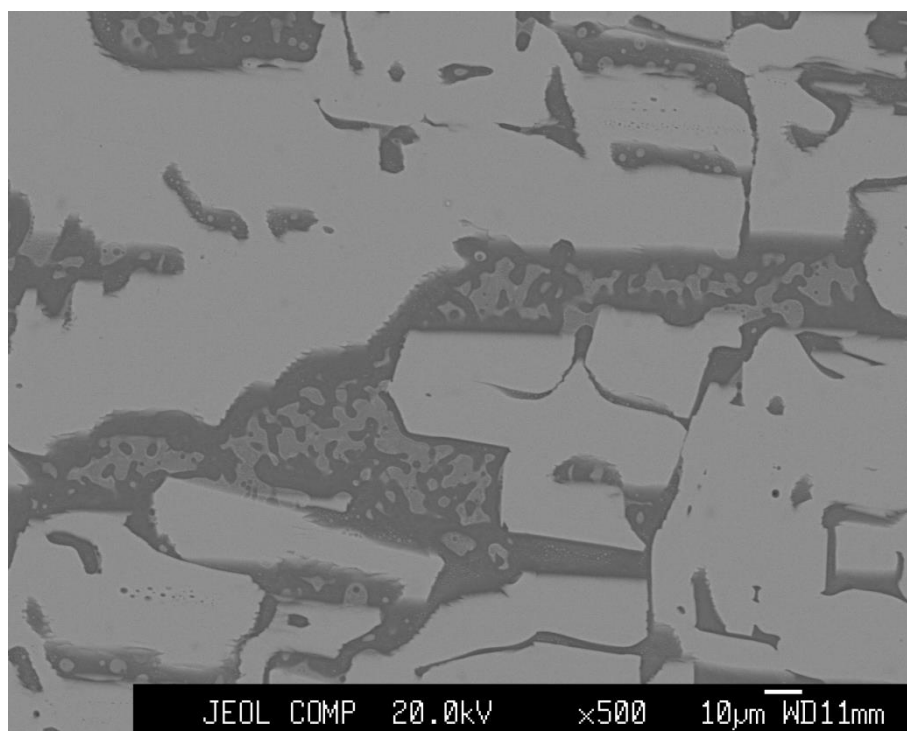


*Figure 6.2.14 Showing CRT09/2008 large fayalite grains (light grey) in matrix.*

| Element                                       | Na <sub>2</sub> O | MgO   | K <sub>2</sub> O | TiO <sub>2</sub> | MnO  |
|---|-------------------|-------|------------------|------------------|------|
| CRT09-2008 Lath near large prill              | 0.01              | 0.47  | 0.09             | 0.01             | 0.13 |
| CRT09-2008 Inter-lath material nr large prill | 0.72              | 0.12  | 5.07             | 0.18             | 0.06 |
| CRT09-2008 Large grain/lath                   | BDL               | 0.28  | 0.05             | BDL              | 0.10 |
| CRT09-2008 Inter grain/lath mid-density       | 0.84              | 0.01  | 4.60             | 0.74             | 0.03 |
| CRT09-2008 Matrix1                            | 1.03              | 0.01  | 7.06             | 0.37             | 0.02 |
| CRT09-2008 Lath nr second prill               | 0.05              | 0.52  | 0.37             | BDL              | 0.13 |
| CRT09-2008 Matrix nr second prill             | 0.68              | 0.005 | 5.23             | 0.53             | 0.02 |

*Table 6.2.9 Showing minor elements present in observable phases of CRT09/2008.*

| Element            | Fe    | P    | Na    | K    | Co   | Cu   | As   |
|--------------------|-------|------|-------|------|------|------|------|
| CRT09-2008 Prill 1 | 95.06 | 0.07 | 0.013 | 0.03 | 0.23 | 0.09 | 0.05 |
| CRT09-2008 Pril 2  | 96.15 | BDL  | 0.038 | 0.02 | 0.19 | 0.20 | 0.02 |

*Table 6.2.10 Showing elements present in large metallic prills in CRT09/2008.*

Although much smaller than many similar artefacts of Roman date, the presence of iron prills and extensive fayalite with limited wüstite would indicate that the piece was produced in a small smithing hearth.

A small suspected smithing hearth was found during excavation although further evidence, such as hammer scale, generated by magnetic detection of soil samples gathered in close proximity to this feature would strengthen this interpretation.

#### **CRT09/1017**

This sample contained four highly similar pieces of slag. Appearing light grey in appearance at fractured surfaces.

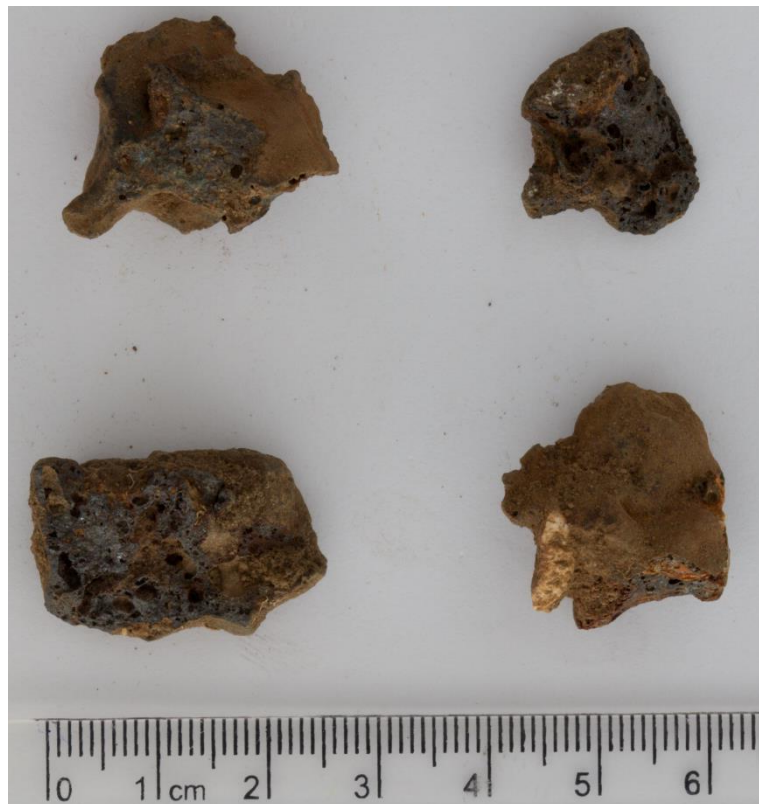


*Figure 6.2.15 Showing the four pieces of slag comprising CRT09/1017.*

One specimen was sampled for analysis based upon the degree of similarity between the four examples. Upon examination under the optical microscope this sample proved to be very different from the rest of the assemblage.

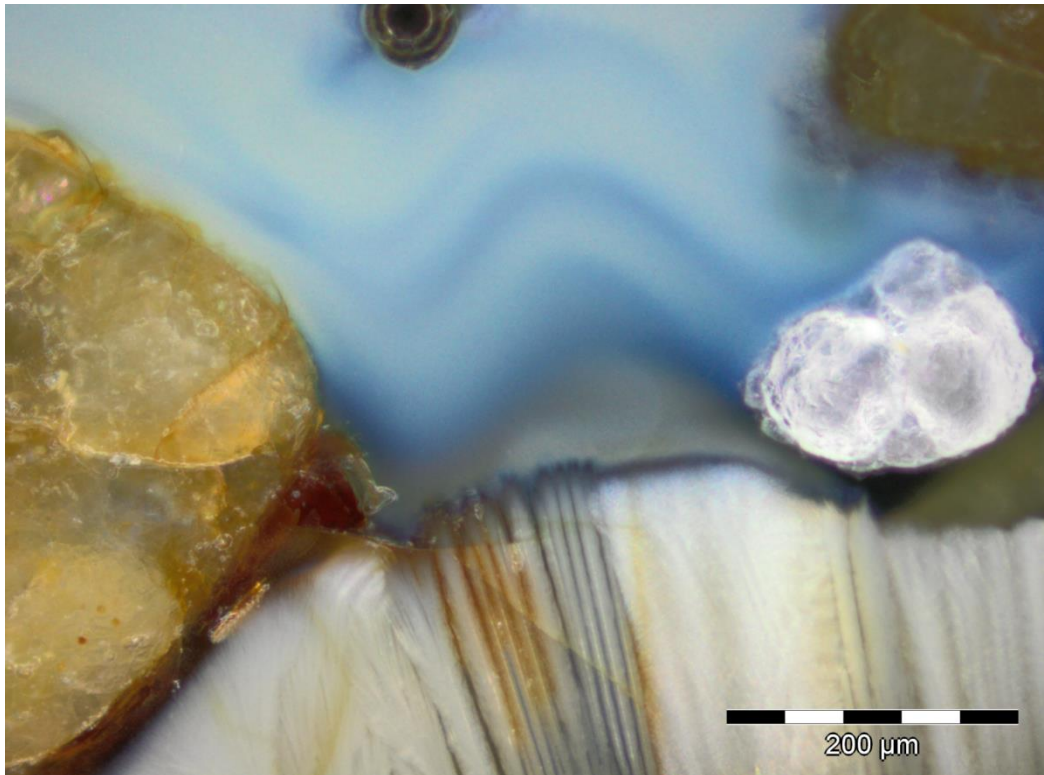


Figure 6.2.16 Showing glassy region with blue colouring with feathered fayalite (white) and silica grains.

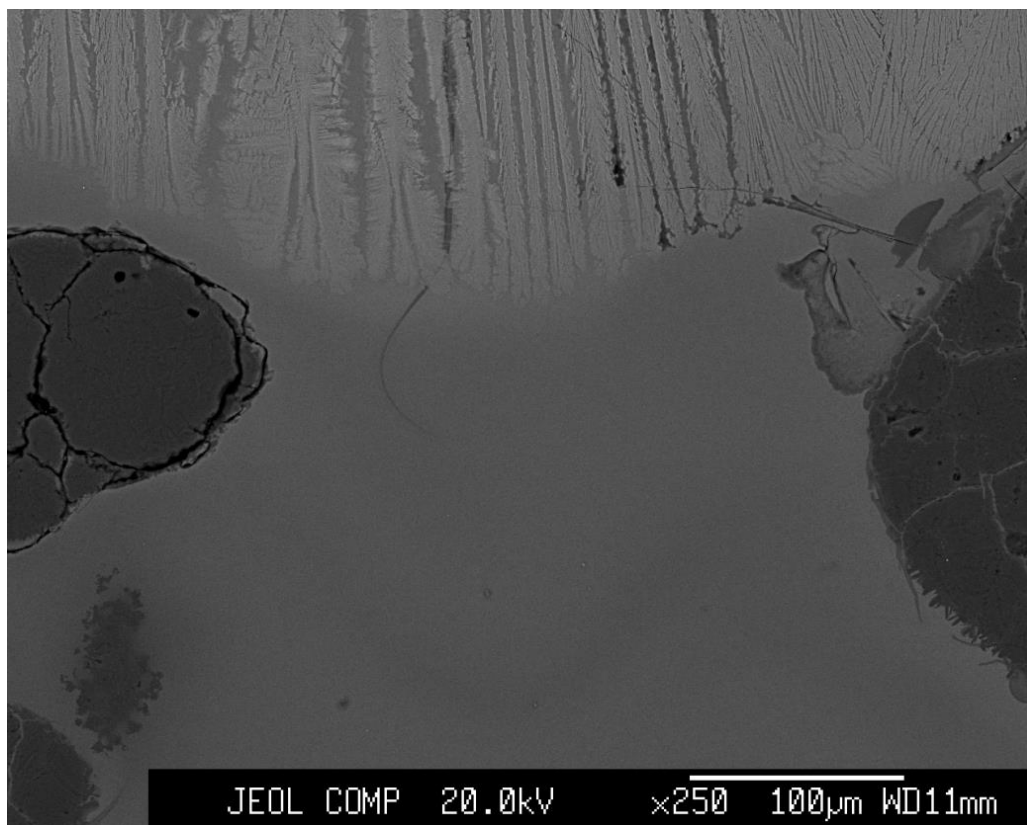


Figure 6.2.17 Showing a region of glassy slag (grey centre) with feathered fayalite laths (top).



In backscatter detection the glassy phase with pale blue colouring appears approximately homogenous, with a slight decrease in relative density arising at the regions of darker colouration.

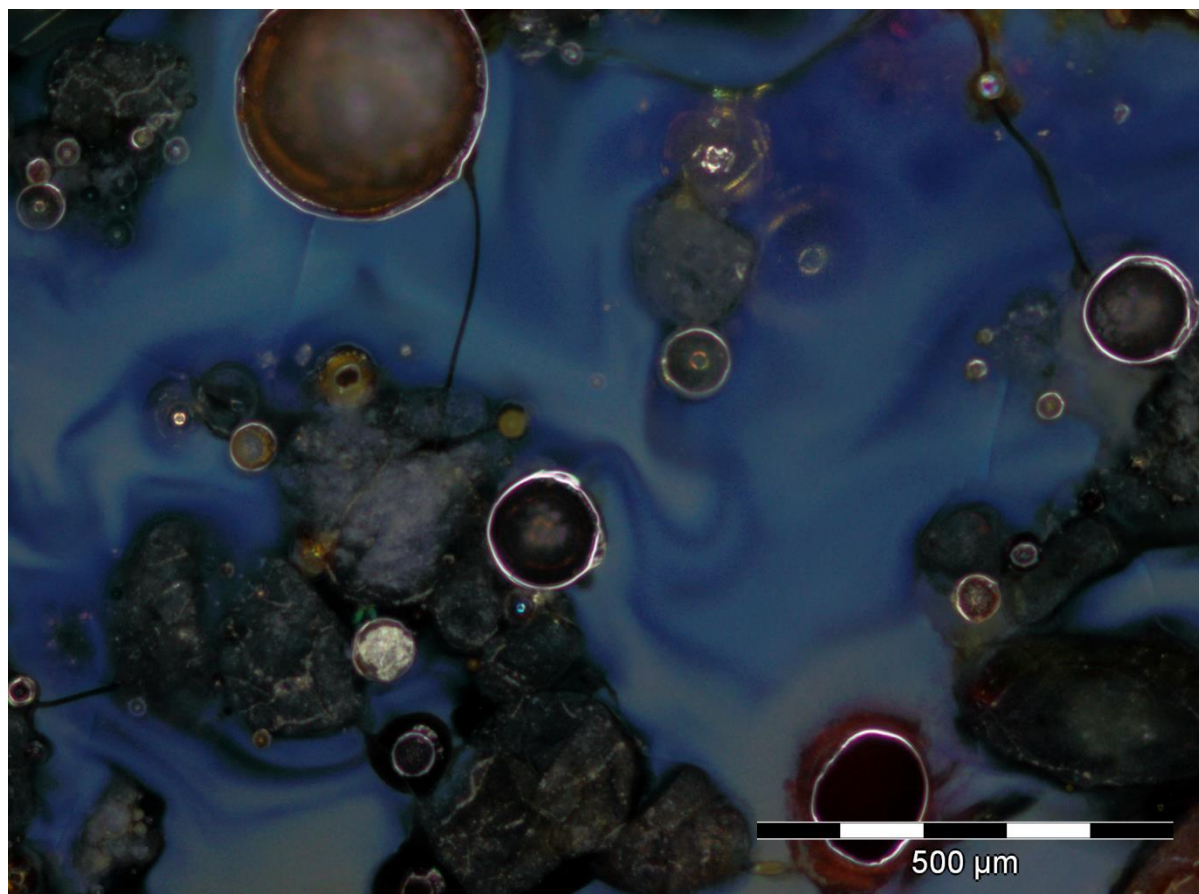


Figure 6.2.18 Showing striking blue colouration in glassy slag of CRT09/1017.

The striking near cobalt blue colour of this glassy phase appears more prominently in these specimens than in the rest of the assemblage. This would suggest that the impurities, most likely reduced iron, present have resulted in the blue appearance, while the lack of wüstite and fayalite suggest that the slag pieces have not formed in a region of significant iron content.

| Element     | FeO   | SiO <sub>2</sub> | P <sub>2</sub> O <sub>5</sub> | Na <sub>2</sub> O | MgO  | Al <sub>2</sub> O <sub>3</sub> | K <sub>2</sub> O | CaO  |
|-------------|-------|------------------|-------------------------------|-------------------|------|--------------------------------|------------------|------|
| Blue colour | 19.78 | 61.80            | 0.21                          | 0.83              | 0.64 | 3.62                           | 3.96             | 6.07 |

Table 6.2.11 Showing major elements and appreciable phosphorus content of blue coloured slag in CRT09/1017.

| Element     | TiO <sub>2</sub> | MnO  | CoO  | CuO  | SO <sub>3</sub> |
|-------------|------------------|------|------|------|-----------------|
| Blue colour | 0.23             | 0.19 | 0.03 | 0.09 | 0.08            |

*Table 6.2.12 Showing minor elements and appreciable phosphorus content of blue coloured slag in CRT09/1017.*

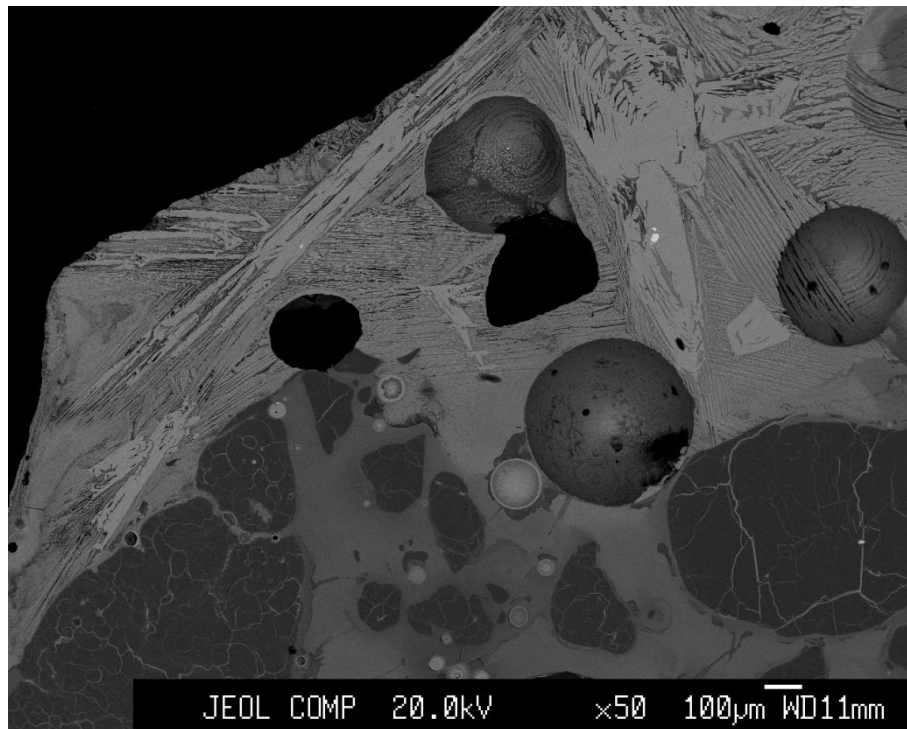


*Figure 6.2.19 Showing significant fayalite growth, glassy slag and unreacted silica.*

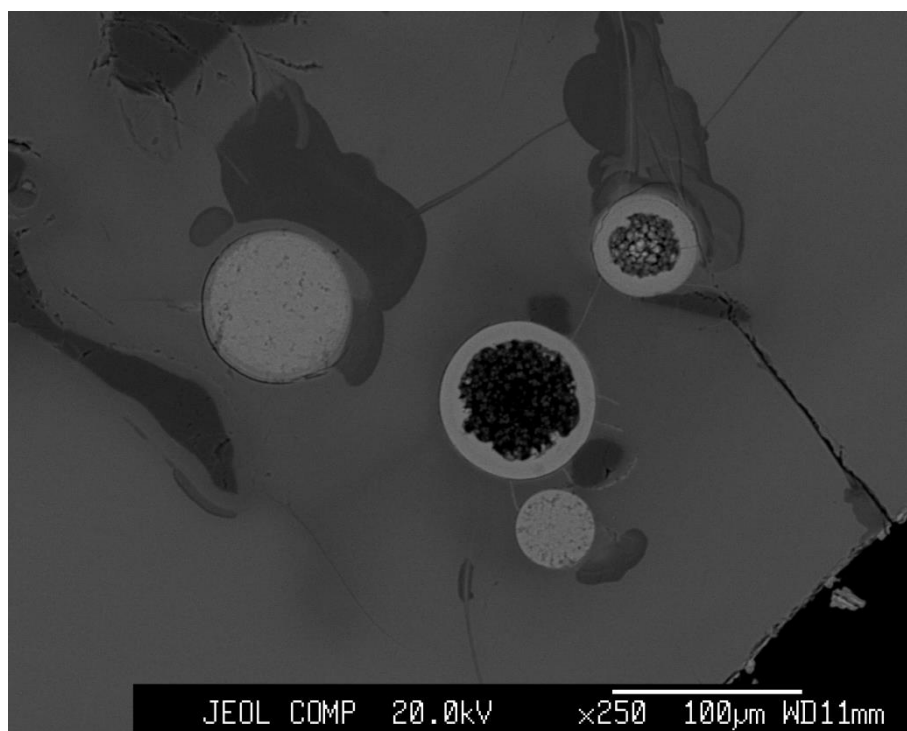


*Figure 6.2.20 Showing glassy slag surrounding oxidised iron prills.*

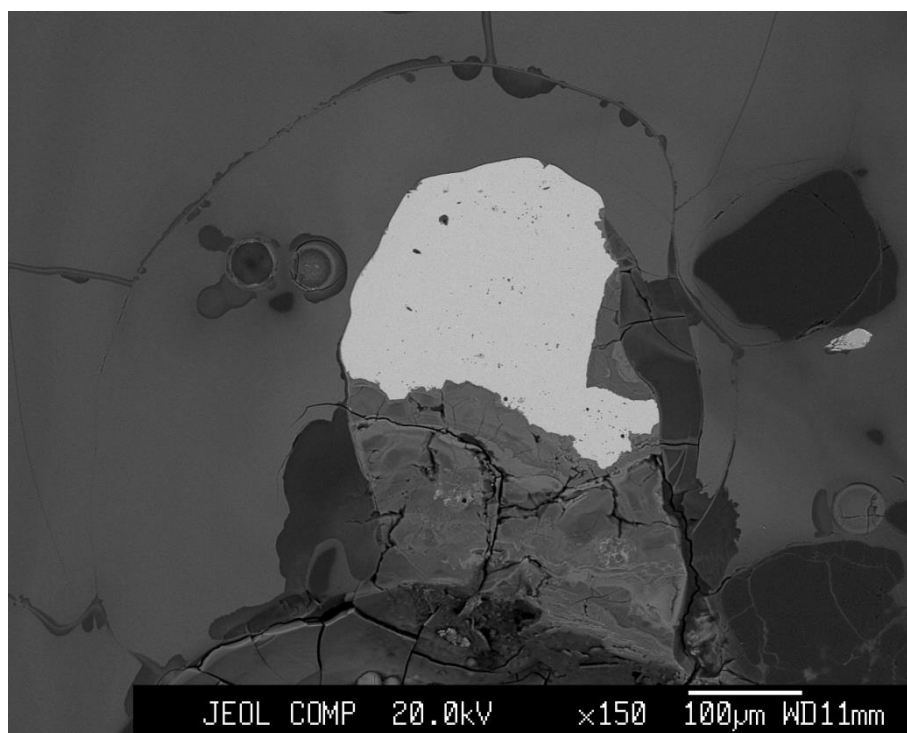


*Figure 6.2.21 Showing large iron prill surrounded by glassy slag and silica grains.*

| Element    | Fe    | P    |
|------------|-------|------|
| Iron Prill | 94.32 | 0.42 |

*Table 6.2.13 Showing major elements detected in iron prill.*

| Element    | Na   | S    | K    | Co   | Ni   | Cu   | As   | Pb   |
|------------|------|------|------|------|------|------|------|------|
| Iron Prill | 0.01 | 0.01 | 0.01 | 0.20 | 0.24 | 0.20 | 0.20 | 0.05 |

*Table 6.2.14 Showing minor elements detected in iron prill.*

### **CRT09/1137/q6**

This sample comprised of a dark slag adhering to a piece of siliceous material. When examined in bright field the microstructure proved to be varied across the slag body. Wüstite were observed to increase in size as distance from the adhering rock increased. Fayalite laths were seen to have a more feathered appearance in closer proximity to the rock and formed larger grains at the distal end of the slag. This would suggest that the slag cooled more rapidly when in contact with the stone, as a slower cooling time allows for greater dendrite and crystal growth. This may indicate that this sample was formed as the slag dripped and landed upon the stone and underwent cooling at a varied rate.

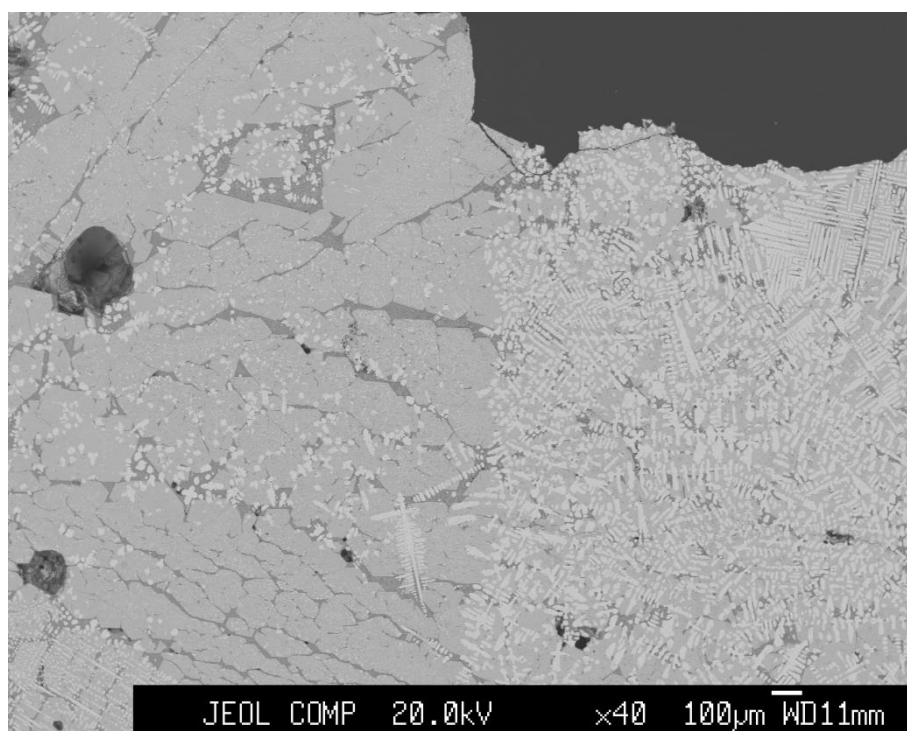


*Figure 6.2.22 Showing the major phases present in CRT09/1137/q6. Large fayalite grains with wüstite and matrix (left) and well developed wüstite dendrites, large fayalite grains and matrix (right).*

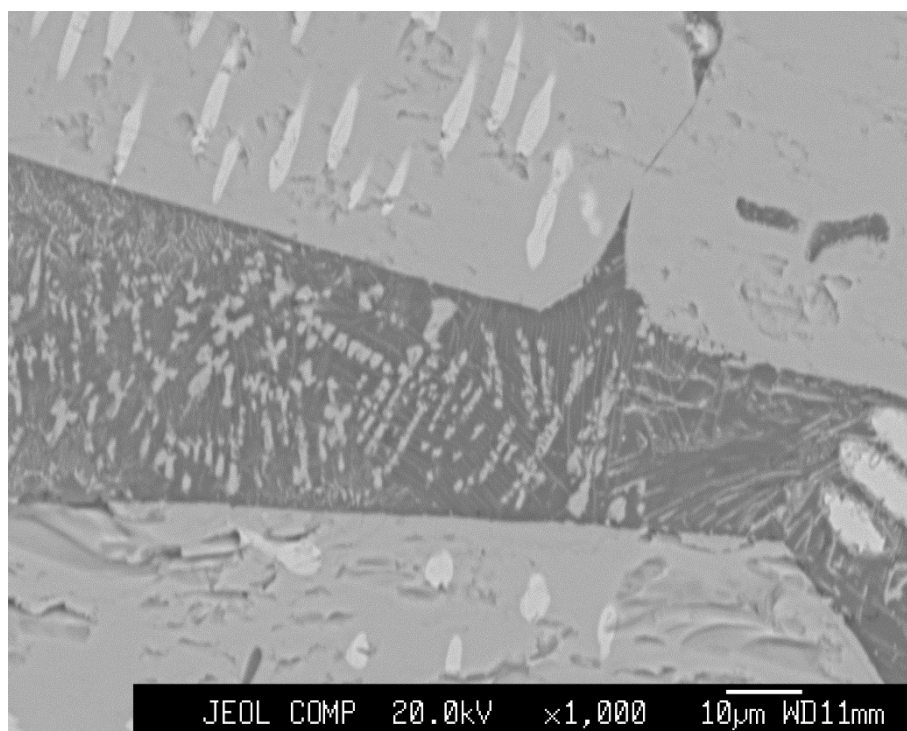


*Figure 6.2.23 Showing ultra-fine wüstite dendrites (light grey) within glassy matrix (dark grey) between fayalite grains (mid- grey) in CRT09/1137/q6.*

| Element       | FeO  | SiO <sub>2</sub> | Na <sub>2</sub> O | Al <sub>2</sub> O <sub>3</sub> | K <sub>2</sub> O | CaO   |
|---------------|------|------------------|-------------------|--------------------------------|------------------|-------|
| Glassy matrix | 0.98 | 48.77            | 2.29              | 31.08                          | 1.38             | 13.97 |

*Table 6.2.15 Showing major elements present in glassy matrix of CRT09/06.*

| Element       | P <sub>2</sub> O <sub>5</sub> | MgO  | SO <sub>3</sub> | TiO <sub>2</sub> | CuO  | BaO  |
|---------------|-------------------------------|------|-----------------|------------------|------|------|
| Glassy matrix | 0.04                          | 0.06 | 0.01            | 0.05             | 0.01 | 0.02 |

*Table 6.2.16 Showing minor elements present in glassy matrix of CRT09/06.*

| Element   | FeO   | SiO <sub>2</sub> | P <sub>2</sub> O <sub>5</sub> | Na <sub>2</sub> O | MgO  | Al <sub>2</sub> O <sub>3</sub> | SO <sub>3</sub> | K <sub>2</sub> O | CaO  | TiO <sub>2</sub> |
|-----------|-------|------------------|-------------------------------|-------------------|------|--------------------------------|-----------------|------------------|------|------------------|
| Slag body | 23.95 | 44.38            | 0.26                          | 1.39              | 1.24 | 16.78                          | 0.53            | 2.58             | 6.82 | 0.80             |

*Table 6.2.17 Showing major elements present in the main slag body of CRT09/06.*

| Element   | MnO  | CoO  | CuO  | BaO  |
|-----------|------|------|------|------|
| Slag body | 0.08 | 0.04 | 0.05 | 0.01 |

*Table 6.2.18 Showing minor elements present in the main slag body of CRT09/06.*

### **CRT09/1137/q13**

This piece was initially identified as slag by the excavators due to the shape and impressions upon the surface. The colour of the piece was more orange than the positively identified slag samples which would suggest a larger quantity of  $\text{Fe}_2\text{O}_3$  being present. This would indicate that the piece was formed in a more oxidising environment.



*Figure 6.2.24 Showing sample CRT09/1137/q13 prior to sampling.*



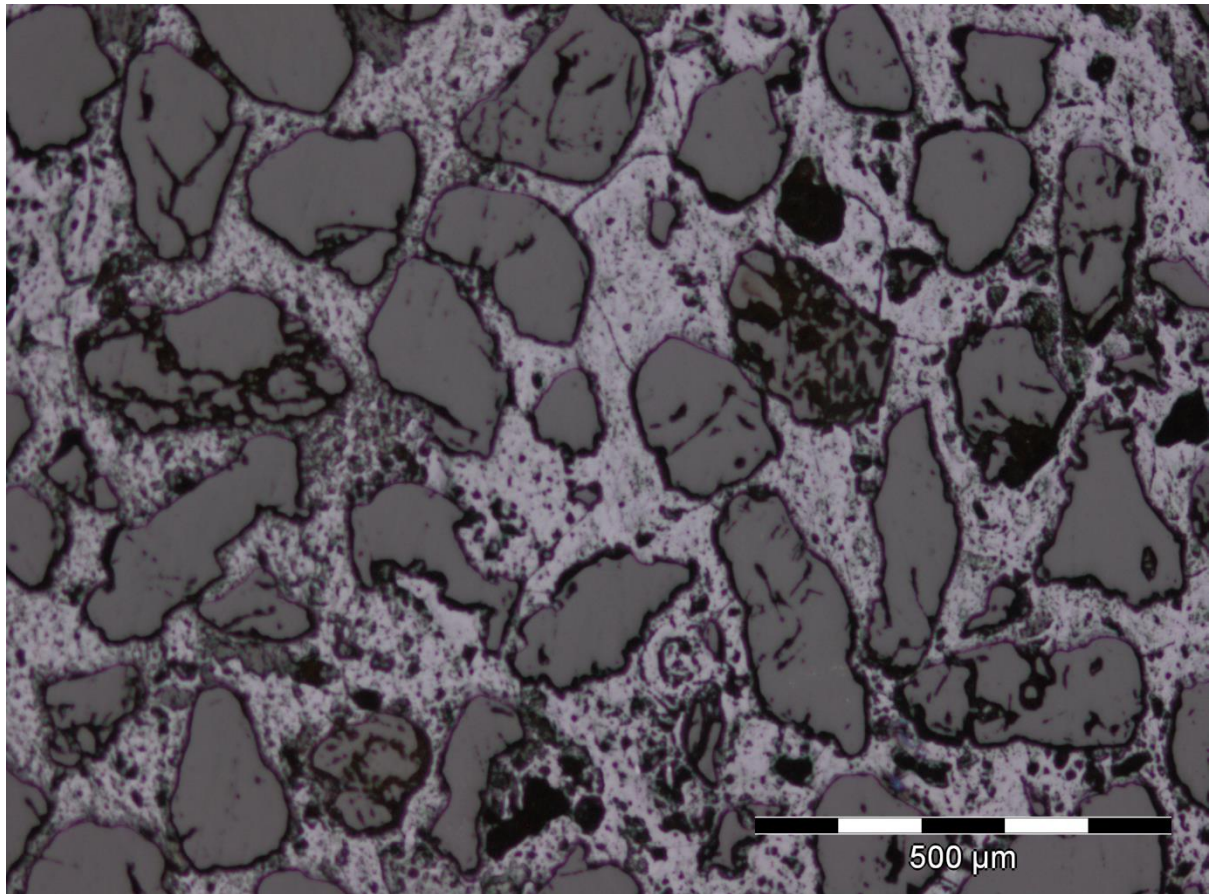


*Figure 6.2.25 Showing bright field image of silica grains and iron rich matrix of CRT09/1137/q13.*

Upon sampling it was found that this piece was not slag, but rather a piece of possible ore material.

Unlike the smelting slag which appears to be black to the eye, this material was a dull orange-brown with a metallic lustre when sectioned. This was revealed to be caused by grains of siliceous material surrounded by a more reflective matrix when examined under the microscope.



### **CRT09/1187**

This sample was also identified as slag during excavation, like the previously discussed piece. Upon sampling it proved to be similar in structure to CRT09/1137/q13.



*Figure 6.2.26 Showing sample CRT09/1187 prior to sampling.*

In this case there was observable banding relating to the abundance of the more reflective material. This did not appear to be as apparent when examining the sample with the microscope, which can be a common occurrence due to the different angles that a sample can be observed from when in hand.

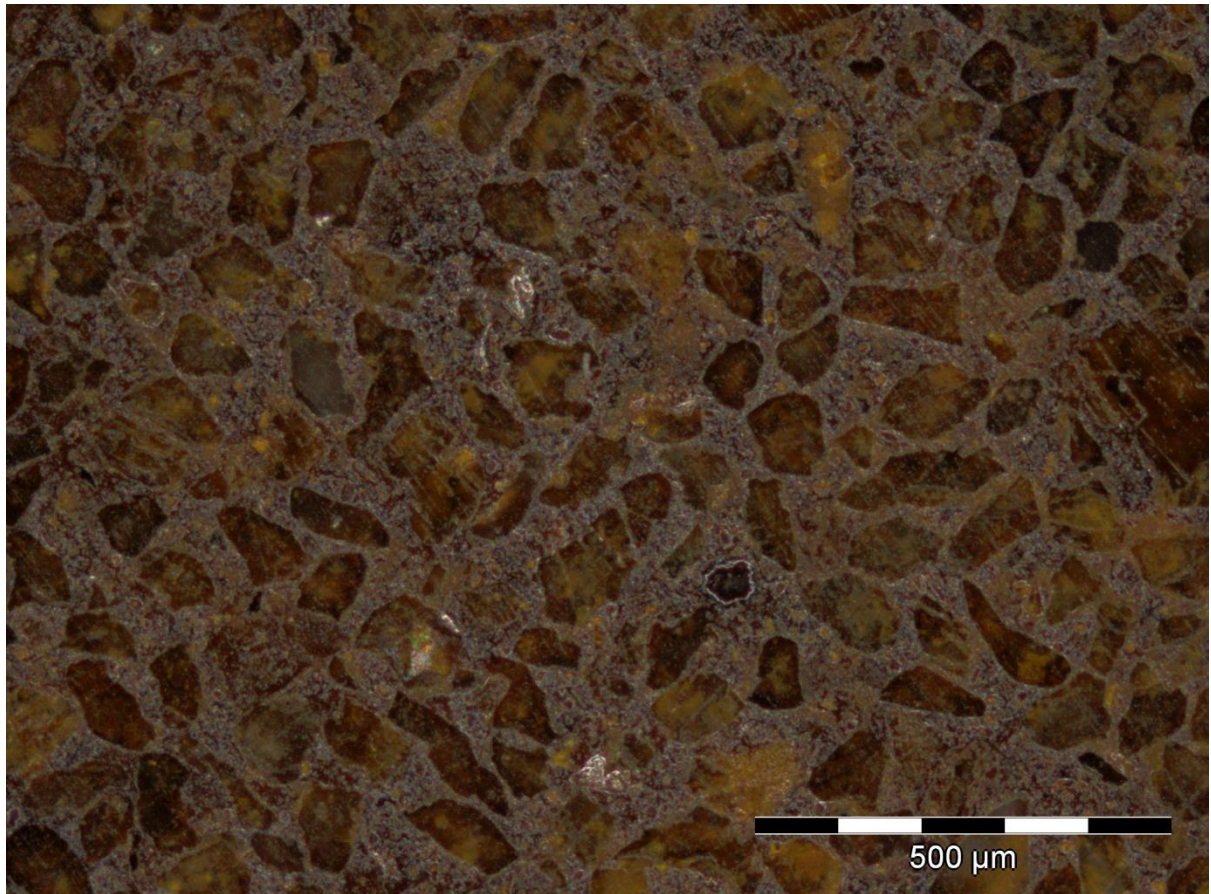


*Figure 6.2.27 Showing dark field image of silica grains in iron rich matrix of CRT09/1187.*

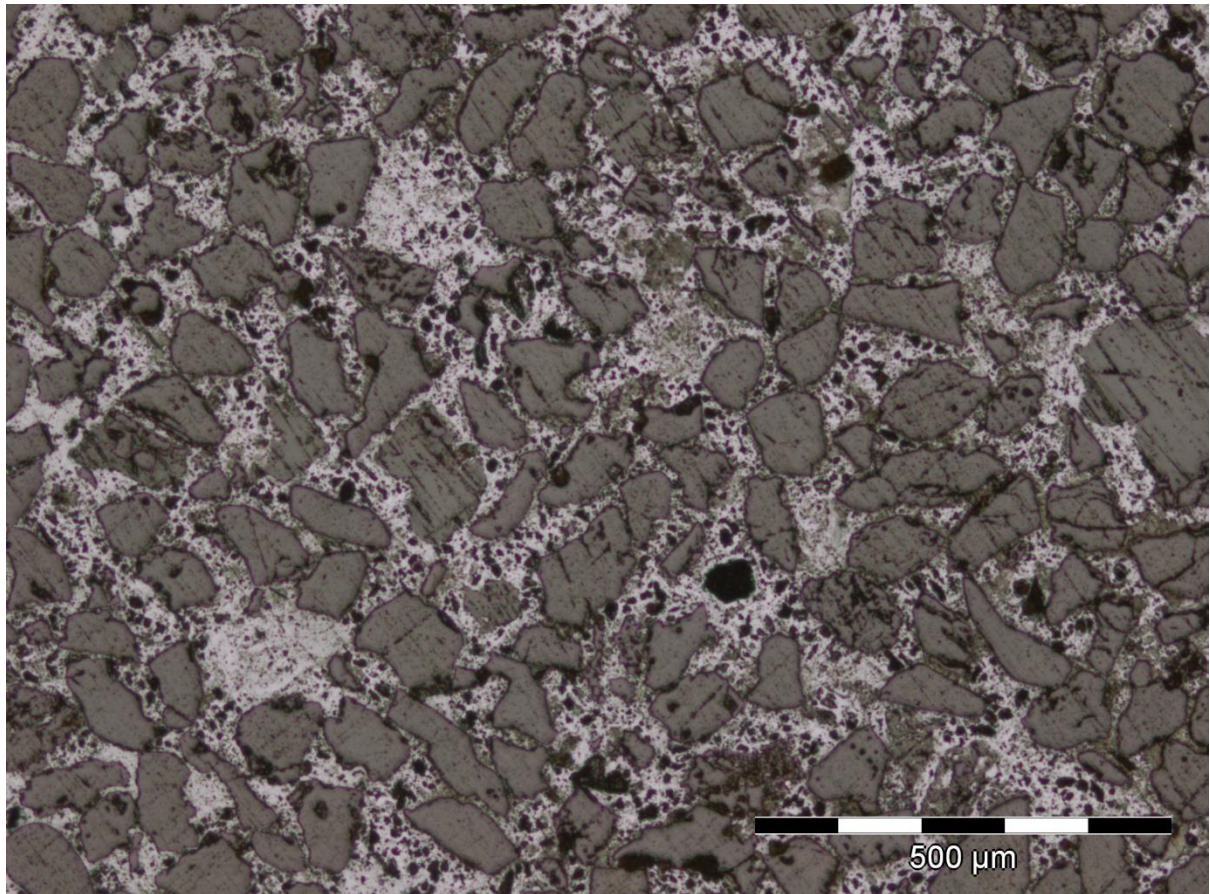


*Figure 6.2.28 Showing bright field image of silica grains in iron rich matrix of CRT09/1187.*

The two samples, CRT09/1137/q13 and CRT09/1187 may not be the ore material exploited in the production of the iron slag found on site. However, they do demonstrate that conditions in the area were suitable for the formation of potential ore materials in the past.



### **CRT09/1198**

This specimen was far lighter in colour than all of the other samples studied, as shown below.



*Figure 6.2.29 Showing sample CRT09/1198 prior to sampling.*

Upon optical examination the section showed a clear granular structure with no dendrites or eutectic. Further evidence from EMPA demonstrated that the vast majority of the material comprised of silica. This appeared as a near uniform grey in backscatter detection.

As can be seen from the analytical data below, it is clear that this sample is not an ironworking slag, the quantity of silica is simply too high to allow for this interpretation.

Given the 98% silica total and granular structure, it is most likely that this sample is of a geological origin than a result of iron smelting.

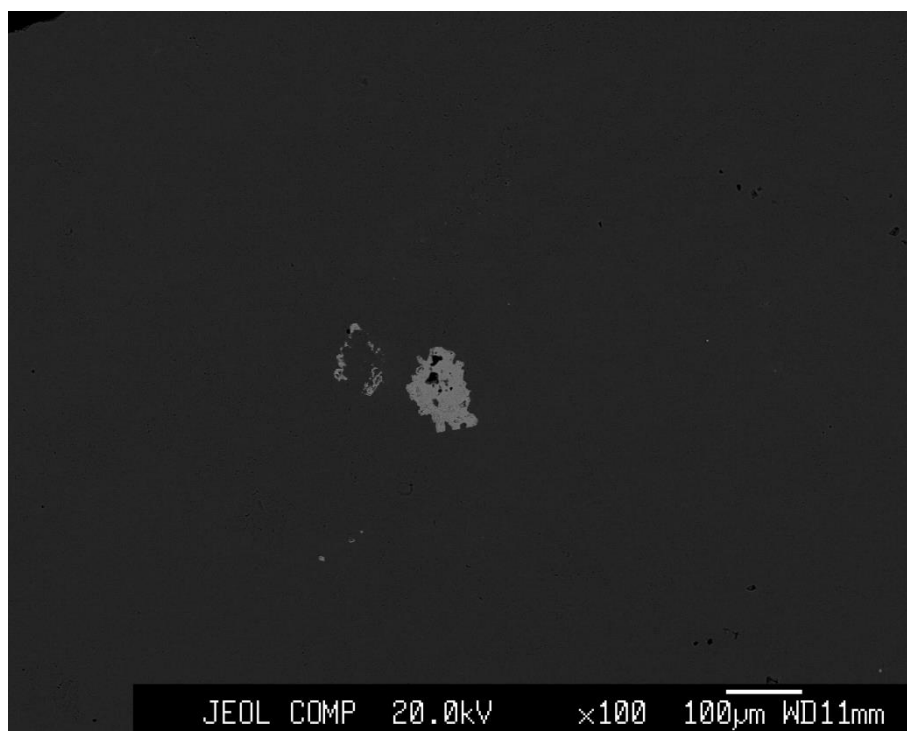


*Figure 6.2.30 Showing the singular metal rich inclusion within CRT09/1198.*

| Element   | FeO   | SiO <sub>2</sub> | Al <sub>2</sub> O <sub>3</sub> | SO <sub>3</sub> | Cl   | CaO  | CuO  |
|-----------|-------|------------------|--------------------------------|-----------------|------|------|------|
| Main body | 0.048 | 95.96            | 0.089                          | 0.02            | 0.04 | 0.03 | 0.02 |

*Table 6.2.19 Showing composition of silaceous body of CRT09/1198.*

### **CRT09/01 unstratified**

This sample comprised of a metallic iron prill surrounded by slag. The metallic portion is not representative of the overall bloom composition due to its size. However, the slag appears to be similar to that observed in other samples.



*Figure 6.2.31 Showing CRT09/01 unstratified prior to sampling.*

Examination by bright field microscopy revealed a very clear boundary between the metallic prill with its surrounding slag and the main slag body of the piece. This was marked by a very large, well defined growth of wüstite, which separated the region with well developed wüstite dendrites from the slag surrounding the prill.

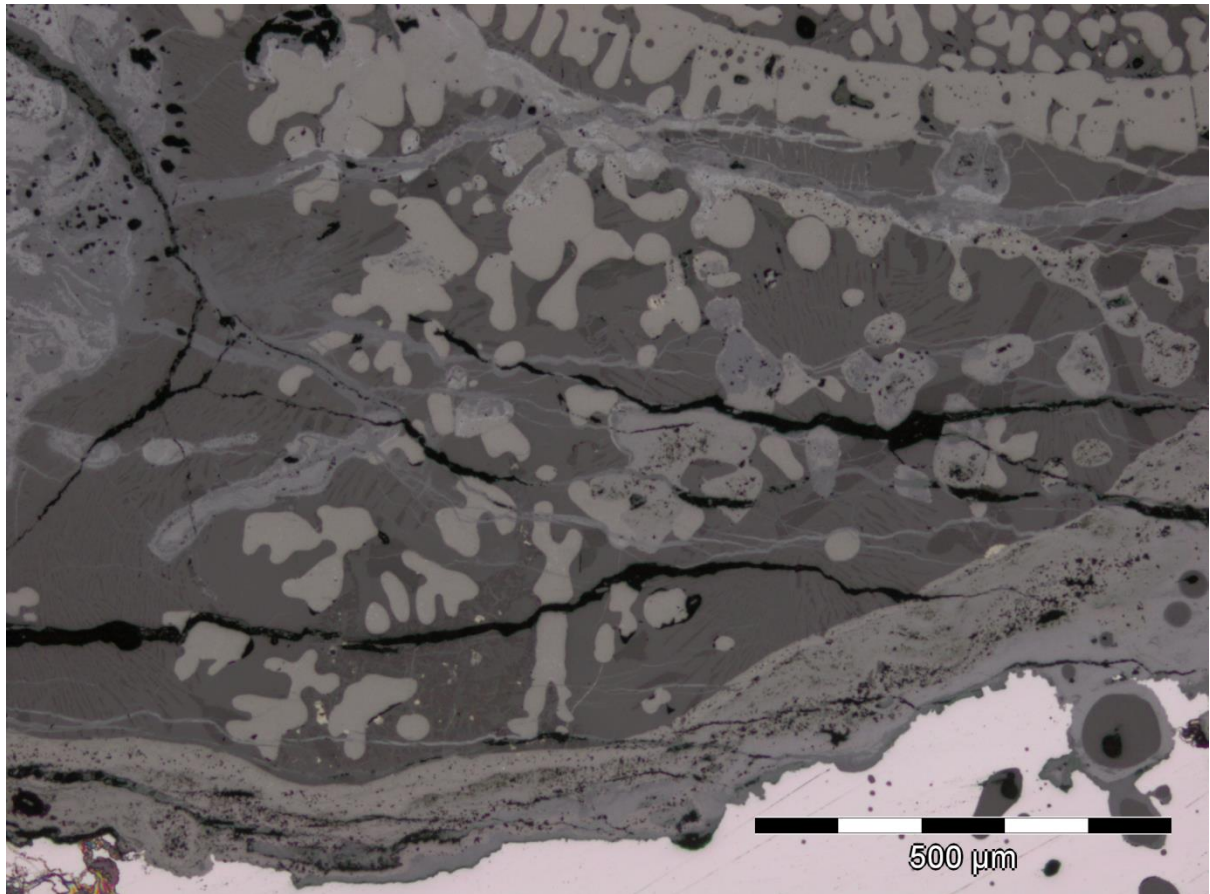


*Figure 6.2.32 Showing bright field image of slag in close proximity to iron prill (bottom) with limitation of large wüstite development (top right) in sample CRT09/01 unstratified.*

| Element    | Fe    | P    | Na   | K    | Co   | Cu   | As   | Pb     |
|------------|-------|------|------|------|------|------|------|--------|
| Iron prill | 96.27 | 0.32 | 0.02 | 0.01 | 0.17 | 0.04 | 0.08 | 0.0376 |

*Table 6.2.20 Showing detected elements in Iron prill of CRT09/01 unstratified.*

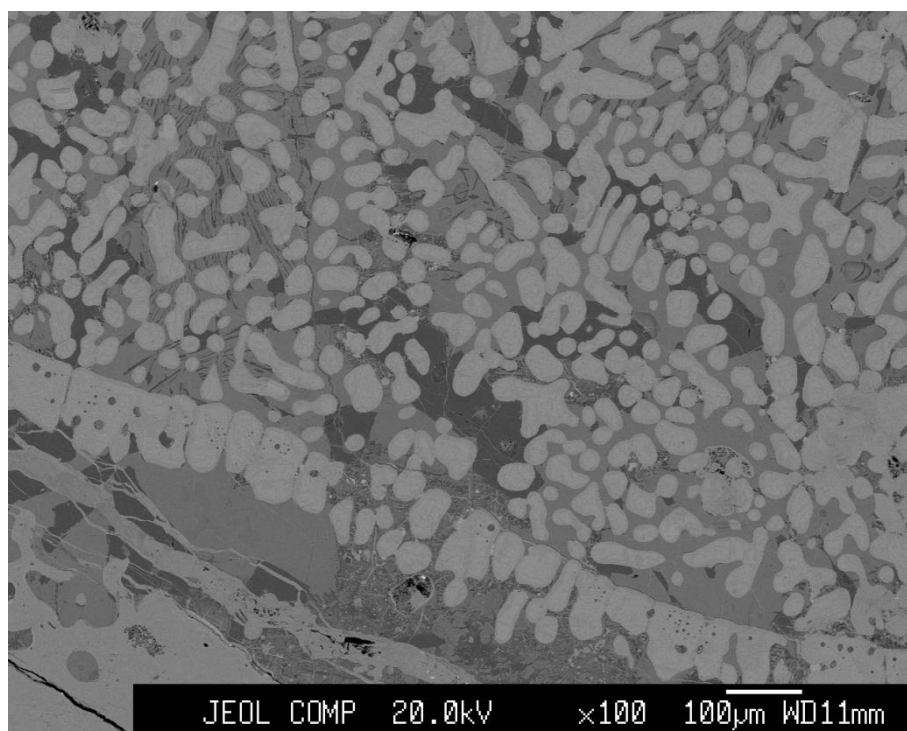


*Figure 6.2.33 Showing CRT09/01 unstratified sample with clear separation of the well-developed wüstite-rich slag (top) from the wüstite-poor slag surrounding the metal prill (bottom left).*



## CRT09/06

This slag drip had several small pores and was dark in colour throughout. A small highly reflective flake was observed in one are, which was revealed to be of far higher density than the rest of the slag by compositional imaging during EMPA. This very marked difference in density may indicate that this thin feature may be a flake of metallic iron which never consolidated with the main bloom during smelting. Such features have also been observed in experimental slags produced as part of the Lincolnshire Limewoods project in 2008.

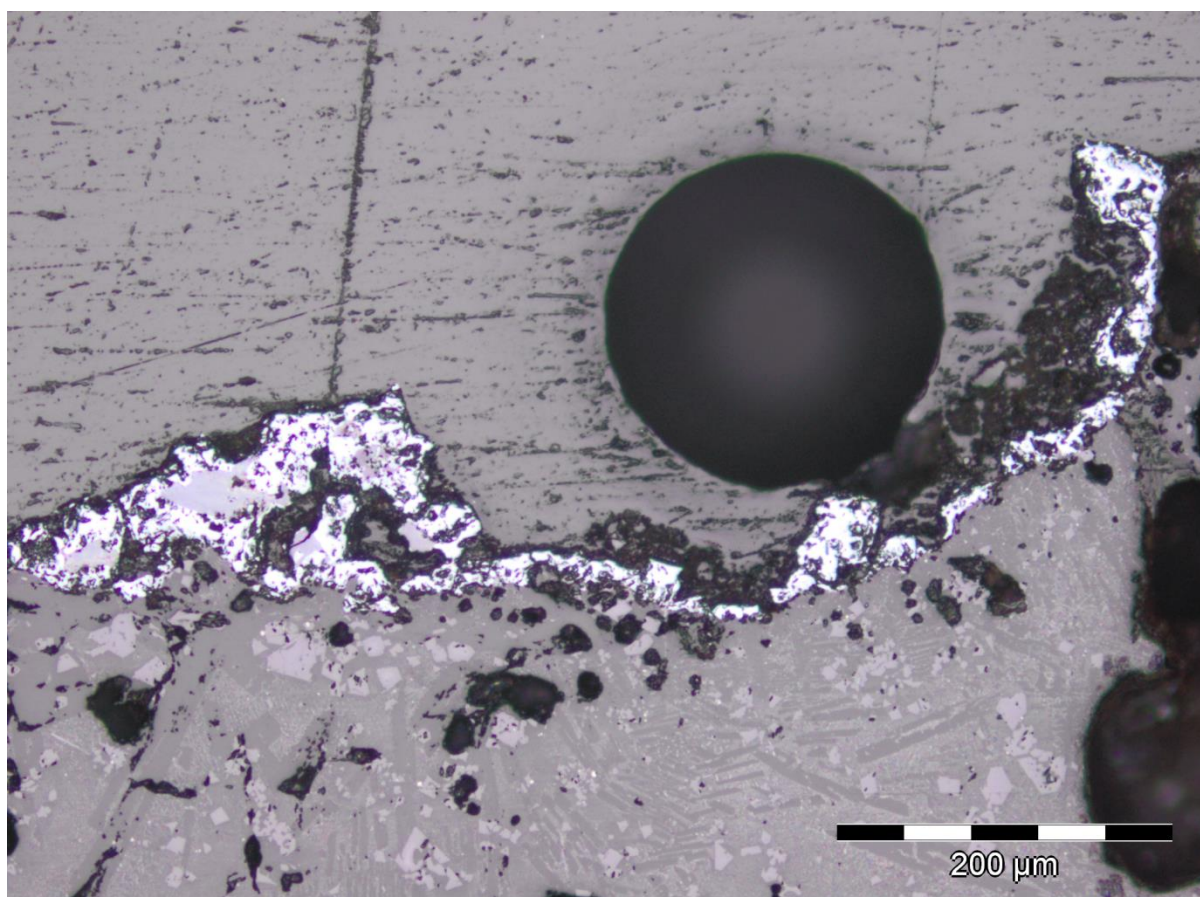


Figure 6.2.34 Showing bright field image of oxidised iron flake (bright white) in sample CRT9/06.

| Element             | FeO   | SiO <sub>2</sub> | Al <sub>2</sub> O <sub>3</sub> |
|---------------------|-------|------------------|--------------------------------|
| Oxidised iron flake | 82.75 | 1.21             | 1.93                           |

Table 6.2.21 Showing major elements detected (%) in oxidised iron flake in CRT09/06.

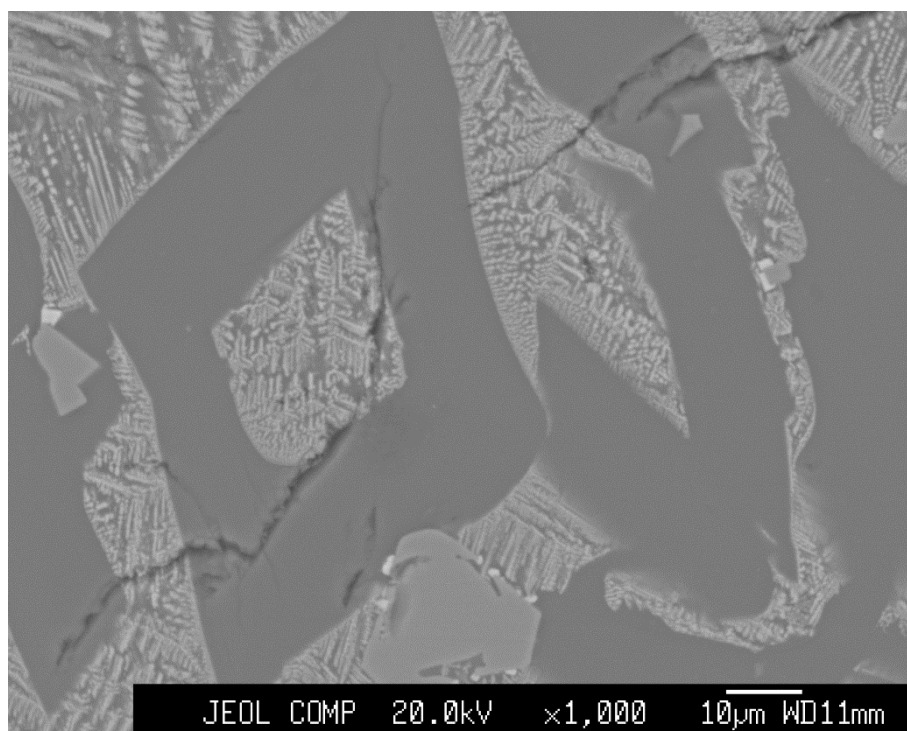


Figure 6.2.35 Showing fine wüstite dendrite growth surrounded by glassy slag in sample CRT09/06.

| Element | FeO   | SiO <sub>2</sub> | P <sub>2</sub> O <sub>5</sub> | N <sub>2</sub> O | MgO  | Al <sub>2</sub> O <sub>3</sub> | K <sub>2</sub> O | CaO  |
|---------|-------|------------------|-------------------------------|------------------|------|--------------------------------|------------------|------|
| Slag    | 23.96 | 44.38            | 0.26                          | 1.39             | 1.24 | 16.79                          | 2.58             | 6.82 |
| Body    |       |                  |                               |                  |      |                                |                  |      |

Table 6.2.22 showing major elements detected (%) in the slag body of CRT09/06

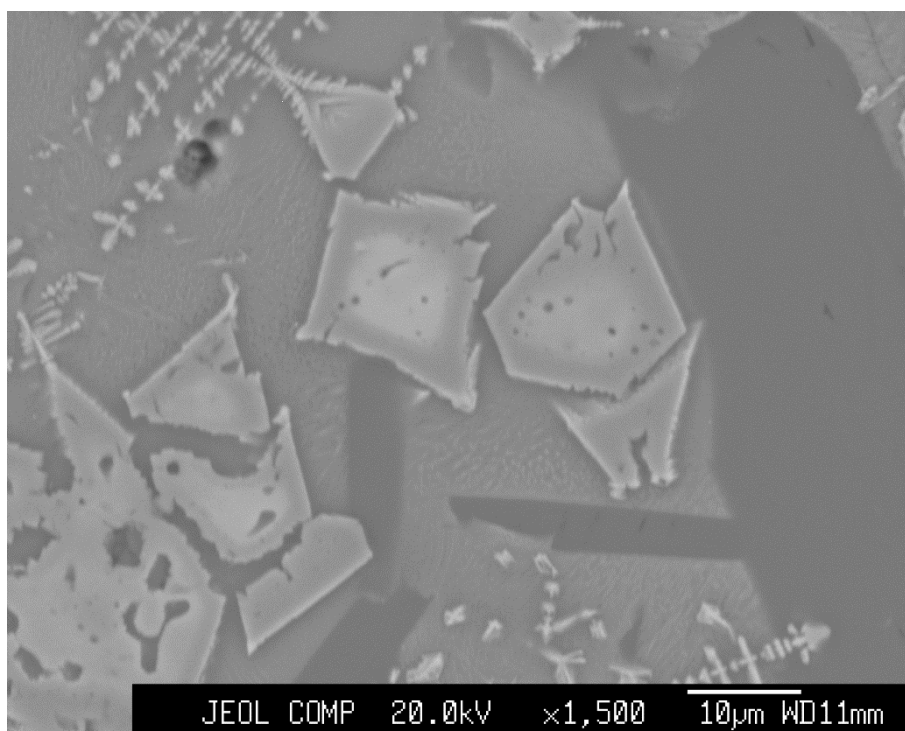
| Element | SO <sub>3</sub> | TiO <sub>2</sub> | MnO  | CoO  | CuO  | BaO  |
|---------|-----------------|------------------|------|------|------|------|
| Slag    | 0.53            | 0.80             | 0.08 | 0.04 | 0.05 | 0.01 |
| Body    |                 |                  |      |      |      |      |

Table 6.2.23 showing minor elements detected (%) in the slag body of CRT09/06

The white and black inclusions appear to be the same material which have experienced different conditions and are not likely to be fuel ash slags as they are surrounded by the more typical fayalitic slag with wüstite dendrites. This may suggest that they are small inclusions of fuel material which have partially reacted.

### CRT09/09a

This sample was dark in colour with a large white inclusion and several large pores. Upon microscopic observation other inclusions were also recorded, which appeared to be similar in structure to the white inclusion but of a dark grey colour. Very fine wüstite dendrites were observed throughout the slag with fayalite laths and a larger quantity of glassy matrix in comparison to other samples.



*Figure 6.2.36 Showing CRT09/09a ultra-fine wüstite dendrites and slight coring of wüstite skeletal structures.*

| Element                          | FeO   | SiO <sub>2</sub> | MgO  | Al <sub>2</sub> O <sub>3</sub> | TiO <sub>2</sub> |
|----------------------------------|-------|------------------|------|--------------------------------|------------------|
| Cored<br>Feature High<br>density | 59.92 | 0.88             | 2.23 | 34.15                          | 1.38             |

*Table 6.2.24 Showing major elements detected (%) in cored structures in figure 6.2.36 above.*

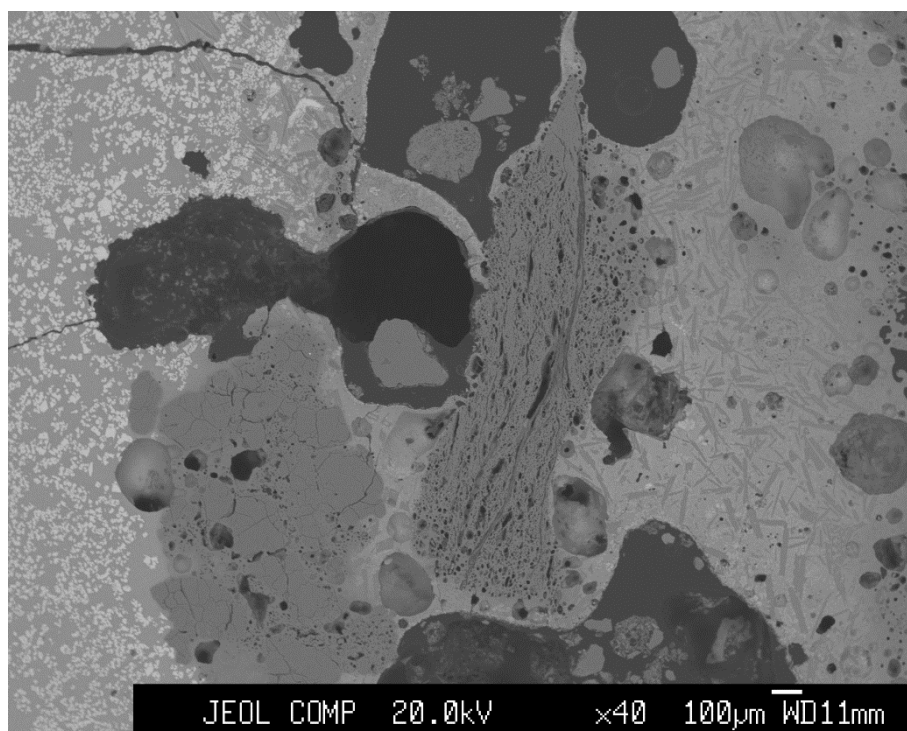


*Figure 6.2.37 Showing CRT09/09a wüstite rich slag (left), probably fuel ash slag inclusion (centre) and fayalite rich slag with well-developed fayalite (right).*

#### **CRT09/09b**

Sample CRT09/09b proved to be significantly different to the rest of the samples as it cut far faster than any other piece. Upon microscopic examination it appeared to be far more porous than the rest of the slags with a grey/black appearance.

CRT09/09a also contained material which paralleled that of CRT09/09b, which would suggest that it is not a conventional smelting slag, but rather that it may be fuel ash slag. Part of the external surface of the sample had a white appearance, which when examined during EMPA compositional imaging was found to contain angular crystals in a low density matrix.

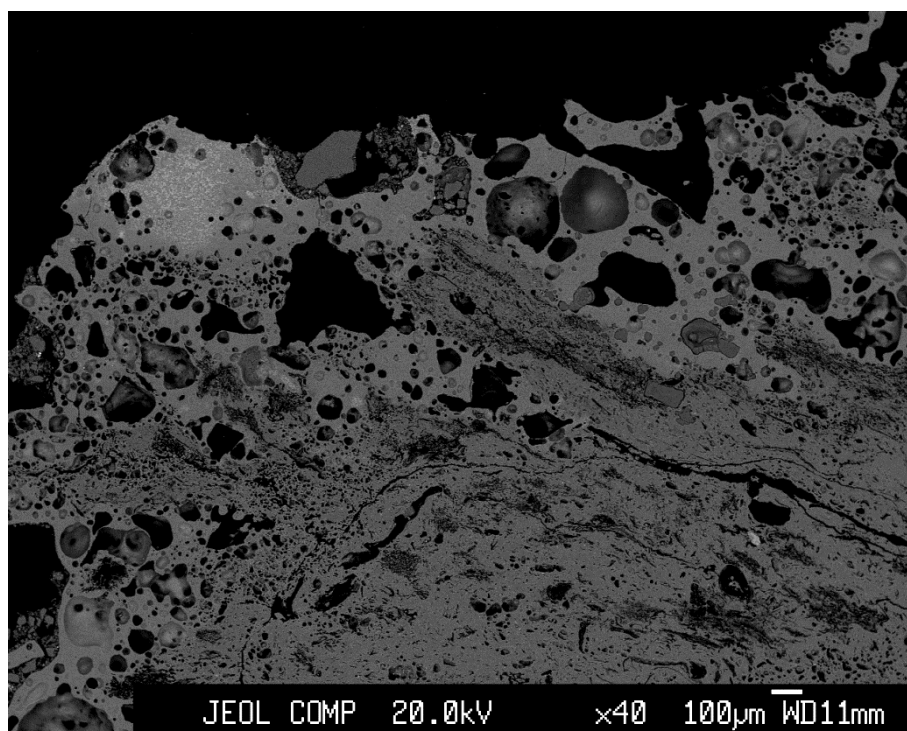


*Figure 6.2.38 Showing the highly porous, low density nature, vitrified structures (top right) and fine higher density crystals in the optically white region (top left) of CRT09/09b.*

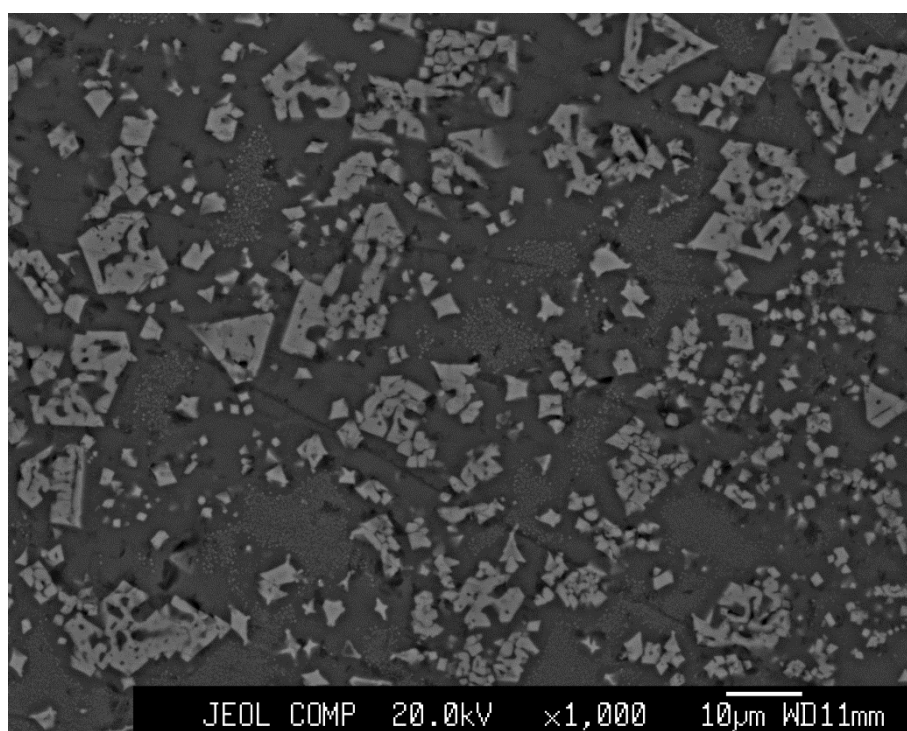


*Figure 6.2.39 Showing CRT09/09b angular crystals in low density matrix with micro-wüstite in the optically white region.*

| Element                          | FeO   | SiO <sub>2</sub> | Al <sub>2</sub> O <sub>3</sub> |
|----------------------------------|-------|------------------|--------------------------------|
| CRT09-09b crystals in white area | 34.20 | 30.50            | 35.40                          |

*Table 6.2.25 Showing major elements present in observed crystals in white region of CRT09/09b.*

This change in colour and the vitrified appearance of the extreme surfaces may indicate the formation of well-developed fuel-ash slag. An inclusion of this material was found within another sample (CRT09/09a), where the main body comprised predominantly of fayalite and wüstite with limited glassy matrix (Figure 6.2.37). Hence the inclusion in sample CRT09/09a may represent the conversion of an unreacted fuel inclusion into fuel ash slag during cooling.

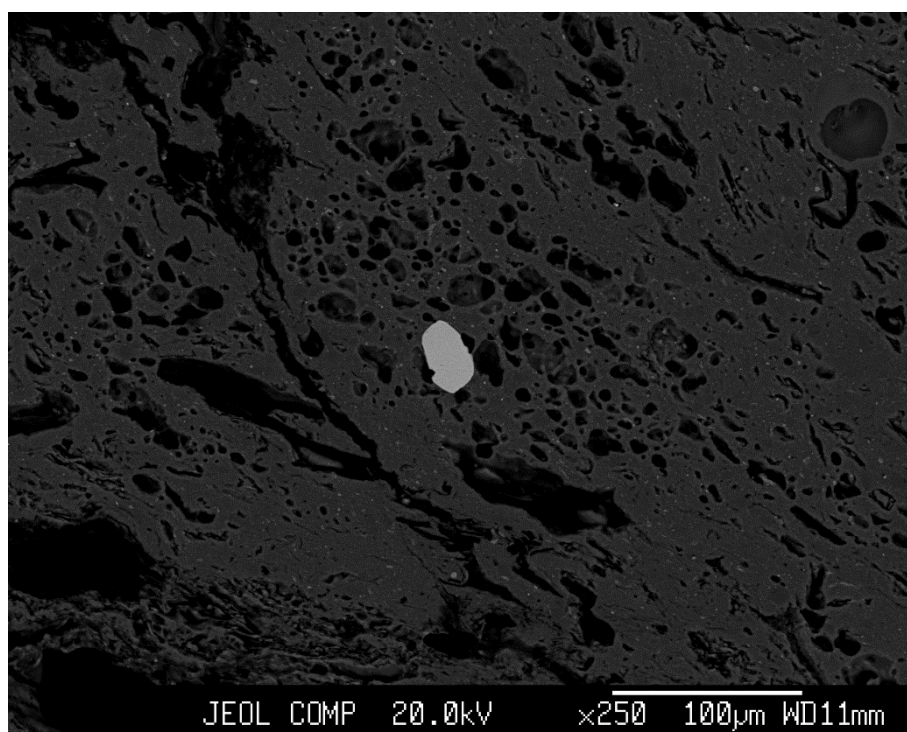


*Figure 6.2.40 Showing bright inclusion of weathered cassiterite within fuel ash slag CRT09/09b.*

| Element               | Fe   | Si  | Mg   | Al   | Ca   | Sn    | O     |
|-----------------------|------|-----|------|------|------|-------|-------|
| Cassiterite inclusion | 0.33 | 4.9 | 0.97 | 4.67 | 0.92 | 79.01 | 23.39 |

*Table 6.2.26 Showing major elements detected in weathered cassiterite inclusion.*

The presence of this tin oxide inclusion may indicate that the piece did not originate from an ironworking process. Inclusions of high tin content are extremely rare in iron slags, as such this inclusion may indicate the presence of a non-ferrous metallurgical activity nearby which may have contributed tin as a contaminant or that this piece was produced during non-ferrous metal working.



## Unanalysed samples

As explained in the sampling section, not all of the samples from the assemblage were analysed due to the limitation of time and the functionality of the equipment available. The unanalysed samples have been recorded here as further evidence of the ironworking activity occurring at the site. Many of these pieces are diagnostic of either smelting or smithing, while some may have originated from either process.

### CRT09/200



*Figure 6.2.41 showing sample CRT09/200 post-cleaning.*

This fayalitic run appears very pale in colour, which suggests a relatively low FeO content. This does not rule out the possibility that it originated from a smelting operation however, as pale coloured smelting slags can occur if they cool in a low oxygen atmosphere. Similar pieces have been seen experimentally and so it may be possible that it formed during either smithing or smelting. Fayalite laths are clearly visible on the surface of this piece which indicate that it experienced a lengthy cooling allowing large crystal growth. This would suggest that it either cooled in a smithing hearth or

inside the furnace where it would stay far hotter for longer, rather than cooling outside of either structure where rapid cooling of the surface would not allow large fayalite laths to develop.

**CRT10/2077**



*Figure 6.2.42 showing sample CRT10/2077 post-cleaning.*

This slag is far lower in density than the smelting examples and approximately conforms to the plano-convex shape of smithing hearth bottoms. The very low density caused by extensive porosity and the light colour of the slag combined with the morphology demonstrate that it is a smithing slag rather than a primary smelting slag.



**CRT10/3034**



*Figure 6.2.43 showing sample CRT10/3034 post-cleaning.*

This piece of vitrified hearth lining exhibits the usual red colouration of the majority of such material in this assemblage. It does not have a high enough density to be comprised of slag, however the grey areas of denser material may be slag adhering to the vitrified ceramic.

**CRT10/4006**



*Figure 6.2.44 showing sample CRT10/4006 post-cleaning.*

This piece of slag exhibits the flowed surface and dark colouring associated with tap slag. The large void seen towards the top of the piece appears to have been the result of a large gas pocket or potentially the slag cooling around a stone which has since been lost.

**CRT10/4018**



*Figure 6.2.45 showing sample CRT10/4018 post-cleaning.*

This small porous drip has a dark outer original surface and several fresh fracture surfaces. The piece is less dense than CRT10/4029 (overleaf) although the dark colour would suggest that it may be from smelting. As the piece possesses significant porosity this would impact upon the apparent density as large portions of the overall volume are accounted for by voids.

**CRT10/4029**



*Figure 6.2.46 showing sample CRT10/4029 post-cleaning.*

This small sample of high density slag is indicative of smelting activity, but like much of the smelting evidence from inside the settlement it is only a fragment of a much larger piece. The flowed, dark surface indicates that it formed either during a tapping action or perhaps within the furnace or hearth following bloom extraction.



*Figure 6.2.47 showing sample CRT10/4047 post-cleaning.*

This piece is unique amongst the assemblage as it does not conform to the usual plano-convex shape of the smithing hearth bottoms. It is also of significantly higher density than many of the other pieces of comparable size. The interesting approximately vertical voids appear to be the result of the slag collecting around fuel although the apparent upper and lower surfaces, both visible in this image would suggest that the slag pooled in a small depression. The fragment has a rounded shape with a roughly 90 degree change in angle between the extremities of the broken surface. This indicates that the surviving portion was one part of a much larger piece of material, which may have been broken deliberately to make it easier to dispose of.

**CRT11/6605**



*Figure 6.2.48 showing sample CRT11/6605 post-cleaning.*

This piece while appearing to be predominantly comprised of vitrified hearth lining also has some slag as evidenced by the grey surface of a fresh fracture approximately centre image. It is not possible to categorically identify which process this material originated from as slag adhering to hearth lining can occur in both primary and secondary ironworking assemblages. The complete vitrification of the hearth lining indicates that temperatures potentially in excess of 1000°C were reached.

## Discussion

As many of the samples were recovered from contexts located towards the centre of the settlement, the small amount of smelting evidence is a result of secondary deposition. That there is any evidence of smelting at all within the assemblage suggests that there was active iron production in the vicinity of Caistor, most likely towards the edge of the settlement, and that the majority of the remains have either yet to be discovered or have been removed in subsequent time periods.

The ore used in the production of iron at Venta Icenorum has still to be successfully identified. The phosphorus content of the potentially naturally occurring ore nodules recovered during excavation may indicate that locally available material was exploited. The phosphorus content of the ores is high enough to allow for the recorded phosphorus content of the slags analysed here.

The large quantity of smithing evidence, in the form of hearth bottoms and possible smithing slags, further supports the identification of an active smithing hearth in the forum towards the latter stages of the chronology of the site. While this is a clear demonstration of the re-appropriation of space which occurred towards the end of the Roman period, it also demonstrates, by way of quantity, that there was a relatively high demand for iron artefacts in the locality. The re-use of Roman buildings for purposes different to that of their original purpose is not unknown. Rogers (2005) demonstrates that the later use of large Roman buildings as later metalworking locations appear to be more common than initially perceived. This is most notable in the Basilica of Cirencester which became an active location for both iron smithing and copper alloy casting (Rogers 2005). As the site underwent some redevelopment and increased construction activity, it would be expected that a large quantity of nails and iron tools would be produced and maintained by the smithy in the settlement. The demolition layer sealing the context which yielded the majority of the material would suggest that the forum was used as a site of refuse disposal prior to the act of demolition. This would indicate that the forum had been out of use for some time prior to the destruction of the remaining architecture.

The large quantity of heavily, and completely vitrified hearth lining demonstrates that high temperature processes were being carried out in the area. The material could have originated from any of the high temperature pyro-technological processes that were employed at the time, and while it is most likely to have originated from smithing hearths, since it was recovered from contexts that also contained smithing hearth bottoms, it may also have been associated with copper alloy working.

The limited quantity of smelting slag recovered from the excavated areas within the settlement is a relatively common occurrence. Smelting is an activity which produces large quantities of dust, noise and pollution as well as posing a significant fire risk to nearby structures. Conversely smithing is a generally safer activity which can be conducted inside or under cover, provided there is reasonable ventilation to help maintain relatively comfortable working conditions. This may further go towards explaining why large buildings were selected for conversion to metalworking areas. The Forum at

Venta Icenorum would have had at least one open side which would allow for air flow and customer access. Any potential segmentation of the roofed space would also allow for purposing areas for the heath, slag deposition and fuel storage. In the renowned case of the Cirencester Basilica (Rogers 2005), the large internal space would help to mitigate stifling temperatures, while the internal walls acted to differentiate working areas for different metallurgical practices.

## **Conclusions**

The site of Venta Icenorum had a fully functioning iron economy, with both smelting and smithing represented within the archaeological material. As the recovered evidence for smelting is limited, it may be assumed that the site of the smelting furnaces was beyond the excavated area potentially being responsible for one if not multiple magnetic anomalies detected during magnetometer survey. The ore used to produce iron at the site may have been a locally available bog ore or nodular ore, similar in nature to the nodules recovered during excavation.

The smithy in the forum appears to have been active towards the end of the Roman period with slags being found within the demolition material of the forum. This further suggests that the use of the forum had changed during the Late Roman period, as iron smithing rarely occurred in the centre of a settlement, let alone in the forum itself. The large number of smithing hearth bottoms recovered from phase 6 may be a result of both an intensification of activity associated with site development and also more successful recovery due to the location of the material in the forum.

The later phase 8 material exhibits no significant differences in morphology to the phase 6 slags. This suggests that it may be residual Roman material which was part of the road surface that later became incorporated into subsequent contexts. There is no discernable difference in the vitrified hearth lining from either phase, which indicates that a similar, if not the same, clay was being used to build the smithing hearths and potentially furnaces as well.

The remaining phase 12 pieces are undoubtedly earlier and a result of being missed during previous excavations. This material contained the most diagnostic evidence of primary iron production, including tap slag and a very dense piece which had a distinct appearance setting it apart from the rest of the assemblage. The recovery from trench backfill contexts is far from ideal, however these pieces provide proof of iron smelting in the nearby vicinity. While excavating Roman settlements for evidence of activity within them, for which excavating the Forum is ideal, understanding how a settlement interacts with the surrounding area is just as important. The large features found during geophysical prospection beyond the limits of Venta Icenorum may provide further evidence of settlement-landscape interaction which would allow for a fuller interpretation of how the site operated and potentially locate the site of iron production hinted at by the presence of diagnostic smelting slag.



## **Saxon case studies**

Following the end of the Roman period, the arrival of Germanic peoples and culture instigated a dramatic and significant change in Britain. The significant cultural differences of the arriving peoples that would create Anglo-Saxon England are reflected in almost every aspect of the cultural remains which define the period.

### **6.3 Quarrington**

An archaeological site at the village of Quarrington, just outside Sleaford, central Lincolnshire, demonstrates the changes in architecture, material culture and settlement pattern that occurred and then became established over the 6<sup>th</sup> and 7<sup>th</sup> centuries A.D. Quarrington is initially described as a hamlet in the opening line of the report, while later in the same paragraph it is referred to as a village (Taylor *et al.* 2003: 231). The presence of the medieval church clearly defines the settlement as a village and not a hamlet. This should have been made clear at the start of the report to avoid ambiguity.

The site is located on the south side of a slight east-west ridge between the River Slea to the north and Moor Drain, a partially canalised stream, to the south (Taylor *et al.* 2003: 233). The underlying geology of the site consists of Lincolnshire Limestone and cornbrash interlaced with ice-wedge polygons (Taylor, C. Allen *et al.* 2003: 231). The name of the stream would suggest that the area was significantly wetter than it is today, which may hint at the possibility of bog ore availability.

The site was identified in 1992 when trial trenches revealed ditches and pits of Early-Middle Saxon date. Subsequent magnetometer survey revealed a widespread distribution of linear geophysical anomalies across an area which was the site of a since completed housing development. A total area of 1.67ha was examined between October 1993 and July 1995.

In the Southern part of the site, a series of linear and curvilinear ditches were excavated, all of which contained pottery of Early Saxon date. A linear ditch on a north west- south east alignment also had several short, parallel gullies on either side. The ditch yielded Early Saxon pottery, while the gullies were found to contain Mid-Saxon pottery. These features were interpreted as possible track ways, which remained in use after the earlier ditch had become in-filled (Taylor *et al.* 2003: 237).

Adjacent to the track system, on the western side, were numerous post holes (Taylor *et al.* 2003: 237). After examination, three round houses were identified (structures 3, 5, 6) each of which were

6m in diameter with south facing entrances (Taylor *et al.* 2003: 237). Ceramic dating evidence was found in post holes of two of the structures, dating to the Early Saxon period.

This settlement area was limited by an east-west aligned ditch to the south and a north-south fence line to the east (Taylor *et al.* 2003: 237). Further to the east a north-south curvilinear ditch was found that appeared to enclose an area to the east and exclude settlement structures (Taylor *et al.* 2003: 237). Further Early Saxon pottery was recovered from all of these ditches (Taylor *et al.* 2003: 237).

Metallurgical activity was identified in structure 8, a 5x3.5m area partially encircled by pits (pit group A) (Taylor *et al.* 2003: 240). This produced both primary and secondary iron slags as well as evidence of copper alloy working. The iron smelting material was recovered from or near the pit group associated with structure 8 (Taylor *et al.* 2003: 241). Stamp-decorated and stabbed sherds indicate that the features most likely date to the 6<sup>th</sup>-7<sup>th</sup> centuries AD. Only Early Saxon pottery was used as crucibles, firmly dating the copper alloy working on the site (Taylor *et al.* 2003: 244).

Given the relatively reliable dating of the metallurgical debris by the ceramic assemblages associated with the features, the iron slags are Early Saxon in date. The analysis of the assemblage was carried out by Jane Cowgill who identified several categories of material. The specialist report also highlights several features of the assemblage which make such a complete interpretation difficult. The slag assemblage is described as being “uncharacteristic” with the majority of the pieces “not conforming with normal morphological traits” (Taylor *et al.* 2003: 256). The uncharacteristic nature of the material makes the table of identified slag (Taylor *et al.* 2003: 257) potentially questionable, as no non-diagnostic or dense ironworking slag was recorded. The identification of tap slag as being the only smelting evidence suggests that the rest of the smelting material associated with a tapping furnace had not been found. The means of the slag production were not successfully interpreted due to the unusual appearance of the assemblage (Taylor *et al.* 2003: 256). The lack of slag blocks in neighbouring East Anglia at this time is used by Cowgill to suggest that the smelting technology in use was a tapped shaft furnace (Taylor *et al.* 2003: 256). Cowgill cites McDonnell in the statement that slag blocks are not found in East Anglia, however McDonnell clearly states in the cited paper that slag blocks “have been found in eastern England from Lincolnshire in the north to Hampshire in the south, with a high concentration in East Anglia” (McDonnell 1989: 374). This apparently contradicts that statement of Cowgill, as slag blocks are found at Little Totham in Essex dated to the 6th-7th centuries A.D. by radiocarbon and thermoluminescence dating methods (Cranstone 1988: 4).

The location of the smelting activity was postulated as being on the fringe of the settlement, due to the large quantities of dust produced by the crushing of both ore and charcoal. Similarly, the smithy is interpreted as being some distance from the investigation site based upon the quantity of smithing slag recovered (Taylor *et al.* 2003: 257). Interestingly, a small number of thin, flat, plate-like slags were identified as probable smelting debris. While the dimensions of the pieces are not stated, they may

have originated from bloom consolidation, rather than being produced in the furnace. This would account for the thickness and apparent flatness of the specimens. Similarly the “flowed droplets” which exhibit no flat surfaces (Taylor *et al.* 2003: 256) may also have been produced during the early stages of bloom smithing. When slag is ejected from a bloom some of it may behave in a similar manner to slag ejected from a fold weld (Dungworth and Wilkes 2009), forming spheroidal slag, which is not the same as hammerscale despite being produced in the same operation.

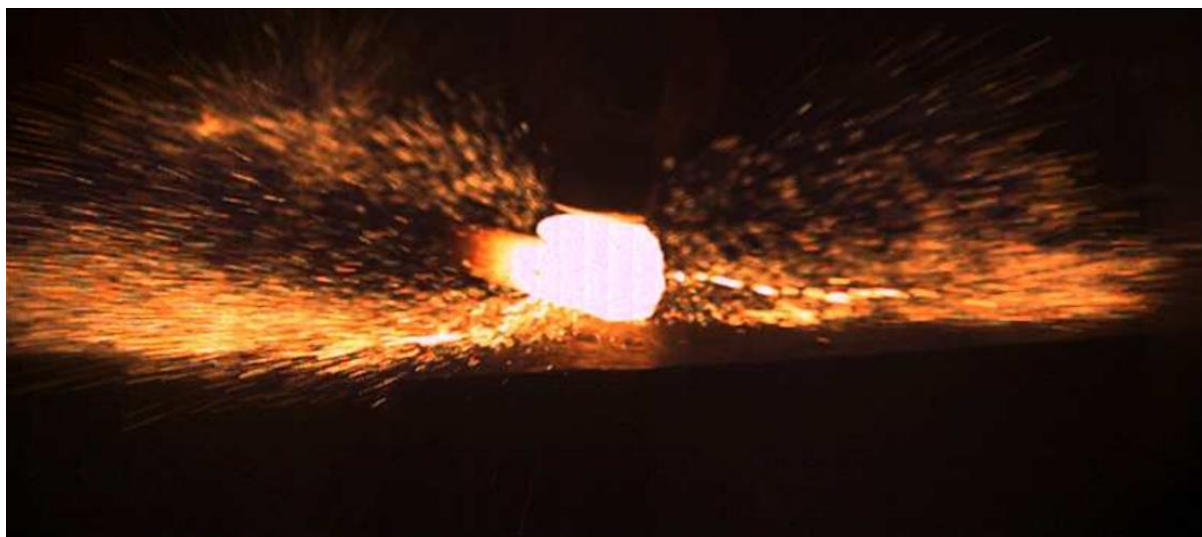


*Figure 6.3.1 showing the ejection of slag from a fold weld (after Dungworth and Wilkes 2009).*

As the droplets of slag cool while travelling through the air, they commonly do not possess any flat surfaces; this evidence is in agreement with the interpretation put forward by Cowgill (Taylor *et al.* 2003: 256).

If these slag droplets and plates originated from bloom consolidation then it would support the limited evidence of smelting provided by the tap slag that primary production of iron was being undertaken in the vicinity of the site. In order to efficiently consolidate a bloom into a billet, it is best to commence forging as soon as it is removed from the furnace. This ensures that the minimum quantity of charcoal is required to maintain the bloom at a forgeable temperature, as it does not require heating from ambient to a temperature of approximately 900°C.

A number of more “normal” smithing slags were recovered from Mid-Saxon contexts. This was interpreted as a reflection of a change in smithing techniques employed at the site (Taylor *et al.* 2003: 257-258), although it may also reflect a change in smithing operation entirely as all the smelting evidence came from earlier phases.

In light of these more recent findings concerning spheroidal slag and the difference in possible ore exploitation between the Roman and the Early Saxon periods, a re-analysis of the slag was undertaken to evaluate the practices occurring at Quarrington.

The initial assessment of material from the site of Quarrington, while being conducted in a similar manner to many other such reports, has some shortcomings. The material was assessed without being washed and some of the pieces present in the Lincolnshire Archives are not recorded in the report.

Some pieces of slag, originally identified as smelting slag, were found to be significantly different from the others in the group. Some of these, such as the two pieces in context QCH93 024, more closely resemble fuel than slag. Another piece of tap slag also in the slag recovered from context QCH93 024 proved to be significantly smaller than the original report claimed, as approximately one third of the piece comprised of the sandy, silt soil that had not been washed off.

These examples demonstrate the importance of cleaning metallurgical debris prior to assessment as adhering soil can obscure diagnostic features and, depending on soil character, significantly alter the shape and mass of a piece leading to an incorrect interpretation. I argue therefore, that all slag assemblages should be thoroughly washed as part of post-excavation standard practice. This is the case with other portions of site assemblages, such as faunal remains, where diagnostic features might only be visible when the pieces are clean. Consequently, it may be argued that all classes of material should be cleaned to ensure correct recording, rather than greater attention being lavished upon the most prevalent or currently fashionable finds groups.

The washing of slag can be a rougher post-excavation treatment than that received by other archaeological materials. The exception to this is vitrified hearth lining exhibiting the orange colouring diagnostic of oxidising conditions, which is far more fragile and friable than the other materials associated with pyrotechnological processes. Washing the material ensures that pieces can be viewed in their clean, unobscured state reaching the most accurate descriptions and resultant interpretations.

While the previously undocumented pieces do not contribute any major modifications to the interpretation of activity at the site, they are significant diagnostic pieces which further strengthen the overall conclusions presented in the original report.

A second, large piece of stone (1.8kg) with red colouring similar to the small piece in the report was found. This again is likely to represent discarded material from ore beneficiation, as the iron rich portions are minimal in comparison to the undesirable host rock.

Further evidence of smithing and smelting are also present among the unreported materials. A smithing hearth bottom with fuel inclusions which was light in colour with some red-purple

colouration in places exhibited a potential layered structure. There appeared to be a primary hearth bottom with a second forming on top.

A large piece of smelting slag with a smooth, relatively flat top surface was identified (QCH93 +). Unlike the smithing slag, this piece had a dark grey interior and had a significantly higher density. It is likely that this piece is a small furnace bottom, and hence a small furnace, which would account for the small quantity of tap slag reported by Cowgill.

Another sample, recovered from context 1164, was originally reported as tap slag. Following cleaning and observation this piece appears to be a smithing hearth bottom, see below figure 6.6.2.



*Figure 6.3.2 showing the profile of slag exhibiting plano-convex form.*

Within a group of slag recovered from context 1389 there were several low density, light colour pieces but also two very dark, dense pieces with evident high iron content on the basis of the dark red-orange to brown colouring of their surfaces. Parts of the lower surfaces displayed more evidence of fluidity and dark grey colouring comparable with larger pieces of furnace slag. When sampled these pieces had a dark grey interior, darker than the sampled smithing slag. This has guided the interpretation that these small pieces originated from smelting.

With these pieces now fully examined a corrected report of the Quarrington material assessed here is presented below incorporating the new interpretations and adjusted mass recordings.

| Context/find number | Mass (g) | Number of Pieces | Interpretation  |
|---------------------|----------|------------------|---|
| QCH93 024           | 136      | 13               | Smelting tap/flow   |
| QCH93 200 149       |          | 2                | Small drip and potential SHB  |
| QCH93 273           | 24       | 2                | Smithing plate and small drip   |
| QCH93 355           |          | 3                | 2 smithing plates and small flow slag                                   |
| QCH93 411           | 4        | 1                | Small drip  |
| QCH93 577           | 32       | 1                | Tap/flow slag   |
| QCH93 1164          | 100      | 1                | Possible smithing hearth bottom   |
| QCH93 +             | 1036     | 1                | Small furnace bottom  |
| QCH93 +B            | 14       | 1                | Smelting gromp  |
| QCH93 +G            | 8        | 2                | High density slags, one has an extremely pronounced plano-convex shape. |
| QCH93 +R            | 4        | 1                | Drip  |
| QCH93 1389          | 29       | 15               | Smelting tap/drip   |

*Table 6.3.1 Revised list of Quarrington smelting slag.*

### Sampled material



*Figure 6.3.3 showing smelting slag from context QCH93 024.*



*Figure 6.3.4 showing unstratified smelting slag QCH93 +*

This piece is the unstratified pooled smelting slag that is diagnostic of smelting activity. Unlike the small drips seen previously this piece has a mass exceeding 1kg and has been called a small furnace bottom due to the indentation in the upper surface.

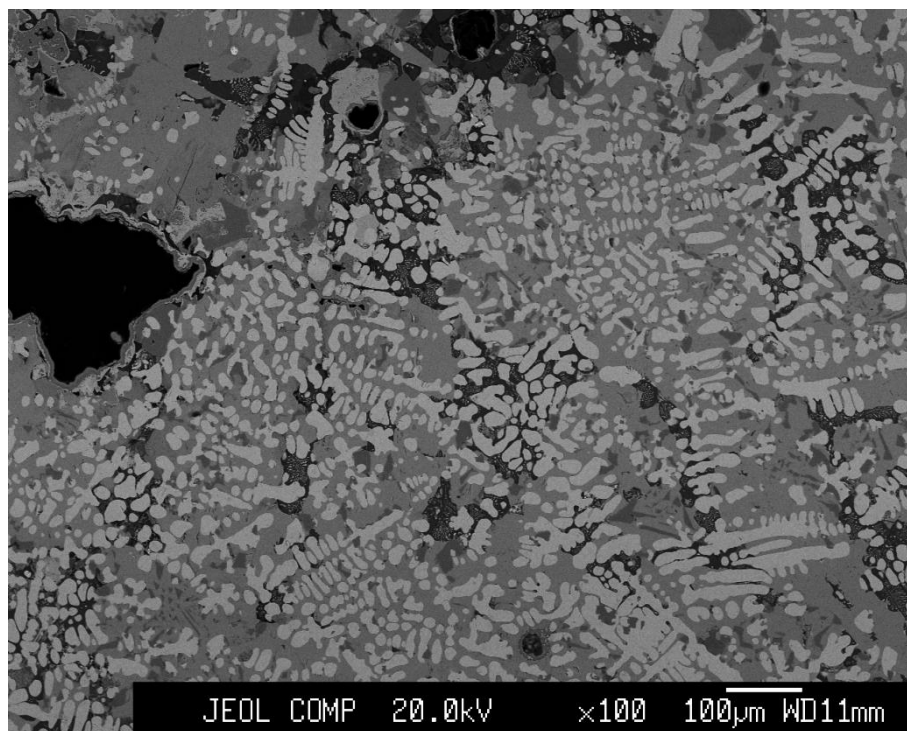


*Figure 6.3.5 showing backscatter electron image of QCH93+ sample with well developed globular wüstite dendrites, fayalite grains and low density matrix, and significant pores.*

The high concentration of wüstite found in the sample of slag from QCH93+ demonstrates that it originated from primary production. This, along with the lack of a flowed surface morphology, further strengthens the argument that it is a small furnace bottom.

| Element          | FeO   | SiO <sub>2</sub> | P <sub>2</sub> O <sub>5</sub> | Na <sub>2</sub> O | Al <sub>2</sub> O <sub>3</sub> | K <sub>2</sub> O | CaO  |
|------------------|-------|------------------|-------------------------------|-------------------|--------------------------------|------------------|------|
| QCH93 + wüstite  | 91.07 | 0.32             | 0.02                          | 0.051             | 0.75                           | 0.06             | 0.03 |
| QCH93 + fayalite | 64.04 | 29.67            | 0.13                          | BDL               | 0.30                           | 0.02             | 0.31 |
| QCH93 + matrix   | 5.66  | 53.31            | 0.24                          | 0.91              | 25.11                          | 17.36            | 0.31 |

*Table 6.3.2 Showing major elements detected in the main mineral phases of slag QCH93+*





*Figure 6.3.6 showing unstratified smelting slag drip QCH93 +R.*

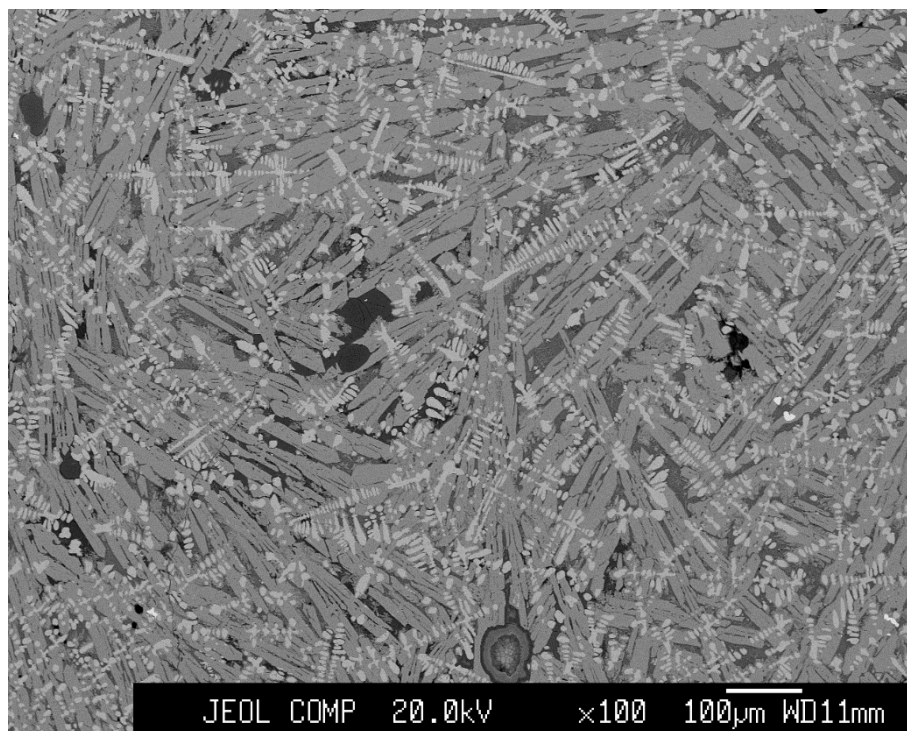


*Figure 6.3.7 showing backscatter electron image of QCH93 +R sample with well-developed wüstite dendrites, fayalite laths and low density matrix, characteristic of the smelting slags recovered from the site.*

| Element           | FeO   | SiO <sub>2</sub> | P <sub>2</sub> O <sub>5</sub> | Na <sub>2</sub> O | Al <sub>2</sub> O <sub>3</sub> | K <sub>2</sub> O | CaO  |
|-------------------|-------|------------------|-------------------------------|-------------------|--------------------------------|------------------|------|
| QCH93 +R wüstite  | 78.27 | 8.95             | 0.08                          | 0.15              | 7.92                           | 0.24             | 0.43 |
| QCH93 +R fayalite | 64.84 | 30.04            | 0.07                          | BDL               | 0.78                           | 0.11             | 0.48 |
| QCH93 +R matrix   | 43.53 | 34.32            | 0.36                          | 1.33              | 11.11                          | 4.30             | 4.23 |

*Table 6.3.3 Showing major elements detected in the main mineral phases of slag QCH93+R*

## 6.4 Flixborough

The settlement site of Flixborough is one that underwent a long period of occupation and yielded deep stratigraphy dating from the Mid- to Late Saxon periods. The excavations produced a detailed image of the activity which occurred throughout the habitation of the site with distinct changes in status and function evident. While Ironworking evidence was recovered from several of the identified phases, the vast majority was dated to the 10<sup>th</sup>-century A.D. (Loveluck 2007: 29). This was marked by a large increase in the quantity of smelting slags and the appearance of large slag blocks.

The earlier of the two main phases of iron production was associated with faunal remains which may indicate consumption related to hunting and high status. This may suggest that the ironworking slags may have been involved in the supply of raw materials, finished artefacts and maintenance of ferrous objects.

The distinct lack of iron slags in the following monastic phase demonstrates a change in economic strategy. This is reflected in the monastic consumption of high quality window glass and the reduced number of hunted animals appearing in the faunal assemblage. Such a significant change in behaviour is not only a result of the construction of a monastery but also a product of the monastic community distancing themselves culturally from what occurred previously.

In the 10<sup>th</sup>-century iron production and smithing appear to return on a far greater scale than had been present prior to the monastic phase (Evans and Loveluck 2009: 324-348). This increase in production may be a result of several factors including increased demand, both locally and for export to nearby settlements, the identification of large quantities of suitable ores within close proximity, and potentially a change in technology that allowed other materials, such as the available Frodingham ironstone to be exploited more successfully. This is certainly a possibility with both bog ore and ironstone found in a roasted condition which would suggest that a level of experimentation was occurring into the potential for smelting the ironstone. This viewpoint may be countered by the abundant presence of ironstone at and surrounding the site. It may have been that pieces of ironstone became roasted coincidentally during other ore preparation. While this may have been the case, it seems somewhat unlikely as the complete roasting of a piece of iron ore requires it to be placed

entirely into oxidising conditions. If these pieces were buried during roasting then parts of the pieces would not have undergone complete oxidation.

The continued presence of smithing slags demonstrates that iron was being worked into artefacts throughout the occupation of the site; however the increased appearance of smithing evidence during the 10<sup>th</sup>-century indicates that the major economic activity changed drastically between the ninth and tenth centuries to focus on the working of iron and the production of ferrous artefacts.

Large quantities of the material were recovered from contexts identified as dumps which would indicate an organised system of slag and rubbish disposal. Given the quantity, and inferred scale of iron production in the 10<sup>th</sup>-century it is to be expected that the disposal of the slag would have to be conducted in an organised manner. As the production of the metallic blooms had to be coordinated and planned, so to the disposal of resultant slag would also have to be organised to avoid the build-up of slag heaps in locations central to activity.

With these possibilities of multiple ore exploitation and potential technological change in mind, it was important to sample material from both of the major iron production phases to allow for a comparison between the phosphorus content of the respective slags. The bog ore accessible at Flixborough will have been produced from the Frodingham ironstone which is also situated within walking distance of the site. However, the two ores should be distinguishable based on phosphorus content, which should have a direct impact upon the phosphorus present in the slags produced from them.

## Sampled material



*Figure 6.4.1 showing large tapped slag from context FLX89 51.*

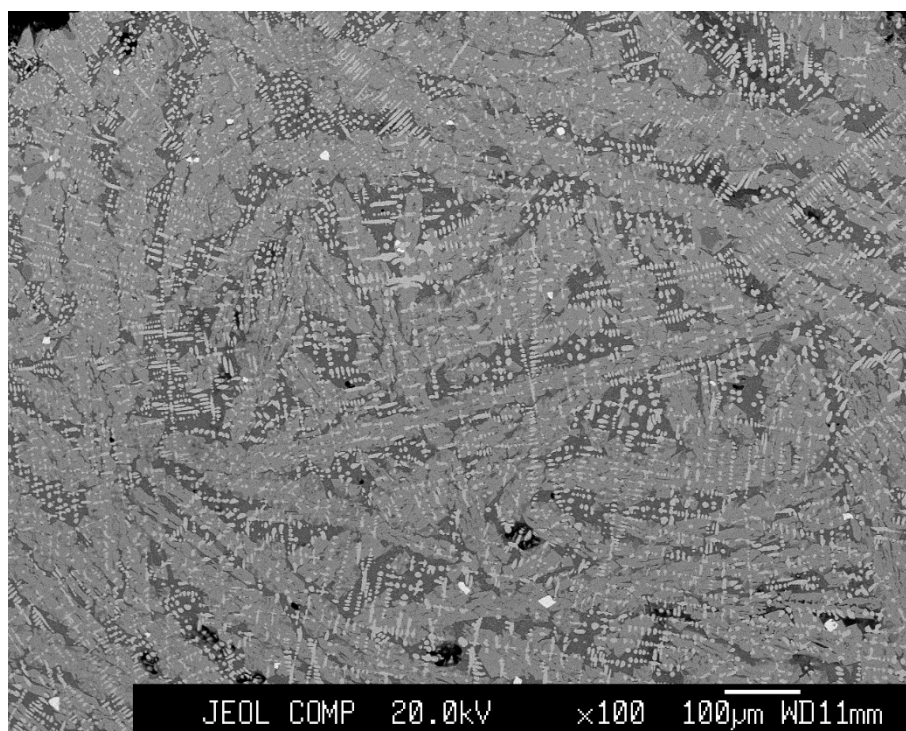


Figure 6.4.2 showing backscatter electron image of slag sample from context FLX89 51, with fine wüstite dendrites, fayalite laths, glassy matrix and metallic iron (bright white).

| Element                     | FeO   | SiO <sub>2</sub> | P <sub>2</sub> O <sub>5</sub> | Na <sub>2</sub> O | Al <sub>2</sub> O <sub>3</sub> | K <sub>2</sub> O | CaO   |
|-----------------------------|-------|------------------|-------------------------------|-------------------|--------------------------------|------------------|-------|
| FLX89 51 large tap wüstite  | 60.15 | 16.73            | 1.80                          | 1.19              | 8.74                           | 3.56             | 5.23  |
| FLX89 51 large tap fayalite | 61.04 | 27.41            | 0.31                          | 0.08              | 5.94                           | 0.031            | 0.80  |
| FLX89 51 large tap matrix   | 27.40 | 35.65            | 2.45                          | 1.71              | 16.76                          | 6.74             | 10.62 |

Table 6.4.1 Showing major elements detected in the main mineral phases of large tap slag from context FLX89 51.



*Figure 6.4.3 showing smelting slag gromp from context FLX89 51.*

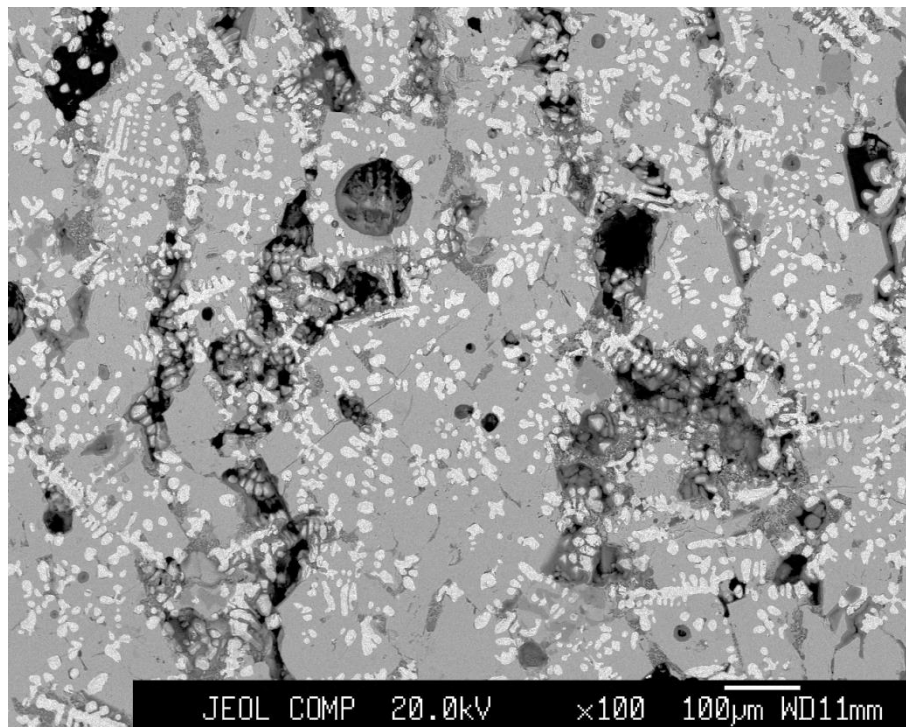


*Figure 6.4.4 showing backscatter electron image of slag sample from context FLX89 51, with globular wüstite dendrites, extensive fayalite grains, limited glassy matrix, and notable porosity.*



| Element                     | FeO   | SiO <sub>2</sub> | P <sub>2</sub> O <sub>5</sub> | Al <sub>2</sub> O <sub>3</sub> | CaO  | MnO  |
|-----------------------------|-------|------------------|-------------------------------|--------------------------------|------|------|
| FLX89 51 small tap wüstite  | 92.55 | 0.35             | 0.05                          | 0.60                           | 0.04 | 0.84 |
| FLX89 51 small tap fayalite | 62.48 | 29.60            | 0.50                          | 0.20                           | 0.73 | 2.89 |
| FLX89 51 small tap matrix   | 46.61 | 0.74             | 0.02                          | 51.64                          | 0.21 | 0.84 |

*Table 6.4.2 Showing major elements detected in the main mineral phases of the smelting group from context FLX89 51*



*Figure 6.4.5 showing flowed smelting slag from context FLX89 2176 (a and b, left and right respectively).*

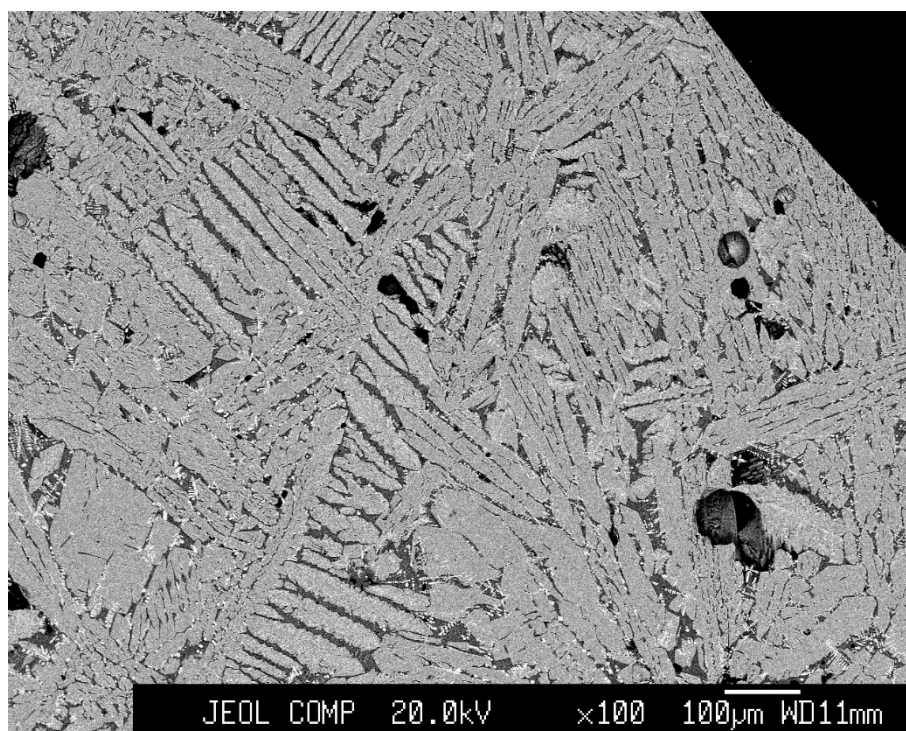


Figure 6.4.6 showing backscatter electron image of slag sample FLX89 2176a, with fine wüstite dendrites, fayalite laths, glassy matrix, and porosity.

| Element              | FeO   | SiO <sub>2</sub> | P <sub>2</sub> O <sub>5</sub> | Al <sub>2</sub> O <sub>3</sub> | Na <sub>2</sub> O | K <sub>2</sub> O | CaO   | MnO  |
|----------------------|-------|------------------|-------------------------------|--------------------------------|-------------------|------------------|-------|------|
| FLX89 2176a wüstite  | 75.69 | 12.87            | 0.77                          | 3.14                           | 0.18              | 0.41             | 1.43  | 0.97 |
| FLX89 2176a fayalite | 63.27 | 29.78            | 0.17                          | 0.15                           | 0.05              | 0.02             | 0.52  | 2.23 |
| FLX89 2176a matrix   | 27.60 | 33.75            | 4.48                          | 14.51                          | 0.77              | 4.92             | 11.82 | 0.60 |

Table 6.4.3 Showing major elements detected in the main mineral phases of the smelting slag FLX89 2176a

The far finer wüstite seen in figure 6.4.8 when compared to that in the previous samples (figures 6.4.6 and 6.4.7) indicates that the slag experienced a more rapid cooling. This is a result of the greater surface area to volume ratio of the thinner flows from which these pieces originated.



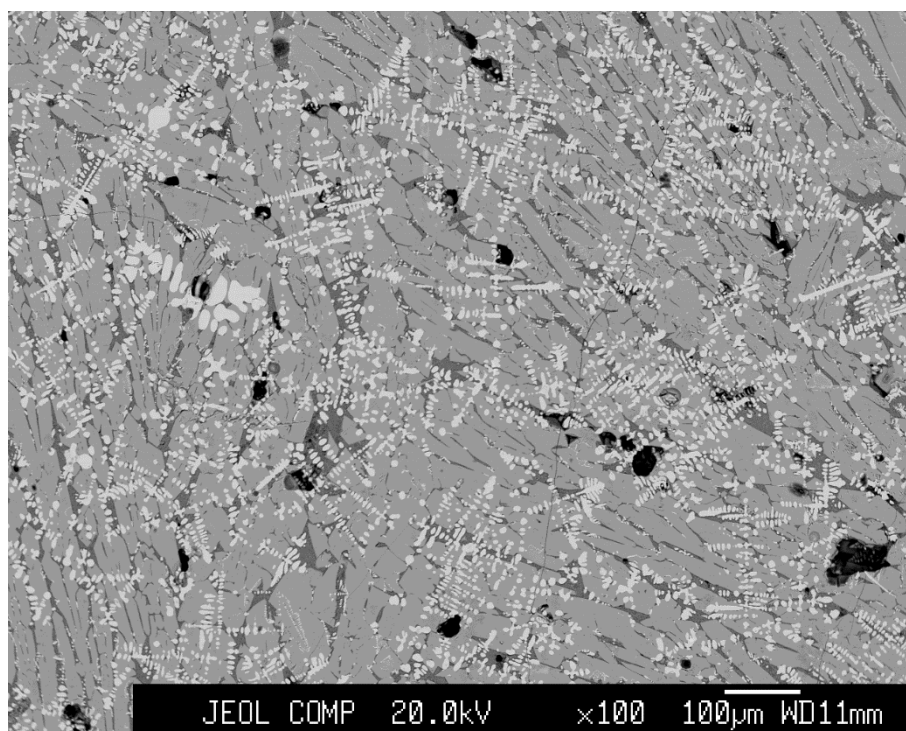


Figure 6.4.7 showing backscatter electron image of slag sample from context FLX89 2176b, with fine wüstite dendrites and occasional globular wüstite, well developed fayalite laths, glassy matrix, and porosity.

| Element              | FeO   | SiO <sub>2</sub> | P <sub>2</sub> O <sub>5</sub> | Na <sub>2</sub> O | Al <sub>2</sub> O <sub>3</sub> | K <sub>2</sub> O | CaO   | MnO  |
|----------------------|-------|------------------|-------------------------------|-------------------|--------------------------------|------------------|-------|------|
| FLX89 2176b wüstite  | 91.33 | 0.96             | 0.11                          | 0.11              | 0.53                           | 0.02             | 0.05  | 0.74 |
| FLX89 2176b fayalite | 62.61 | 29.50            | 0.42                          | 0.07              | 0.17                           | 0.02             | 0.90  | 2.75 |
| FLX89 2176b matrix   | 30.00 | 31.23            | 5.86                          | 0.74              | 11.01                          | 4.93             | 14.17 | 0.97 |

Table 6.4.4 Showing major elements detected in the main mineral phases of the smelting slag FLX89 2176b



*Figure 6.4.8 Showing flowed smelting slag from context FLX89 1427.*

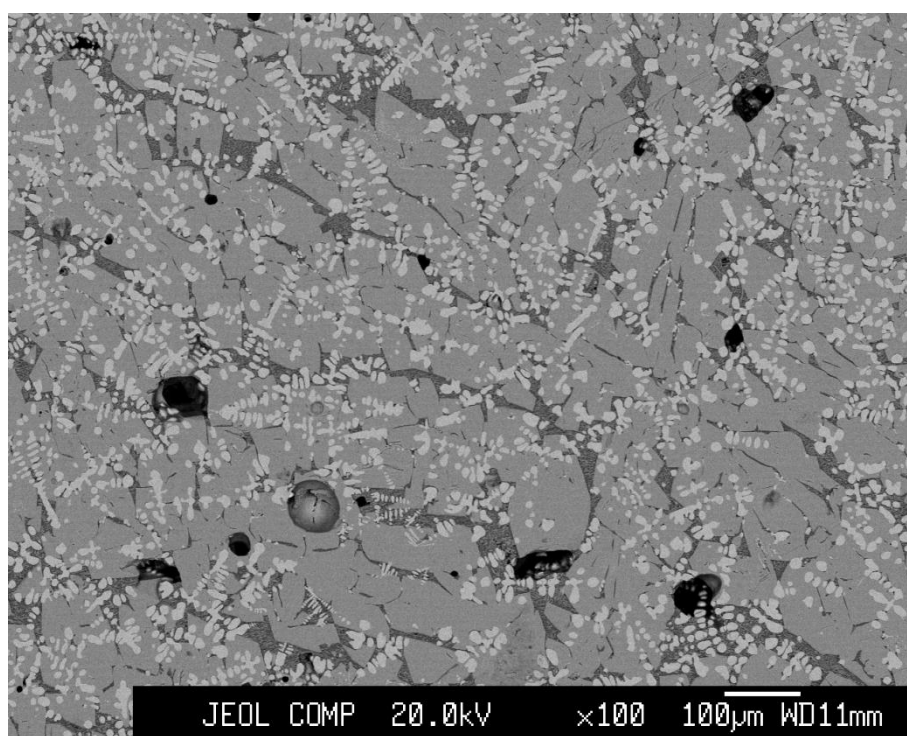


*Figure 6.4.9 Showing backscatter electron image of slag sample from context FLX89 1427, with fine wüstite dendrites and occasional globular wüstite, well developed fayalite laths, glassy matrix, and porosity.*

| Element                | FeO   | SiO <sub>2</sub> | P <sub>2</sub> O <sub>5</sub> | Na <sub>2</sub> O | Al <sub>2</sub> O <sub>3</sub> | K <sub>2</sub> O | CaO   | MnO  |
|------------------------|-------|------------------|-------------------------------|-------------------|--------------------------------|------------------|-------|------|
| FLX89 1427<br>wüstite  | 81.31 | 6.31             | 1.40                          | 0.20              | 3.19                           | 0.88             | 2.70  | 0.84 |
| FLX89 1427<br>fayalite | 62.53 | 30.34            | 0.39                          | BDL               | 0.18                           | 0.02             | 0.88  | 2.88 |
| FLX89 1427<br>matrix   | 29.11 | 31.35            | 7.12                          | 0.86              | 12.0                           | 4.94             | 14.16 | 0.99 |

*Table 6.4.5 Showing major elements detected in the main mineral phases of the smelting slag FLX89 1427*



*Figure 6.4.10 Showing roasted ore sample from context FLX89 17513.*

This is a sample of roasted ore, which is representative of the other pieces recovered and examined as part of the complete assemblage.



*Figure 6.4.11 showing smelting slag from context FLX89 2823.*



*Figure 6.4.12 showing smelting slag group from context FLX89 1995.*

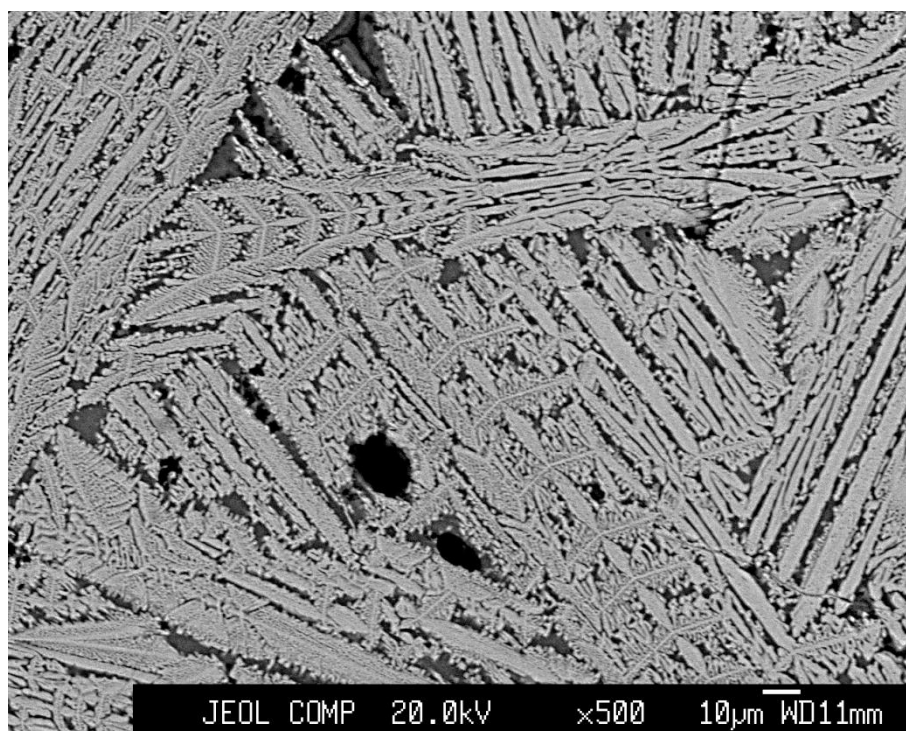


Figure 6.4.13 showing backscatter electron image of slag sample from context FLX89 1995, with no visible wüstite, feathered fayalite laths, glassy matrix, and porosity.

| Element             | FeO   | SiO <sub>2</sub> | P <sub>2</sub> O <sub>5</sub> | Na <sub>2</sub> O | Al <sub>2</sub> O <sub>3</sub> | K <sub>2</sub> O | CaO  | MnO  |
|---------------------|-------|------------------|-------------------------------|-------------------|--------------------------------|------------------|------|------|
| FLX89 1995 fayalite | 59.56 | 33.83            | 0.56                          | 0.12              | 1.41                           | 0.38             | 0.71 | 1.66 |
| FLX89 1995 matrix   | 26.94 | 46.52            | 4.32                          | 0.24              | 12.59                          | 2.00             | 6.51 | 0.64 |

Table 6.4.6 Showing major elements detected in the main mineral phases of the smelting slag FLX89 1995

This sample has the characteristics of a smelting slag, although the lack of visible wüstite and rapidly cooled fayalite may suggest that it was a result of a particularly gangue-rich reaction. The microstructure contrasts greatly with the other pieces examined where all three major phases are clearly visible.





*Figure 6.4.14 showing large smelting slag piece from context FLX89 10393 10449.*

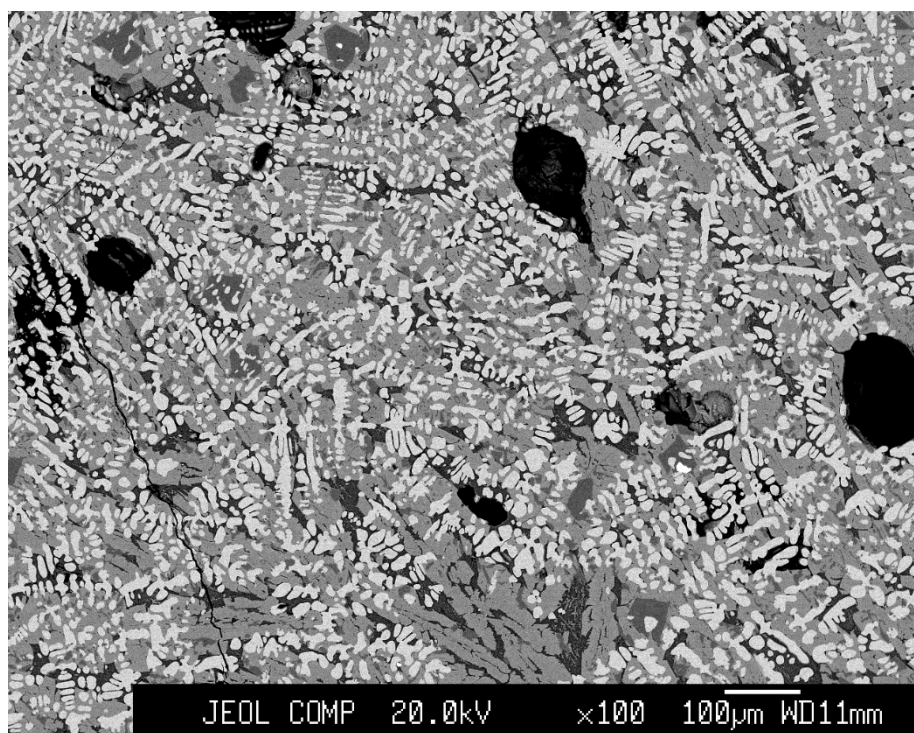


Figure 6.4.15 showing backscatter electron image of slag sample from context FLX89 10393 10449, with well-developed wüstite dendrites, fayalite laths, glassy matrix, and pores.

| Element                       | FeO   | SiO <sub>2</sub> | P <sub>2</sub> O <sub>5</sub> | Na <sub>2</sub> O | Al <sub>2</sub> O <sub>3</sub> | K <sub>2</sub> O | CaO  | MgO  |
|-------------------------------|-------|------------------|-------------------------------|-------------------|--------------------------------|------------------|------|------|
| FLX98 10393<br>10449 wüstite  | 92.19 | 0.46             | 0.03                          | 0.04              | 0.79                           | 0.03             | 0.09 | 0.12 |
| FLX98 10393<br>10449 fayalite | 60.95 | 29.78            | 0.76                          | 0.07              | 0.86                           | 0.04             | 0.95 | 3.39 |
| FLX98 10393<br>10449 matrix   | 28.55 | 21.09            | 3.22                          | 3.01              | 31.98                          | 2.07             | 8.58 | 1.17 |

Table 6.4.7 Showing major elements detected in the main mineral phases of the smelting slag FLX89 10393 10449



*Figure 6.7.16 showing large smelting slag with flowed surface FLX89 2024.*



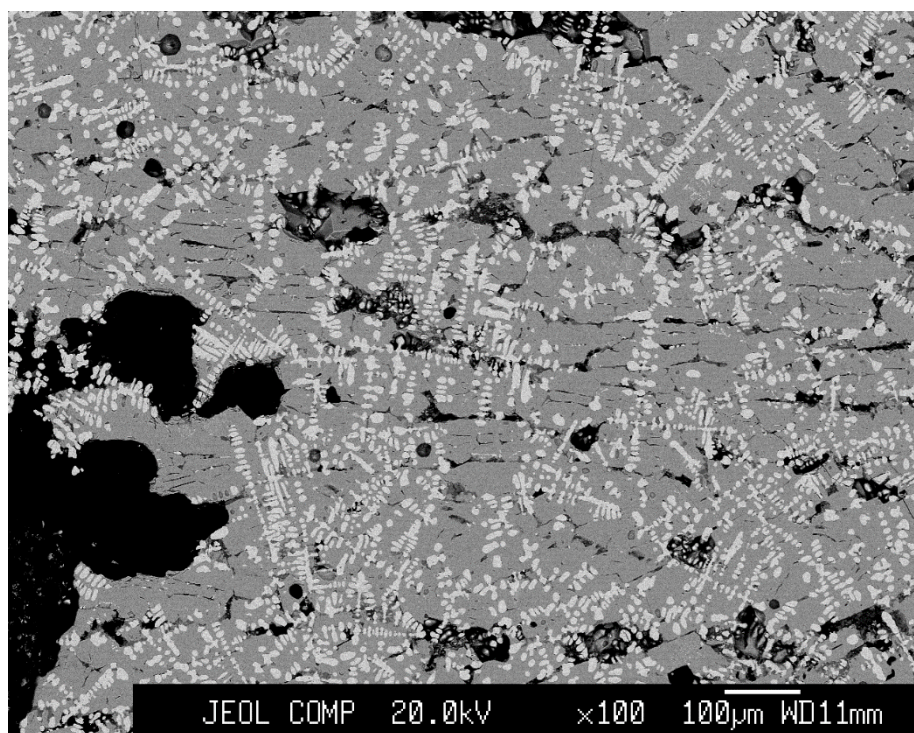


Figure 6.4.17 showing backscatter electron image of slag sample from context FLX89 2024, with well-developed wüstite dendrites and occasional globular wüstite, extensive fayalite grains, limited glassy matrix, and significant pores.

| Element             | FeO   | SiO <sub>2</sub> | P <sub>2</sub> O <sub>5</sub> | Al <sub>2</sub> O <sub>3</sub> |
|---------------------|-------|------------------|-------------------------------|--------------------------------|
| FLX89 2024 wüstite  | 87.16 | 4.61             | 0.36                          | 1.36                           |
| FLX89 2024 fayalite | 65.35 | 29.18            | 0.801                         | 0.34                           |
| FLX89 2024 matrix   | 75.20 | 14.52            | 0.99                          | 4.27                           |

Table 6.4.8 Showing major elements detected in the main mineral phases of the smelting slag FLX89 2024



*Figure 6.4.18 showing sample of material from FLX89 800 with slag encasing iron- rich stone.*



*Figure 6.4.19 showing smelting slag ribbon from context FLX89 3256 5286.*

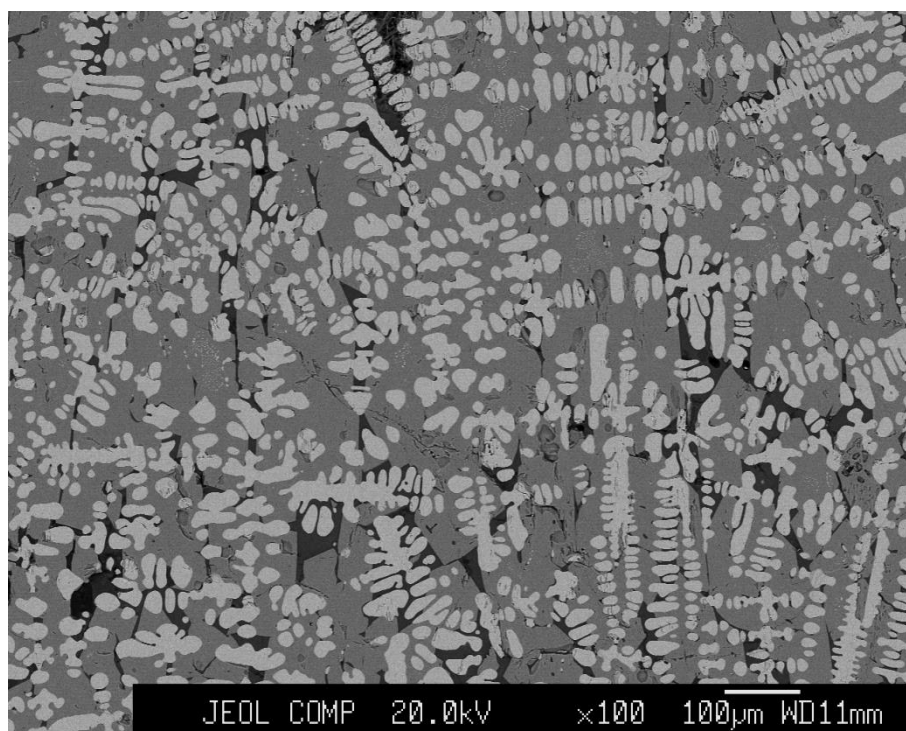


Figure 6.4.20 showing backscatter electron image of slag sample from context FLX89 3256 5286, with well-developed wüstite dendrites and occasional globular wüstite, extensive fayalite grains, and glassy matrix.

| Element                     | FeO   | SiO <sub>2</sub> | P <sub>2</sub> O <sub>5</sub> | Na <sub>2</sub> O | Al <sub>2</sub> O <sub>3</sub> | K <sub>2</sub> O | CaO  |
|-----------------------------|-------|------------------|-------------------------------|-------------------|--------------------------------|------------------|------|
| FLX89 3256 5286<br>wüstite  | 93.78 | 0.32             | 0.03                          | 0.07              | 0.84                           | 0.02             | BDL  |
| FLX89 3256 5286<br>fayalite | 66.32 | 29.94            | 0.45                          | BDL               | 0.20                           | 0.02             | 0.22 |
| FLX89 3256 5286<br>matrix   | 30.86 | 35.24            | 5.1                           | 1.63              | 17.48                          | 7.51             | 4.92 |

Table 6.4.9 Showing major elements detected in the main mineral phases of the smelting slag FLX89 3256 5286



*Figure 6.4.21 showing smelting slag from context FLX89 674*



*Figure 6.4.22 showing smelting slag from context FLX89 10394 10546*



*Figure 6.4.23 showing tap slags from context FLX89 3107 – analysed samples tap slag number 2, tap slag number 4 and tap number slag 5 indicated by red numbers. The pieces are arranged to show archaeological and fresh breaks to allow for clearer association.*



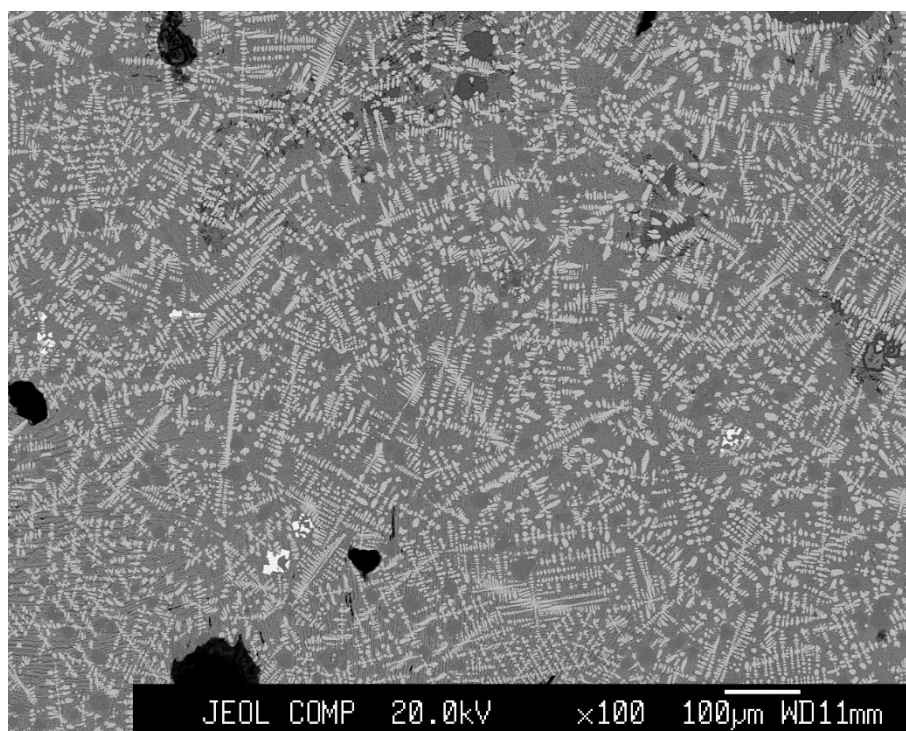


Figure 6.4.24 showing backscatter electron image of slag sample tap slag number 2 from context FLX89 3107, with wüstite dendrites, extensive fayalite grains, glassy matrix, and occasional metallic iron (bright white).

| Element                        | FeO   | SiO <sub>2</sub> | P <sub>2</sub> O <sub>5</sub> | Na <sub>2</sub> O | Al <sub>2</sub> O <sub>3</sub> | K <sub>2</sub> O | CaO  | MgO  |
|--------------------------------|-------|------------------|-------------------------------|-------------------|--------------------------------|------------------|------|------|
| FLX89 3107 Tap slag 2 wüstite  | 63.17 | 19.28            | 1.70                          | 0.93              | 7.13                           | 0.72             | 3.95 | 2.37 |
| FLX89 3107 Tap slag 2 fayalite | 43.76 | 29.23            | 2.88                          | 1.51              | 11.45                          | 1.49             | 7.77 | 1.88 |
| FLX89 3107 Tap slag 2 matrix   | 36.92 | 32.59            | 2.33                          | 2.00              | 14.14                          | 1.65             | 7.95 | 2.20 |

Table 6.4.10 Showing major elements detected in the main mineral phases of tap slag 2 from context FLX89 3107

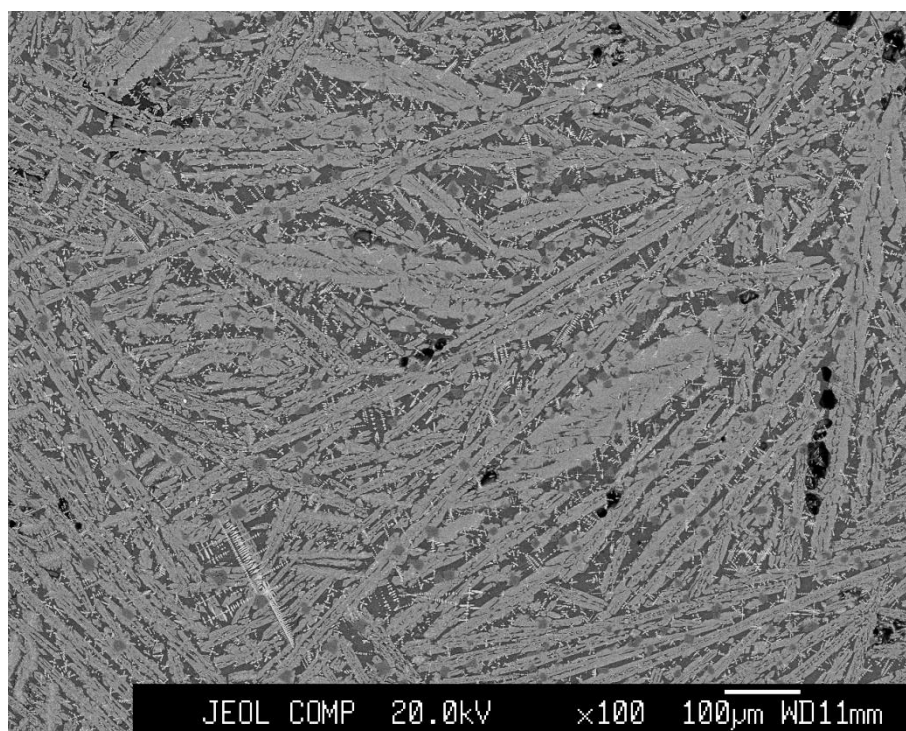


Figure 6.4.25 showing backscatter electron image of slag sample tap slag number 4 from context FLX89 3107, with fine wüstite dendrites, fayalite laths and glassy matrix

| Element                         | FeO   | SiO <sub>2</sub> | P <sub>2</sub> O <sub>5</sub> | Na <sub>2</sub> O | Al <sub>2</sub> O <sub>3</sub> | K <sub>2</sub> O | CaO   | MgO  |
|---------------------------------|-------|------------------|-------------------------------|-------------------|--------------------------------|------------------|-------|------|
| FLX89 3107<br>Tap 4<br>wüstite  | 33.89 | 29.29            | 2.67                          | 2.43              | 15.43                          | 2.63             | 10.31 | 0.09 |
| FLX89 3107<br>Tap 4<br>fayalite | 57.6  | 29.81            | 0.66                          | 0.16              | 1.98                           | 0.28             | 2.00  | 3.64 |
| FLX89 3107<br>Tap 4<br>matrix   | 34.47 | 30.31            | 2.55                          | 2.23              | 18.19                          | 2.41             | 9.76  | 0.15 |

Table 6.4.11 Showing major elements detected in the main mineral phases of tap slag 4 from context FLX89 3107

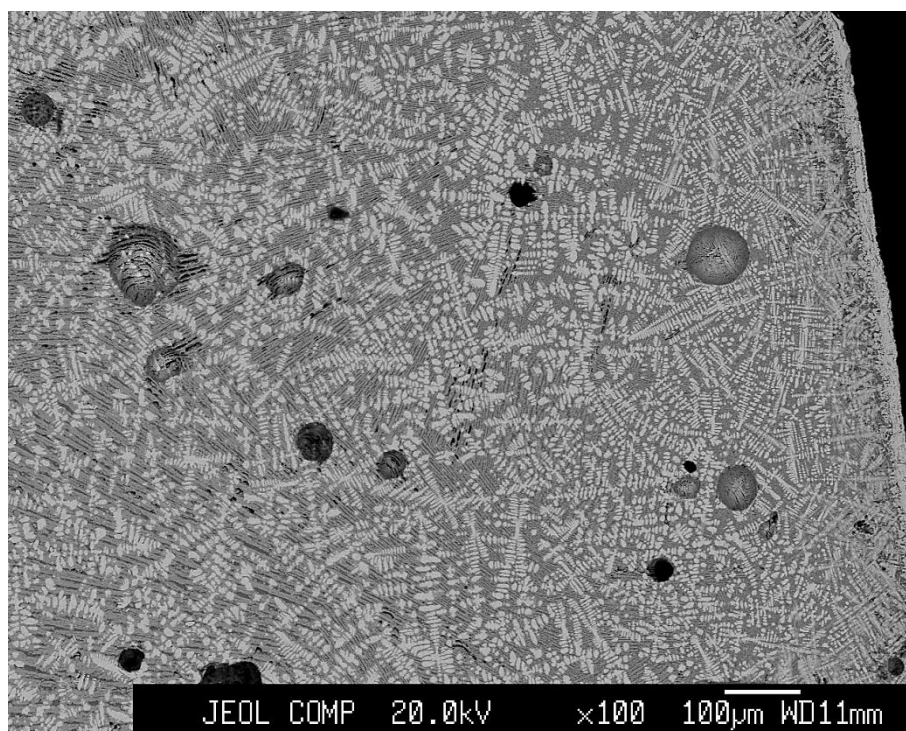


Figure 6.4.26 showing backscatter electron image of slag sample tap slag number 5 from context FLX89 3107, with fine wüstite dendrites, fayalite laths, glassy matrix porosity and magnetite skin (far left).

| Element                         | FeO   | SiO <sub>2</sub> | P <sub>2</sub> O <sub>5</sub> | Na <sub>2</sub> O | MgO  | Al <sub>2</sub> O <sub>3</sub> | K <sub>2</sub> O | CaO   |
|---------------------------------|-------|------------------|-------------------------------|-------------------|------|--------------------------------|------------------|-------|
| FLX89 3107<br>Tap 5<br>wüstite  | 85.89 | 3.30             | 0.19                          | 0.10              | 0.54 | 3.42                           | 0.08             | 0.32  |
| FLX89 3107<br>Tap 5<br>fayalite | 60.30 | 18.09            | 1.81                          | 0.56              | 1.53 | 10.03                          | 0.26             | 2.22  |
| FLX89 3107<br>Tap 5<br>matrix   | 19.23 | 34.50            | 5.76                          | 3.28              | 0.05 | 15.45                          | 4.954            | 16.15 |

Table 6.4.12 Showing major elements detected in the main mineral phases of tap slag 5 from context FLX89 3107





*Figure 6.7.27 showing smelting/furnace slag piece from context FLX89 3107.*

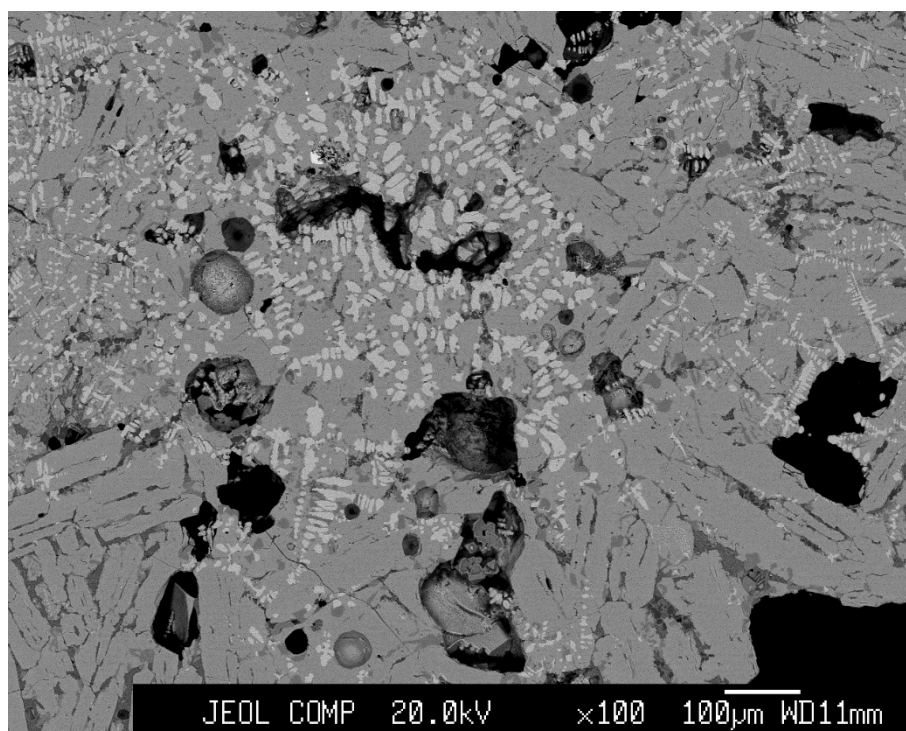


Figure 6.4.28 showing backscatter electron image of furnace slag sample from context FLX89 3107, with fine wüstite dendrites (top right) and globular wüstite (centre), fayalite grains, glassy matrix, and significant porosity.

| Element                                       | FeO   | SiO <sub>2</sub> | P <sub>2</sub> O <sub>5</sub> | Na <sub>2</sub> O | MgO  | Al <sub>2</sub> O <sub>3</sub> | K <sub>2</sub> O | CaO   |
|---|-------|------------------|-------------------------------|-------------------|------|--------------------------------|------------------|-------|
| FLX89 3107<br>Medium furnace<br>slag wüstite  | 90.05 | 0.27             | 0.04                          | BDL               | 0.17 | 2.98                           | 0.021            | 0.04  |
| FLX89 3107<br>Medium furnace<br>slag fayalite | 63.77 | 30.16            | 0.37                          | 0.05              | 2.29 | 0.36                           | 0.021            | 0.56  |
| FLX89 3107<br>Medium furnace<br>slag matrix   | 28.38 | 31.11            | 4.78                          | 3.64              | 0.12 | 16.10                          | 5.32             | 10.29 |

Table 6.4.13 Showing major elements detected in the main mineral phases of the medium furnace slag from context FLX89 3107



*Figure 6.4.29 showing largest furnace slag piece from context FLX89 3107.*

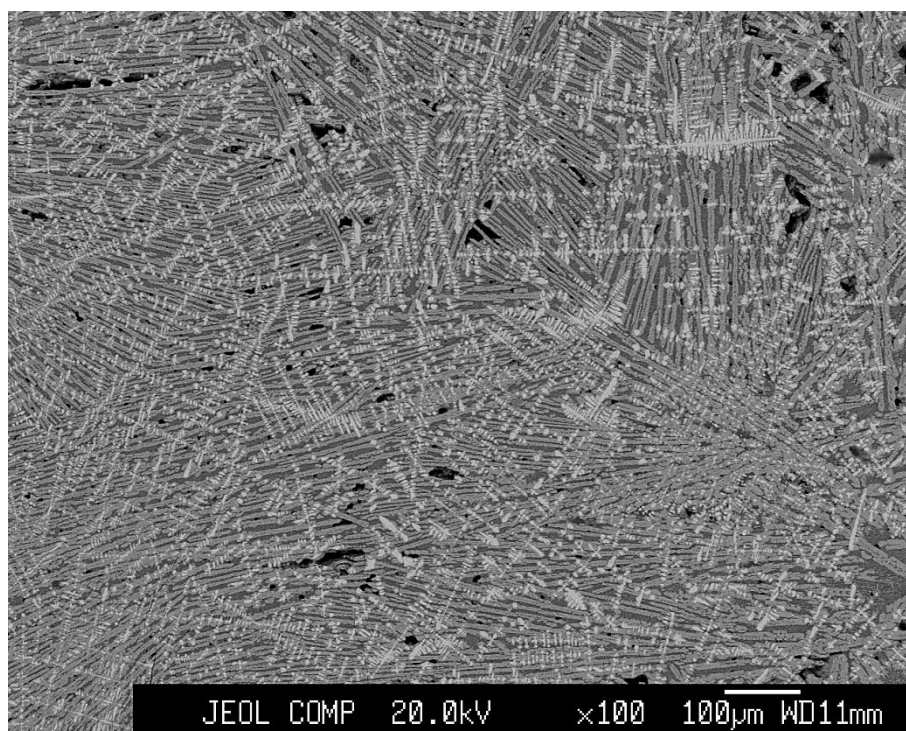


Figure 6.4.30 showing backscatter electron image of large furnace slag sample from context FLX89 3107, with fine wüstite dendrites, fine fayalite laths, glassy matrix.

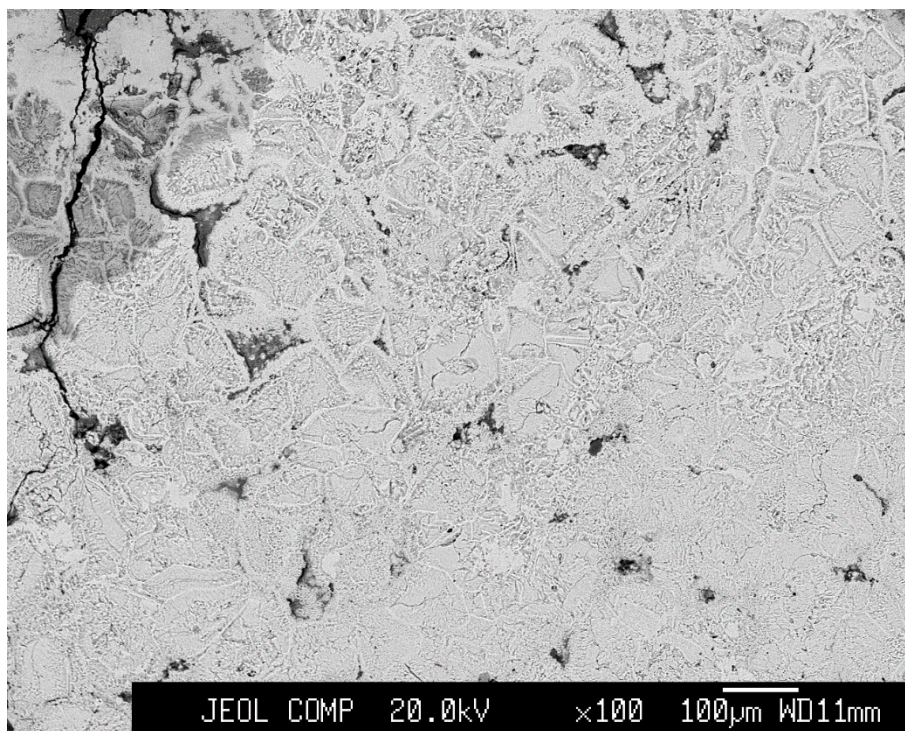
| Element   | FeO   | SiO <sub>2</sub> | P <sub>2</sub> O <sub>5</sub> | Na <sub>2</sub> O | MgO  | Al <sub>2</sub> O <sub>3</sub> | K <sub>2</sub> O | CaO   |
|---|-------|------------------|-------------------------------|-------------------|------|--------------------------------|------------------|-------|
| FLX89 3107<br>Large<br>furnace slag<br>wüstite  | 59.37 | 17.37            | 1.447                         | 0.47              | 1.44 | 11.05                          | 0.71             | 4.81  |
| FLX89 3107<br>Large<br>furnace slag<br>fayalite | 38.60 | 29.24            | 3.23                          | 1.60              | 1.34 | 14.88                          | 2.49             | 9.62  |
| FLX89 3107<br>Large<br>furnace slag<br>matrix   | 21.44 | 38.67            | 1.60                          | 3.89              | 0.37 | 18.37                          | 4.99             | 10.74 |

Table 6.4.14 Showing major elements detected in the main mineral phases of the large furnace slag from context FLX89 3107





*Figure 6.4.31 showing small ore piece from context FLX89 503 14333.*



*Figure 6.4.32 showing backscatter electron image of ore sample from context FLX89 503 14333.*

| Element                     | FeO   | SiO <sub>2</sub> | P <sub>2</sub> O <sub>5</sub> | Al <sub>2</sub> O <sub>3</sub> | CaO  | MnO  |
|-----------------------------|-------|------------------|-------------------------------|--------------------------------|------|------|
| FLX89 803 14333 tech sample | 79.32 | 1.73             | 0.86                          | 0.74                           | 0.52 | 1.06 |

Table 6.4.15 Showing major elements detected within the sample of ore FLX89 503 14333.

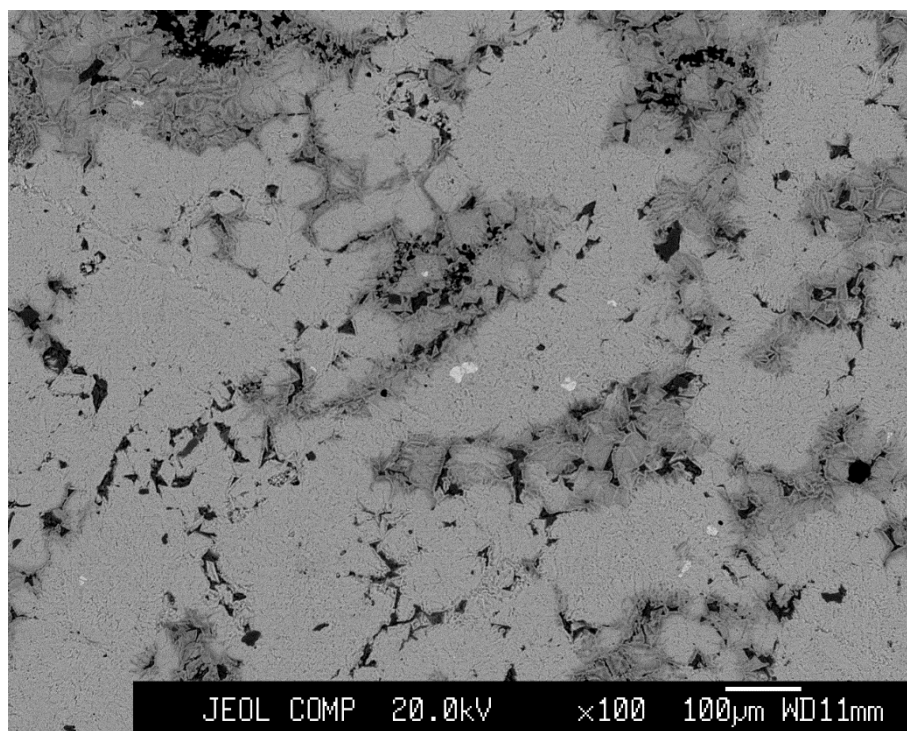


Figure 6.4.33 Showing microstructure of ore sample recovered from context FLX89 800, multiple FeS inclusions (bright white) visible within ore body.

| Element                   | FeO   | SiO <sub>2</sub> | P <sub>2</sub> O <sub>5</sub> | MgO  | Al <sub>2</sub> O <sub>3</sub> | CaO  | MnO  |
|---------------------------|-------|------------------|-------------------------------|------|--------------------------------|------|------|
| FLX89 800 average density | 69.76 | 2.12             | 2.07                          | 0.50 | 0.30                           | 1.09 | 3.30 |

Table 6.4.16 showing main elements detected in the average density ore body of sample recovered from context FLX89 800.

| Element                  | Fe    | S     | O     | P    |
|--------------------------|-------|-------|-------|------|
| FLX89 800 FeS inclusions | 48.98 | 33.82 | 11.59 | 0.48 |

Table 6.4.17 Showing main elements detected in FeS inclusions found in the ore sample recovered from context FLX89 800.

The outstanding question from the original monograph report concerning iron smelting was whether Frodingham Ironstone was being used as a viable ore during the periods of iron smelting at Flixborough. This led to the sampling of several ores in the hope of finding pieces of both which could be imaged during EMPA examination to provide definitive proof alongside compositional data, see figures 6.4.32 and 6.4.33. As discussed later in chapter 7, the use of ironstone as a viable ore during the early medieval period is an aspect of metal production which may prove to be of great significance as it would allow a greater amount of iron to be produced in England without having to rely upon importing raw materials from elsewhere.

# Chapter 7

## Data Interpretation

|     |   |     |
|-----|---|-----|
| 7.1 | <i>Introduction</i>   | 248 |
| 7.2 | <i>East Yorkshire</i>   | 249 |
| 7.3 | <i>Caistor</i>  | 262 |
| 7.4 | <i>Quarrington</i>  | 268 |
| 7.5 | <i>Flixborough</i>  | 276 |
| 7.6 | <i>Possibility for different reaction conditions and ore exploitation</i> | 285 |
| 7.7 | <i>Implications of the demonstration of the production of fresh metal</i> | 287 |
| 7.8 | <i>Overall Synthesis</i>  | 289 |

### 7.1 Introduction

This section addresses the observation and interpretation of the data produced from the chemical analyses of the slag samples. There are several chemical behaviours which have a direct impact upon the composition of the analysed phase, most notably the matrix, and the resultant data which will now be discussed. Previously in chapter 3 the major phases of iron slags have been defined - wüstite, fayalite and the matrix phases. The matrix phase, being the last to form, is where the majority of trace and minor elements are found (Blakelock *et al.* 2009; Paynter 2006), the later formation of this phase results in it being enriched in the trace and minor elements making it more useful and informative for provenance studies (Blakelock *et al.* 2009; Paynter 2006).

Phosphorus is a minor element that can vary in concentration within a sample based on multiple factors. The first of these is the heterogeneous distribution of phosphorus within the ore, a result of natural variability, which can cause some slag to contain a greater proportion of phosphorus. The presence of phosphorus can also be affected by the availability of free oxygen (Godfrey 2007) which will reduce the phosphorus content of the slag by forming volatile  $P_4O_6$ . This has a double effect on the smelt by reducing phosphorus content but also causing a reduced yield of iron due to a less reducing reaction atmosphere. The other significant contributor to the distribution of phosphorus is calcium (Godfrey 2007). Calcium is far more reactive than iron and will preferentially react with



phosphorus to form calcium phosphate, which is stable even at the temperatures reached during iron smelting. If Calcium is present then the proportion of phosphorus detected during analysis of that area of the matrix will be significantly higher than is commonly detected in other areas of the same sample.

The data plots are phase composition averages, calculated from a total of 5 analyses per major phase. They are presented on x-y scatter plots using the FeO:SiO<sub>2</sub> ratio on the x-axis as this ratio is a direct result of the mineral phase being analysed. Wüstite which is almost entirely FeO has an exceptionally high FeO:SiO<sub>2</sub> value, Fayalite has an approximate value of 2 and the matrix phase is found in a wider band between 0 to 1. The reason for the matrix having a wider range of composition in comparison to the other mineral species is because it can contain some wüstite that is less than 1µm in size which is too small to completely avoid during spot analyses, as seen in figure 6.2.23, as well as being a result of varying iron and silica content prior to solidification.

Mixed signal results are also produced due to the behaviour of the electron beam as covered in chapter 4. In cases where this has occurred the FeO:SiO<sub>2</sub> ratio reflects this by being shifted away from the main phase ratios. For example a mixed fayalite-wüstite analysis would produce a FeO:SiO<sub>2</sub> value in excess of 2.5, and be clearly shifted to the right of the other fayalite points which would have values closer to 2.

The y-axis presents the percentage P<sub>2</sub>O<sub>5</sub> content, which as previously stated, is affected by the presence of calcium and the availability of free O<sub>2</sub> within the reaction atmosphere.

## **7.2 East Yorkshire**

### Average compositions

The Foulness Valley slags, while being only a total of eight samples from three sites are considered together as they are assumed to be contemporary with each other due to the shift in occupation locations during the later Roman period away from the Foulness Valley, and the change in activity to ceramic production. The elevated phosphorus content of the majority of the points, in excess of 2.5% P<sub>2</sub>O<sub>5</sub>, demonstrate the result of using a high phosphorus bog ore. The outlier with more than 7% P<sub>2</sub>O<sub>5</sub> is a result of the presence of higher levels of calcium. The fayalite group seen in figure 7.2.4, found at an FeO: SiO<sub>2</sub> value of 2.1, is relatively confined with only one point having a higher phosphorus content. This may have resulted from a phosphorus rich matrix phase being partially analysed below the observable fayalite, although there is no significant shift to the left of the FeO:SiO<sub>2</sub> ratio.

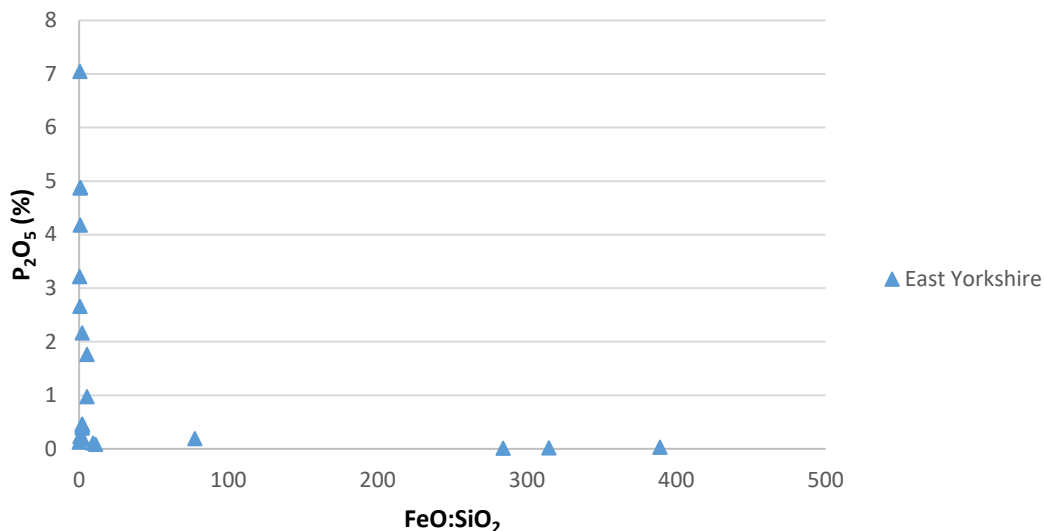


Figure 7.2.1 Complete phase average compositions for East Yorkshire assemblage.

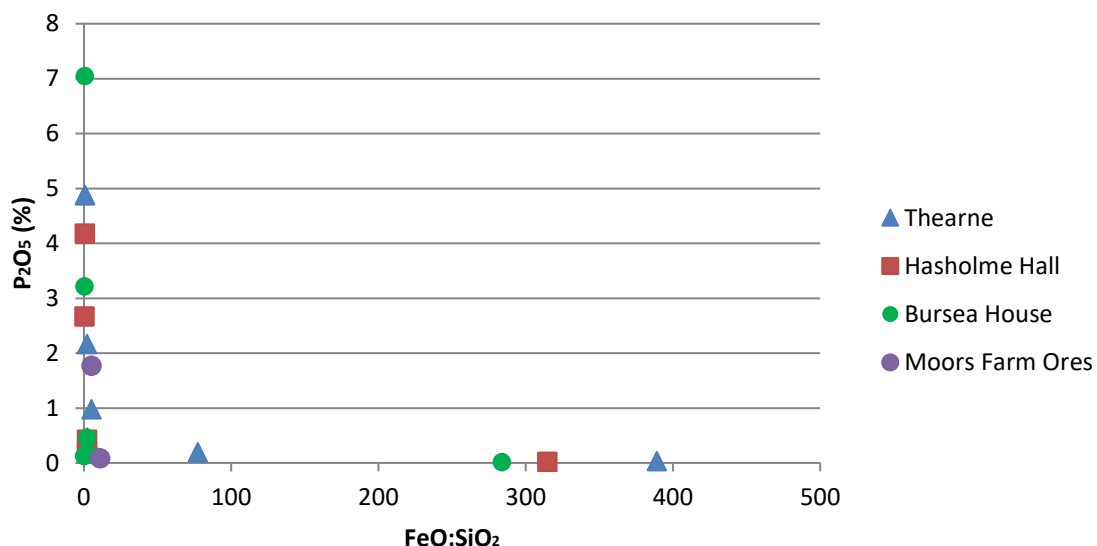


Figure 7.2.2 Complete phase average compositions for East Yorkshire assemblage by site.

The following figures, 7.2.3 and 7.2.4, show the matrix and fayalite phase data more clearly after the removal of the wüstite points. By including the wüstite data on the graphs above, the rest of the data is compressed to as it all has values FeO:SiO<sub>2</sub> of less than 3, making it impossible to properly observe.

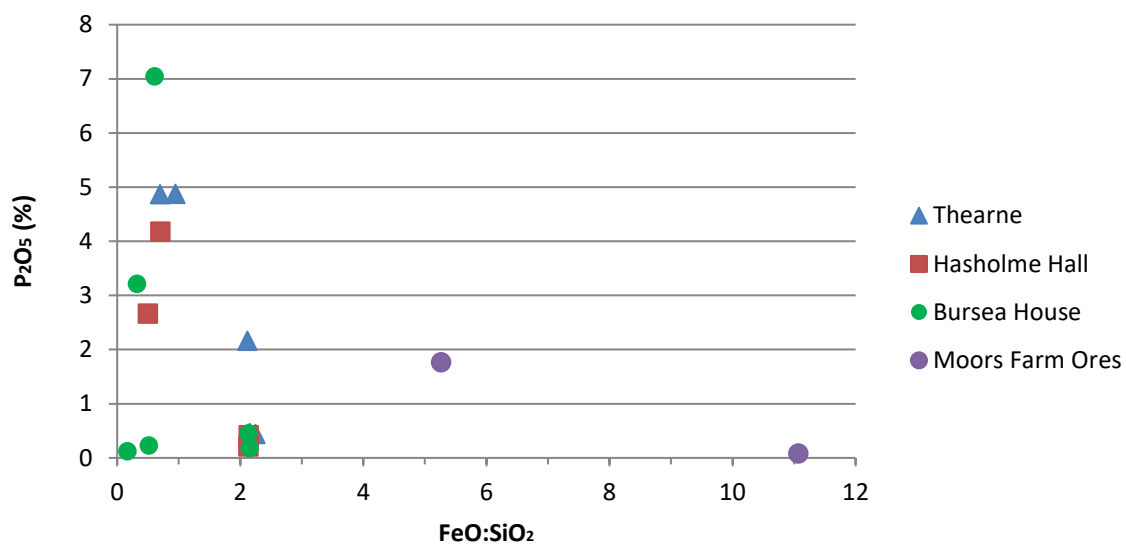


Figure 7.2.3 Matrix and Fayalite phase average compositions by site with ores for comparison.

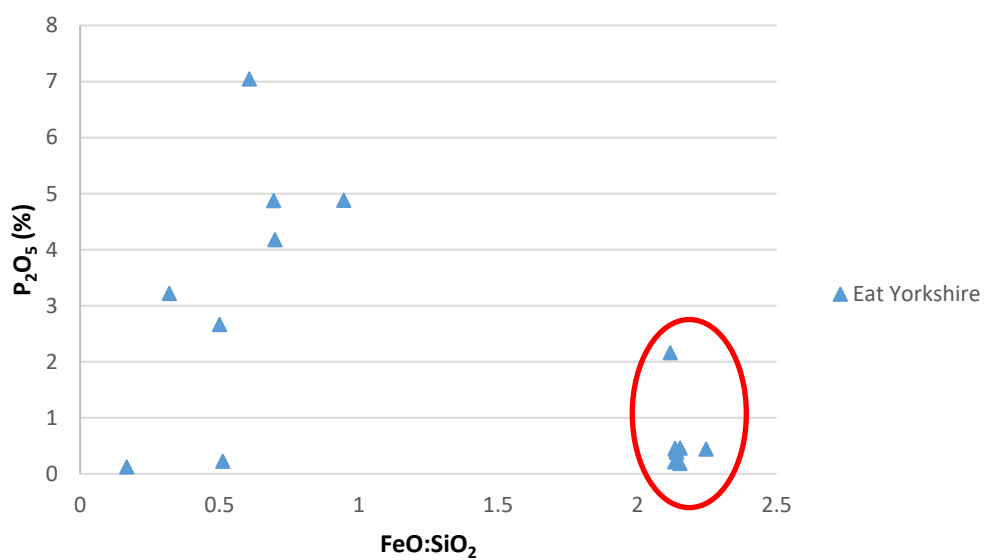
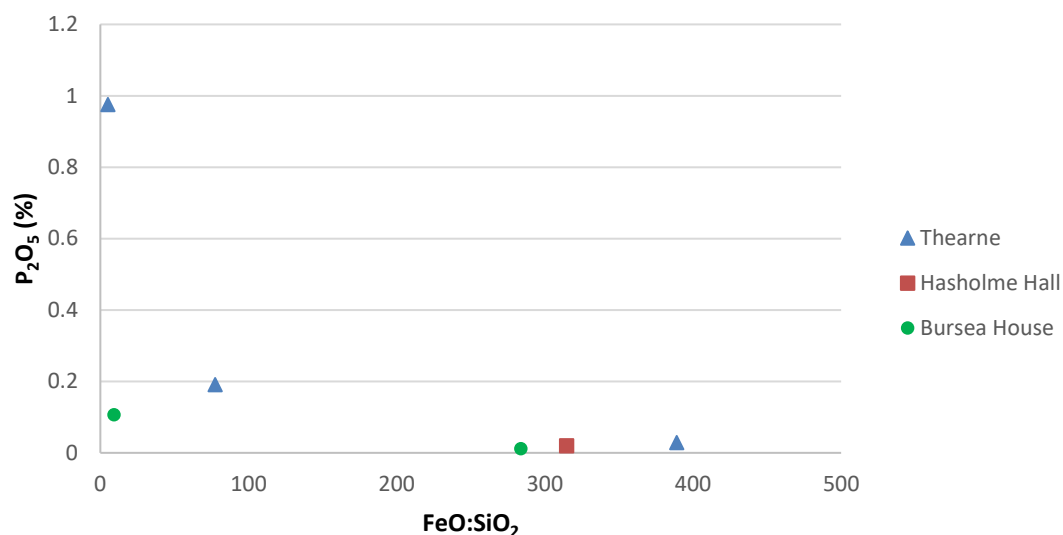


Figure 7.2.4 Fayalite (red circle) and matrix phase average compositions for all East Yorkshire slag samples.



*Figure 7.2.5 Wüstite phase average composition per site.*

The wüstite phase averages clearly show the effect of mixed signal results. The plots from Thearne, Hasholme Hall and Bursea House that plot closely to the X-axis illustrate what good, approximately single phase data produce. While the other 2 plots from Thearne and the single Bursea House plot with FeO:SiO<sub>2</sub> values of less than 100 very clearly illustrate the effects of multi-phase detection during analysis, not only in reduced FeO and increased SiO<sub>2</sub> content – skewing the plots to the left, but also in increased P<sub>2</sub>O<sub>5</sub> content.

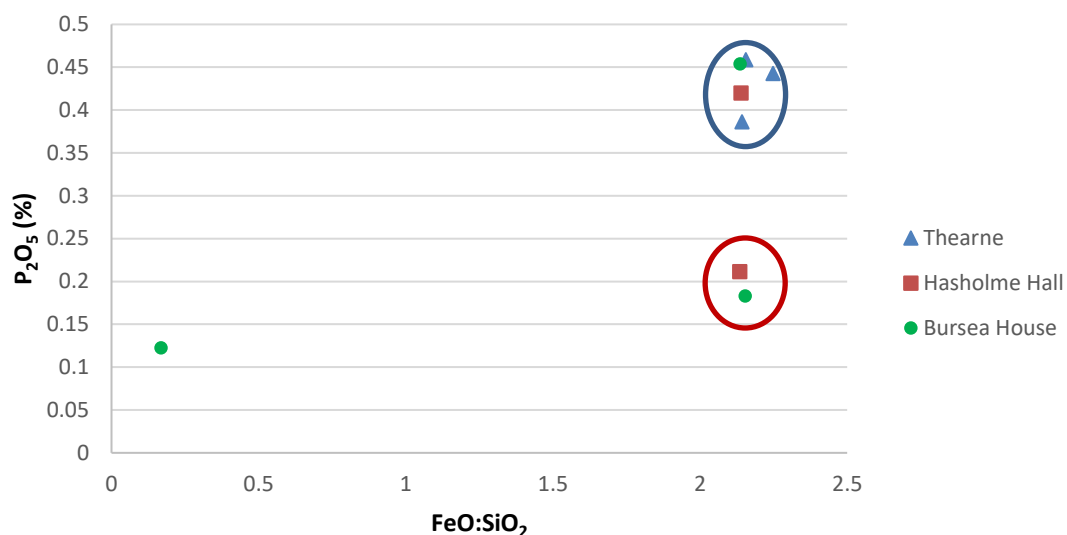


Figure 7.2.6 Fayalite phase average composition per site with higher and lower phosphorus groupings circled in blue and red respectively.

|                              | FeO $\bar{x}$ :SiO <sub>2</sub> $\bar{x}$ | FeO:SiO <sub>2</sub> $\sigma$ | $\sigma/\bar{x}$ | P <sub>2</sub> O <sub>5</sub> $\bar{x}$ | P <sub>2</sub> O <sub>5</sub> $\sigma$ | $\sigma/\bar{x}$ |
|------------------------------|---|-------------------------------|------------------|---|--|------------------|
| Thearne drip1 fayalite       | 2.1546                                    | 0.0256                        | 0.0119           | 0.4588                                  | 0.2592                                 | 0.5650           |
| Thearne drip2 fayalite       | 2.1416                                    | 0.0224                        | 0.0104           | 0.3864                                  | 0.0958                                 | 0.2479           |
| Thearne drip3 fayalite       | 2.2473                                    | 0.0365                        | 0.0162           | 0.4428                                  | 0.1066                                 | 0.2408           |
| Hasholme Hall small fayalite | 2.1392                                    | 0.0328                        | 0.0153           | 0.4198                                  | 0.1569                                 | 0.3738           |
| Hasholme Hall large fayalite | 2.1342                                    | 0.0096                        | 0.0045           | 0.2116                                  | 0.0965                                 | 0.4559           |
| Bursea house smith fayalite  | 2.1526                                    | 0.0054                        | 0.0025           | 0.1830                                  | 0.0619                                 | 0.3382           |
| Bursea House smelt fayalite  | 2.1358                                    | 0.0145                        | 0.0068           | 0.4540                                  | 0.5577                                 | 1.2283           |
| Bursea House green fayalite  | 0.1680                                    | 0.0765                        | 0.4551           | 0.1224                                  | 0.0703                                 | 0.5747           |

Table 7.2.1 showing phase mean compositions, mean phosphorus content, associated standard deviations, and coefficients of variation for the East Yorkshire fayalite data.

The average fayalite phase compositions of the Foulness assemblage plot in 2 distinct groups, see figure 7.2.6 above. The slag from the site of Thearne has a relatively consistent  $P_2O_5$  content between 0.38 – 0.46%, which is also found in a sample from both Bursea House and Hasholme Hall. The group with a lower  $P_2O_5$  content of between 0.18-0.21% is found only at Bursea House and Hasholme Hall. The outlier from Bursea House was produced from a piece of slag which is green in colour and has no visible wüstite. The unique colour of this piece within the entire assemblage is a result of a far greater olivine mineral content which may indicate that it was produced by a different process, or from very different reaction component, than that of the Iron Age slags.

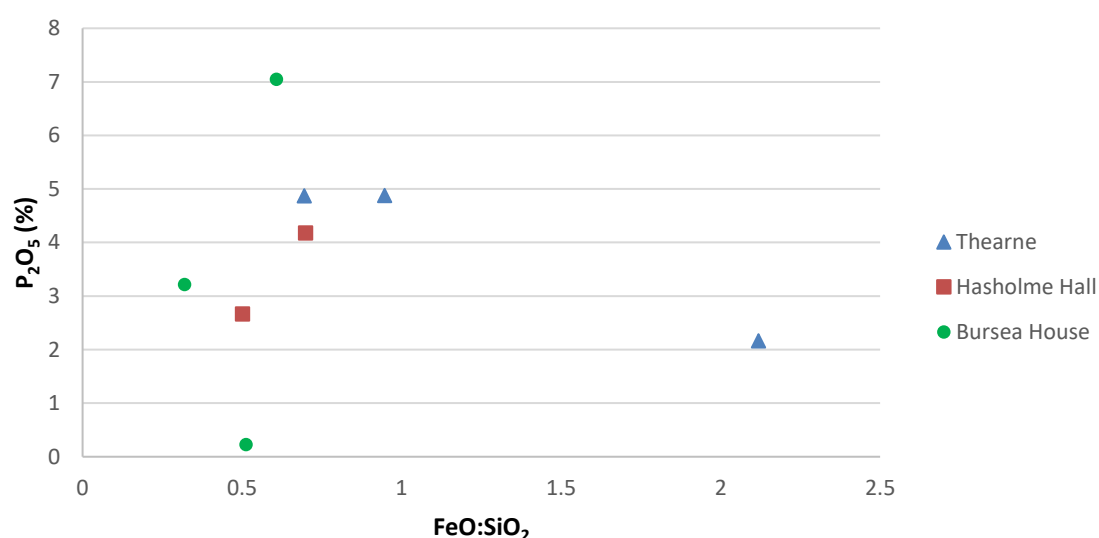


Figure 7.2.7 Matrix phase average composition per site.

|                            | <b>FeO <math>\bar{x}</math>:SiO<sub>2</sub> <math>\bar{x}</math></b> | <b>FeO:SiO<sub>2</sub> <math>\sigma</math></b> | <b><math>\sigma/\bar{x}</math></b> | <b>P<sub>2</sub>O<sub>5</sub> <math>\bar{x}</math></b> | <b>P<sub>2</sub>O<sub>5</sub> <math>\sigma</math></b> | <b><math>\sigma/\bar{x}</math></b> |
|----------------------------|--|--|------------------------------------|--|---|------------------------------------|
| Thearne drip1 matrix       | 2.1190   | 20.6492  | 9.7446                             | 2.1618   | 3.5532  | 1.6436                             |
| Thearne drip2 matrix       | 0.9463   | 0.1239   | 0.1309                             | 4.8760   | 0.5418  | 0.1111                             |
| Thearne drip3 matrix       | 0.6948   | 0.1219   | 0.1755                             | 4.8720   | 0.7181  | 0.1474                             |
| Hasholme Hall small matrix | 0.5009   | 0.1959   | 0.3912                             | 2.6626   | 1.5467  | 0.5809                             |
| Hasholme Hall large matrix | 0.6994   | 0.0451   | 0.0645                             | 4.1780   | 0.2538  | 0.0608                             |
| Burse House smith matrix   | 0.6074   | 0.8575   | 1.4117                             | 7.0446   | 8.6124  | 1.2225                             |
| Burse House smelt matrix   | 0.3199   | 0.5458   | 1.7063                             | 3.2142   | 4.4430  | 1.3823                             |
| Burse House green matrix   | 0.5126   | 5.5899   | 10.9049                            | 0.2268   | 0.0850  | 0.3749                             |

*Table 7.2.2 showing phase mean compositions, mean phosphorus content, associated standard deviations, and coefficients of variation for the East Yorkshire matrix data.*

The average matrix phase compositions show that the majority of iron slag matrix exists within a band of composition between 0.3-1.0 FeO:SiO<sub>2</sub>. The outlier from Thearne with 2.16% P<sub>2</sub>O<sub>5</sub> and an FeO:SiO<sub>2</sub> value of 2.12 is a result of a mixed signal analysis. The phosphorus content detected from the matrix analysed within that set of 5 analyses shows that phosphorus was still present in a significant quantity.

## Raw data plots

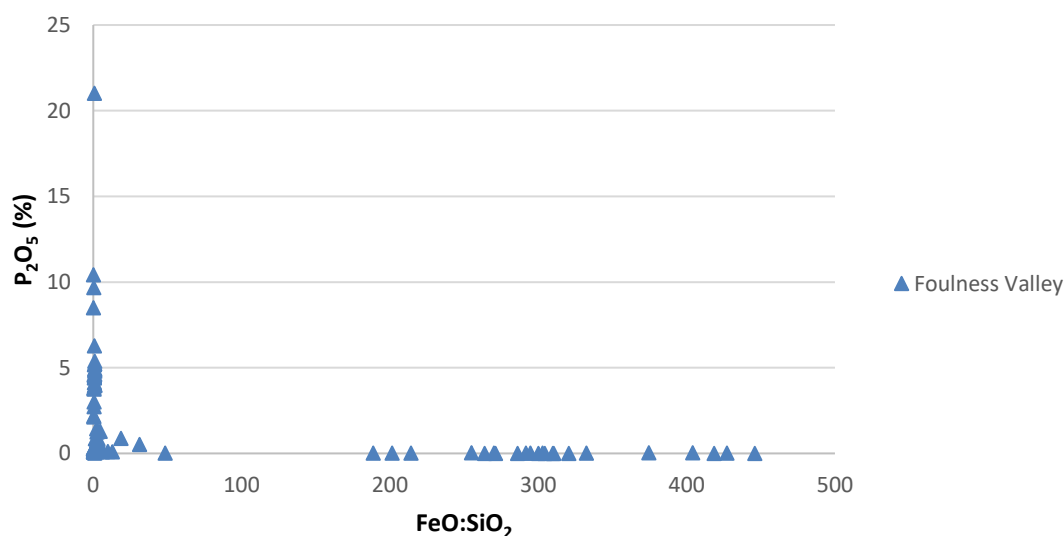


Figure 7.2.8 Complete phase composition analyses for East Yorkshire assemblage.

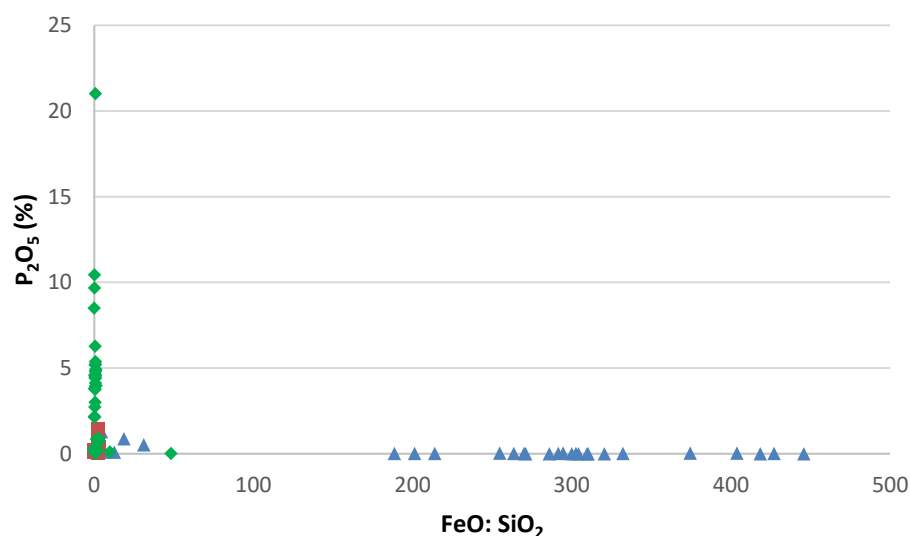


Figure 7.2.9 Complete phase composition analyses for East Yorkshire assemblage by phase.

The complete raw data when divided into the 3 major phases, presented in figure 7.2.9 above, clearly demonstrates that wüstite does not host phosphorus. The range of  $FeO:SiO_2$  values between 188- 446 show that even in analysed areas which appear to be entirely comprised of a single phase, the presence of other phases beneath the surface will alter the overall compositional data. This is particularly apparent with the lower  $FeO:SiO_2$  value wüstite plots, which appear close close to the origin in the above graph . These very low ratio wüstite points are the result of a small quantity of



wüstite being present at the surface of the analysed point with other materials being unobservable beneath. This is further corroborated by the slightly elevated  $P_2O_5$  content observed in two of the three outliers.

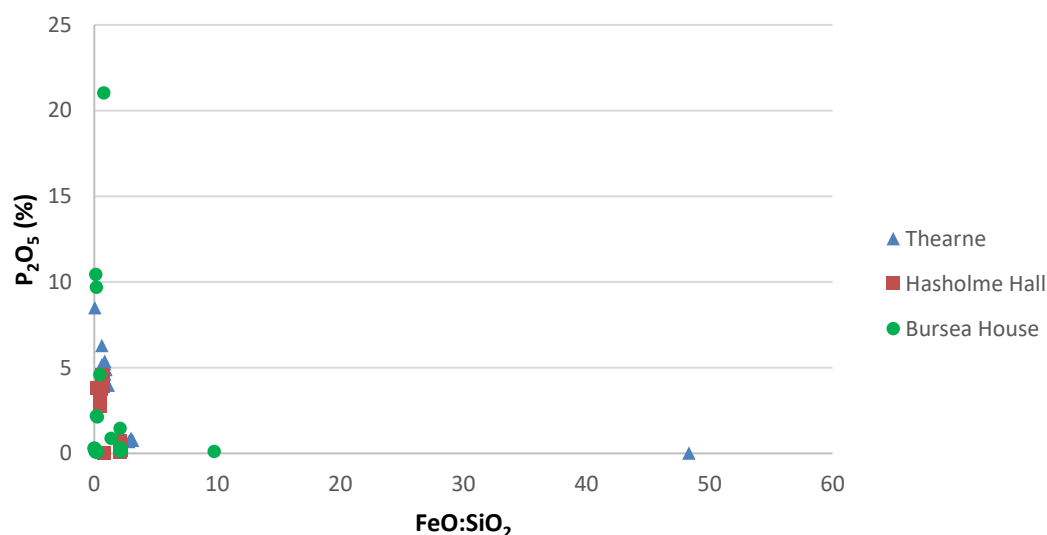


Figure 7.2.10 Complete phase composition analyses of fayalite and matrix phase of East Yorkshire assemblage.

There is also a high value point from Thearne in the fayalite and matrix phase graph above. This is a result of wüstite being present in the analysed volume of the spot beneath the observed surface, skewing the  $FeO:SiO_2$  value to the right, as the ratio value is far greater than the maximum value of approximately 2 which can be generated by a mixed matrix-fayalite result. The matrix points plotting approximately along the y-axis show some significant variation in  $P_2O_5$  content. The Bursea House analyses being the most wide ranging, with values between 0.3-21%. This exceptionally high phosphorus content is a result of the presence of calcium effectively enriching the analysed area in phosphorus to levels far beyond that seen in the rest of the material.

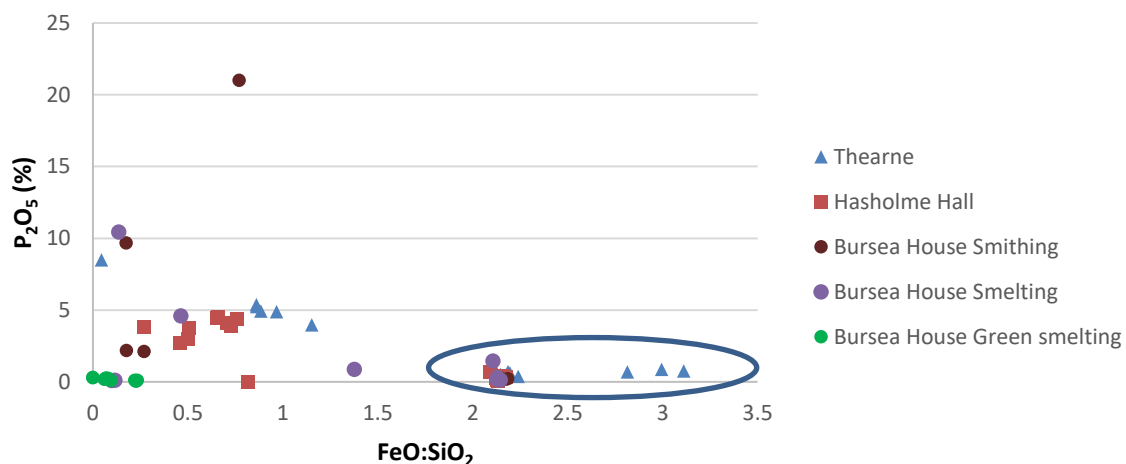


Figure 7.2.11 Complete phase composition analyses of fayalite (circled in blue) and matrix phase of East Yorkshire Assemblage after removal of extreme outliers.

Upon removing the widely dispersed outliers it became apparent that the Bursea House material could also provide further information as that material contained smithing, as well as smelting slag, see figure 6.1.5. The graph above illustrates the complete composition analyses for each site by type of slag analysed. The fayalite group at the approximate FeO:SiO<sub>2</sub> value of 2 contains points from all of the Iron Age smelting and smithing slag, as can be seen in closer detail in figure 7.2.12. The green coloured smelting slag from Bursea House, which by morphology appears to be contemporary with the rest of the assemblage, is again constantly close to the origin, which further suggests that it is not a result of the same smelting process that made the rest of the assemblage.

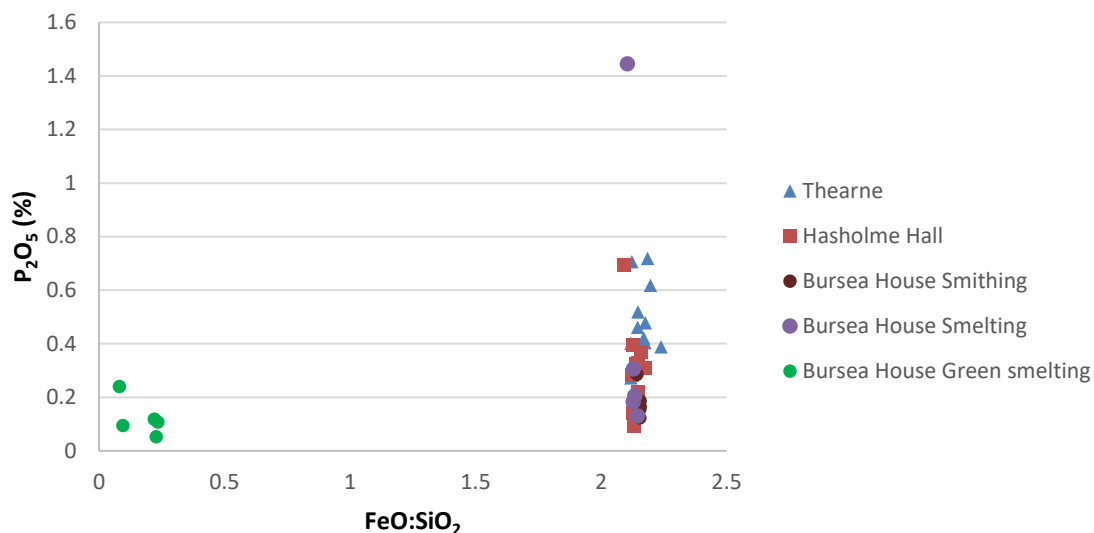
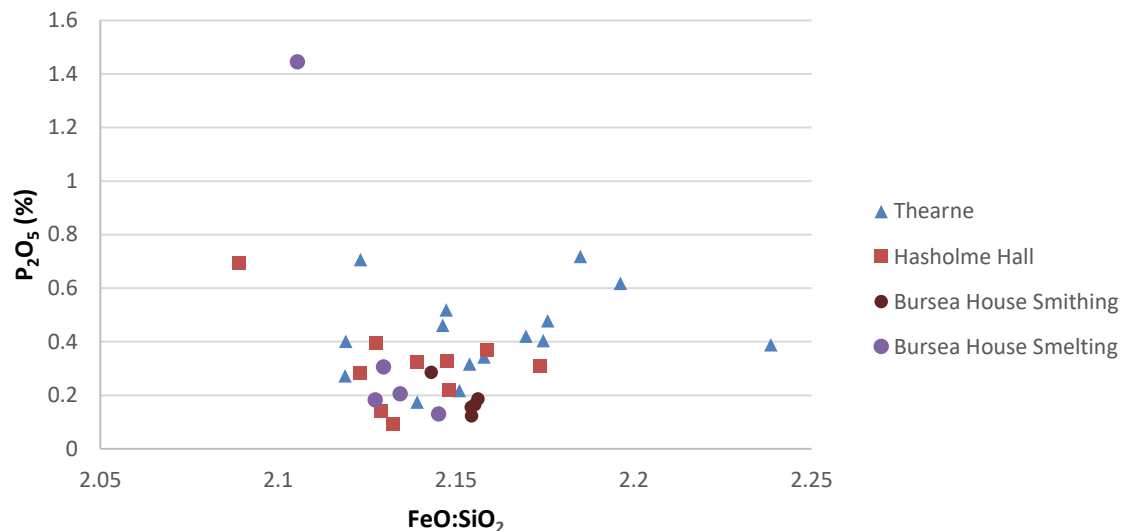


Figure 7.2.12 Complete fayalite phase analyses of East Yorkshire assemblage.

Examining only the fayalite phase of the East Yorkshire assemblage shows that the green coloured slag data plots within the matrix band where the average matrix compositions are found. This is due to a far lower iron content than all of the other material. Such a low iron content, accompanied with the lack of visible wüstite, suggests that this slag was produced from a smelt which included a very large proportion of silica, possibly a significant failure of the furnace lining, skewing the reaction conditions towards the production of fayalite and matrix phases at the expense of free, available wüstite. This would account for the pale green colour of the slag, as it may be seen to be an extreme case of the conditions which produce the recognised pale yellow slag seen in the experimental assemblage in chapter 5.



*Figure 7.2.13 Complete fayalite phase analyses of East Yorkshire assemblage after removal of the green smelting slag.*

With the exclusion of the anomalous green slag, the rest of the fayalite plots show a generally tighter grouping. The outlier from Bursea House containing in excess of 1% more P<sub>2</sub>O<sub>5</sub> than the rest of the analysed points of that sample is again due to the presence of calcium, this also applies to the single point from Hasholme Hall with 0.69% P<sub>2</sub>O<sub>5</sub>. The Thearne material is more varied in composition than the other samples.

This data set forms a useful control set as it demonstrates that high phosphorus ore produces slag which is significantly rich in phosphorus, and that it is found within the matrix phase. The relatively wide spread of the matrix points between 0.16- 0.95 FeO:SiO<sub>2</sub> illustrates the variability in Iron Age smelting when using a material with a variable silica content. As the data from the sites do not group distinctly, in either fayalite (figure 7.2.13) or matrix (figure 7.2.14) analysis it is not possible to identify individual Holmes based upon the chemical composition of the slag.

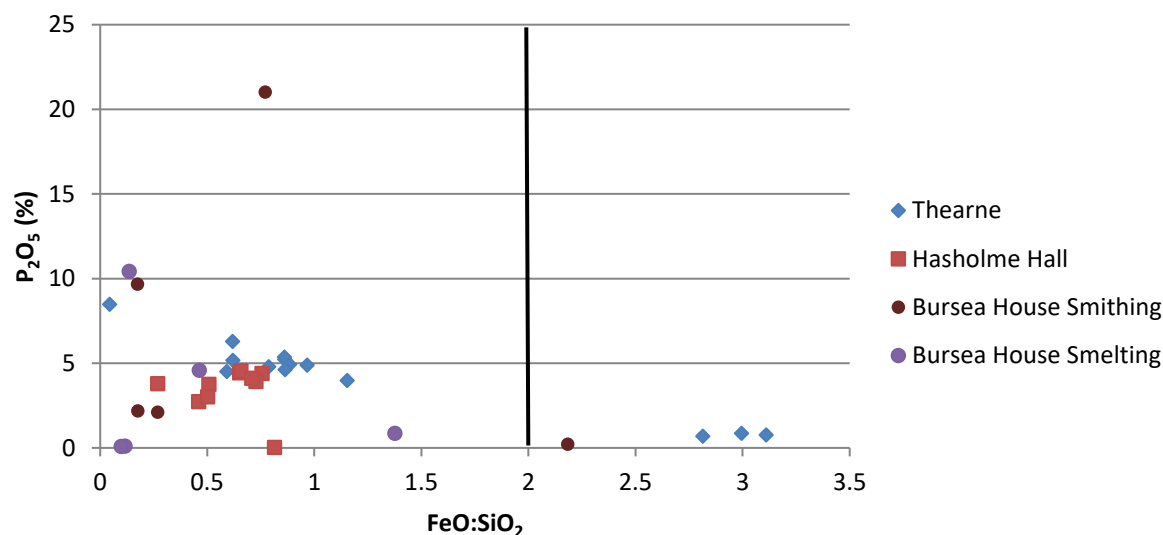


Figure 7.2.14 showing complete matrix data with outlier fayalite rich analyses beyond  $\text{FeO}:\text{SiO}_2$  value of 2 shown by the black line.

The complete matrix data plots reveal some outliers which resulted from the analysis of fayalite and wüstite, namely the individual points to the right of  $\text{FeO}:\text{SiO}_2$  value of 2, highlighted by the line applied to the above figure. These values are the result of fayalite and wüstite being present below the surface of the sample, within the analysed volume as described in chapter 4.

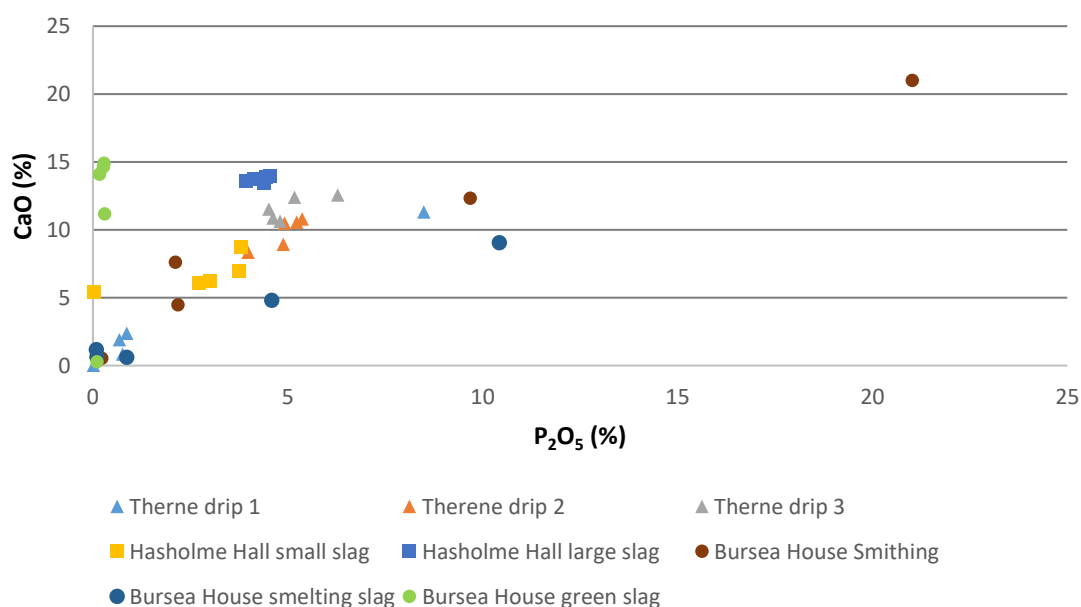


Figure 7.2.15 showing  $\text{P}_2\text{O}_5$  against  $\text{CaO}$  in matrix of analysed East Yorkshire slags.

The trends in  $P_2O_5$  and CaO content shown in figure 7.2.15 demonstrate that phosphorus content increases with the presence of calcium. The most notable variation occurs within the smithing slag, which experiences a greater contribution from fuel ash and the metal being worked. This would explain the very high value outlier and the wide range in phosphorus content. The green slag, contains a significant quantity of calcium, but very little phosphorus in comparison to the rest of the assemblage. Due to the greater reducing atmosphere which generated this material, the phosphorus oxides are reduced and may be lost in waste gasses, or possibly kept within the metallic products, while calcium cannot be reduced by carbon monoxide. This most likely has the effect of depleting the slag of phosphorus, while the calcium oxides remain.

### 7.3 Caistor

#### Average Compositions

The site of Caistor is in close proximity to an estuarine floodplain, as is Flixborough. However the data demonstrate that the slag appears to have been produced from a bedded ore with all of the major points plotting with less than 1%  $P_2O_5$ . The single point at approximately 5%  $P_2O_5$  is a result of the analysed matrix containing 7.7% Calcium.

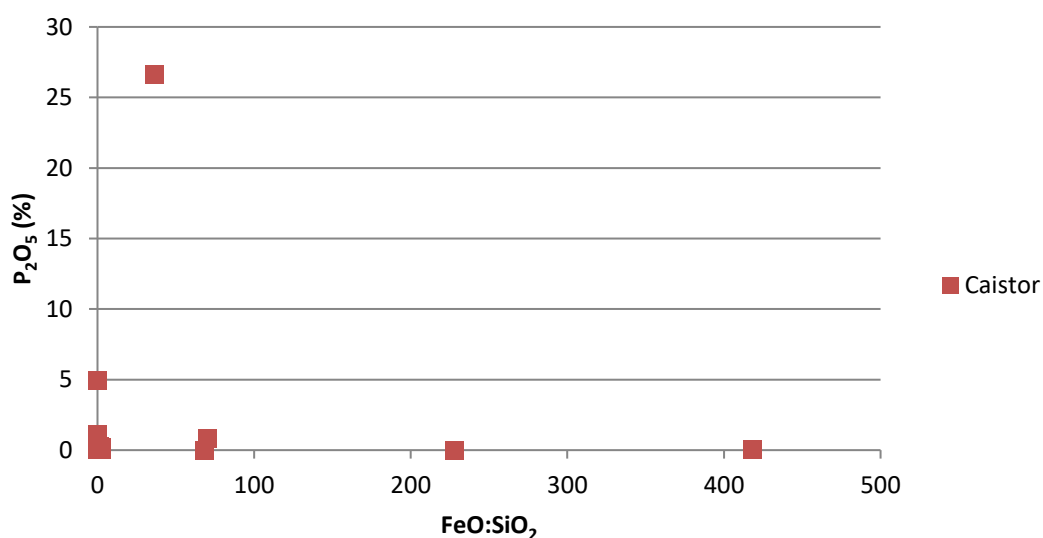


Figure 7.3.1 Complete phase average data for the Caistor assemblage.

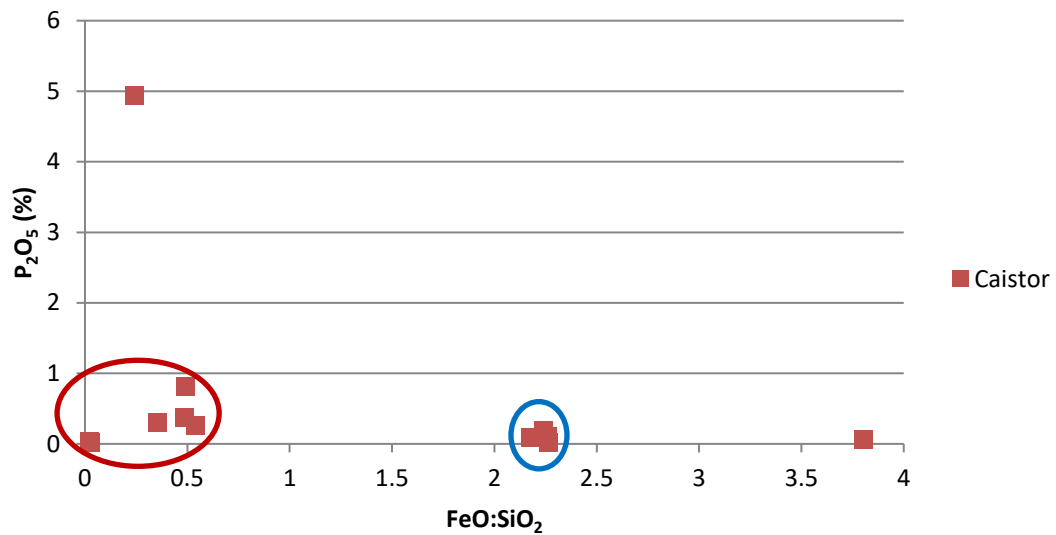


Figure 7.3.2 Complete fayalite, circled in blue, and matrix, circled in red, phase average compositions for Caistor assemblage.

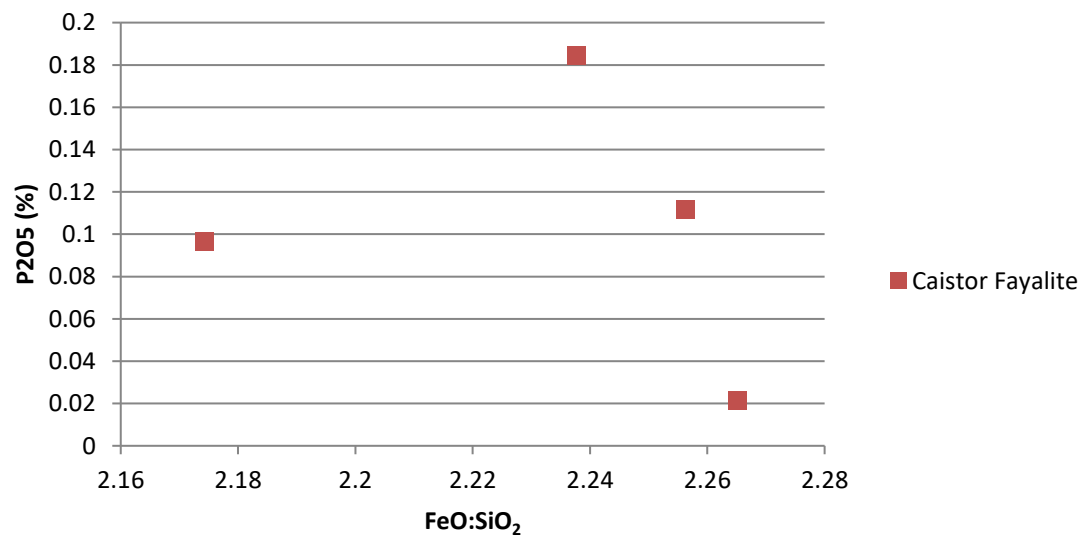


Figure 7.3.3 Fayalite phase average for Caistor assemblage.

|  | $\text{FeO}\bar{X}:\text{SiO}_2\bar{X}$ | $\text{FeO}:\text{SiO}_2 \sigma$ | $\sigma/\bar{X}$ | $\text{P}_2\text{O}_5 \bar{X}$ | $\text{P}_2\text{O}_5 \sigma$ | $\sigma/\bar{X}$ |
|--|---|----------------------------------|------------------|--------------------------------|-------------------------------|------------------|
| CRT09-01 unstratified fayalite             | 2.2378                                  | 0.2553                           | 0.1141           | 0.1844                         | 0.0952                        | 0.5162           |
| CRT09-1017 Fayalite laths                  | 2.1743                                  | 0.0354                           | 0.0163           | 0.0966                         | 0.0332                        | 0.3432           |
| CRT09-09a Potential Fyalite? with dendrite | 0.4856                                  | 0.0729                           | 0.1501           | 0.3740                         | 0.0468                        | 0.1251           |
| CRT09-09a Cored feature low density        | 3.8042                                  | 28.4088                          | 7.4677           | 0.0783                         | 0.0631                        | 0.8065           |
| CRT09-1137.Q6 Fayalite grains              | 2.2563                                  | 0.0252                           | 0.0112           | 0.1118                         | 0.0435                        | 0.3887           |
| CRT09-2008 Large grain/lath                | 2.2652                                  | 0.0189                           | 0.0083           | 0.0216                         | 0.0083                        | 0.3854           |

Table 7.3.1 showing phase mean compositions, mean phosphorus content, associated standard deviations, and coefficients of variation for the Caistor fayalite data.

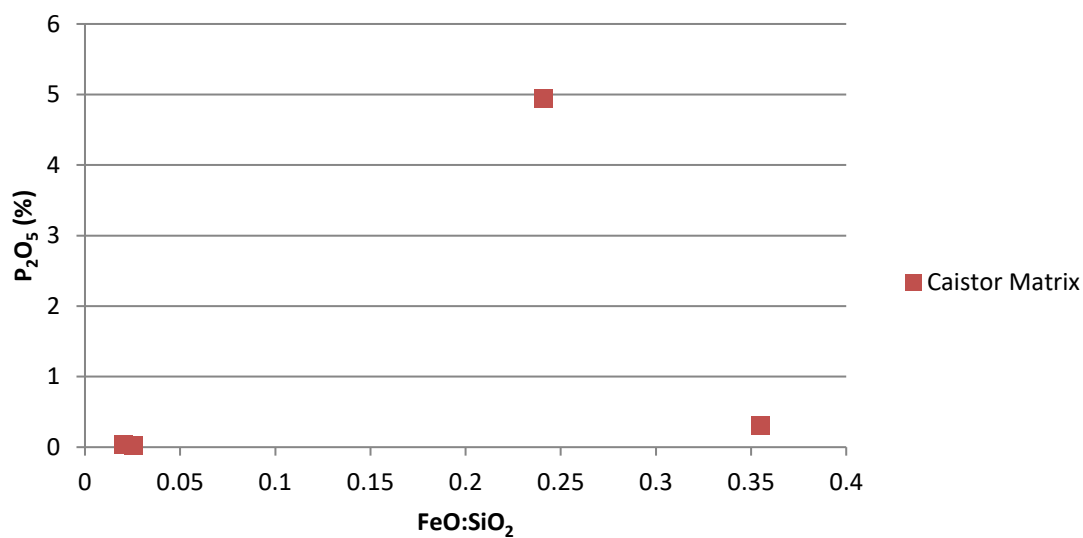


Figure 7.3.4 Matrix phase average for Caistor assemblage.



|                                     | <b>FeO<math>\bar{x}</math>:SiO<math>_2\bar{x}</math></b> | <b>FeO:SiO<math>_2</math> <math>\sigma</math></b> | <b><math>\sigma/\bar{x}</math></b> | <b>P<math>_2</math>O<math>_5</math> <math>\bar{x}</math></b> | <b>P<math>_2</math>O<math>_5</math> <math>\sigma</math></b> | <b><math>\sigma/\bar{x}</math></b> |
|-------------------------------------|--|---|------------------------------------|--|---|------------------------------------|
| CRT09-01 unstratified matrix        | 0.0273   | 13.7440   | 503.3383                           | 26.6120  | 1.0412  | 0.0391                             |
| CRT09-09a Glassy matrix             | 0.0254   | 0.0043  | 0.1707                             | 0.0340   | 0.0077  | 0.2278                             |
| CRT09-1137.Q6 Glassy matrix         | 0.2412   | 0.1074  | 0.4452                             | 4.9440   | 1.2593  | 0.2547                             |
| CRT09-06 Glassy matrix              | 0.0201   | 0.0034  | 0.1686                             | 0.0364   | 0.0173  | 0.4753                             |
| CRT09-06 Slag away from glassy area | 0.5398   | 0.0193  | 0.0357                             | 0.2566   | 0.0319  | 0.1244                             |
| CRT09-2008 Inter grain/lath         | 0.4917   | 0.1039  | 0.2113                             | 0.8170   | 0.1974  | 0.2417                             |
| CRT09-2008 Matrix                   | 0.3553   | 0.1788  | 0.5033                             | 0.3028   | 0.0708  | 0.2337                             |

*Table 7.3.2 showing phase mean compositions, mean phosphorus content, associated standard deviations, and coefficients of variation for the Caistor matrix data.*

The close grouping of the matrix average compositions as well as the fayalite around FeO:SiO $_2$  2.1-2.3 demonstrates a well-controlled, consistent set of reaction conditions. This is also a partial result of the level of control over the raw material used. If a bedded ore was the metal source, then it would be more likely to have a more consistent overall silica content following processing than the bog ores seen in the Foulness assemblage. This would partially explain the close grouping of the phases, although that does not exclude the likelihood of heterogeneous phosphorus and calcium distribution within the raw material. The single point at FeO: SiO $_2$  3.8 is a result of a fayalite and wüstite mixed signal. The increased FeO detected shifted the point the right, away from the mineral fayalite point.

### Raw data plots

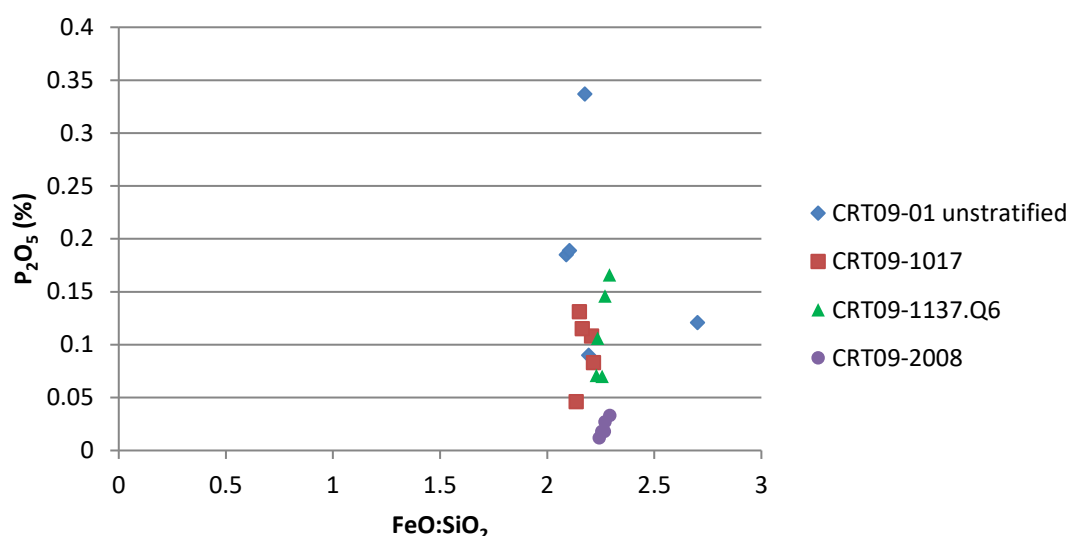


Figure 7.3.5 Complete phase composition analyses of fayalite phase Caistor assemblage.

The individual point compositions of the fayalite phases in the Caistor samples are much more closely grouped than the average composition plots would suggest. This highlights the effect of using averaged data, which can be skewed as a result of outliers and the number of data entries used to calculate the average value. The coefficients of variation indicate that the fayalite analysed in CRT09-01 has a higher P<sub>2</sub>O<sub>5</sub> variability than the identified fayalite in the other samples, which proved to be reliably identified with low  $\sigma/\bar{X}$  values for FeO:SiO<sub>2</sub>. In contrast, the cored features in sample CRT09-09a are far more variable in terms of P<sub>2</sub>O<sub>5</sub> content with a  $\sigma/\bar{X}$  value of 0.8065 and a FeO:SiO<sub>2</sub> value of 7.4677 which indicates that the analyses detected very wide ranging compositions.

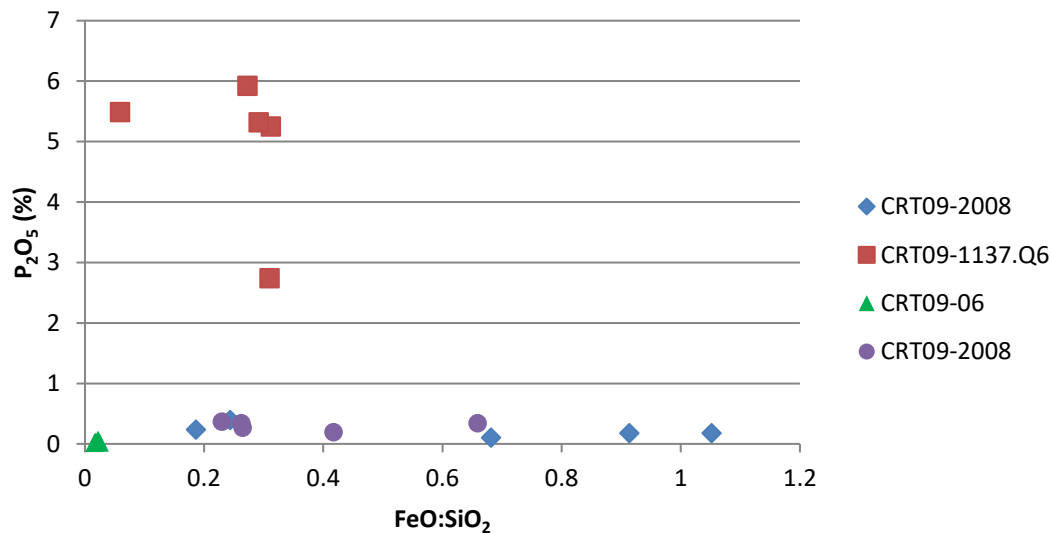


Figure 7.3.6 Complete phase composition analyses of matrix phase Caistor assemblage.

The complete matrix data shown in figure 7.3.6 above shows that one sample contained far more phosphorus than the others. This is partially due to the presence of calcium in the analysed areas, but is also a reflection of the heterogeneous nature of the iron ore in use.

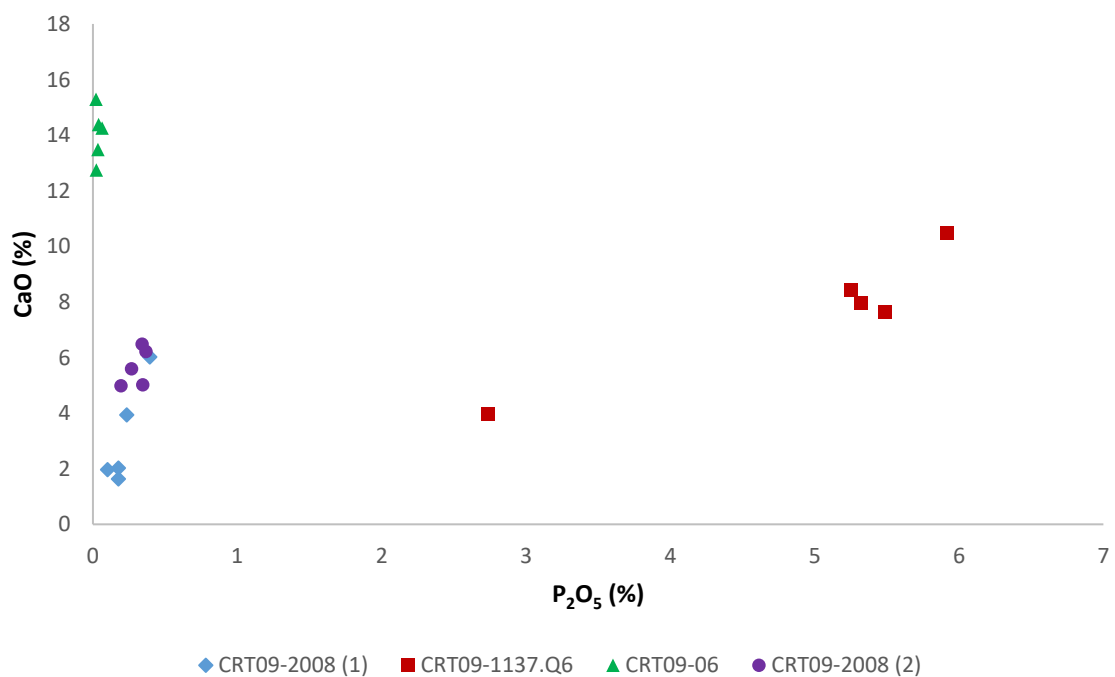


Figure 7.3.7 showing  $P_2O_5$  against  $CaO$  in matrix of analysed Caistor slags.

The trends in  $P_2O_5$  and  $CaO$  content shown in figure 7.3.7 demonstrate that the sampling 1137.Q6 has elevated phosphorus levels and greater calcium content than both of the samples from CRT09-2008. It

is interesting that the sample CRT09-06 shows a similar behaviour, both in terms of  $\text{FeO}:\text{SiO}_2$  and  $\text{CaO}$  relationships compared to  $\text{P}_2\text{O}_5$  content as the green slag from Bursea House.

## 7.4 Quarrington

### Average Compositions

The Quarrington data does not suggest the use of a high phosphorus bog ore. All except one of the matrix points contain less than 1%  $\text{P}_2\text{O}_5$ . The outlier is a result of the presence of approximately 5% calcium, which preferentially reacts with phosphorus to form calcium phosphate. The overall data demonstrates that the overall control of the silica content was not as exacting as in the previous Roman smelting, with the remaining matrix material containing a far wider range of silica values.

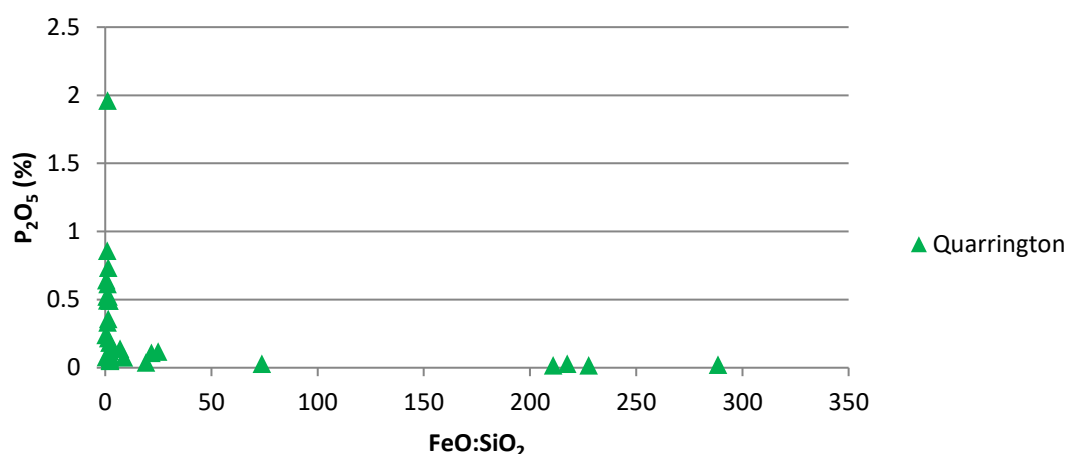


Figure 7.4.1 Complete phase average compositions for Quarrington assemblage.

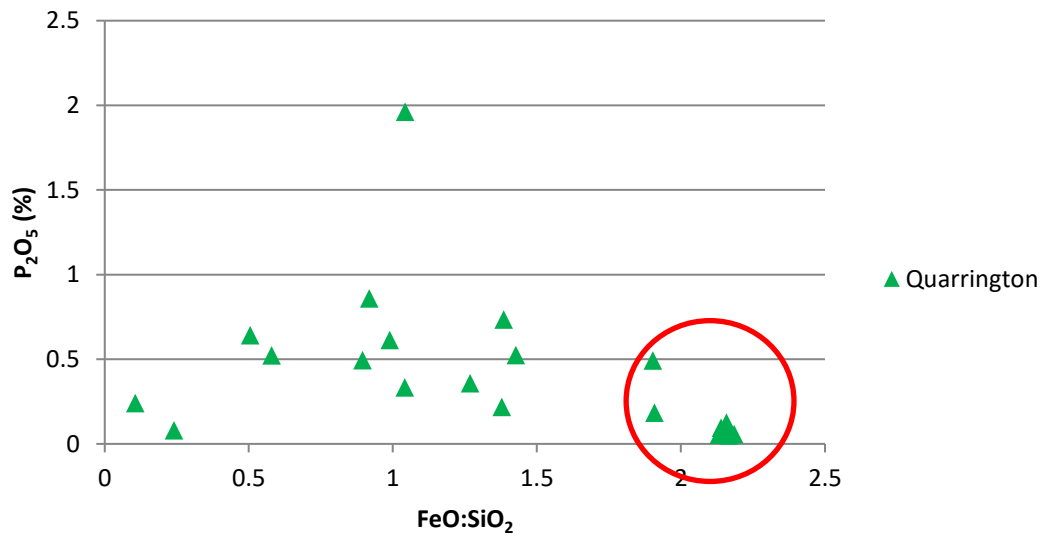


Figure 7.4.2 Complete fayalite (circled in red) and matrix phase average compositions for Quarrington assemblage.

|                              | <b>FeO <math>\bar{x}</math>:SiO<sub>2</sub> <math>\bar{x}</math></b> | <b>FeO:SiO<sub>2</sub> <math>\sigma</math></b> | <b><math>\sigma/\bar{x}</math></b> | <b>P<sub>2</sub>O<sub>5</sub> <math>\bar{x}</math></b> | <b>P<sub>2</sub>O<sub>5</sub> <math>\sigma</math></b> | <b><math>\sigma/\bar{x}</math></b> |
|------------------------------|--|--|------------------------------------|--|---|------------------------------------|
| QCH93 024 tap 1<br>fayalite  | 2.1318   | 0.0382   | 0.0179                             | 0.0542   | 0.0115  | 0.2129                             |
| QCH93 024 tap 2<br>fayalite  | 2.1852   | 0.0151   | 0.0069                             | 0.0586   | 0.0232  | 0.3963                             |
| QCH93 024 tap 3<br>fayalite  | 2.1618   | 0.0305   | 0.0141                             | 0.0938   | 0.0234  | 0.2500                             |
| QCH93 024 tap 4<br>fayalite  | 2.1398   | 0.9550   | 0.4463                             | 0.0948   | 0.0395  | 0.4169                             |
| QCH93 024 tap 5<br>fayalite  | 2.1658   | 0.0291   | 0.0134                             | 0.0502   | 0.0216  | 0.4308                             |
| QCH93 1389 tap 1<br>fayalite | 1.3786   | 0.0574   | 0.0417                             | 0.2180   | 0.0167  | 0.0767                             |
| QCH93 1389 tap 2<br>fayalite | 1.9025   | 0.1274   | 0.0670                             | 0.4934   | 0.1938  | 0.3928                             |
| QCH93 1389 tap 3<br>fayalite | 1.4274   | 0.3290   | 0.2305                             | 0.5244   | 0.1479  | 0.2821                             |
| QCH93 1389 plate<br>fayalite | 1.9086   | 0.2089   | 0.1095                             | 0.1844   | 0.0611  | 0.3312                             |
| QCH93 + fayalite             | 2.1588   | 0.0922   | 0.0427                             | 0.1250   | 0.0335  | 0.2680                             |
| QCH93 +R fayalite            | 2.1589   | 0.0195   | 0.0090                             | 0.0734   | 0.0091  | 0.1243                             |

*Table 7.4.1 showing phase mean compositions, mean phosphorus content, associated standard deviations, and coefficients of variation for the Quarrington fayalite data.*

|                            | <b>FeO <math>\bar{x}</math>:SiO<sub>2</sub> <math>\bar{x}</math></b> | <b>FeO:SiO<sub>2</sub> <math>\sigma</math></b> | <b><math>\sigma/\bar{x}</math></b> | <b>P<sub>2</sub>O<sub>5</sub> <math>\bar{x}</math></b> | <b>P<sub>2</sub>O<sub>5</sub> <math>\sigma</math></b> | <b><math>\sigma/\bar{x}</math></b> |
|----------------------------|--|--|------------------------------------|--|---|------------------------------------|
| QCH93 024 tap<br>1 matrix  | 0.5056   | 0.2152   | 0.4257                             | 0.6424   | 0.1247  | 0.1941                             |
| QCH93 024 tap<br>2 matrix  | 1.0412   | 0.3226   | 0.3099                             | 0.3338   | 0.0529  | 0.1586                             |
| QCH93 024 tap<br>3 matrix  | 0.2407   | 0.3724   | 1.5469                             | 0.0804   | 0.0596  | 0.7419                             |
| QCH93 024 tap<br>4 matrix  | 0.9900   | 0.2175   | 0.2197                             | 0.6146   | 0.0905  | 0.1472                             |
| QCH93 024 tap<br>5 matrix  | 0.8950   | 0.1357   | 0.1516                             | 0.4942   | 0.0546  | 0.1106                             |
| QCH93 1389 tap<br>1 matrix | 0.5799   | 0.5996   | 1.0339                             | 0.5233   | 0.4611  | 0.8811                             |
| QCH93 1389 tap<br>2 matrix | 1.0425   | 0.3092   | 0.2966                             | 1.9613   | 1.0767  | 0.5490                             |
| QCH93 1389 tap<br>3 matrix | 1.3847   | 1.2471   | 0.9006                             | 0.7338   | 0.2463  | 0.3357                             |
| QCH93 1389<br>plate matrix | 0.9186   | 0.6428   | 0.6997                             | 0.8596   | 0.3747  | 0.4359                             |
| QCH93 + matrix             | 0.1063   | 0.1087   | 1.0228                             | 0.2420   | 0.2464  | 1.0181                             |
| QCH93 +R<br>matrix         | 1.2683   | 0.6011   | 0.4739                             | 0.3582   | 0.2095  | 0.5847                             |

*Table 7.4.2 showing phase mean compositions, mean phosphorus content, associated standard deviations, and coefficients of variation for the Quarrington matrix data.*

The phase average plots for Quarrington show a very tight grouping, circled in red in figure 7.4.2 above, at a FeO:SiO<sub>2</sub> value of 2.1 with 2 outlier points at values of approximately 1.9. The wider scatter of points at values of less than 1.5 represents the matrix average values.

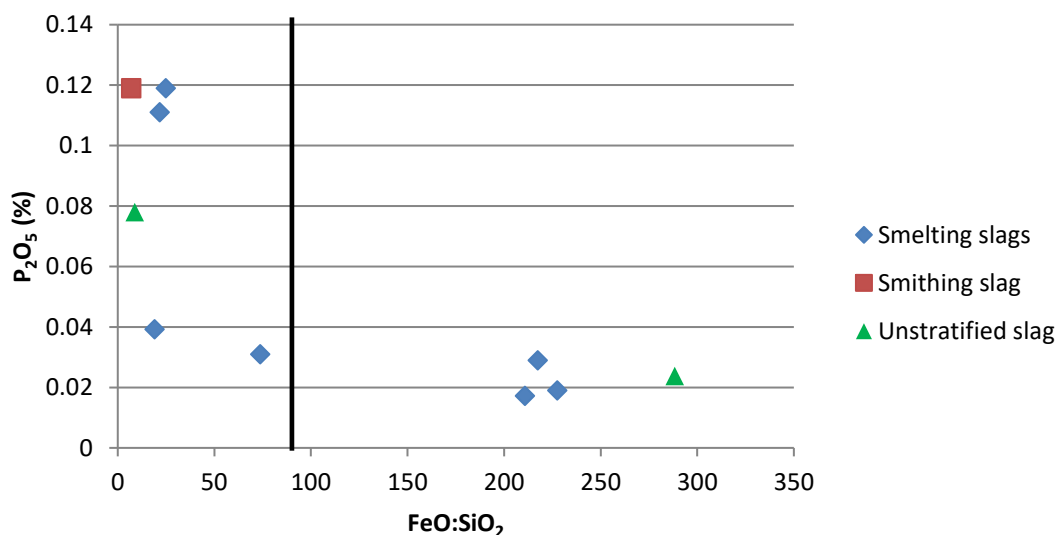


Figure 7.4.3 Wüstite phase average compositions for the Quarrington assemblage.

The wüstite average compositions show some mixed signal responses, left of the black line, where a large proportion of matrix was analysed. None of the points have an FeO:SiO<sub>2</sub> value in excess of 300, which as seen in the Foulness assemblage data is associated with an FeO content greater than 80%. This is more common amongst wüstite analyses because of the significantly higher atomic weight of wüstite in comparison to the other phases. If any matrix phase is beneath the wüstite it is not visible during electron microscopy, whereas wüstite can be seen within areas that are comprised mostly of the matrix phase.



## Raw data plots

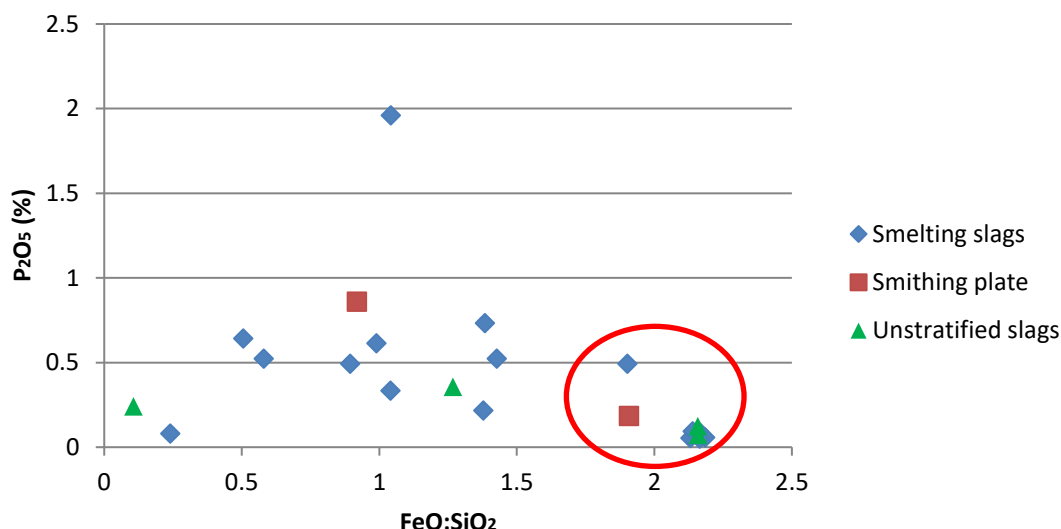


Figure 7.4.4 Complete fayalite (red circle) and matrix phase average compositions for the Quarrington assemblage by sample type.

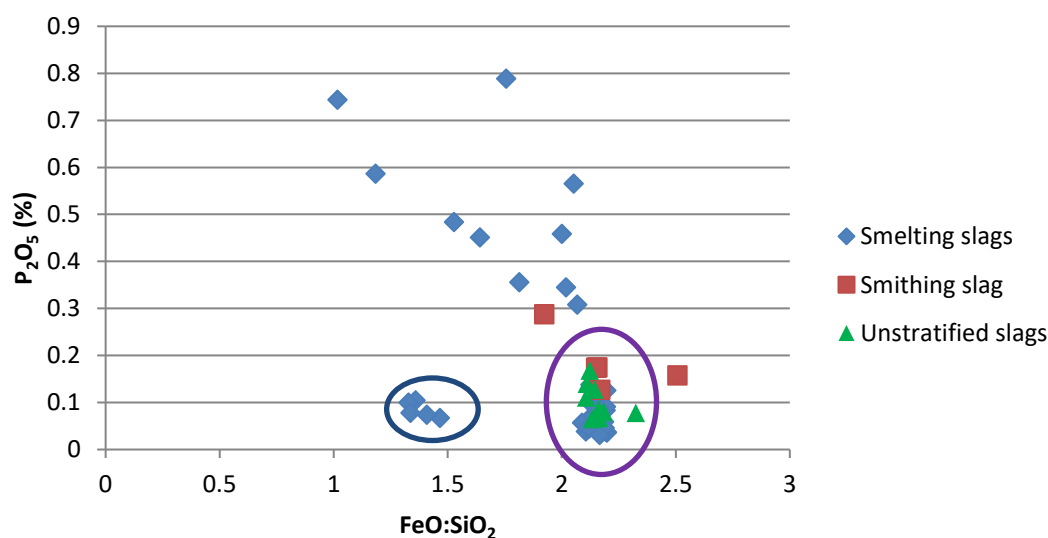


Figure 7.4.5 Complete fayalite data for the analysed Quarrington assemblage.

Within the raw fayalite data for Quarrington above (figure 7.4.5) there appear to be three distinct groupings of points within the stratified smelting slags (blue diamonds). The main group, which plots in the same region as the unstratified smelting slags and two of the smithing slag points, circled in purple, conform to the recognised composition of fayalite with an  $FeO:SiO_2$  value of approximately 2. The second group, which appears between 1.35-1.46 circled in blue, and has a similar  $P_2O_5$  content to the main group would appear to be the result of analysing a small portion of matrix along with the fayalite, only slightly increasing the presence of  $SiO_2$ , without a major increase in  $P_2O_5$ . The third group, with a far larger scatter all contain  $P_2O_5$  in excess of 0.3%.

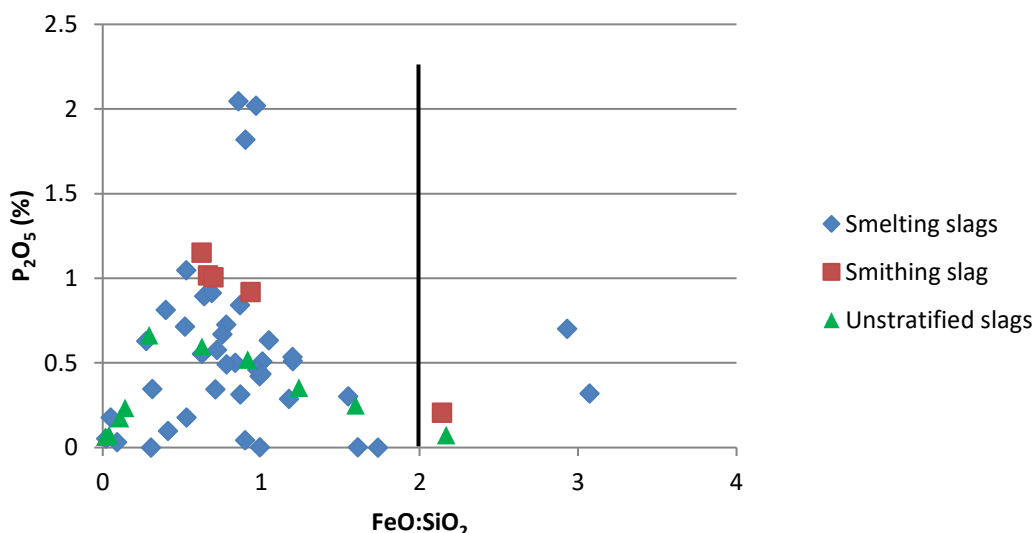
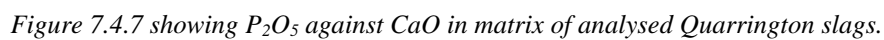


Figure 7.4.6 Complete matrix data for the analysed Quarrington assemblage, showing the fayalite composition limit (black vertical line) at an FeO:SiO<sub>2</sub> value of 2.

The complete matrix data illustrates that the smelting material is more varied in phosphorus content than the smithing slag. This is to be expected as the smelting slag is produced in a far larger volume, from a more variable material than the slag formed during smithing. It is notable that 4 of the 5 smithing points contained phosphorus in levels which plot close to the upper limit of the main cloud of smelting points at a P<sub>2</sub>O<sub>5</sub> content of approximately 1%, excluding the 3 points with greater P<sub>2</sub>O<sub>5</sub> contents. This would suggest that the slag was produced from a material relatively rich in phosphorus, as smithing slag can only derive the iron required to form slag from the surface of the worked metal. This also results in smithing slag containing greater levels of minor elements in comparison to smelting slag as the reaction conditions do not allow for the same amount of loss to the atmosphere. Thus the P<sub>2</sub>O<sub>5</sub> content of smithing slag is more even more closely related to the material being worked than a smelting slag is to its ore.

The unstratified smelting slags fall within the main cloud of data, while the smithing slag appears to have been formed from the forging of material richer in phosphorus, which may have originated from the smelting on site. The low phosphorus contents of less than 1% seen in all but 4 smelting slag analyses, taken with the remains of what are presumed to be processed ore remains, would suggest the use of a bedded ore sourced from the limestone ridge rather than a high phosphorus bog ore.



275

## 7.5 Flixborough

### Average Compositions

Flixborough is unique amongst the assemblages examined in this study as it contains material from two different periods of production. During these two periods it is suggested in the original literature that different ore was used, with bog ore being exploited during the earlier 8<sup>th</sup>-century phase of iron production and the beginning of experimental use of Frodingham Ironstone in the later 10<sup>th</sup>-century (Starley 1999). Hypothetically, if the smelting conditions were the same at both time periods then the plotted points would separate based on phosphorus content, with the data from the earlier phase plotting higher on the y-axis due to the higher phosphorus content of bog ore. As can be seen from the graph below, this is not entirely the case.

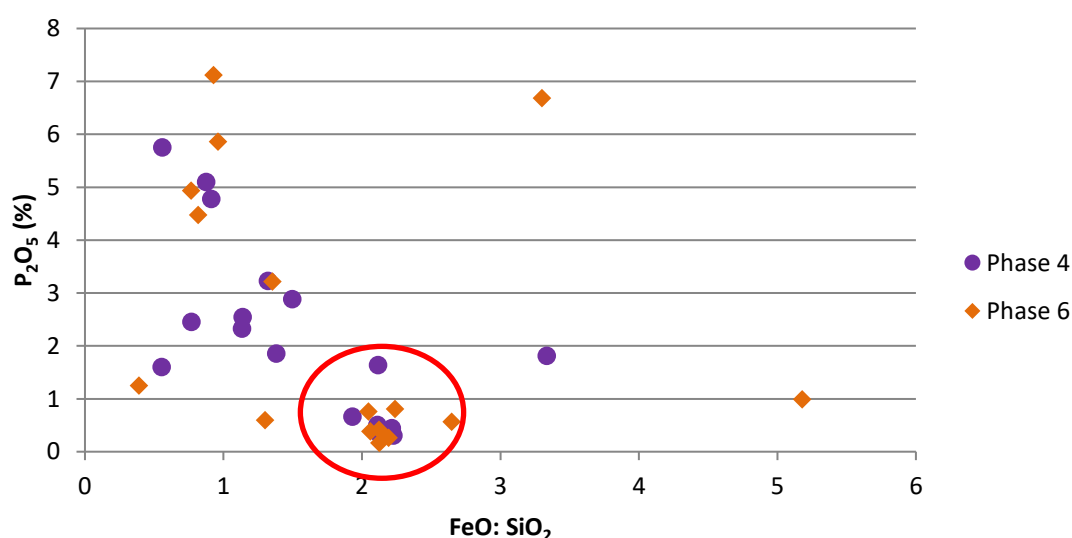


Figure 7.5.1 Phase average for 8<sup>th</sup>-century and 10<sup>th</sup>-century fayalite, circled in red, and matrix to the left of that group.

|   | <b>FeO <math>\bar{x}</math>:SiO<sub>2</sub> <math>\bar{x}</math></b> | <b>FeO:SiO<sub>2</sub> <math>\sigma</math></b> | <b><math>\sigma/\bar{x}</math></b> | <b>P<sub>2</sub>O<sub>5</sub> <math>\bar{x}</math></b> | <b>P<sub>2</sub>O<sub>5</sub> <math>\sigma</math></b> | <b><math>\sigma/\bar{x}</math></b> |
|---|--|--|------------------------------------|--|---|------------------------------------|
| FLX89 51 small tap fayalite             | 2.1106   | 0.0192   | 0.0091                             | 0.5054   | 0.1946  | 0.3850                             |
| FLX89 51 large tap fayalite             | 2.2272   | 0.2224   | 0.0999                             | 0.3096   | 0.0963  | 0.3111                             |
| FLX89 3256 5286 fayalite                | 2.2149   | 0.0243   | 0.0110                             | 0.4474   | 0.1204  | 0.2691                             |
| FLX89 3107 Tap slag 1 fayalite          | 2.1161   | 5.4353   | 2.5685                             | 1.6406   | 0.7023  | 0.4281                             |
| FLX89 3107 Tap slag 2 fayalite          | 1.4971   | 0.9015   | 0.6022                             | 2.8828   | 0.7454  | 0.2586                             |
| FLX89 3107 Tap slag 4 fayalite          | 1.9320   | 0.1089   | 0.0564                             | 0.6624   | 0.3509  | 0.5297                             |
| FLX89 3107 Tap slag 5 fayalite          | 3.3333   | 5.9213   | 1.7764                             | 1.8120   | 1.7225  | 0.9506                             |
| FLX89 3107 Medium furnace slag fayalite | 2.1145   | 0.0365   | 0.0173                             | 0.3660   | 0.1360  | 0.3716                             |
| FLX89 3107 Large furnace slag fayalite  | 1.3201   | 1.1290   | 0.8552                             | 3.2324   | 1.3250  | 0.4099                             |

*Table 7.5.1 showing phase mean compositions, mean phosphorus content, associated standard deviations, and coefficients of variation for 8<sup>th</sup>-century Flixborough fayalite data.*

|                               | <b>FeO <math>\bar{x}</math>:SiO<sub>2</sub> <math>\bar{x}</math></b> | <b>FeO:SiO<sub>2</sub> <math>\sigma</math></b> | <b><math>\sigma/\bar{x}</math></b> | <b>P<sub>2</sub>O<sub>5</sub> <math>\bar{x}</math></b> | <b>P<sub>2</sub>O<sub>5</sub> <math>\sigma</math></b> | <b><math>\sigma/\bar{x}</math></b> |
|-------------------------------|--|--|------------------------------------|--|---|------------------------------------|
| FLX89 2176 a<br>fayalite      | 2.1249   | 0.0304   | 0.0143                             | 0.1673   | 0.1057  | 0.6320                             |
| FLX89 2176 b<br>fayalite      | 2.1221   | 0.0193   | 0.0091                             | 0.4160   | 0.1850  | 0.4446                             |
| FLX89 1427<br>fayalite        | 2.0610   | 0.0228   | 0.0111                             | 0.3886   | 0.0948  | 0.2440                             |
| FLX89 4 2823<br>fayalite      | 1.2989   | 0.7029   | 0.5411                             | 0.6004   | 0.3643  | 0.6068                             |
| FLX98 10393<br>10449 fayalite | 2.0463   | 0.0353   | 0.0172                             | 0.7630   | 0.1217  | 0.1595                             |
| FLX89 2024<br>fayalite        | 2.2394   | 0.0203   | 0.0091                             | 0.8070   | 0.2242  | 0.2778                             |
| FLX89 664<br>fayalite         | 2.1912   | 0.9796   | 0.4471                             | 0.2633   | 0.0981  | 0.3725                             |
| FLX89 10384<br>10846 fayalite | 2.6475   | 20.8813  | 7.8872                             | 0.5672   | 0.4566  | 0.8051                             |

*Table 7.5.2 showing phase mean compositions, mean phosphorus content, associated standard deviations, and coefficients of variation for 10<sup>th</sup>-century Flixborough fayalite data.*

|  | FeO $\bar{x}$ :SiO <sub>2</sub> $\bar{x}$ | FeO:SiO <sub>2</sub> $\sigma$ | $\sigma/\bar{x}$ | P <sub>2</sub> O <sub>5</sub> $\bar{x}$ | P <sub>2</sub> O <sub>5</sub> $\sigma$ | $\sigma/\bar{x}$ |
|--|---|-------------------------------|------------------|---|--|------------------|
| FLX89 51<br>small tap<br>matrix                | 62.6789                                   | 38.9656                       | 0.6217           | 0.0223                                  | 0.0142                                 | 0.6338           |
| FLX89 51<br>large tap<br>matrix                | 0.7687                                    | 0.5981                        | 0.7781           | 2.4532                                  | 1.5225                                 | 0.6206           |
| FLX89 3256<br>5286 matrix                      | 0.8758                                    | 0.2430                        | 0.2775           | 5.1000                                  | 0.6153                                 | 0.1206           |
| FLX89 3107<br>Tap slag 1<br>matrix             | 1.3801                                    | 0.2585                        | 0.1873           | 1.8580                                  | 0.4275                                 | 0.2301           |
| FLX89 3107<br>Tap slag 2<br>matrix             | 1.1327                                    | 0.3155                        | 0.2786           | 2.3276                                  | 1.3196                                 | 0.5669           |
| FLX89 3107<br>Tap slag 4<br>matrix             | 1.1372                                    | 1.3583                        | 1.1945           | 2.5452                                  | 0.8289                                 | 0.3257           |
| FLX89 3107<br>Tap slag5<br>matrix              | 0.5575                                    | 0.1005                        | 0.1803           | 5.7550                                  | 3.3665                                 | 0.5850           |
| FLX89 3107<br>Medium<br>furnace slag<br>matrix | 0.9122                                    | 2.7775                        | 3.0450           | 4.7812                                  | 4.6174                                 | 0.9657           |
| FLX89 3107<br>Large furnace<br>slag matrix     | 0.5545                                    | 0.3549                        | 0.6400           | 1.6025                                  | 1.5850                                 | 0.9891           |

*Table 7.5.3 showing phase mean compositions, mean phosphorus content, associated standard deviations, and coefficients of variation for 8<sup>th</sup>-century Flixborough matrix data.*

|                             | <b>FeO <math>\bar{x}</math>:SiO<sub>2</sub> <math>\bar{x}</math></b> | <b>FeO:SiO<sub>2</sub> <math>\sigma</math></b> | <b><math>\sigma/\bar{x}</math></b> | <b>P<sub>2</sub>O<sub>5</sub> <math>\bar{x}</math></b> | <b>P<sub>2</sub>O<sub>5</sub> <math>\sigma</math></b> | <b><math>\sigma/\bar{x}</math></b> |
|-----------------------------|--|--|------------------------------------|--|---|------------------------------------|
| FLX89 2176 a<br>matrix      | 0.8179   | 0.0543   | 0.0664                             | 4.4780   | 0.1946  | 0.043                              |
| FLX89 2176 b<br>matrix      | 0.9605   | 0.0864   | 0.0899                             | 5.8600   | 1.1304  | 0.193                              |
| FLX89 1427<br>matrix        | 0.9284   | 0.0478   | 0.0515                             | 7.1200   | 0.9703  | 0.136                              |
| FLX89 4 2823<br>matrix      | 0.3883   | 0.0747   | 0.1923                             | 1.2538   | 0.1123  | 0.089                              |
| FLX98 10393<br>10449 matrix | 1.3536   | 40.0435  | 29.583                             | 3.2182   | 3.3267  | 1.034                              |
| FLX89 2024<br>matrix        | 5.1794   | 91.4898  | 17.664                             | 0.9938   | 0.8314  | 0.836                              |
| FLX89 664<br>matrix         | 0.7663   | 0.0920   | 0.1201                             | 4.9360   | 0.6070  | 0.123                              |
| FLX89 10384<br>10846 matrix | 3.2997   | 119.8070                                       | 36.309                             | 6.6854   | 13.9525   | 2.087                              |

*Table 7.5.4 showing phase mean compositions, mean phosphorus content, associated standard deviations, and coefficients of variation for 10<sup>th</sup> century Flixborough matrix data.*



### Raw data plots

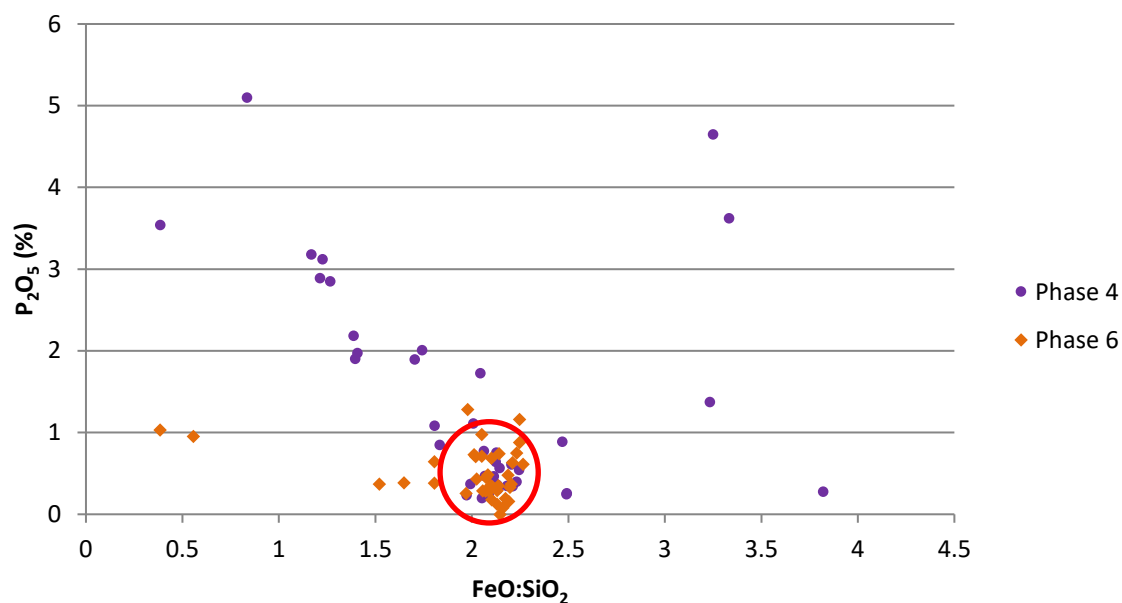


*Figure 7.5.2 Fayalite plots with the exclusion of two major outliers from the 8<sup>th</sup>-century, highlighting the major grouping of points from Phases 4 and 6 at  $FeO:SiO_2$  values of 2 and showing clear outliers in the phase 4 data.*

The fayalite analyses show that the 8<sup>th</sup>-century slags produced many mixed signal responses. Although there was a group that plotted in the same region as the clear group of 10<sup>th</sup> century fayalite points that is circled in red. The overlapping of the fayalite group from both phases demonstrates a similar chemical composition with near identical phosphorus levels.

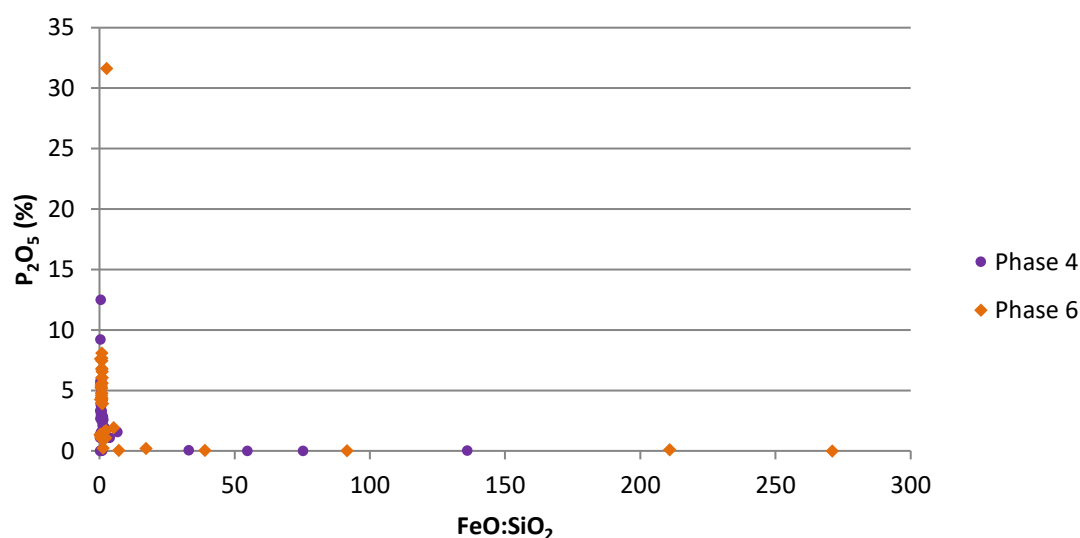


Figure 7.5.3 Matrix phase analyses including mixed signal outliers.

The mixed signal outliers along the x-axis seen in the complete matrix analysis are the result of wüstite being detected within the analysed volume of the outlying points. The extreme outliers along the y-axis, namely the points from the 8<sup>th</sup>-century material with 9.19% and 12.48%  $P_2O_5$  and the single point from the 10<sup>th</sup>-century slags with in excess of 30%  $P_2O_5$ , are caused by the presence of elevated levels of calcium in comparison to the rest of the assemblage. This demonstrates the variable composition of smelting slags even across a cross sectional area of less than 2cm<sup>2</sup>.

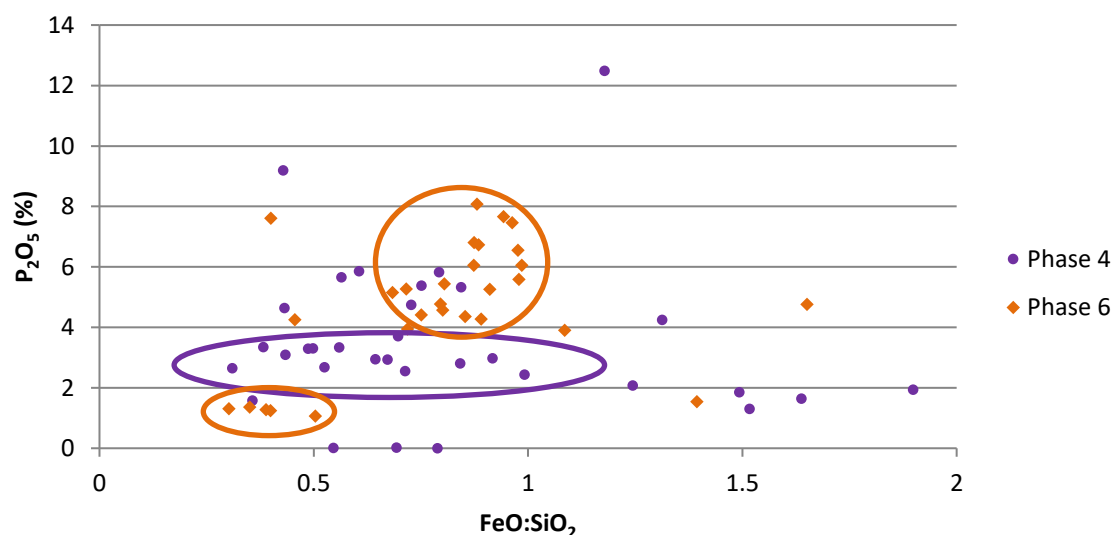


Figure 7.5.4 Matrix phase analyses excluding mixed signal outliers with  $FeO:SiO_2 > 2$ .

Upon closer examination of the matrix results, after the removal of the outliers, there appears to be a slight difference between the 8<sup>th</sup>-century and 10<sup>th</sup>-century matrix composition.

There is a group within the earlier production phase which range from approximately 2.4– 3.7%  $P_2O_5$  within the matrix ( $FeO:SiO_2$  between 0.5-1.5), circled in purple in figure 7.5.4. This is consistent with the use of a bog ore which does not contain as high a proportion of phosphorus as seen in the Foulness Valley. As the narrow horizontal group of 8<sup>th</sup>-century points, circled in purple, lies within a relatively consistent  $P_2O_5$  content, it may be that these were produced using the same kind of ore. The variable silica  $FeO:SiO_2$  ratio is most likely caused by variability in the material the slag was formed from during smelting.

The later phase matrix data suggest that there is something different occurring during the 10<sup>th</sup>-century, with both distinctly low and high phosphorus contents being detected, see the groups marked with orange circles above in figure 7.5.4. This may be a result of different ores being exploited although phosphorus content alone does not always reflect raw materials, as it is also influenced by the reaction conditions in which the material is produced. For this reason a second plot was generated from the data examining the  $P_2O_5$  content against the presence of  $SO_3$  see figure 7.6.1 below. This is far more indicative of the availability of free oxygen and can provide further evidence to imply which ore was being used.

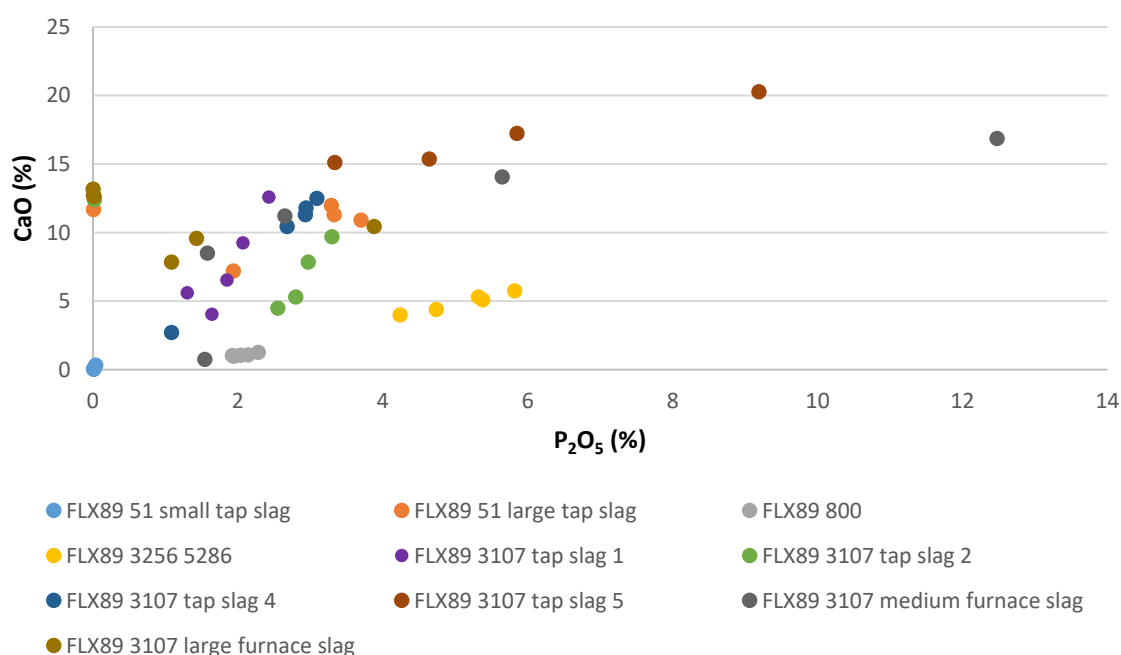


Figure 7.5.5 showing  $P_2O_5$  against CaO in matrix of analysed Flixborough phase 4 (8<sup>th</sup>-century) slags.

The  $P_2O_5$  against CaO plot for the 8<sup>th</sup>-century slags from Flixbrough shows that there is a main body of data with groups of outliers. Tap slag 5 in particular has higher CaO values than the rest of the assemblage. This may suggest that the ore from which this slag originated contained more calcium than the lower value pieces, as fuel ash contribution should be approximately similar for all of the slags as they were produced during a single phase of site occupation, where the technology would be

anticipated to be broadly similar. The general trend seen in the other assemblages continues here with an increase in phosphorus content being related to an increase in calcium.

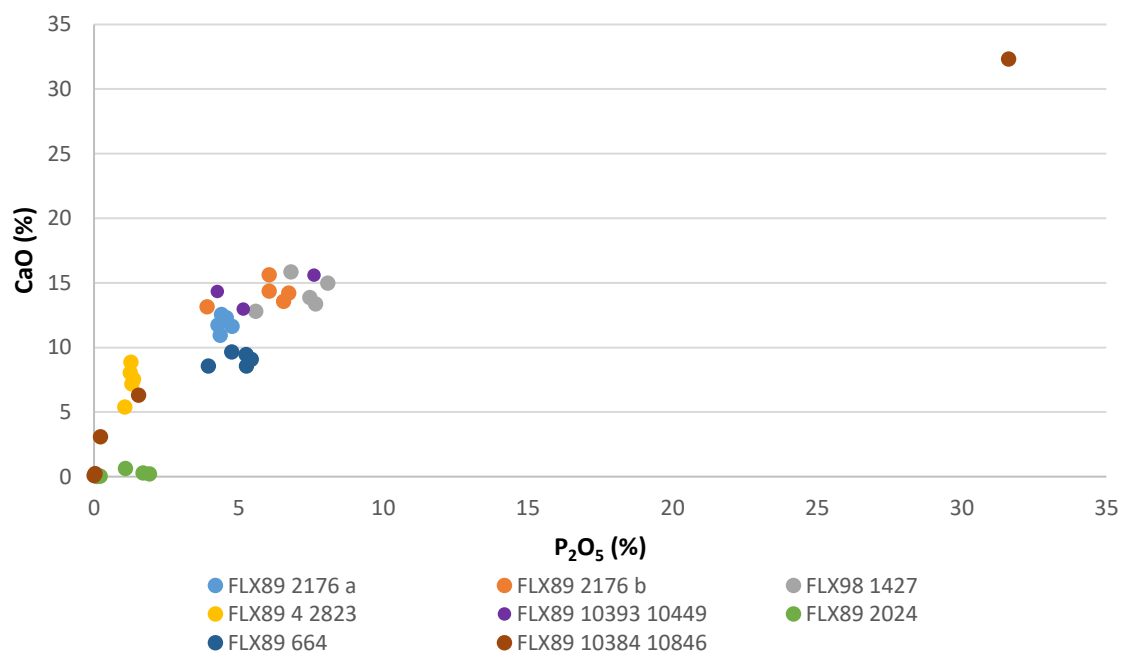


Figure 7.5.6 showing P<sub>2</sub>O<sub>5</sub> against CaO in matrix of analysed Flixborough phase 6 (10<sup>th</sup> century) slags.

The P<sub>2</sub>O<sub>5</sub> against CaO plot for the later 10<sup>th</sup> century iron slags shows a larger proportion of samples having higher CaO content when compared to the earlier 8<sup>th</sup>-century material. As the charcoal supply for the smelting most likely did not change between the periods of activity, the increase in CaO can be more firmly placed upon the use of different ore as this is the only locally available raw material which would show significant differences in composition. The trend of increasing P<sub>2</sub>O<sub>5</sub> in relation to increased CaO content is also clearly demonstrated here, with a notable outlier with in excess of 30% of both oxides. This outlier is most likely the result of unintentional analysis of calcium phosphate beneath the observable surface of the sample.

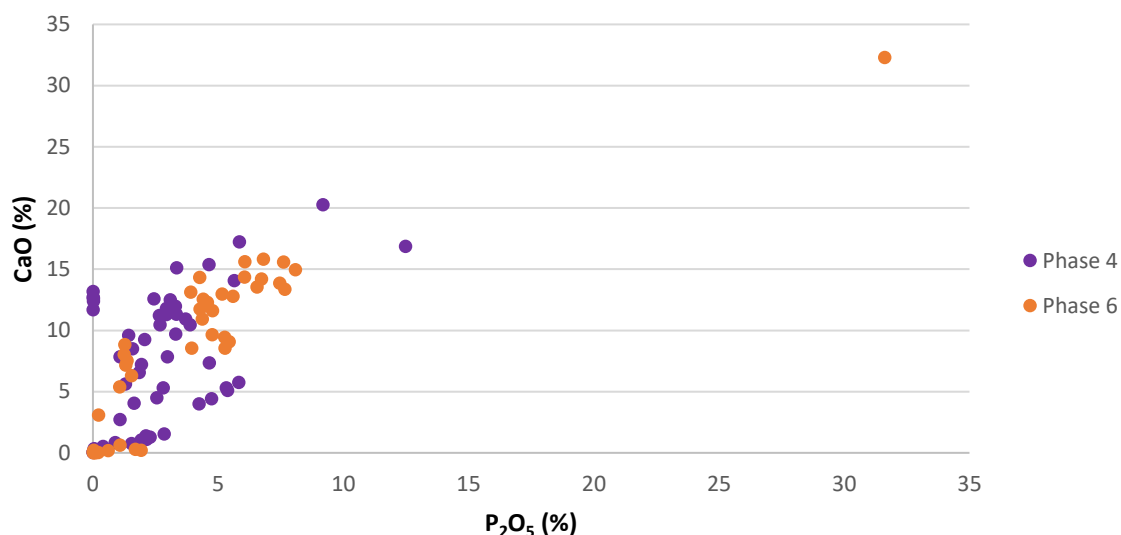


Figure 7.5.7 showing comparison of  $P_2O_5$  against CaO in matrix of all analysed Flixborough slags by site phase.

The combined plot of  $P_2O_5$  against CaO shown above in figure 7.5.7 shows a similar behaviour to the  $FeO:SiO_2$  against  $P_2O_5$  shown in figure 7.5.4. The large group of points from the 8<sup>th</sup>-century, phase 4, material plotting between the groups of later phase slags is consistent between the graphs. This suggests that the earlier material was produced using different conditions and likely a different ore. The use of a different ore is also supported by the greater calcium content shown in the phase 6 data, with a large group plotting between approximately 12-15% CaO. As there is also a group of later data which plots in the same area as the earlier slags, it may be suggested that this ore was also in use at the later time, alongside the ore responsible for the higher calcium content.

## 7.6 Possibility for different reaction conditions and ore exploitation

Both phosphorus and sulphur are volatile and will, at least partially, be removed during roasting and smelting as oxide gasses. For their presence to be detected within smelting slags, there has to be a limited availability of free oxygen for reaction. Sulphur is of particular interest when it comes to ore identification in this case as it is particularly susceptible to oxidation (Kaczorek *et al.* 2004), which is why secondary ores are oxides and carbonates rather than sulphides – which are the primary ores. For sulphur to be present in any significant quantity then it must originate from the ore, as charcoal contains almost no sulphur and it does not enter the system through the clay from which the furnace is built. If this is the case, then any significant sulphur content must have originated from the bedded Frodingham Ironstone and not the available bog ore which has undergone further oxidation in the

aqueous environment of its formation, as we have seen in chapter three from the study by Kaczorek *et al.* (2004) of bog ore formation processes.

The following data plot was created in an attempt to address this by presenting the data in a way which would indicate if an ore with higher sulphur content was being used.

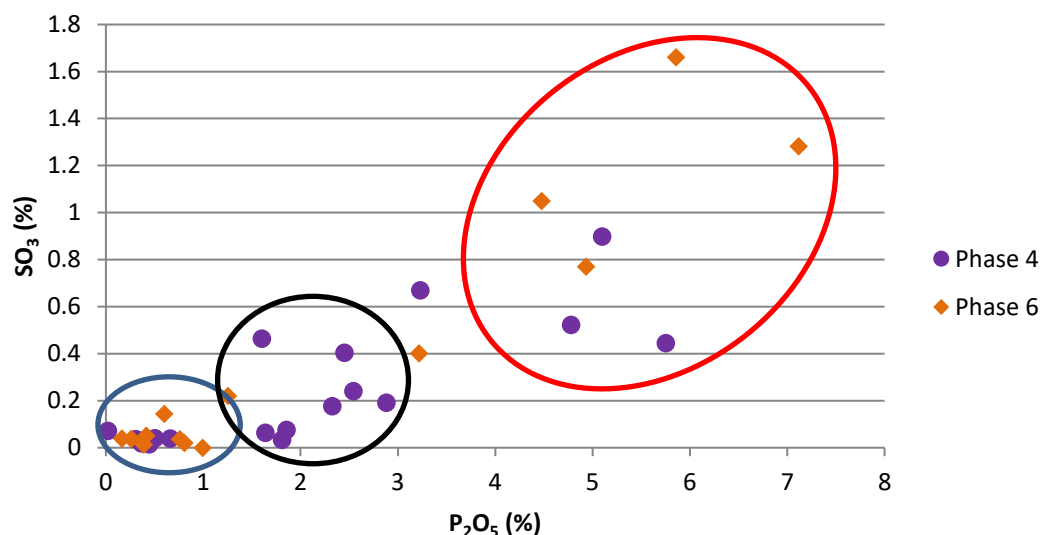


Figure 7.6.1  $P_2O_5$  against  $SO_3$  scatter plot for Flixborough data.

The graph above clearly shows there are two very different groupings of results in the 10<sup>th</sup>-century data. The majority of the points, circled in blue, contain less than 1%  $P_2O_5$  and less than 0.1%  $SO_3$ . There is a clear gap in the data between 3.3-4.5%  $P_2O_5$  which may suggest the use of a different ore. The elevated levels of  $SO_3$  in the points above 4.5%  $P_2O_5$ , circled in red, can only have originated from an ore which contains sulphur, most likely FeS. This is also supported by the 8<sup>th</sup>-century data which has several plots in the same low value region as the later data, but also has a small number with no overlapping 10<sup>th</sup>-century points. This 8<sup>th</sup>-century group circled in black most likely resulted from the exploitation of bog ore which produces a higher, though slightly more variable, phosphorus content.

The three points with higher sulphur levels in the 8<sup>th</sup>-century data further support the evidence from context 800, which yielded a piece of iron ore with FeS inclusions. It would appear, based on the limited data set, that some experimentation occurred during the sixth-seventh centuries into the use of iron stone as a viable raw material, while having similar reaction conditions to those smelts using the bog ore, as indicated by the lower phosphorus points with similar sulphur values (between 0.4-0.67%  $SO_3$ ).

The later data, which illustrate significant differences in SO<sub>3</sub> content not only show the return to the use of ironstone but show that the reaction conditions were different to those used previously. The increased size of the slag pieces seen during the 10<sup>th</sup>-century may demonstrate that the smelting operation increased in scale, used more powerful bellows, but also consumed significantly more charcoal which would limit the availability of free O<sub>2</sub>, thus allowing the survival of SO<sub>3</sub> within the slag.

The other important point to be taken from this SO<sub>3</sub> presence in both the 8<sup>th</sup>-century and 10<sup>th</sup>-century materials is that bedded ore was used in both periods. This shows a level of continuity in the ore sourcing strategies employed in Anglo-Saxon England where bedded ore has been seen to be exploited in Kent (Kelly 1995) through historical sources and now also at Quarrington and Flixborough by archaeological finds. As bog ore was also used at Flixborough the choice to use both ore deposits may reflect another aspect of the exploitation strategy and the decision making processes of the Saxon smelters. As both deposits are within a short walk from the site, the use of both ores is not unexpected. The argument that all iron production in Britain since the Iron Age until the Late Medieval period (Cowgill pers. com. 2014) was conducted using exclusively bog ore has been shown to be false, as it is contradicted by evidence from Rockingham Forest (Foard 2001: 68), Quarrington (see section 7.4), and also Flixborough (see sections 7.5 and figure 7.6.1 above). The archaeological finds of roasted Frodingham Ironstone at Flixborough and the chemical composition analyses shown here prove that the ironstone was being used to produce bloom iron while bog ore was also being used. The reasoning for the use of both may be a result of recognising that the ores produced metal with different working properties, but may also reflect the common human choice to use what is at hand.

## **7.7 Implications of the demonstration of the production of fresh metal**

The chronological implications of the findings from Quarrington are significant as they have proven that primary iron production occurs during the late 5<sup>th</sup> and early 6<sup>th</sup> centuries A.D. In Eastern England Anglo-Saxon communities were using both bedded and bog ore sources from this early date when available. This contrasts with the previous paradigms of technological collapse, loss of skill, and subsequently scavenging old scrap metal to supply demand, and the mass importation of new metal from the Netherlands (Fleming 2012: 5, 13). Fleming describes the event of the Roman withdrawal from Britain as a “calamitous material impoverishment” (Fleming 2012: 5). By stating that the Roman metal production was of the order 2,250 tonnes of clean, new bloom iron per year in Britain (Fleming 2012: 6), it seems extremely unlikely that anywhere could produce a comparable quantity for export, which is usually seen as the use of material surplus to local demand, as suggested by the importation model. The use of emotive language such as “awesome” as a means of describing the scale of Roman

production (Fleming 2012: 8) is an example of temporal, and classical, chauvinism where the ability of the classical Roman people is seen as being far superior to that of the contemporary and later non-Roman peoples. This is an unfair assessment of the knowledge of the people involved in iron production, with words such as “specialist” (Fleming 2012: 6, 12, 14) being used solely to describe those individuals involved in Roman period smelting, while Fleming states that “the knowledge of most skilled workers formerly involved in the various enterprises that stood behind it would have rapidly disappeared” (Fleming 2012: 14). This would suggest that the iron smelters simply forgot how to produce the product they based their livelihoods on, which, after a lifetime of experience, is not possible without the passing of generations, as seen in the Van Der Merwe and Avery (1987) study discussed in chapter 2. Contrary to the suggestion that iron production and specialist working was not carried out from the late 5<sup>th</sup> until the late 7<sup>th</sup> century A.D. (Fleming 2012: 36), the high number of iron grave goods from the Garton-Elmswell area near Driffield, East Yorkshire would suggest that the community not only had an inheritance of knowledge from the previous Roman period, but also the capability to exploit the available iron ores in the vicinity to produce the raw material required (Loveluck 1996: 45-46).

The argument posed by Fleming that large scale iron smelting sites have not been found in Eastern England is currently correct (Fleming 2012: 14). No sites have been found that match the scale of Snorup in Denmark (Smekalova *et al.* 1993), however the focus of Anglo-Saxon settlement archaeology in England has been the core habitation areas of settlements rather than their peripheries (Hamerow 2007), rather than the “Utmark” or “offsite” locations where primary iron production occurred during the Early Medieval period. It is highly unlikely that many of the early iron production sites will be found, however it is also not practical to suggest that the entirety of the demand for fresh iron could be met by importing bar metal from the continent. If it were the case that all of the fresh iron was imported, then it would have to be supported by a dedicated export market for another commodity, which is not attested in the archaeological record. It may be argued that the traded commodity was perishable, although Fleming makes no attempt to provide an example, and suggesting that such goods were not available in ready quantities locally in the Netherlands seems questionable at best. Also, the scavenging of old scrap as a primary means of iron supply cannot account for the production of high quality tools from fresh metal. Instead the metal economy is far more complex, with the use of new metal, new scrap and old scrap to fulfil different purposes. This further strengthens the case for there being no major technological collapse across Eastern England between the 5<sup>th</sup> and 7<sup>th</sup> centuries A.D.



## 7.8 Overall Synthesis

When considered together all of the data supports the standing assumption that the use of high phosphorus ore results in the production of slags with higher phosphorus content. This proves that bog ore is the raw material responsible for the production of phosphoric iron.

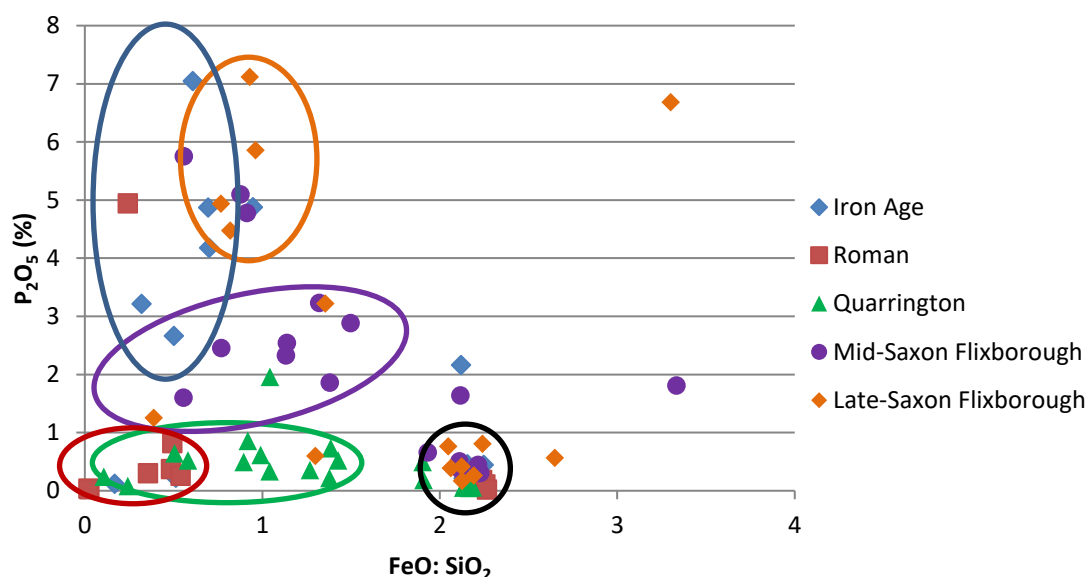


Figure 7.8.1 Combined phase average plot for all assemblages, the points circled in black represent the reliable fayalite analyses of the complete assemblage.

It is interesting to note that the matrix analyses from the Roman material, circled in red, using a bedded ore is generally grouped closer together than any other examined in this study with 5 of the 6 average composition points being between FeO:SiO<sub>2</sub> of 0.05 and 0.5 and the same points all being below 1% P<sub>2</sub>O<sub>5</sub>. This supports the generally accepted view that Roman smelting was far more controlled than that which came before or after (Fleming 2012), as demonstrated by comparing the dispersal of the Iron Age and Saxon matrix points to the Roman data plots. The outliers with high P<sub>2</sub>O<sub>5</sub> content in all cases are a direct result of the presence of calcium. This is a common occurrence due to the reaction with calcium to form Calcium phosphate which is intentionally caused today to remove phosphorus from blast furnace products.

My examination of the different phases at Flixborough has also provided new evidence for the development and experimentation of iron smelting during the Saxon period. Previously it was believed that ironstone was used during the 10<sup>th</sup>-century A.D., but now the exploitation and exploration of this material can be pushed back a further two centuries. While this may not have met with a great deal of success, as evidenced by the continued use of bog ore in the later phases of the site, it would appear that the first steps of technological exploration were taken earlier and were later

returned to. What is clear from this attempted use of the ironstone is that the smelting community made an association between the rust-orange colour of the stone and iron. This is most likely due to an association with the colour of iron rich water associated with bog ore which then became linked to the colour of the ironstone.

Today, we apply our knowledge of chemistry and prior knowledge gained by ore analyses to decide if a bloom will have steel, phosphoric iron or predominantly ferritic characteristics. In the past, it is far more likely that bloom workability was something that the smelters would have understood as a result of being exposed to too much fuel, or a result of the ore they used. They did not make predictions as modern experimental archaeologists do on the yield of metal based on the previously informed assumption that the ore in use had a composition of at least 60% viable iron oxide. To approach experiments in this way, while useful for us to understand the reduction and expected bloom formation, is a compromise due to our lack of practical smelting experience. Instead, past smelters knew their materials far better than we do today and would be able to predict the approximate size of bloom they would produce in a given smelt based on experience. They would not calculate a yield as we do to a given percentage; however they would have an understanding of how much workable metal they could produce from their regular quality of ore.

The same can be said about the production of slag. While the accepted method of bulk sampling, normalising, and plotting on an  $\text{FeO-SiO}_2\text{-Al}_2\text{O}_3$  diagram allows us to assess the overall system, with neatly plotted points falling within the usual range, it masks the high variability occurring within each individual smelt. The direct careful selection of material implied by studying African smelting, where bedded ore bodies are of very high quality and bog ore is rarely exploited, as seen in the ethnographic literature discussed in chapter 3, may also skew our interpretation of material selection. In my own experience preparing ore for smelting is a labour intensive process. This may account for why we find very little ore at known smelting sites, as the smelters expended a large amount of time and effort in obtaining and preparing the material, they most likely did not wish to waste their effort and so incorporated a greater quantity of the processed ore into the charge, with only the least desirable portion being discarded. This may in part explain why we struggle to produce large quantities slag in modern experiments, as we are too selective and driven by our need to accurately predict our outcome based on percent yield of bloom rather than smelting what we have to hand to produce as much as we can without being guided by our modern perception of how ore was used.

The other aspect of bloom production the data touches upon is the production of specific materials. Today we know what causes bloomery iron to behave in specific ways due to metallographic studies and chemical analyses. In the past the presence of phosphorus within an ore was not known, so the idea that past smelters could produce phosphoric iron or clean ferritic iron by choice of ore is plausible if the smelters had other means of assessing their metallic products. It is more probable that

the different materials were all regarded as types of iron that were recognisably different in terms of their working properties. The behaviour of phosphoric iron during working and the distinct colour difference would become associated with iron produced in a given location, leading to specific selection of materials for secondary production. In many cases the production of a bloom which is entirely a single material is impossible, as the smelting environment is extremely heterogeneous throughout. Certainly, the use of a high phosphorus ore, such as that found in East Yorkshire would produce a bloom with a greater phosphoric character than the bedded ores used in Quarrington or Caistor. However, some regions in these blooms would be more easily carburised than others, most commonly towards the surface where the bloom iron is in contact with slag and free oxygen, which will reduce the phosphorus content, allowing for subsequent carburisation by charcoal contact. So to say that high phosphorus ore produces high phosphorus metal and high phosphorus slag is true as a general rule. The shortcoming of this generalisation is that it oversimplifies the heterogeneity of the final product. Through consolidation and subsequent forging the ferritic and Fe-P material towards the centre of the bloom will be preserved, while the Fe-P-C and Fe-C rich surface will be removed. This will result in the production of bar metal which appears to be more homogeneous in composition.

So in summary the major findings from examining the complete body of data are that:

- 1) High phosphorus ores do indeed produce high phosphorus slags and thus high phosphorus metal, as shown by the East Yorkshire data.
- 2) In Britain iron smelting sites use the ore that is proximally available, until the large scale importation of phosphorus free ores, and do not show a preference towards bog ores when geological ore beds are accessible, regardless of time period, as indicated by the Caistor and Quarrington data.
- 3) Anglo-Saxon smelters could recognise different ore deposits and their occurrence in roasted condition at Flixborough is not a coincidence, but rather the result of their use.
- 4) The evidence from Quarrington and Flixborough demonstrate that there was no technological collapse and impoverishment of knowledge following the end of the Roman period.

# Chapter 8

## Conclusions

|            |  |            |
|------------|--|------------|
| <b>8.1</b> | <b><i>Conclusions</i></b>                  | <b>292</b> |
| <b>8.2</b> | <b><i>Further research suggestions</i></b> | <b>294</b> |

### 8.1 Conclusions

This investigation of archaeological and experimental materials has produced several responses to the aims stated at the outset of this research. As discussed in section 7.8, the standing assumption that the use of high phosphorus ore results in high phosphorus slag and thus a bloom with a greater proportion of phosphorus has been found to be true. The data from East Yorkshire, where a phosphorus rich bog ore was the raw material, shows a consistently higher phosphorus content than the slags from sites using bedded ore such as Quarrington and Caistor (figures 7.2.14, 7.3.6, 7.4.6). The material from Flixborough also demonstrates the impact of reaction conditions on the preservation of phosphorus. This is reflected in the two distinct groups, one of which has an elevated level of phosphorus comparable to the Foulness Valley samples but also a higher sulphur content (figure 7.5.4).

This finding supports the conclusion that, on a basic level, what goes in determines what comes out of an iron smelt. The archaeological data coupled with the practical experience I have gained demonstrates that, although Evans proposed a means to control phosphorus partitioning between slag and bloom, it is not possible to produce a bloom comprised entirely of a single material with our current level of knowledge and ability, as discussed in chapter 3. This is a result of the heterogeneous nature of an iron smelt, where the ore used combined with the variable reaction conditions through the active reaction space produces a bloom with ferritic, phosphoric and carbon steel regions (figures 4.6.1, 4.6.2). That artefacts appear to be manufactured from bars of relatively uniform composition would appear to be a result of the processing undertaken between bloom production and final artefact smithing. During consolidation and subsequent smithing the carbon rich exterior of a bloom will be lost as hammerscale, leaving the core to form the final bar. Due to carbon diffusion during the smelt the core portion of the bloom which is formed first and then isolated from the charcoal by subsequently formed iron flakes is typically less rich in carbon and therefore appears more homogeneous during metallographic analysis.

This work has also provided information about the ore sourcing strategies employed at different times. In the Foulness Valley, where each iron production site is found upon an island, or promontory called a 'holme' of iron rich sand surrounded by bog land, the ore used is unsurprisingly bog ore. It is readily available and also renewed by the leaching of the iron minerals from the 'holmes'. By contrast the site of Quarrington had access to bedded ore in the nearby chalk indicated by the appearance of the possible ore pieces held in the Lincolnshire Archives, but also demonstrated by the high CaO content of the slags shown in figure 7.4.7. As the fenlands were much further from the site, the closer, bedded deposits were exploited. Flixborough is a unique case with the availability of both Frodingham Ironstone and also bog ore produced from this ore bed, both being present within a 10m distance. The archaeological data, both in terms of finds as well as elemental analyses, show that both sources were exploited to produce iron at the site. Furthermore there appears to be no significant change in sourcing strategy between the two phases of iron production, apart from the presumed increase in extraction to supply the greater scale of production implied by the far larger slag finds from the 10th-century. That Anglo-Saxon iron smelters were sourcing and exploiting both bog ore and bedded ores is not surprising, as they were aware of both types of deposit and the signifiers of their presence, as discussed in chapters 2 and 7. All these indications of using the proximally available ore leads to the conclusion that, in England where iron ore is relatively common, smelting groups would seek out the nearest accessible source. This is the first time that these nationally important assemblages have been examined for chemical composition. The findings are the most significant to be made in the study of Anglo-Saxon iron production in recent years, proving the use of bedded iron ores at both Quarrington and Flixborough.

The data generated from the Roman material was produced from a very limited sample but still demonstrates a closer grouping of compositions than is seen in the other assemblages, as shown in chapter 7. While this supports the idea of Roman smelting being more efficient in terms of iron recovery, as less FeO was detected during the analyses of the non-wüstite phases (figures 7.3.5, 7.3.6), the small quantity of data may artificially enhance this perceived efficient iron recovery due to the limited number of pieces analysed. Further analytical study would serve to substantiate this possibility.

The experiment has also yielded helpful results for explaining the appearance of smelting slags with light coloured interiors, as shown in chapter 4. It has been demonstrated that these are the result of increased oxygen supply, leading to greater iron extraction, but also may be influenced by the incorporation of large quantities of furnace lining into the smelt due to slumping and failure of the furnace wall. The subsequent increase in iron-poor material increases the production of iron silicates, reducing the free iron oxide content, which causes the slag to appear lighter in colour with a reduced perceived mass (figures 4.6.6 – 4.6.10).

The other crucial finding is that there was no technological collapse following the end of the Roman period, as demonstrated by the data and archaeological finds shown in chapters 6 and 7. Instead, production focus shifted to more rural locations, with a main purpose of satisfying local demand. The iron economy may have been supplemented by importing and scavenging material, but that alone is not a credible means to supply enough iron and steel to meet demand.

## **8.2 Further research**

The findings of this work demonstrate that further study is required in several areas of ferrous metallurgy. Some of which are listed below in the anticipation that they can be carried out at a future date.

The material from the Foulness Valley requires a more in-depth study with a complete categorisation and chemical compositional study. This will provide useful data for comparison with other sites where bog ore may have been used, and also provide a better understanding of the smelting technology in use in that area during the Iron Age. Further survey work should also be carried out examining the sand ‘holmes’ found in the Hull Valley to test the working theory that iron working sites can be found on them in the same way as in the Foulness Valley. Thearne already provides some evidence that this is the case, although a wider field survey and mapping investigation may give a greater quantity of evidence for the intense level of iron production activity occurring in East Yorkshire in both river valleys during the late Iron Age.

Bulk sample analysis should be conducted on these slags to produce bulk compositions. These would provide a greater body of analytical data which will allow inclusion into and expansion of existing datasets. Care must be taken when plotting bulk samples however, as demonstrated by the significantly different composition of areas seen in archaeological smelting slags regardless of time period (figures 6.2.22, 6.2.37, 6.4.28). In order to obtain a representative composition, multiple samples must be taken to account for different compositional regions.

Further examination of the material from Flixborough would increase the dataset presented here. By doing so the conclusions concerning Ironstone exploitation would be more substantially supported. The large quantity of material which has yet to be analysed will yield far more data with which to support the findings presented in chapter 7.

A standard experimental framework with a centralised location would be of great benefit to future research. This would reduce the number of variables experienced in a series of smelts and between smelting campaigns, which would increase the reliability of results.

## Bibliography

Abdu, B. and R. Gordon (2004). Iron Artefacts from the Land of Kush. Journal of Archaeological Science **31** (7): 979-998.

Agricola [1556] (Hoover H.C. and L.H. Hoover trans. 1950) De re metallica New York, Dover Publications.

Anon. (820-830). Stuttgart Psalter, Württembergische Landesbibliothek Stuttgart.

Attenborough, F. L. (1922). The laws of the earliest English kings. Cambridge, Cambridge university press.

Azéma, A., B. Mille, P. Echegut and D. D. S. Meneses (2011). An experimental study of the welding techniques used on large Greek and Roman bronze statues. Historical Metallurgy **45** (2): 71-80.

Azoulay, H., E. Conforto, P. Refait and C. Rémazeilles (2013). Study of ferrous corrosion products on iron archaeological objects by electron backscattered diffraction (EBSD). Applied Physics A **110**: 379-388.

Balasubramaniam, R. and Gouthama (2003). Alloy design of ductile phosphoric iron ideas from archaeometallurgy. Bulletin of Materials Science **26** (5): 483 - 491.

Balasubramaniam, R. and A. V. R. Kumar (2003). Corrosion Resistance of the Dhar Iron Pillar. Corrosion Science **45**: 2451-2465.

Bayley, J., D. Dungworth and S. Paynter (2001). Centre for Archaeology Guidelines: Archaeometallurgy. London, English Heritage.

Beck, B. and M. Senn (2000). Zur Eisenverhüttung im Durachtal in. K. Bünteli, M. Höneisen and K. Zubler Berslingen-ein verschwundenes Dorf bei Schaffhausen. Schaffhausen. **Schaffhauser Archäologie** **3**: 241-269.

Binford, L. R. (1967). Smudge pits and hide smoking: The use of analogy in archaeological reasoning. American Antiquity **32** (1): 1-12.

Birch, T. (2011). Living on the edge: making and moving iron from the 'outside' in Anglo-Saxon England. Landscape History **31** (1): 5-23.

Biringuccio, V. [1540]. (Smith, C.S. and M.T. Gnudi 1990 trans.) The Pyrotechnia of Vannoccio Biringuccio. New York, Dover Publications.

Blakelock, E., M. Martín-Torres, H. A. Veldhuijzen and T. Young (2009). Slag inclusions in iron objects and the quest for provenance: an experiment and a case study. Journal of Archaeological Science **36** (8): 1745-1757.

Blakelock, E. and J. G. McDonnell (2007). A review of the metallographic analysis of Early Medieval knives. Historical Metallurgy **41** (1): 40-56.

Blakelock, E. and J. G. McDonnell (2011). Early medieval knife manufacture in Britain; a comparison between rural and urban settlements (AD 400-1000) in. J. Hošek, H. Cleere and L. Mihok The Archaeometallurgy of Iron: Recent Developments in Archaeological and Scientific Research. Prague, Institute of Archaeology of the ASCR: 123-136.

Boonstra, A., T. v. d. Manakker and W. v. Dijk (1997). Experiments with a slag-tapping and a slag pit furnace in Nørby. Early iron production - Archaeology, technology and experiments. Nordic Iron Seminar, Lejre, July 22nd to 28th, 1996. Technical Report 3 (1997). L. Chr: 73-80.

Brauns, M., R. Schwab, G. Gassmann, G. Wieland and E. Pernicka (2013). Provenance of Iron Age iron in southern Germany: a new approach. Journal of Archaeological Science **40** (2): 841-849.

Buchwald, V. F. (2005). Iron and steel in ancient times. Historisk-filosofiske Skrifter **29**. Copenhagen: The Royal Academy of Science and Letters.

Caboi, L. and C. Dunikowski (2004). "Les systems de production siderurgiques chez les Celtes au nord de La France." Pre-Actes, XXVIIIe colloque international AFEAF.

Carlie, A. (2012). Forging for the household or specialized production? The social organization of Early Ironworking in Skåne: Excavations at Brunnshög. Acta Archaeologica **83**: 55-81.

Champion, T. C. (ed), 1989. Centre and Periphery: comparative studies in archaeology. London, Unwin Hyman.



Charlton, M. F., P. Crew, Th. Rehren and S.J. Sheenan (2010). Explaining the evolution of ironmaking recipes – An example from northwest Wales. Journal of Anthropological Archaeology **29**: 352-367.

Charlton, M. F., E. Blakelock, M. Martinon-Torres and T. Young (2012). Investigating the production provenance of iron artifacts with multivariate methods. Journal of Archaeological Science **39** (7): 2280-2293.

Cherry, J. F. (1990). The first colonization of the Mediterranean islands: a review of recent research. Journal of Mediterranean Archaeology **3** (2): 145-221.

Childs, S. T. (1991). Style, technology, and iron smelting furnaces in Bantu-speaking Africa. Journal of Anthropological Archaeology **10**: 332-359.

Chirikure, S. (2006). New light on Njanja iron working: Towards a systematic encounter between ethnohistory and archaeometallurgy. South African Archaeological Bulletin **61** (184): 142-151.

Cleere, H. (1971). Ironmaking in a Roman furnace. Britannia **2**: 203-217.

Clogg, P. (1999). The Welham Bridge slag in. P. Halkon and M. Millet Rural settlement and industry : Studies of the Iron Age and Roman archaeology of lowland East Yorkshire, Yorkshire Archaeological Report 4. Leeds, Yorkshire Archaeological Society.

Condron, F. (1997). Iron production in Leicestershire, Rutland and Northamptonshire in antiquity. Transactions of the Leicestershire Archaeological and Historical Society **71**: 1-20.

Coustures, M. P., D. Béziat, F. Tollon, C. Domergue, L. Long and A. Rebiscoul (2003). The use of trace element analysis of entrapped slag inclusions to establish ore – bar iron links: Examples from two Gallo-Roman iron-making sites in France (Les Martys, Montagne Noire, and Les Ferrys, Loiret). Archaeometry **45** (4): 599-613.

Craddock, P. T. (1998). New light on the production of crucible steel in Asia. Bulletin of the Metals Museum **29**: 41-66.

Craddock, P. T. and B. R. Craddock (1996). The Beginnings of Metallurgy in South-West. Mining History: The bulletin of the Peak District Mines Historical Society **13** (2): 52-63.

Craddock, P. T. and D. Gale (1988). Evidence for early mining and extractive metallurgy in the British Isles: Problems and potentials in. E. A. Slater and J. O. Tate Science and Archaeology Glasgow 1987 (British Archaeological Reports British Series). Oxford, Archaeopress. **196 (i)**.

Cranstone, D. (1988). Historical Metallurgy Society Newsletter. **11** (Summer).

Crew, P. (1991) Experimental iron smelting and bloom smithing, linked to archaeological evidence from two sites in north Wales, Archeologie Experimentale, Tome 1 – Le Feu: le metal, la ceramique, Editions Errance, Paris: 160-163.

Crew, P. (1991) The experimental production of prehistoric bar iron, Historical Metallurgy **25**: 21-36.

Crew, P and C. Salter (1993) Currency bars with welded tips in Espelund, A. (ed) 1993 Bloomery ironworking during 2000 years **3** Trondheim: 11-30.

Crew, P. (1994) Currency bars in Great Britain, in Mangin, M. (ed) (1994) La siderurgie ancienne de l'est de la France, dans son context européen (Besançon): 345-350.

Crew, P., M. Charlton, P. Dillmann, P. Fluzin, C. Salter and E. Truffaut (2011) Cast iron from a bloomery furnace in Hošek, J., H. Cleere, and L. Mihok (eds) 2011 The archaeometallurgy of iron: Recent developments in archaeological and scientific research, Prague 239-262, 313-316.

Crew, P. (2013) Twenty five years of bloomery experiments: Perspectives and prospects in D. Dungworth and R.C.P. Doonan (2013) Accidental and experimental archaeometallurgy. London, Historical Metallurgy Society: 23-50.

Crowder, W. (1857). An attempt to determine the average compositions of the Rosedale, Whitby and Cleveland Ironstones. Edinburgh New Philosophical Journal new series **5**: 35-52.

David, N. and Y. L. Bléis (1988). Dokwaza: Last of the African iron masters. University of Calgary: Department of Communications Media.: 50 minutes.

Degryse, P., J. Schneider, N. Kellens, M. Waelkens and Ph. Muchez (2007). Tracing the resources of iron working at ancient Sagalassos (South-west Turkey): A combined lead and strontium isotope study on iron artefacts and ores. Archaeometry **49** (1): 75-86.

Degryse, P., J. C. Schneider and P. Muchez (2009). Combined Pb-Sr isotopic analysis in provenancing late Roman iron raw materials in the territory of Sagalassos (SW Turkey). Archaeological and Anthropological Sciences **1** (2): 155-159.

Desaulty, A.-M., C. Mariet, P. Dillmann, J. L. Joron and P. Fluzin (2008). A provenance study of iron archaeological artefacts by Inductively Coupled Plasma-Mass Spectrometry multi-elemental analysis. Spectrochimica Acta Part B **63**: 1253-1362.

Devos, W., M. Senn-Luder, C. Moor and C. Salter (2000). Laser ablation inductively coupled plasma mass spectrometry (LA-ICP-MS) for spatially resolved trace analysis of early-medieval archaeological iron finds Fresenius Journal of Analytical Chemistry **366** (8): 873-880.

Diinhoff, S. (2005). The issue of infield and outfield in. I. Holm, S. Innselset and I. Øye Utmark: the outfield as industry and ideology in the Iron Age and the Middle Ages. Bergen, University of Bergen. 1: 109-118.

Dillman, P. and M. L'Heritier (2007). Slag inclusion analysis for studying ferrous alloys employed in French medieval buildings Supply of materials and diffusion of smelting processes. Journal of Archaeological Science **34**: 1810-1923.

Dixon, N. (2004). The Crannogs of Scotland: An underwater archaeology. Stroud, Tempus.

Dowd, M. A. and N. Fairburn (2005). Excavations at Farranastack Evidence for the use of Shaft Furnaces in Medieval iron production. Journal of Irish Archaeology **14**: 115-121.

Dungworth, D. (2001). Metal working evidence from Housesteads Roman Fort, Northumberland CfA report. Portsmouth, English Heritage. **109/2001**.

Dungworth, D. (2012). "Book Review :The Archaeometallurgy of Iron edited by Jiri Hošek, Henry Cleere and L'ubomír Mihok". Retrieved 10/12/2012, 2012, from [http://www.prehistoricsociety.org/files/reviews/The\\_Archaeometallurgy\\_of\\_Iron\\_final\\_review.pdf](http://www.prehistoricsociety.org/files/reviews/The_Archaeometallurgy_of_Iron_final_review.pdf).

D. Dungworth and R.C.P. Doonan (2013) Accidental and experimental archaeometallurgy. London, Historical Metallurgy Society.

Dungworth, D. and L. Mephram (2012). Prehistoric iron smelting in London: Evidence from Shooters Hill. Historical Metallurgy **46** (1): 1-8.

Dungworth, D. and R. Wilkes (2009). Understanding hammerscale: the use of high speed film and electron microscopy. Historical Metallurgy **43**: 33-46.

Edmonds, M. (1990) Description, understanding and the chaîne opératoire. Archaeological review from Cambridge **9**: 55-70.

Ehrenreich, R. M. (1985). Trade, technology and the ironworking community in the Iron Age of Southern Britain. British Archaeological Reports British Series Oxford, Archaeopress. **144**.

Ellingham, H. J. T. (1944) Transactions and communications. Journal of the Society of Chemical Industry **63** (5): 125-160.

Eschenlohr, L. (2001). Recherches archéologique sur le district sidérurgique du Jura centrale suisse. Lausanne. **Cahiers d'archéologie romande No. 88**.

Eschenlohr, L. and V. Serneels (1991). Les bas fourneaux mérovingiens de Boécourt, Les Boulies (JU/Suisse), Porrentruy. **Cahier d'archéologie jurassienne 3**.

Espelund, A. (1997). The Evenstad Process - Description, Excavation and Metallurgical Evaluation. Early Iron Production - Archaeology, Technology and Experiments, Lejre.

Estanislau, T. (1999). The Catalan Process for the direct production of malleable iron and its spread to Europe and the Americas. Contributions to Science **1** (2): 225-232.

Evans, D. H. and C. Loveluck, Eds. (2009). Life and economy at Early Medieval Flixborough c. A.D. 600-1000 - The artefact evidence. Oxford, Oxbow books.

Evison, V. I. (1987). Dover: the Buckland Anglo-Saxon cemetery. London, Historic Buildings and Monuments Commission of England.

Fell, D. (2007). Archaeological evaluation: Land at Wakerley, Northamptonshire, Volume 1: The Trial Trenches. Milton Keynes, Archaeological Services and Consultancy Ltd.

Fell, V. (2005). Fiskerton: Scientific analysis of corrosion layers on archaeological iron artefacts and from experimental iron samples buried for up to 18 months CfA Reports. Portsmouth, English Heritage. **65/2005**.

Fleming, R. (2012). Recycling in Britain after the fall of Rome's metal economy. Past and Present **201**: 3-44.

Friede, H. M., A. A. Hejja, A. Koursaris and R. H. Steel (1984). Thermal aspects of the smelting of iron ore in reconstructed South African Iron Age furnaces. Journal of the South African Institute of Mining and Metallurgy **84** (9): 285-297.

Fulford, M. G., J.R.L. Allen, C. Gaffney, J. Gater, G.C. Boon and I. Figueiral (1992). Iron-Making at the Chesters Villa, Woolaston, Gloucestershire: Survey and Excavation. Britannia **23**: 159-215.

Ganzelewski, M. (1997). Die frühe Verhüttung von Raseneisenerzen am Kammberg bei Joldelund (Schleswig-Holstein). University of Bochum. **PhD Thesis**.

Giles, M. (2007). Making metal and forging relations Ironworking in the British Iron Age. Oxford journal of archaeology **26** (4): 395-413.

Gilmour, B. J. (2007). Swords, Seaxes and Saxons: Pattern-welding and edged weapon technology from Late Roman Britain to Anglo-Saxon England in. M. Henig and T. J. Smith Collectanea Antiqua: Essays in memory of Sonia Chadwick Hawkes (British Archaeological Reports International Series). Oxford, Archaeopress.

Girbal, B. (2013). Experimenting with the bowl furnace in. D. Dungworth and R.C.P. Doonan (2013) Accidental and experimental archaeometallurgy. London, Historical Metallurgy Society: 83-92.

Godfrey, E. (2007). The Technology of Ancient and Medieval Directly Reduced Phosphoric Iron. . University of Bradford, University of Bradford. **PhD thesis**.

Godfrey, E. and M. van Nie (2004). A Germanic ultrahigh carbon steel punch of the Late Roman-Iron Age. Journal of Archaeological Science **31** (8): 1117-1125.

Goodhew, P. J., J. Humphreys and R. Beanland (2001). Electron microscopy and analysis. London, Taylor and Francis.

Goodway, M. (1987). Phosphorus in Antique Iron Music Wire. Science **236**: 927-932.

Gutiérrez-Zugasti, I. and D. Cuenca-Solana (2015). Ornaments from the Magdalenian burial area in El Mirón Cave (Cantabria, northern Spain). Were they grave goods? Journal of Archaeological Science **60**: 112-124.

Halkon, P. (2008). Archaeology and environment in a changing East Yorkshire landscape: The Foulness Valley c. 800 B.C. to c. A.D. 400. BAR British Series. Oxford. **472**.

Halkon, P. (2011). Iron, landscape and power in Iron Age East Yorkshire. Archaeological Journal **168**: 133-165.

Halkon, P. and M. Millet, Eds. (1999). Rural settlement and industry: Studies in the Iron Age and Roman archaeology of Lowland East Yorkshire, Yorkshire Archaeology Report 4. Leeds, Yorkshire Archaeology Society.

Hall, N. (2007). Telephone House, High Street, Southampton: An investigation of Medieval gold threads. Research Department Report Series. London, English Heritage. 20/2007.

Hall, N. (2008). An experimental investigation into the interaction of carbon with phosphoric iron. Undergraduate dissertation. Bradford, University of Bradford.

Hall, N. (2009). Ironworking debris in. S. S. Frere and R. L. Fitts Excavations at Bowes and Lease Rigg Roman forts, Yorkshire Archaeological Report 6. Leeds, Yorkshire Archaeological Society.

Hall, N. (2012). Experimental investigation into the production of phosphoric iron through forge enrichment. Masters of Science dissertation, University of Nottingham.

Hallimond, A.F. (1925) Iron ores: Bedded ores of England and Wales. Petrography and chemistry Special reports on the mineral resources of Great Britain **29**.

Hammerow, H. (2007) Agrarian production and the emporia of mid Saxon England, ca. A.D. 65-850 in Henning, J. (2007) Post-Roman towns, trade and settlement in Europe and Byzantium. Berlin, Walter de Gruyter: 219-232.

Hart, C. R. (1975). The Early Charters of Northern England and the North Midlands. Leicester, Leicester University Press.

Hauptmann, A. (2014). The investigation of archaeometallurgical slag in. B. W. Roberts and C. Thornton Archaeometallurgy in global perspective. New York, Springer: 91-105.

Hawthorne, J.G. and C.S. Smith (trans.) 1979 Theophilus: On Divers Arts. New York, Dover Publications.

Heimann, R. B., U. Kreher, J. Oexle, V. Hirsekorn, O. Ullrich, D. Janke, B. Lychatz, B. Ullrich, H. Lindner and B. Wagenbreth (1998). Archaeometallurgical investigations into the iron production technology in Upper Lusatia, Saxony, from the Early Iron Age (Billendorf period) to the 12th century AD. European Journal of Mineralogy **10** (5): 1015-1035.

Henderson, J. (2000) The science and archaeology of materials. Oxon, Routledge.

Hinton, D. A. (2000). A Smith in Lindsey: The Anglo-Saxon grave at Tattershall Thorpe, Lincolnshire. The Society for Medieval archaeology monograph series. London. **16**.

Hinton, D. A. (2003). Anglo-Saxon smiths and myths in. D. Scragg Textual and material culture in Anglo-Saxon England: Thomas Northcote Toller and the Toller Memorial Lectures. Cambridge, D.S. Brewer.

Holm, I., S. Innselset, and I. Øye (eds) (2005). 'Utmark': The outfield as industry and ideology in the Iron Age and the Middle Ages, UBAS (University of Bergen Archaeological Service) International 1 Bergen.

Horden, P. and N. Purcell (2000). The corrupting sea: A study of Mediterranean history. Oxford, Blackwell.

Høst-Madsen, L. and V. F. Buchwald (1999). The characterization and provenancing of ore, slag and iron from the Iron Age settlement at Snorup. Historical Metallurgy **33** (2): 57-67.

Jöns, H. (1999). Iron production in Northern Germany during the Iron Age. Settlement and Landscape, Århus, Jutland Archaeological Society.

Kaczorek, D. and M. Sommer (2003). Micromorphology, chemistry, and mineralogy of bog iron ores from Poland. Catena **54**: 393-402.

Kaczorek, D., M. Sommer, I. Andruschkewitsch, L. Oktabaa, Z. Czerwinskia and K. Stahrc (2004). A comparative micromorphological and chemical study of "Raseneisenstein" (bog iron ore) and "Ortstein". Geoderma **121**: 83-94.

Kapp, L., H. Kapp and Y. Yoshihara (1987). The craft of the Japanese sword. Tokyo, Kodansha International.

Karbowniczec, M. (2006). Metallurgical process in ancient shaft furnace - theoretical considerations. Metallurgija **12** (2-3): 145-154.

Keipura, R. T. and B. R. Sanders (1985). Metals handbook 9th edition volume 9: Metallography and microstructures. Ohio USA, American Society for Metals.

Kelly, S. E., Ed. (1995). Charters of St Augustine's Abbey, Canterbury, and Minster-in-Thamet. Anglo-Saxon Charters 4. Oxford, Oxford University Press.

Kubaschewki, O. (1982) Iron – Binary phase diagrams. Berlin, Springer-Verlag.

Kumar, V. and R. Balasubramaniam (2002). On the origin of high phosphorus content in ancient Indian iron. Metals, Materials and Processes **14** (1): 1-14.

Landuydt, C. J. (1990). Micromorphology of iron minerals from bog ores of the Belgian Campine area in. L. A. Douglas Soil micromorphology. A basic and applied science. Amsterdam, Elsevier: 289-294.

Le Coze, J. (2000). Purification of Iron and Steels a continuous effort from 2000 BC to AD 2000. Materials Transactions, Japan Insitiute of Metals **41** (1): 219-232.

Leroi-Gourhan, A. (1993). Gesture and speech. Cambridge, Massachusetts, MIT press.

Lewis, A. (1994). Bronze Age mines of the Great Orme: Interim report. Bulletin of the Peak District Mines Historical Society **12** (3): 31-36.

Lindholm, D., W. Roggenkamp, S. Bittlestone (trans.) and A. Bittlestone (trans.) (1969) Stave churches in Norway, London, Rudolf Steiner Press.

Loveluck, C. (1996). The development of the Anglo-Saxon ladscape, economy and society. Anglo-Saxon studies in archaeology and history **9**: 25-48.

Loveluck, C. (2007). Rural settlement, lifestyle and social change in the latter first millennium AD - Anglo-Saxon Flixborough in its wider context. Oxford, Oxbow books.



Lyngstrøm, H. S. (2011). Iron from Zealandic bog iron ore- more than a theoretical possibility? Nordiske Fortidsminder Serie C **8**: 139-146.

MacGregor, M., G.W. Lee and G. V. Wilson (1920). Special reports on the mineral resources of Great Britain Vol. XI Iron ores (continued) The Iron ores of Scotland. Edinburgh, HMSO.

Marzinzik, S. (2003). Early Anglo-Saxon belt buckles (late fifth to early eighth centuries A.D.): Their classification and context. British Archaeological Reports British Series. Oxford. 357.

McDonnell, J. G. (1987a). Analysis of Eight Iron Knives and Four Other Tools from Hamwih, Southampton. Ancient Monuments Laboratory Report 137/1987. Centre for Archaeology, English Heritage.

McDonnell, J. G. (1987b). Metallurgical Analysis of Six Iron Knives from Hamwic, Southampton. Ancient Monuments Laboratory Report 93/1987. Centre for Archaeology, English Heritage.

McDonnell, J. G. (1988). The Ironworking Slags from North Cave. Ancient Monument Laboratory Report 91/1988. London, English Heritage.

McDonnell, J. G. (1988). Ore to artefact: A study of early ironworking in. E. A. Slater and J. O. Tate (1988) Science and Archaeology Glasgow 1987 (British Archaeological Reports British Series). Oxford, Archaeopress. **196 (i)**.

McDonnell, J. G. (1989). Iron and Its Alloys in the Fifth to Eleventh Centuries AD in England. World Archaeology **20** (3): 373-382.

McDonnell, J. G. (1992). The Metallurgical Analysis of the Ironworking Slags and Iron Artefacts in. P. Ottaway Anglo-Scandinavian Ironwork from Coppergate, York. Vol: 17/6. York, York Archaeological Trust/Council of British Archaeology.

McDonnell, J. G., E. Blakelock, S. R. Robinson, N. Chabot, A. B. Daoust and V. Castagnino (2012). The Iron Economy of Saxon Wharram Percy: Modelling the Saxon iron-working landscape. in. W. S. Wharram. (2012) A study of Settlement on the Yorkshire Wolds, XIII. A History of Wharram Percy and its Neighbours. York, York University Archaeological Publications.

Michell, J. (1989). A little history of Astro-Archaeology: stages in the transformation of heresy. London, Thames and Hudson.

- Mighall, T. M., I. D. L. Foster, P. Crew, A. S. Chapman and A. Finn (2009). Using mineral magnetism to characterise ironworking and to detect its evidence in peat bogs. Journal of Archaeological Science **36** (1): 130-139.
- Mihok, L. (2006). Beginnings of iron smelting in the central carpathians region. Metalurgija **12** (2-3): 173-184.
- Militzer, M. and J. Wieting (1989). Segregation mechanisms of temper embrittlement Acta Metallurgica **37** (10): 2585-2593.
- Miller, D. and G. Whitelaw (1994). Early Iron Age metal working from the site of KwaGandaganda, Natal, South Africa. The South African archaeological bulletin **49** (160): 79-89.
- Miller, D. E. and N. J. v. d. Merwe (1994). Early metal working in Sub-Saharan Africa: A review of recent research. Journal of African History **35** (1): 1-36.
- Morton, G.R. and J. Wingrove (1969) Constitution of bloomery slags: Part 1 – Roman, Journal of the Iron and Steel Institute: 1556-1564.
- Muhly, J. D., R. Maddin, T. Stetch and E. Özgen (1985). Iron in Anatolia and the nature of the Hittite iron industry. Anatolian Studies **35**: 67-84.
- Navasaitis, J. and A. Selskiene (2007). Metallographic examination of cast iron lump produced in the bloomery iron making process. Materials Science (Medžiagotyra) **13** (2): 167-173.
- Navasaitis, J., A. Selskienė and G. Žaldarys (2010). The study of trace elements in bloomery iron. Materials Science (Medžiagotyra). **16** (2): 113-118.
- Ottaway, P. (1987). Anglo-Scandinavian knives from 16-22 Coppergate, York in. B. G. Scott and H. Cleere The crafts of the blacksmith: Essays presented to R F Tylecote at the 1984 symposium of the UISPP Comité pour la Sidérurgie Ancienne held in Belfast, N Ireland, 16-21 September 1984. Belfast, Ulster Museum/UISPP Comité pour la Sidérurgie Ancienne: 83-86.
- Ottaway, P. (1992). Anglo-Scandinavian ironwork from 16-22 Coppergate, Published for the York Archaeological Trust by the Council for British Archaeology.

Øye, I. (2005). Introduction in. I. Holm, S. Innselset and I. Øye Utmark: the outfield as industry and ideology in the Iron Age and the Middle Ages. Bergen, Univeristy of Bergen. 1: 9-20.

Park, J.-S. and T. Rehren (2011). Large-scale 2nd to 3rd century AD bloomery iron smelting in Korea. Journal of Archaeological Science **38** (6): 1180-1190.

Paynter, S. (2006). Regional variations in bloomery smelting slag of the iron age and Romano-British periods. Archaeometry **48**: 271-292.

Paynter, S. (2011). Pre-industrial ironworks. London, English Heritage.

Paynter, S., E. Blakelock and G. Hatton (2012). Ias Tan y Bwlch, Snowdonia National Park Bloomery iron smelting - experimentation and archaeology. English Heritage Research Department Reports. Portsmouth, English Heritage. 25.

Pearce, M. (2014). Belief systems of past miners. Archelologica Postmedievale.

Pearson, M. P. (1999). Food, sex and death: Cosmologies in the British Iron Age with particular reference to East Yorkshire. Cambridge Archaeological Journal **9**: 43-69.

Percy, J. (1864). Metallurgy: the art of extracting metals from their ores, and adapting them to various purposes of manufacture: Iron and Steel. London, John Murray.

Piaskowski, J. (1989). Phosphorus in Iron Ore and Slag, and in Bloomery Iron. Archaeomaterials **3** (1): 47-59.

Piccardo, P., M. G. Ienco, R. Baladubramaniam and P. Dillmann (2004). Detecting Non-Uniform Phosphorus Distribution in Ancient Indian Iron by Colour Metallography. Curent Science **87** (5): 650-653.

Pine, J. (2003). The excavation of a late Iron Age/Roman settlement and iron production site at the Whitehall Brick and Tile Works, Arborfield Garrison, Berkshire. Berkshire Archaeological Journal **76**: 37-67.

Pliny, t. E. (1952). Pliny, Natural History, with an English translation by H. Rackham. Cambridge, MA, Harvard University Press. **IX, Libri XXXIII-XXXV**.

Potter, J.F. (1977) Eocene, lower Bracklesham Beds, iron workings in Surrey, Proceedings of the Geological Association **88** (4): 229-241.

Pryce, T. O., C. Chiemsisouraj, V. Zeitoun and H. Forestier (2011b). An 8th-9th century AD iron smelting workshop near Saphim Village, NW Lao PDR. Historical Metallurgy **45** (2): 81-89.

Pryce, T. O., M. Pollard, M. Martín-Torres and V. C. Pigott (2011a). Southeast Asia's first isotopically defined Prehistoric copper production system: When did extractive metallurgy begin in the Khao Wong Prachan Valley of Central Thailand? Archaeometry **53** (1): 146-163.

Radivojević, M. (2013) Archaeometallurgy of the Vinča culture: A case study of the site of Belovode in eastern Serbia. Historical Metallurgy **41** (1) 13-32

Raghavan, V. (1988). Phase diagrams of ternary iron alloys. Part 3. Ternary systems containing iron and phosphorus. Indian Institute of Metals: 229.

Rehder, J. E. (2000). The Mastery and uses of Fire in Antiquity. Montreal, McGill-Queens University Press.

Rehren Th., M. Charlton, S. Chirikure, J. Humphris, A. Ige and H. A. Veldhuijzen (2007). Decisions set in slag: The human factor in African iron smelting in. S. La Niece, D. Hook and P. Craddock Metals and mines studies in archaeometallurgy. London, Archetype: 211-218.

Rogers, A. (2005). Metalworking and Late Roman power: a study of towns in later Roman Britain. in. J. Bruhn, B. Croxford and D. Grigoropoulos TRAC 2004: Proceedings of the Fourteenth Annual Theoretical Roman Archaeology Conference Durham 2004. Oxford, Oxbow Books: 27-38.

Ross, M., A.G. Sisco and C.S. Smith (2015) Bergbuchlein, the little book on ores: The first mining book ever printed. Oxshott, Oxshott press.

Rubinson, S. R. (2010). An archaeometallurgical study of Early Medieval iron technology: An examination of the quality and use of iron alloys in iron artefacts from Early Medieval Britain. University of Bradford, University of Bradford. **PhD thesis**.

Salter, C. J. (1989). The scientific investigation of the iron industry in Iron Age Britain in. J. Henderson Scientific analysis in archaeology and its interpretation. Oxford, Oxford University Committee for Archaeology and UCLA Institute of Archaeology.

Salter, C. and P. Crew (1997) High phosphorus steel from experimentally smelted bog-iron ore in Crew, P. and S. Crew (eds) 1997, Early ironworking in Europe: Archaeology and experiment, Maentwrog: 83-84.

Samuels, L. E. (1980). Optical microscopy of carbon steels. Ohio, USA. ASM.

Saunders, L. (2013). An American bloomery in Sussex in. D. Dungworth and R. C. P. Doonan (2013) Accidental and Experimental archaeometallurgy. London, Historical Metallurgy Society: 107-110.

Saunders, W. H. L. and H. G. Williams III (2002). Practical bloomery smelting in. P. B. Vandiver, M. Goodway and J. L. Mass Materials Issues in Art and Archaeology VI, **712**: 579-588.

Saunders, W. H. L. and H. G. Williams III (2002). Practical Bloomery Smelting. Materials Research Society symposium proceedings **712**: 579-588.

Saunders, W. H. L. and S. Williams (2002). A practical treatise on the smelting and smithing of bloomery iron. Historical Metallurgy **36** (2): 122-131.

Schmidt, P. R. (1997). Iron technology in East Africa: Symbolism, science, and archaeology. Oxford, James Currey.

Schmidt, P. R. and D.H. Avery (1983). More evidence for an advanced prehistoric iron technology in Africa. Journal of Field Archaeology **10** (4): 421-434.

Schürmann, E. (1958). Die Reduktion des Eisens im Rennfeuer. Stahl und Eisen **78** (19): 1297-1308.

Schwab, R., D. Heger, B. Höppner and E. Pernicka (2006). The Provenance of iron artefacts from Manching: A multi-technique approach. Archaeometry **48** (3): 433-452.

Scott, D. A. (1991). Metallography and microstructure of ancient and historic metals. Singapore, The J. Paul Getty Trust.

Selskiene, A. (2007). Examination of smelting and smithing slags formed in bloomery iron-making process. Chemija **18** (2): 22-28.

Senn, M., U. Gfeller, B. Guénette-Beck, P. Lienemann and A. Ulrich (2010). Tools to qualify experiments with bloomery furnaces. Archaeometry **52** (1): 131-145.

Serneels, V. (1993). Archéométrie des scories de fer. Recherches sur la sidérurgie ancienne en Suisse occidentale. Lausanne. **Cahiers d'archéologie romande No. 61.**

Serneels, V. (2002). Analyses chimiques des matières premières et produits de l'opération de réductions dans le four basque d'Agorregi in. M. M. Urteaga Agorregiko burdinola eta errotak (Aia, Gipuzkoa). San Sebastian, Departamento de Cultura, Euskera, Juventud y Deportes. **Arkeologia 3**: 93-121.

Serneels, V. and B. Beck (1998). Les scories du Mont Chemin et l'utilisation de la magnétite pour fabriquer du fer par la méthode directe de réduction. Minaria Helvetica **18b**: 43-65.

Serneels, V. and P. Crew (1997) Ore-slag relationships from experimentally smelted bog-iron ore in Crew, P. and S. Crew (eds) 1997, Early ironworking in Europe: Archaeology and experiment, Maentwrog: 78-82.

Shepherd, D. J. (1997). The ritual significance of slag in Finnish Iron Age burials. Fennoscandia archaeologica **XIV**: 13-22.

Sim, D. (1998). Beyond the bloom: Bloom refining and iron artifact production in the Roman world. British Archaeological Reports International Series. Oxford, Archaeopress. 725.

Smekalova, T., O. Voss and N. Abrahamsen (1993). Magnetic investigation of iron-smelting centres at Snorup, Denmark. Archaeologica Polona **31**: 83-103.

Smith, T. (2013) A report on the Wealden Iron Research Group smelt in D. Dungworth and R. C. P. Doonan (2013) Accidental and Experimental archaeometallurgy. London, Historical Metallurgy Society: 99-106.

Srinivasan, S. and S. Ranganathan (2004). India's legendary Wootz Steel: An advanced material of the Ancient World. Bangalore, India, Tata Steel.

Starley, D. (1999). The analysis of middle Saxon ironwork and ironworking debris from Flixborough, South Humberside. Ancient monuments laboratory reports (New Series) 35/1999. Centre for Archaeology, English Heritage.

Stead, J. E. (1918). Iron, carbon and phosphorus. Journal of the Iron and Steel Institute **97**: 389-412.

Stewart, J. W., J. A. Charles and E. R. Wallach (2000a). Iron-phosphorus-carbon system part 1 - Mechanical properties of low carbon iron-phosphorus alloys. Materials Science and Technology **16**: 275-282.

Stewart, J. W., J. A. Charles and E. R. Wallach (2000b). Iron-phosphorus-carbon system part 2 - Metallographic behaviour of Oberhoffer's Reagent. Materials Science and Technology **16**: 275-282.

Stewart, J. W., J. A. Charles and E. R. Wallach (2000c). Iron-phosphorus-carbon system part 3 - Metallography of low carbon-phosphorus alloys. Materials Science and Technology **16**: 291-303.

Stoops, G. (1983). SEM and light microscopic observations of minerals in bog ores of the Belgian Campine. Geoderma **30**: 179-186.

Swanton, M. (1993). Anglo-Saxon Prose. London, Orion.

Taylor, G., C. Allen, J. Bayley, J. Cowgill, V. Fryer, C. Palmer, B. Precious, J. Rackham, T. Roper and J. Young (2003). An early to middle Saxon settlement at Quarrington, Lincolnshire. The Antiquaries Journal **83**: 231-280.

Thiele, A. and J. Hošek (2015) Estimation of phosphorus content in archaeological iron objects by means of optical metallography and hardness measurements. Acta Polytechnica Hungarica **12** (4): 113-126.

Thompson, L. (2004). Ancient weapons in Britain. Barnsley, Pen and Sword Military.

Tylecote, R. F. (1968). The phosphorus content of iron from the bloomery site at West Runton, Norfolk. Bulletin of the Historical Metallurgy Group **2** (2): 83.

Tylecote, R. F. (1970). The composition of metal artifacts: a guide to provenance? Antiquity **44**: 19-25.

Tylecote, R. F. (1970). Recent work on early ironworking sites in the Stamford area. Bulletin of the Historical Metallurgy Group **4** (1): 24-27.

Tylecote, R. F. (1990). The prehistory of metallurgy in the British Isles. London, The Institute of Metals.

Tylecote, R. F., J. N. Austen and A. E. Wraith (1971). The mechanism of the bloomery process in shaft furnaces. Journal of the Iron and Steel Institute **212**: 342-363.

Ulmschneider, K. (2000). Settlement, economy and the 'productive' site: Middle Anglo-Saxon Lincolnshire A.D. 650/780. Medieval Archaeology **44** (1): 53-79.

Vallbona, A. V. (1997). An investigation of the behaviour of phosphorus in the production of bloomery iron: a study of archaeological phosphorus-rich iron. University of Bradford, University of Bradford. **PhD thesis**.

Van der Merwe, N. J. and D. H. Avery (1987). Science and magic in African technology Traditional iron smelting in Malawi. Africa: Journal of the International African Institute **57** (2): 143-172.

Vega, E., P. Dillmann, M. Lheritier, P. Fluzin, P. Crew and P. Benott (2003). Forging of Phosphoric Iron. An Analytical and Experimental Approach. Proceedings of the International Conference on Archaeometallurgy in Europe. Milan, Italy, Associazione Italiana di Metallurgia.

Voss, O. (1996). Snorup- an iron producing settlement in West Jutland, 1st to 7th Century A.D. The Importance of Ironmaking, Norberg Jernkontorets Bergshistoriska Utskot.

Waanders, F. B., L. R. Tiedt, M. C. Brink and A. A. Bisschoff (2005). From ore to tool - Iron Age iron smelting in the largest and oldest meteorite crater in the world. Hyperfine Interactions **161** (1-4): 21-31.

Wang, Q. and P. Crew (2013) Three ores, three irons and three knives in Humphris, J. and T. Rehren (eds.) 2013 The world of iron, London, Archetype: 393-401

Webster, L. (1991). The Franks Casket in. L. Webster and J. Backhouse The making of England: Anglo-Saxon art and culture A.D. 600-900. London, British Museum Press.

Weeks, L. (1999). Lead isotope analyses from Tell Abraq, United Arab Emirates New data regarding the 'tin problem' in Western Asia. Antiquity **73**: 46-64.

Weeks, L., E. Keall, V. Pashley, J. Evans and S. Stock (2009). Lead Isotope analysis of Bronze Age copper-based artefacts from Al-Midamman, Yemen: Towards the identification of an indigenous metal production and exchange system in the Southern Red Sea region. Archaeometry **51** (4): 576-597.



Wheeler, J. (2011). Charcoal analysis of industrial fuelwood from medieval and early modern iron-working sites in Bilsdale and Rievaulx, North Yorkshire, UK: evidence for species selection and woodland management. Environmental Archaeology **16** (1): 16-35.

Wood, I. N. (1990). Ripon, Francia and the Franks Casket in the Early Middle Ages. Northern History 26 (1-19).

Wynne, E. and R.F. Tylecote (1958). An experimental investigation into primitive iron-smelting technique, Journal of the Iron and Steel Institute, **190**: 339-348

Young, T. (1993). Sedimentary iron ores in. R. A. D. Patrick and D. A. Polya Mineralization in the British Isles. London, Chapman and Hall: 446-489.

Zitzmann, A. (1977) The iron ore deposits of Europe and adjacent areas, explanatory notes to the international map of the iron ore deposits of Europe 1:2500000. Hannover, Bundesanstalt für Geowissenschaften und Rohstoffe.